

**Kinetic mechanism, ammonia channeling
and domain cross-talk in *Plasmodium
falciparum* GMP synthetase: an
amidotransferase**

A Thesis Submitted for the Award of the Degree of

Doctor of Philosophy

By

Bhat Javaid Yousuf



**Molecular Biology and Genetics Unit
Jawaharlal Nehru Centre for Advanced Scientific
Research (A Deemed University)
Jakkur, Bangalore-560064
India.**

October 2010

DECLARATION

I hereby declare that this thesis entitled “**Kinetic mechanism, ammonia channeling and domain cross-talk in *Plasmodium falciparum* GMP synthetase: an amidotransferase**” is an authentic record of the research work carried out by me under the supervision of Prof. Hemalatha Balaram at the Molecular Biology and Genetics Unit, Jawaharlal Nehru Centre for Advanced Scientific Research, Bangalore, India and that this work has not been submitted elsewhere for the award of any other degree.

In keeping with the general practice of reporting scientific observations, due acknowledgements have been made wherever the work described has been based on the findings of other investigators. Any omission, which might have occurred by oversight or misjudgement, is regretted.

(Bhat Javaid Yousuf)

Place:

Date:



Hemalatha Balaram, Ph. D.

Professor

CERTIFICATE

This is to certify that the work described in this thesis entitled “**Kinetic mechanism, ammonia channeling and domain cross-talk in *Plasmodium falciparum* GMP synthetase: an amidotransferase**” is the result of investigations carried out by Mr. Bhat Javaid Yousuf in the Molecular Biology and Genetics Unit, Jawaharlal Nehru Centre for Advanced Scientific Research, Bangalore, India under my supervision, and that the results presented in this thesis have not previously formed the basis for the award of any other diploma, degree or fellowship.

(Hemalatha Balaram)

Place:

Date:

Acknowledgements

Listing all the people whose help was sought, directly or indirectly, during the course of this study is indeed a difficult task however, an utmost attempt has been done to acknowledge all.

I express my sincere gratitude to Prof. Hemalatha Balaram, my research supervisor, without whom this dissertation would definitely not have attained the current form. I heartily thank her for the constant guidance, encouragement and invaluable support provided to me. Her appreciation for new ideas and their promotion and for creating a supportive work environment in the laboratory is highly acknowledged.

Working with Prof. Siddhartha P. Sarma, Molecular Biophysics Unit, Indian Institute of Science, Bangalore, was indeed a privilege. The NMR experiments performed during this study would not have been brought off without his consistent efforts and investment of his precious time. I extend my unfeigned thankfulness to him for the guidance, encouragement and the permission to use his laboratory facilities, unlimitedly.

Prof. Elizabeth A. Komives, University of California, San Diego, was very kind in providing helpful suggestions, protocols and software for the H/D exchange experiments. Dr. Zhongqi Zhang, Amgen Inc, CA, gifted the MagTran software that was used for calculation of the peptide centroid masses. I gratefully acknowledge both of them for the help.

*A mutant strain of *E. coli* (*guaA*⁻) was generously provided by Yale Genetic Stock Center that formed the production factory for PfGMP synthetase. I sincerely thank them for the kind gift.*

Prof. Dipankar Chatterjee (MBU, IISC) and Prof. M.R.S Rao, the former chairpersons and Prof. Anuranjan Anand, the current chairman of MBGU, are highly acknowledged for their suggestions and constructive criticism. I particularly thank Prof. M. R. S. Rao for his critical comments and salutary advice during my routine work presentations in the department. I thank all other MBGU faculties, Prof. Tapas K. Kundu, Prof. Namita Surolia, Prof. Ranga Udaykumar, Prof. Maneesha Inamdar and Prof. Kaustav Sanyal for allowing me to use their lab equipments.

It was an immense pleasure to be a student of some great teachers at JNCASR, Professors- Amitabh Joshi, Anuranjan Anand, Hemalatha Balaram, Tapas K. Kundu and Vijay K. Sharma and IISC, Prof P. Balaram. I owe my deepest gratitude to all of them. Teachers at Jammu University, Professors- B. K Bajaj, I. D. Pandey, Jyoti Vakhlu, Manoj K. Dhar, K.L. Dhar, Roshan L. Mattoo and Sanjana Koul were all generous and supportive during my M. Sc. studies and I sincerely thank them all. I am particularly grateful to Prof. R. L. Mattoo, my M. Sc. research supervisor, who continues to be a great source of

encouragement and guidance for me.

I acknowledge Kallol Gupta, Dr. Suman K. Thakur and Dr. Sabreesh from Prof. P. Balaram's lab at IISC, for their time to time help in mass spectrometry experiments.

A wonderful group of colleagues in lab made my stay here an enjoyable and memorable one. I take this opportunity to thank all my labmates, both past, Dr. Chetan, Dr. Mylarappa, Dr. Chetana, Shilpa, Shastri, Bopanna, Sujay, Dr. Mousumi, Dr. Sonali, Dr. Subhra, Roopa and Kavita and present, Dr. Vasudeva, Dr. Srinivas Rao, Vinay, Bharath, Bala, Moumita, Vidhi, Sanjeev, Sourav, Sonia, Vijay, Prasoon, Arpit and Debarati for their help, support, suggestions and encouragement. Shastri, Roopa and Kavita are greatly acknowledged for their specific support. Vinay makes a special reference for being a fantastic friend to share views with and for proof reading some part of this thesis. Bharath's unlimited help particularly in running computer softwares is highly acknowledged. My special thanks to Dr. Vasudeva for his help in formatting and proofreading the thesis. I am also indebted to extend my sincere thanks to all the lab members of Prof. Siddhartha P. Sarma, particularly to Ashwani, Megha, Rajesh and Rustam for their unfettered support during the NMR experimentation.

The company of my batch mates, Arif, Gayatri, Manohar, Pavan, Srikanth, Sairam, and Venkatesh Bhat was marvelous and I thank all of them for their help.

During my stay here, I came across a number of wonderful friends at JNC, IISC and NCBS. Without naming, I wholeheartedly thank all of them for their moral support and time to time help. I specially thank Shahnawaz, EOBU, for teaching me ANOVA analysis and Tariq, IISC for his constant help. Also, I owe special thanks to Mr. Peer Mehboob and his family for providing me a home-like atmosphere here in JNC.

I acknowledge NMR spectroscopy and mass spectrometry facilities at IISC and MALDI-TOF-mass spectrometry, DNA sequencing and confocal microscopy facilities at JNC.

I thank CSIR and DST for the financial assistance during my Ph. D. and DBT for the travel grant.

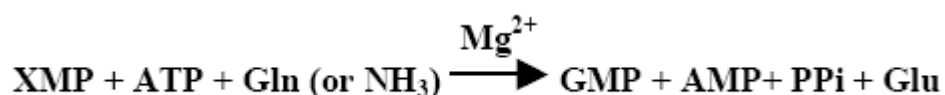
I also sincerely thank administrative staff of JNCASR including library and complab, for their immense support.

The incredible encouragement, motivation and moral support provided by my family members is beyond description. I thank my father, mother, sisters and in-law brothers for their constant support, and dedicate this thesis to my loving father and mother. I also thank my uncles, G. N. Qadri, who has always been a source of inspiration for me and M. Hussain for their constant encouragement.

Thesis summary

Amidotransferases are a class of enzymes that catalyse the incorporation of nitrogen into a wide variety of substrate molecules, such as amino acids, amino sugars, nucleotides of purines and pyrimidines, coenzymes and antibiotics (*Adv. Enzymol. Relat. Areas. Mol. Biol.* (1998), **72**, 87-144). The aminated products of these reactions serve as entry points for nitrogen into their respective pathways. Most of the amidotransferases are known to utilise both glutamine as well as external ammonia for the nitrogen incorporation reaction. However, when glutamine is used as a source of nitrogen, its hydrolysis is catalysed in a specialized domain called the GAT (glutamine amidotransferase) domain. This domain has evolved a mechanism by which glutamine is hydrolysed using cysteine as a nucleophile (*Cell. Mol. Life Sci.* (1998), **54**, 205–222). Accordingly, amidotransferases have been classified into three classes, depending on the mechanism by which glutamine is hydrolysed in the GAT domain for generating ammonia. G-type amidotransferases use a catalytic triad formed by a set of conserved residues (Cys-His-Glu), while, F-type amidotransferases contain a conserved N-terminal cysteine as the main nucleophilic residue with catalysis being assisted by His and Asp, as has been shown in some cases (*J. Biol. Chem.* (1989), **264**, 16613-16619). In the third class of amidotransferases, though ammonia is generated by glutamine hydrolysis, a consensus motif involved in such a reaction is yet to be identified. All the amidotransferases are modular enzymes, containing two spatially separated domains which are specialized for two different types of chemical reactions. Ammonia channeling and domain cross-talk are the hallmarks of these enzymes (*Curr. Opin. Chem. Biol.* (2006), **10**, 465-472; *Curr. Opin. Struct. Biol.* (2007), **17**, 653-664).

Guanosine monophosphate synthetase or GMP synthetase (E.C. 6.3.5.2) belongs to the G-type class of amidotransferases that catalyses the formation of guanosine monophosphate (GMP) in the purine nucleotide biosynthetic pathway. The reaction catalysed by GMP synthetase involves the irreversible conversion of XMP (xanthosine 5'-monophosphate) to GMP, a reaction that requires ATP and involves the transfer of an amino group from glutamine to the C2 carbon of XMP via an adenylyl-XMP intermediate (*Biochemistry* (1983), **24**, 5343-5350). The enzyme also directly uses ammonia as a source of nitrogen replacing glutamine. GMP synthetase is a Mg^{2+} dependent enzyme. The overall reaction catalysed by GMP synthetase is shown in the scheme below.



GMP synthetases from both prokaryotes and eukaryotes consist of two domains. The C-terminal ATPase (ATP pyrophosphatase) domain catalyses the condensation of XMP with ATP and the N-terminal glutaminase domain (GAT) liberates ammonia by the hydrolysis of glutamine.

Plasmodium falciparum relies solely on purine salvage pathway for the replenishment of purine nucleotides, as the parasite lacks purine *de novo* biosynthetic pathway. Due to the presence of low levels of free guanine in human blood (*Mol. Cell. Biochem.* (1994), **140**, 1–22), GMP production through the enzyme hypoxanthine guanine phosphoribosyl transferase (HGPRT) would be insufficient for the rapidly multiplying parasite during intraerythrocytic stages. Also, both *P. falciparum* and human erythrocytes lack guanosine kinase eliminating the possibility of conversion of guanosine to GMP. Hence, the major source of GMP in *P. falciparum* is through the conversion of XMP to GMP by GMP synthetase. The aim of this study is to understand the biochemical and kinetic aspects of *Plasmodium falciparum* GMP synthetase (PfGMP synthetase) in terms of kinetic mechanism, ammonia channeling and domain cross-talk.

The thesis comprises of four chapters. The first chapter provides a detailed introduction to different classes of amidotransferases. The available literature on different aspects of amidotransferases in terms of ammonia channeling, conformational changes and other biochemical and structural features are summarized. This chapter concludes with the literature survey on GMP synthetases reported from different organisms, in which different aspects of the enzyme function and its regulation are highlighted.

The second chapter presents the work done on biochemical and kinetic aspects of *P. falciparum* GMP synthetase. Primers were designed based on the annotated gene sequence of PfGMP synthetase (PF10_0123) available in the *Plasmodium falciparum* genome database, PlasmoDB (*Nucleic Acids Res.* (2001), **29**, 66-69). The gene was cloned in pQE30 expression vector and over-expressed in an *E. coli* strain deficient in GMP synthetase (*guaA*⁻ mutant). The overall results obtained from these studies on PfGMP synthetase highlighted that the enzyme has many features that are similar to *E. coli* GMP synthetase and distinct from the human counterpart. PfGMP synthetase, though an eukaryotic enzyme shares only 21 % sequence identity with the human enzyme, while a sequence identity of 41 % is shared with the *E. coli* counterpart. The oligomeric state of PfGMP synthetase was found to be dimeric like the *E. coli* enzyme, and is an exception from the eukaryotic counterparts that have been shown to be monomeric. XMP binding in PfGMP synthetase is hyperbolic in nature, while a cooperative behavior operates in the human counterpart and overall catalytic turnover of PfGMP synthetase is 10 fold lower than the human enzyme. The order of substrate (ATP, XMP and glutamine) binding in PfGMP synthetase was elucidated by combination of detailed initial velocity kinetics and, inhibition kinetics using products and a substrate analogue. The

initial velocity kinetics done according to the method of Freiden (*J. Biol. Chem.* (1959), **234**, 2891-2896) followed by fitting of the data to appropriate models suggested that the binding of ATP and XMP follows a steady state ordered mechanism and an irreversible step (ping pong mechanism) occurs between the binding of either ATP or XMP and glutamine. Use of products (GMP and PPI) and a substrate analogue (AMP-PNP) for inhibition kinetics suggested that ATP is the first substrate to bind followed by XMP, and glutamine can bind either before or after the binding of the nucleotides. Overall, these studies suggested that a two-site ping pong mechanism operates in PfGMP synthetase in which the immediate release of glutamate upon glutamine hydrolysis in the GAT domain gives rise to the irreversible step in the whole kinetic mechanism. These studies also led us to conclude that the products formed in the reaction are released in an ordered manner, in which AMP leaves first followed by GMP and then PPI. PfGMP synthetase is a Mg^{2+} dependent enzyme and binding of Mg^{2+} is cooperative in nature. Though Mg^{2+} is used in the formation of MgATP complex, extra binding sites for free Mg^{2+} are present on this enzyme. Psicofuranine and decoynine are the two known potent inhibitors of human and *E. coli* GMP synthetases. However, the effect of these inhibitors on PfGMP synthetase activity was minimal and though psicofuranine reduced the activity by 25%, decoynine did not elicit any effect, suggesting that there may be structural differences across these enzymes.

Ammonia channeling in amidotransferases is an essential process in the catalysis of glutamine dependent amidotransferase reaction. The third chapter focuses on ammonia channeling in *P. falciparum* GMP synthetase. Functional coordination between the two domains in amidotransferases is essential for their efficient catalysis, and binding of substrates in the acceptor domain generally triggers the hydrolytic reaction in the GAT domain. In PfGMP synthetase, though a significant level of leaky glutaminase activity is observed in the absence of substrates in ATPase domain, the enzyme has evolved a mechanism to prevent such a wasteful process during the complete reaction, as in the presence of ATP and XMP a 1:1 stoichiometry in the formation of glutamate and GMP from their respective domains was seen. Differences in the K_m value for glutamine and external ammonia, occurrence of 1:1 stoichiometry in the formation of two products (GMP and glutamate) and pH kinetics of ammonia and glutamine dependent reactions, all indicated channeling of ammonia across domains in PfGMP synthetase. To further validate ammonia channeling in PfGMP synthetase, competition assays were carried out in which both glutamine and ammonia were together provided in the reaction mixture. ^{15}N edited 1H fHSQC (Fast Heteronuclear Single Quantum Coherence) NMR spectroscopy allowed us to quantify the contribution of external $^{15}NH_3$ to the formation of GMP, when both glutamine and $^{15}NH_3$ were together present in the reaction mixture. The proportion of ^{15}N GMP produced by the utilization of $^{15}NH_3$ in the total pool of ^{14}N and ^{15}N GMP in presence of ^{14}N glutamine was

always <50 %, suggesting that indeed the ammonia generated from glutamine is channeled within the protein and does not mix with the outside medium. Presence of saturating concentration of glutamine (15 mM) in the assay did not stop the entry of external $^{15}\text{NH}_3$ (present at subsaturating concentration of 20 mM), indicating that external ammonia could be accessing the adenylyl-XMP intermediate through a route that is different from the one followed by ammonia generated from glutamine. In competition assays where glutamine and $^{15}\text{NH}_3$ were together present, ^{15}N edited ^1H fHSQC NMR spectra also showed the formation of ^{15}N L- glutamine. The formation of ^{15}N L- glutamine is due to the reaction of $^{15}\text{NH}_3$ with the thioester intermediate formed in the GAT domain during the hydrolysis of glutamine and this observation validates the general catalytic mechanism in G-type amidotransferases. The presence of two routes for the entry of external ammonia into PfGMP synthetase was further validated by mutating the active site cysteine (C102) to alanine. Assays done with the C102A mutant for both glutamine and ammonia dependent activities showed that only the latter activity is retained while, as expected, the former activity is completely abolished. Inhibition of ammonia dependent activity seen in presence of glutamine suggested that glutamine was able to bind to the mutant enzyme. Presence of 15 mM glutamine (saturating concentration) in the reaction assay did not completely inhibit the ammonia dependent activity, suggesting that external ammonia may indeed be entering the enzyme through another route. The reciprocal plots of $1/v$ versus $1/\text{substrate}$, in which one of the substrates (either NH_3 , XMP or ATP) was varied at different fixed concentrations of glutamine, were all parallel. This line pattern reflects dead-end inhibition arising from the binding of glutamine to the GAT domain. However, replots of the intercepts (obtained from primary plots) versus glutamine concentration were all hyperbolic. This nature of the replots is indicative of partial inhibition by glutamine, confirming that external ammonia uses two routes for entry into the enzyme.

Domain cross-talk and conformational changes in amidotransferases are known to aid these enzymes in synchronizing the function of GAT and the acceptor domains. The last chapter of this thesis deals with the studies that were carried out to monitor the global and local structural changes in PfGMP synthetase, occurring as a consequence of substrate binding. Binding of substrates, ATP and XMP in the ATPase domain in PfGMP synthetase should regulate the function of GAT domain, in order to carry the whole reaction in a coordinated way. Biochemical assays in which glutaminase activity was measured in presence and absence of ATP and XMP showed that presence of substrates enhanced the glutaminase activity by 40 % as compared to the unliganded form. Similarly, GAT inactivation studies using acivicin and diazo oxo norleucine (DON), the two known structural analogues of glutamine, suggested that rate of inactivation was higher in the presence of substrates. The second order rate constants for inactivation by acivicin and DON in the absence of substrates were 0.18 ± 0.01 and $0.19 \pm 0.01 \text{ min}^{-1} \text{ mM}^{-1}$, respectively, which increased to 1.49 ± 0.34

and $0.95 \pm 0.08 \text{ min}^{-1} \text{ mM}^{-1}$, respectively, in the presence of substrates. Limited proteolysis of PfGMP synthetase with trypsin followed by measurement of the residual activity and visualization of band pattern by SDS-PAGE showed that the enzyme is comparatively resistant to proteolysis in the liganded form when compared to that of the unliganded. Circular dichroism spectroscopy of the ATP and XMP bound form of PfGMP synthetase showed reproducible changes both in the far and near-UV regions, when compared to the unliganded form, suggesting the occurrence of both local and global changes in the liganded form of PfGMP synthetase. Use of ANS (8-anilino-1-naphthalene sulphonic acid) as a probe for conformational changes in PfGMP synthetase showed that complete ligand binding causes a significant decrease in ANS emission intensity compared to the unliganded form. To specifically localize the regions on PfGMP synthetase that undergo change on ligand binding, two approaches were taken; 1) limited proteolysis of PfGMP synthetase in the presence and absence of substrates, and 2) hydrogen/deuterium exchange of liganded and unliganded enzyme and both approaches were followed by MALDI-TOF mass spectrometry. Comparison of MALDI-TOF mass spectra of PfGMP synthetase incubated with different ligand combinations and after being subjected to limited proteolysis, showed complete absence of a $15471 \pm 1 \text{ Da}$ peak in the spectrum when the enzyme was bound to both ATP and XMP. Replacement of ATP in the pre-incubation reaction with its non hydrolysable analogue, AMPPNP showed a similar pattern. The $15471 \pm 1 \text{ Da}$ peak was assigned to a region in the GAT domain of PfGMP synthetase involving the residues Lys³⁷-Lys¹⁷³. This suggested that ligand binding in ATPase domain leads to the inaccessibility of Lys³⁷ and Lys¹⁷³ (both residues in the GAT domain) to trypsin leading to the absence of the peak and, reflecting that ligand binding causes global changes in PfGMP synthetase. A more robust technique which addressed the question whether both local and global changes occur in the enzyme as a consequence of substrate binding, was hydrogen/deuterium exchange (H/DX) followed by mass spectrometry. H/DX of PfGMP synthetase, both in the presence and absence of ATP and XMP followed by pepsin digestion and MALDI-TOF mass spectrometry highlighted regions both in ATPase (300-315 and 423-430) and GAT domain (4-22 and 143-155) that have reduced deuteration when the enzyme was completely liganded. These studies not only supported the results obtained with other probes used in this study, but also showed that the liganded form of PfGMP synthetase undergoes both local as well as global structural changes. All these studies led to the conclusion that a change brought about by ligand binding in ATPase domain is somehow transduced to the GAT domain to synchronize the function of the two catalytic pockets.

In conclusion, the overall study provides a comprehensive view of the biochemical aspects of PfGMP synthetase, the order of substrate binding and product release, ammonia channeling and inter-domain activity coordination as a result of local and global

conformational changes brought about by the binding of substrates. Probably, the binding of substrates leads to the formation of a closed form of the enzyme which may be aiding in the creation of an ammonia channel across the protein.

List of publications

1. **Bhat, J. Y.**, Shastri, B. G., and Balaram, H. (2008). Kinetic and biochemical characterization of *Plasmodium falciparum* GMP synthetase. *Biochem J* 409, 263-273.
2. **Bhat, J. Y.**, Roopa, Kavita S., Sarma, S.P., and Balaram, H. (2010). Ammonia channeling in *Plasmodium falciparum* GMP synthetase, an elucidation by NMR spectroscopy and biochemical assays. (Manuscript under preparation).
3. **Bhat, J.Y.**, Roopa, and Balaram, H. (2010). Ligand induced conformational changes in *Plasmodium falciparum* GMP synthetase, monitored by combination of spectroscopic probes and mass spectrometry. (Manuscript under preparation).

List of Abbreviations

ADA	Adenosine deaminase
ADSS	Adenylosuccinate synthetase
AMP	Adenosine monophosphate
ATP	Adenosine monophosphate
ATPPase	ATP pyrophosphatase
DHB	2,5-dihydroxybenzoic acid
DON	6-diazo-5-oxo-L-norleucine
DTT	Dithiothreitol
ESI	Electrospray Ionisation
fHSQC	Fast Heteronuclear Single Quantum Coherence
FMN	Flavin mononucleotide
GAT	Glutamine amidotransferase
GDP	Guanosine diphosphate
GMP	Guanosine monophosphate
GMPS	Guanosine monophosphate synthetase
HGPRT	Hypoxanthine guanine phosphoribosyltransferase
IMPDH	Inosine monophosphate dehydrogenase
IPTG	Isopropyl thio- β -D-galactopyranoside
MALDI-TOF	Matrix Assisted Laser Desorption/Ionisation Time of Flight
MES	(2-(N-morpholino)ethanesulfonic acid)
NAD	Nicotinamide adenine dinucleotide
NADPH	Nicotinamide adenine dinucleotide phosphate
Ni-NTA	Ni ²⁺ -nitrilotriacetate
AMPPNP	Adenosine 5- $[\beta,\gamma$ -imido]triphosphate
PAGE	Polyacrylamide Gel Electrophoresis
PfASL	<i>P. falciparum</i> adenylosuccinate lyase
PfGMPS	<i>Plasmodium falciparum</i> GMPS
PNP	Purine nucleoside phosphorylase
XMP	Xanthosine monophosphate

Contents

Declaration	i
Certificate	ii
Acknowledgements	iii
Thesis summary	v
List of publications	xi
List of abbreviations	xii

Chapter 1. Introduction to amidotransferases and guanosine monophosphate synthetase

1.1. Summary	1
1.2. Glutamine amidotransferases	1
1.2.1. General description	1
1.2.2. Classification of amidotransferases	2
1.2.2.1. Class I or G-type amidotransferases	3
1.2.2.2. Class II or F-type amidotransferases	4
1.2.2.3. Non-classified amidotransferases	6
1.2.3. General features of glutamine amidotransferases	9
1.2.3.1. Modularity	9
1.2.3.2. Ammonia channeling and domain cross-talk in glutamine-dependent amidotransferases	11
1.3. Amidotransferases in protozoa	11
1.4. Guansoine monophosphate (GMP) synthetase	13
1.4.1. Discovery of GMP synthetase	13
1.4.2. Structural organization of GMP synthetases	14
1.4.3. Moonlighting or non-catalytic functions of GMP synthetases	23
1.5. Purine biosynthesis and the role of GMP synthetase in <i>P. falciparum</i>	25

Chapter 2. *Plasmodium falciparum* GMP synthetase: biochemical and kinetic characterization

2. 1.Summary	31
2.2. Introduction	31

2.2.1. Catalytic mechanism	32
2.2.2. Kinetic mechanism	32
(A) Rapid equilibrium assumption	33
(B) Steady-state assumption	33
2.2.2.1. Initial velocity kinetics without added inhibitors	33
2.2.2.2. Initial velocity kinetics with added inhibitors	35
(A) Competitive inhibition	35
(B) Uncompetitive inhibition	35
(C) Non-competitive inhibition	36
2.2.3. Metal ion dependence of enzyme activity	36
2.2.4. Kinetic and biochemical aspects of GMP synthetases	37
2.2.5. GMP synthetase inhibitors	37
2.3. Materials and methods	39
2.3.1. Materials	39
2.3.2. Cloning, complementation, expression and purification	39
2.3.3. Analytical gel filtration	40
2.3.4. Assay for PfGMPS glutaminase activity	40
2.3.5. Assay for GMP synthetase activity	41
2.3.6. Initial velocity kinetics	42
2.3.7. Kinetics of inhibition by products and substrate analogs	43
2.3.8. Dependence of PfGMPS activity on Mg ²⁺ ions	43
2.4. Results	44
2.4.1. Functional complementation and preliminary characterization of recombinant PfGMP synthetase	44
2.4.2. Kinetic mechanism of PfGMPS	47
2.4.3. Mg ²⁺ requirement for PfGMPS activity	54
2.4.4. Inhibition by nucleosides, nucleotides and purine bases	56
2.5. Discussion	56
Chapter 3. Ammonia channeling in <i>P. falciparum</i> GMP synthetase: biochemical and NMR spectroscopic investigation	
3.1. Summary	61
3.2. Introduction	61

3.2.1. Biochemical and structural aspects of ammonia channeling in glutamine dependent amidotransferases	61
3.2.2. Mechanistic basis of ammonia channeling revealed by computational approaches	66
3.2.3. Ammonia dependant activity in amidotransferases	67
3.3. Materials and methods	69
3.3.1. Materials	69
3.3.2. Assay for PfGMPS activity	70
3.3.3. pH titration of glutamine and ammonium dependent activities	70
3.3.4. Stoichiometry of glutamate and GMP formation	71
3.3.5. Steady state competition assays in presence of both glutamine and external ammonia	72
3.3.6. Enzymatic synthesis of ¹⁵ N GMP	72
3.3.7. NMR measurements	73
3.3.8. Chemical modification of glutaminase domain	73
3.3.9. Construction and biochemical characterization of C102A PfGMPS	74
3.4. Results	75
3.4.1. Biochemical evidence for ammonia channeling	75
3.4.2. Steady state competition assays between glutamine and ammonium	78
3.4.3. Effect of chemical modification and mutagenesis of cysteine 102 on glutamine and ammonium dependent activities	84
3.5. Discussion	90

Chapter 4. Substrate-induced conformational changes in *P. falciparum* GMP synthetase: biochemical and mass spectrometric investigation

4.1. Summary	95
4.2. Introduction	95
4.2.1. Conformational changes in proteins and use of high-resolution mass spectrometry	95
4.2.1.1. Limited proteolysis in conjunction with mass spectrometry (LP-MS)	96
4.2.1.2. Hydrogen-deuterium exchange coupled to mass spectrometry (H/DX MS)	98

4.2.2. Domain cross-talk or inter-domain signaling or amidotransferase allostery	105
4.3. Materials and methods	108
4.3.1. Materials	108
4.3.2. Enzyme preparation and activity assays	108
4.3.3. Irreversible inhibition of PfGMPS	108
4.3.4. Circular dichroism measurements	109
4.3.5. ANS fluorescence measurements	110
4.3.6. Limited tryptic proteolysis of PfGMPS	110
4.3.7. Hydrogen-deuterium exchange (H/DX)	111
4.3.8. MALDI-TOF mass spectrometric analysis of the deuterium- incorporated samples	112
4.3.9. PfGMPS modeling	113
4.4. Results	113
4.4.1. Inter-domain cross-talk	113
4.4.2. Circular dichroism and ANS fluorescence spectroscopy	117
4.4.3. Limited tryptic proteolysis of PfGMPS	120
4.4.4. Substrate-induced conformational changes in PfGMPS monitored by hydrogen-deuterium exchange coupled to MALDI-TOF mass spectrometry	126
4.5. Discussion	133
References	137

CHAPTER 1

Chapter 1 **Introduction to amidotransferases and guanosine monophosphate synthetase**

1.1. Summary

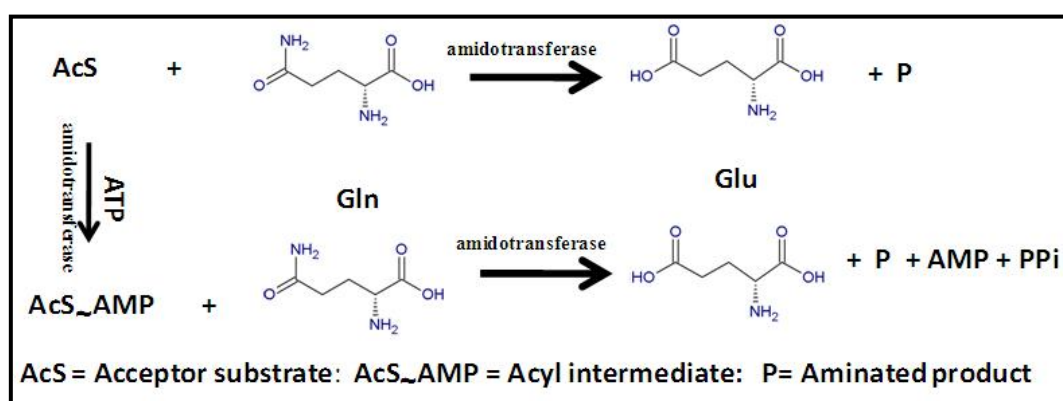
This chapter provides a general introduction to amidotransferases, a class of enzymes that belong to different metabolic pathways. Common features that form the basis of classification of these enzymes are discussed. *P. falciparum* GMP synthetase, an enzyme of purine salvage pathway and a member of amidotransferases, forms the theme of studies reported in this thesis. A brief survey of literature available on GMP synthetases is also included. The chapter concludes with an account on current understanding of the purine biosynthetic pathway in *P. falciparum* and its potential use as antimalarial drug target.

1.2. Glutamine amidotransferases

1.2.1. General description

Glutamine amidotransferases (Gln-ATs) or transamidases, are the enzymes catalyzing amination of a wide variety of metabolites, like amino acids, purines, pyrimidines, amino sugars, coenzymes and antibiotics, that sometimes serve as entry points for nitrogen into the respective pathways. Most of the amidotransferases reported till date can either directly utilize ammonia from an external source or generate it by the hydrolysis of glutamine, needed for the amination of the acceptor molecules. Generally, these enzymes are modular with spatially separated glutaminase and the acceptor domains, specific for catalyzing the complex amidotransferase reaction in two parts, the glutamine hydrolysis and the acceptor amination, respectively. A set of glutamine amidotransferases after glutamine hydrolysis, transfer the generated ammonia directly to the acceptor substrates, with glutamate synthase serving as an example. However, in other cases, the acceptor substrate is first pre-activated by utilization of a molecule of ATP that leads to the

formation of catalytically active intermediate possessing an electron deficient centre. The intermediate finally reacts with ammonia (with lone pair of electrons) in a nucleophilic reaction to proceed to the formation of aminated product (Buchanan, 1973; Massiere and Badet-Denisot, 1998; Zalkin, 1985; Zalkin, 1993; Zalkin and Smith, 1998). Though the final nitrogen-incorporated products differ across amidotransferases, glutamate is the common product whenever glutamine is hydrolyzed. The amidotransferase reaction differs from that catalyzed by aminotransferases or transaminases (E.C. 2.6.1.) as the latter catalyse the transfer of α -amino group from an amino acid to an α -keto acid (generally α -keto glutaric acid), in a pyridoxal phosphate (PLP) dependent reaction (Hirotsu et al., 2005). A general amidotransferase reaction scheme (Scheme 1.1) is shown below:



Scheme 1.1. General amidotransferase reaction showing the transfer of amino group from glutamine to the acceptor molecule

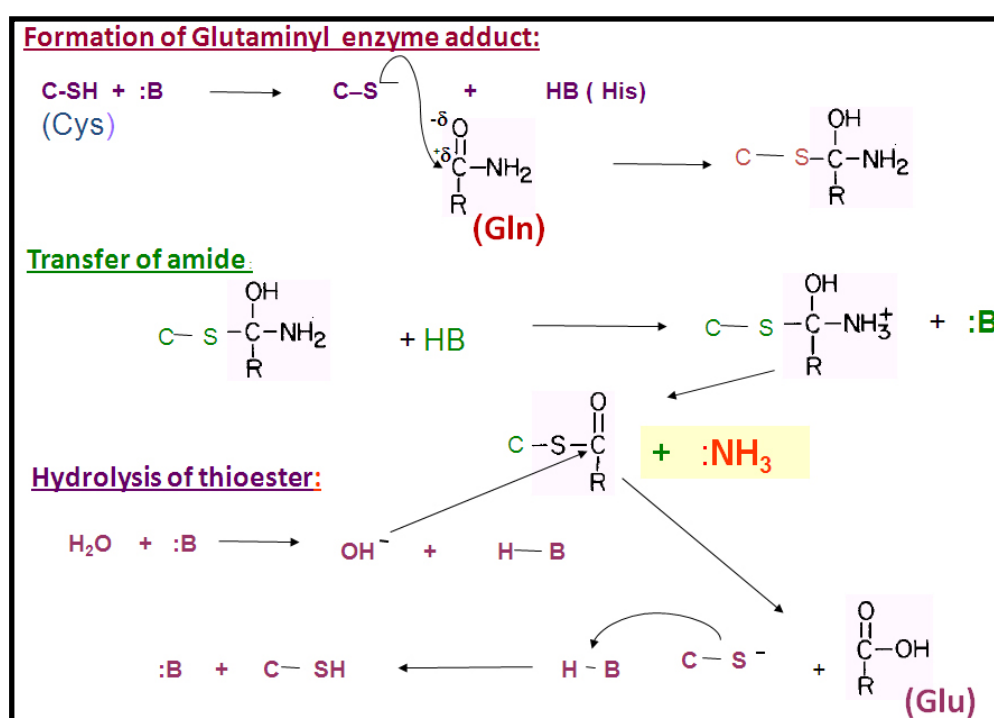
1.2.2. Classification of amidotransferases

Till date International Union of Biochemistry and Molecular Biology (IUBMB) has not proposed any separate official classification for amidotransferases (Webb, 1992). However, Howard Zalkin at Purdue university (Zalkin, 1993), has classified amidotransferases into two distinct classes based on alignment of the gene sequences that were available for these enzymes at that time. The classification was initially based on the conserved residues in primary sequences of the glutaminase domains in these enzymes and subsequent biochemical and structural analysis led to their functional implication. A group of glutamine hydrolyzing enzymes that also incorporate nitrogen into their substrates do not resemble either of the two canonical

amidotransferase classes in terms of the glutaminase domain architecture and hence, have been placed in a separate class (Zalkin, 1985; Zalkin, 1993).

1.2.2.1. Class I or G-type amidotransferases

These enzymes possess a conserved catalytic triad (cysteine, histidine and glutamate) (Tesmer et al., 1996; Thoden et al., 1997) in the glutaminase domain for generating ammonia from glutamine. Anthranilate synthase, an enzyme catalyzing a reaction both in the tryptophan and the folic acid biosynthetic pathways, was first to be reported from class I amidotransferases. This enzyme is encoded by trp-G operon and hence, the name G-type amidotransferases. Scheme 1.2 shows the proposed catalytic mechanism for glutamine hydrolysis in class I amidotransferases (Amuro et al., 1985; Zalkin, 1993).



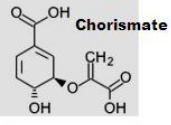
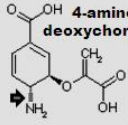
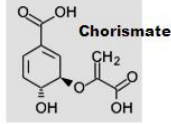
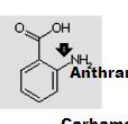
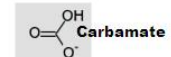
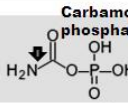
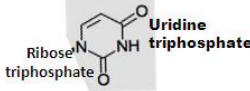
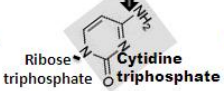
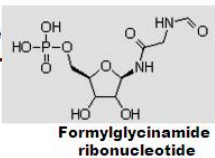
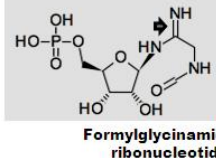
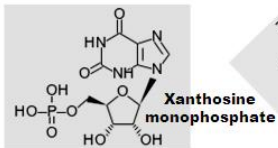
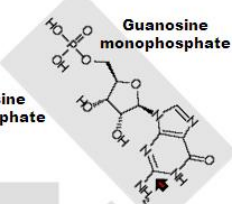
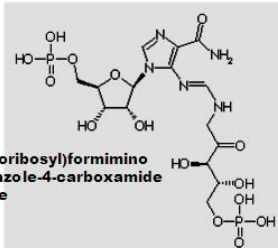
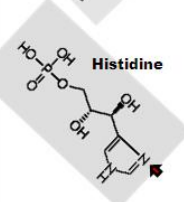
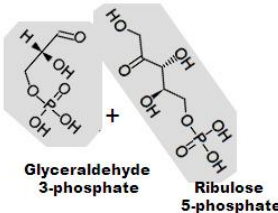
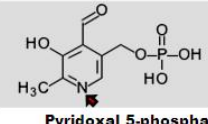
Scheme 1.2. Proposed catalytic mechanism for glutamine hydrolysis in class 1 amidotransferases. During this reaction, thioester intermediate is formed between glutamine and the catalytic cysteine followed by generation of ammonia and release of glutamate.

In this mechanism, a general base (His) assisted cysteine nucleophile forms an adduct with glutamine (glutaminyl-enzyme adduct) and its subsequent protonation drives the reaction towards the release of ammonia. Finally, the catalytic glutamate assists in hydrolysis of the thioester intermediate to release glutamate as a product and prepare the enzyme for another round of catalysis. This mechanism has been supported both by biochemical (isolation of the thioester intermediate) (Chaparian and Evans, 1991; Levitzki and Koshland, 1971; Roux and Walsh, 1992; Schendel et al., 1989) and structural studies (crystal structures containing covalently bound acivicin) (Chaudhuri et al., 2001). The catalytic mechanism in class I amidotransferases resemble that of α/β hydrolases in many aspects (Tesmer et al., 1996). Two prominent mechanistic features shared by these two different families of enzyme are (1) the oxyanion hole that is involved in stabilization of the transient negative charge on glutamine amide oxygen, and (2) the nucleophile elbow, that provides the disallowed backbone conformation to the nucleophilic residue (cysteine). The members of this group (Table 1.1) are either hetero or homo oligomers, where the glutaminase and the acceptor domains are either fused or separate. Site-directed mutagenesis (Miran et al., 1991), structural elucidation (Smith, 1995; Tesmer et al., 1996) and other routine biochemical methods involving chemical labeling have accounted the role of triad residues in catalysis of the glutaminase domain in these enzymes.

1.2.2.2. Class II or F-type amidotransferases

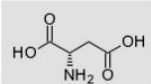
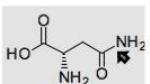
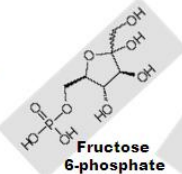
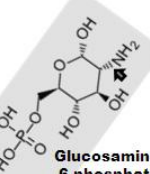
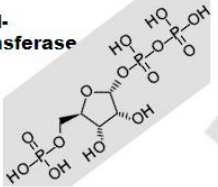
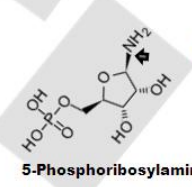
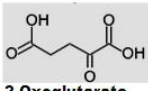
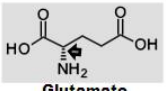
These enzymes are characterized by the presence of a conserved N-terminal nucleophilic cysteine in the glutaminase domain that forms the main catalytic residue during glutamine hydrolysis. Unlike triad glutamine amidotransferases, no consensus assisting residues have been distinguished in class II GATs. Though pH dependent assays in glutamate synthase (Vanoni et al., 1994) and diethylpyrocarbonate labeling (Badet-Denisot and Badet, 1994) and mutational analysis of glutamine-PRPP-amidotransferase (Mei and Zalkin, 1989) have suggested the involvement of histidine in glutamine hydrolysis, alignment of large number of class II primary sequences did not reveal any conserved histidine across the members (Zalkin, 1993). In the absence of any close residue that can increase the nucleophilicity of the catalytic cysteine, it has been proposed that the terminal amino group could be doing the function (Isupov et al., 1996) through involvement of a chain of water molecules, though a clear proof

Table 1.1. Class I amidotransferases, their acceptor substrates, the aminated products, name of the biosynthetic pathway and the respective PDB IDs for those reported in literature. Those marked in red are two-subunit type amidotransferases. Arrows point to the site of nitrogen incorporation. The structures of the molecules were adapted from KEGG pathway database (Kanehisa and Goto, 2000) (<http://www.genome.jp/kegg/pathway.html>).

Enzyme	Acceptor substrate	Product	Biosynthetic Pathway	Structure reported
Aminodeoxychorismate synthase (E.C. 2.6.1.85)	 Chorismate	 4-amino-4-deoxychorismate	Folic acid	<i>E. coli</i> (1K0E)
Anthranilate synthase (E.C. 4.1.3.27)	 Chorismate	 Anthranilate	Tryptophan	<i>S. Solfatarius</i> (1QDL) <i>S. typhimurium</i> (111Q) <i>S. marcescens</i> (117S)
Carbamoyl phosphate synthase (E.C. 6.3.5.5)	 Carbamate	 Carbamoyl phosphate	Arginine, uridine and cytidine triphosphates	<i>E. coli</i> (1T36) (1CE8) (1BXR) (1JDB)
CTP synthetase (E.C.6.3.4.2)	 Uridine triphosphate	 Cytidine triphosphate	Pyrimidine	<i>T. thermophilus</i> (1VCM, VCN, 1VCO) <i>E. coli</i> (1S1M) <i>H. sapiens</i> (2V01)
Formylglycinamide synthetase (EC 6.3.5.)	 Formylglycinamide ribonucleotide	 Formylglycinamide ribonucleotide	Purine	<i>B. subtilis</i> (1TWJ, 1T4A) <i>S. typhimurium</i> (1T3T) <i>T. maritima</i> (3D54) (2HRY, 2HRU, 2HS0, 2HS3, 2HS4)
GMP synthetase (E.C. 6.3.5.2)	 Xanthosine monophosphate	 Guanosine monophosphate	Purine	<i>E. coli</i> (1GPM) <i>P. horikoshii</i> (3A41)
IGP synthase (E.C. 4.1.3. -) (E.C.2.4.2. -)	 N ¹ -(5'-phosphoribosyl)formimino-5-aminoimidazole-4-carboxamide ribonucleotide	 Histidine	Histidine	<i>S. cerevisiae</i> (10X4, 10X5, 10X6) (1JVN) <i>S. olfataricus</i> (1LBL), <i>T. maritima</i> (1K9V 1GPW), <i>T. thermophilus</i> (1KA9)
PLP synthase (E.C. 1.4.3.5)	 Glycerinaldehyde 3-phosphate + Ribulose 5-phosphate	 Pyridoxal 5-phosphate	Vitamin B₆	<i>G. Stearothermophilus</i> (1Z) <i>T. maritima</i> (21SS) <i>B. subtil</i> (2NV0, 2NV1, 2NV2), <i>P. faic</i> (2ABW), <i>S. cerevisiae</i> (3FEM)

for such a mechanism is awaited. This family of enzymes has gained the name F-type amidotransferases due to the reason that pur F operon encoded glutamine PRPP amidotransferase was the first reported member (Zalkin, 1993) from the class. Most members of class II (table 1.2) are two-domain type amidotransferases, i.e. the glutaminase and the acceptor domains are fused in a single polypeptide chain.

Table 1.2. Class II amidotransferases, their acceptor substrates, the aminated products, name of the biosynthetic pathway and the respective PDB IDs for those reported in literature. Arrows point to the site of nitrogen incorporation. Structures of the molecules were adapted from KEGG pathway database (Kanehisa and Goto, 2000) (<http://www.genome.jp/kegg/pathway.html>).

Enzyme	Acceptor substrate	Product	Biosynthetic pathway	Structures reported
Asparagine synthetase (E.C. 6.3.5.4)	 Aspartate	 Asparagine	Asparagine	<i>E. coli</i> (1CT9,11AS, 12AS)
Glucosamine 6-phosphate synthase (E.C. 2.6.1.16)	 Fructose 6-phosphate	 Glucosamine 6-phosphate	Hexosamines	<i>E. coli</i> (1MOR, 1MOS, 2J6H, 2BPJ, 2BPL, 1XFF, 1XFG, 2VF4) <i>C. albicans</i> (2POC, 2PUT, 2PUV, 2PUW), <i>H. sapiens</i> (2ZJ3, 2ZJ4)
Glutaminephosphoribosyl-pyrophosphate amidotransferase (E.C. 2.4.2.14)	 5-Phospho-alpha-D-ribose 1-diphosphate	 5-Phosphoribosylamine	Purines	<i>B. subtilis</i> (1GPH, 1A00), <i>E. coli</i> (1ECF, 1EGG), 1ECB, 1ECC, 1ECJ) <i>H. sapiens</i> (2HCR)
Glutamate synthase (E.C.1.4.7.1)	 2-Oxoglutarate	 Glutamate	Glutamate	<i>Synechocystis sp</i> (10FD, 10FE, 10FF, 1LLW, 1LLZ, 1LM1) <i>A. brasilense</i> (1EA0)

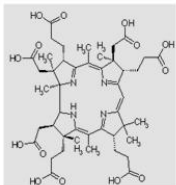
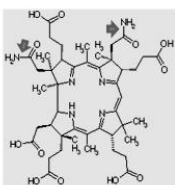
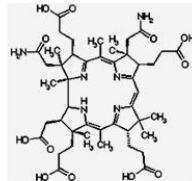
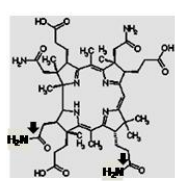
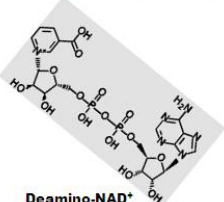
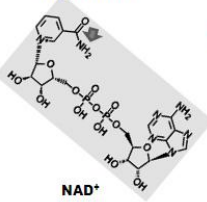
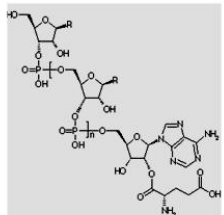
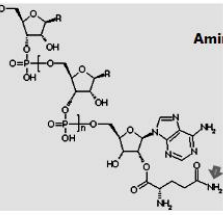
1.2.2.3. Non-classified amidotransferases

In this class of amidotransferases, a set of glutamine utilizing enzymes have been placed that do not fit otherwise to the canonical amidotransferases in terms of geometry of the glutaminase active site involved in glutamine hydrolysis. In NAD synthetase, an enzyme of the NAD biosynthetic pathway, it has been recently proposed that cysteine, lysine and glutamate could form the catalytic motif and their

subsequent replacement with alanine by site-directed mutagenesis led to the complete loss of glutamine utilizing ability (Bellinzoni et al., 2005; LaRonde-LeBlanc et al., 2009). GatCAB and GatDE, are the two glutamine dependent amidotransferases that carry out the amination of either aspartate or glutamate using glutamine, after the two residues get misacylated to tRNA^{Asp} or tRNA^{Gln} by aspartate and glutamyl tRNA synthetases, respectively (Wu et al., 2009). Though, these enzymes can generate ammonia either from glutamine or asparagines, it has been suggested that glutamine serves as a better amide donor than asparagine in *S. aureus* GatCAB compared to *A. aeolicus* GatCAB, where both the substrates are utilized with similar efficiency (Nakamura et al., 2006; Wu J, 2009). These amidotransferases belong to a family of amidases that use Ser-cisSer-Lys motif as a “catalytic scissor” for glutamine hydrolysis with Ser acting as a nucleophile. A recently solved crystal structure of *A. aeolicus* GatCAB co-crystallised with glutamine has confirmed the formation of acyl intermediate at the nucleophile Ser¹⁷¹ with Ser¹⁷¹, cisSer¹⁴⁷, and Lys⁷² forming the catalytic scissor (Wu et al., 2009).

Besides the listed amidotransferases (Table 1.3), arylamine synthetase (chloramphenicol biosynthesis) and aminoDAHP synthase (ansamycines and mitomycines biosynthesis) have been placed in this group. Recent studies have added few new candidates to the list of existing amidotransferases, with their putative reactions and the amidotransferase class being predicted, though a complete biochemical characterization is still awaited. OxyD, an enzyme of tetracycline biosynthesis, is a putative class II amidotransferase resembling asparagine synthetase in terms of the glutaminase domain architecture (Zhang et al., 2006), with either malonyl-CoA or malonyl-ACP as the predicted acceptor substrate and malonamyl-CoA or malonamyl-ACP respectively, as the amidated product. Polyene carboxamide synthase, an enzyme involved in the biosynthesis of polyene macrolide carboxamide AB-400, contains asparagine synthetase-like glutaminase domain and is proposed to be a member of class II of amidotransferases (Miranzo et al., 2010). A member of thioStrepton biosynthetic pathway producing thiopeptide antibiotics, has also been proposed to be a member of class II of amidotransferases (Kelly et al., 2009).

Table 1.3. Unclassified amidotransferases, their acceptor substrates and the aminated products, name of the biosynthetic pathway and the respective PDB IDs for those reported in literature. Those marked in red are two-subunit type amidotransferases. Arrows point to the site of nitrogen incorporation. The structures of the molecules were adapted from KEGG pathway database (Kanehisa and Goto, 2000) (<http://www.genome.jp/kegg/pathway.html>).

Enzyme	Acceptor substrate	Product	Biosynthetic pathway	Structures reported
Cobyrinic acid a,c-diamide synthetase (E.C. 6.3.5.9)	 Cobyrinic acid	 Cobyrinic acid a,c-diamide	Vitamin B ₁₂ (cobalamine)	
Cobyrinic acid synthetase (E.C. 6.3.5.10)	 Cobyrinic acid a,c-diamide	 Cobyrinic acid	Vitamin B ₁₂ (cobalamine)	
NAD synthetase (E.C. 6.3.5.1)	 Deamino-NAD ⁺	 NAD ⁺	Nicotineamide Adenine dinucleotide	<i>B. subtilis</i> (1NSY, 2NSY, 1EE1, 1FYD, 1IFX, 1IH8, 1KQP), <i>E. coli</i> (1WXE, 1WXF, 1WXG, 1WXH, 1WXI), <i>H. pylori</i> (1XNG, 1XNH), <i>B. anthracis</i> (2PZB, 2PZ8), <i>M. tuberculosis</i> (3DLA)
Glu-tRNA^{Gln} amidotransferase (E.C.6.3.5.7)	 glutamyl-tRNA ^{Gln}	 glutaminyl-tRNA ^{Gln}	Aminoacyl-tRNA	<i>P. abyssi</i> (1ZQ1), <i>S. aureus</i> (2DF4, 2DQN, 2F2A, 2G5H, 2G5I), <i>M. thermotrophicus</i> (2D6F), <i>A. aeolicus</i> (3H0L, 3H0M, 3H0R)

1.2.3. General features of glutamine amidotransferases

1.2.3.1. Modularity

All amidotransferases reported till date, are modular in structure; possessing two spatially separate active sites specialized for the catalysis of two chemically different reactions. The domain that catalyses glutamine hydrolysis and hence, producing glutamate and ammonia, is referred to as glutamine amidotransferase domain or glutaminase domain. Structural and biochemical studies on both class I and class II amidotransferases have shown the presence of a conserved cysteine in the glutaminase domain that acts as a nucleophile during glutamine hydrolysis (Isupov et al., 1996; Tesmer et al., 1996; Thoden et al., 1997; van den Heuvel et al., 2004). Different glutamine analogues have been used for locating position of the catalytic cysteine in the glutaminase domain as the mechanism of reaction of the cysteine with these analogues is similar to that followed in the cysteine-glutamine reaction and unlike glutamine, they remain bound to the enzyme covalently (Chittur et al., 2001; Massiere and Badet-Denisot, 1998). The analogues that have been used commonly are acivicin (Tso et al., 1980), diazo-oxo-norleucine (Badet et al., 1987; Hartmann, 1963; Mehlhaff and Schuster, 1991; Vanoni et al., 1994; Vollmer et al., 1983), azaserine (Hartmann, 1963; Mehlhaff and Schuster, 1991; Mizobuchi and Buchanan, 1968; Queener et al., 1973) and chloroacetone (Khedouri et al., 1966; Mantsala and Zalkin, 1976; Trotta et al., 1974).

The second domain in amidotransferases is generally known as the acceptor or synthetase domain and contains the active site that carries out amination of the acceptor substrate, by availing ammonia either from glutaminase domain (hydrolyzing glutamine) or directly from the surrounding medium. The acceptor domains across different amidotransferases differ in the primary sequence and this has been primarily attributed to the differences in reactions occurring in the domain that involve varied acceptor substrates (Tables 1.1, 1.2 and 1.3). Based on the reaction mechanism for amination in the acceptor domain, amidotransferases can be placed into three groups: (1) enzymes where the acceptor substrate is activated by transfer of a phosphate group from ATP before being aminated and produce ADP and Pi as the by-products. e.g CTP synthetase, carbamoyl phosphate synthetase, formoylglycinamide synthetase, Glu-tRNA amidotransferase. (2) amidotransferases like, GMP synthetase, asparagine

synthetase, cobyrinic acid a, c-diamide synthetase, cobyrinic acid synthetase and NAD synthetase, where utilization of ATP is followed by attachment of AMP to the respective substrates for activation, and produces AMP and PPi as by-products. An amino acid motif in the ATPase domain of GMP synthetase, known as P-loop, is highly conserved in the acceptor domains of asparagine and NAD synthetases and binds to PPi of ATP in these enzymes (Tesmer et al., 1996). (3) a third set of amidotransferases (gln:PRPP amidotransferase, anthranilate synthase, aminodeoxychorismate synthase, IGP synthase, glucoseamine-6 phosphate synthase, PLP synthase and glutamate synthase) do not use ATP before the amination process in the acceptor domain and hence, incorporate the amino group directly into the substrates (Massiere and Badet-Denisot, 1998).

While biochemical and structural studies have confirmed that amidotransferase reactions are completed by synchronized catalysis of two physically distant active centers, it has also been revealed that the glutaminase and the acceptor domains may not be part of the same polypeptide, but can be synthesized separately that after interaction catalyze the glutamine dependent amidotransferase reaction. For example, in *E. coli* IGP synthase, the two domains form two distinct polypeptides (Klem and Davisson, 1993), while in *S. cerevisiae* homolog, the two domains are fused in a single polypeptide (Kuenzler et al., 1993) and have been accordingly called as two-subunit or two-domain IGP synthases. This arrangement of domains in amidotransferases has been implicated in their functional regulation as demonstrated in carbamoyl phosphate synthetase (CPS). In mammalian CPS, the enzyme with fused glutaminase and the synthetase domains, deletion of 29 amino acid stretch that links the two domains, resulted in an active enzyme with stimulated glutamine dependent activity and abolished ammonia dependent activity (Guy and Evans, 1997). Similarly, when the two domains of *E. coli* CPS, a two-subunit GAT, were fused into a single polypeptide, the enzyme did not show similar allosteric inhibition by ornithine, as elicited by the native enzyme (Guy et al., 1997). However, like mammalian CPS, the enzyme lost the ammonia utilization property and gained enhanced glutamine dependent activity. Tables 1.1 and 1.3 provide a list of two-subunit amidotransferases (marked in red) that have been characterized and the structures reported in literature.

When the two domains in amidotransferases exist as separate proteins, generally the glutaminase domain specifically interacts with the cognate acceptor

domain, however an exception to this rule is observed in *Bacillus subtilis* and *Acinetobacter calcoaceticus* anthranilate synthases. In these organisms, a single glutaminase domain (TrpG) can couple with two different acceptor domains, TrpE and PabB to form anthranilate and 4-amino-4 deoxychorismate, respectively as the final products. These glutaminase domains are referred to as amphibolic (Slock et al., 1990; Zalkin, 1993).

1.2.3.2. Ammonia channeling and domain cross-talk in glutamine-dependent amidotransferases

Ammonia channeling is a characteristic feature of glutamine-dependent amidotransferases and has due implication in their catalytic mechanism. In this phenomenon, the ammonia generated by glutamine hydrolysis in the glutaminase domain is transferred to the synthetase domain without its diffusion to the surroundings. Defined structural elements that perform the function are known as ammonia tunnels or channels (Mouilleron and Golinelli-Pimpaneau, 2007; Weeks et al., 2006). Recent studies have provided great details of this process.

Domain coordination in amidotransferases is needed for the synchronized function of the domains that perform different individual reactions. Towards the same step, these enzymes undergo large conformational changes upon substrate binding that not only serves the purpose of domain coordination, but also lead to the formation of ammonia tunnels in some cases (Mouilleron and Golinelli-Pimpaneau, 2007).

Detailed account of ammonia channeling and conformational changes in amidotransferases is provided in chapters 3 and 4 of this thesis, respectively.

1.3. Amidotransferases in protozoa

To sustain their complex life cycle, parasites have shaped their metabolism in a fascinating adaptive way, making it logically fair to visualize the existing variations that these organisms harbor in terms of metabolism. Therefore, presence or absence of different metabolic pathways or some of the steps thereof, leads to the subsequent absence of the respective enzymes in these organisms (Ginger, 2006).

Though a detailed description and analysis of many of the amidotransferases in parasitic protozoa is still not reported, few of the enzymes have been studied or at least putatively identified from genome sequencing. Hill et al., (Hill et al., 1981)

reported activity of five of the pyrimidine biosynthetic pathway enzymes including carbamoyl phosphate synthetase (CPS) from crude extracts of many parasitic protozoa *Crithidia fasciculata*, *Trypanosoma cruzi*, *Leishmania major*, *Trichomonas vaginalis*, *Eimeria tenella*, *Toxoplasma gondii*, *Plasmodium berghei*, *Fasciola gigantica*, *Schistosoma mansoni*, *Hymenolepis diminuta*, *Nippostrongylus brasiliensis* and *Trichuris muris*. Characterization of CPS II gene and its localization on *T. cruzi* DNA was reported by Aoki et al (Aoki et al., 1994) and Nara et al (Nara et al., 1998), respectively. Cloning and preliminary characterization of CPS II from *L. mexicana* and *T. cruzi* has also been reported (Nara et al., 1998). Generation of CPS II mutant strains of *T. gondii* and their infection into an immune competent mice did not show any virulence, underscoring role of CPS in the organism (Fox and Bzik, 2002). Recently, CTP synthetase from *T. brucei* (Fijolek et al., 2007) and *P. falciparum* (Hendriks et al., 1998; Yuan, 2005) has been cloned and biochemically characterized, that highlighted differences in the kinetic parameters of these enzymes from that of the human host.

Pyridoxal 5-phosphate synthase from *P. falciparum*, involved in the biosynthesis of vitamin B₆, has been investigated in a detailed manner (Derrer et al., 2010; Gengenbacher et al., 2006). The enzyme consists of two subunits, Pdx1 and Pdx2 with former being the glutaminase domain and latter the synthase domain. Structural characterization of the protein has provided basis for the interaction of its two subunits that also led to the conclusion that its overall structure resembles its homologs from other organisms. In 2000, isolation and characterization of the gene encoding *P. falciparum* GMP synthase was reported by McConkey (McConkey, 2000). Besides the above well characterized glutamine amidotransferases in *P. falciparum*, other members of this class have been annotated. The enzymes that have been listed in *Plasmodium* genome database, PlasmoDB (<http://plasmodb.org>) but still to be characterized are; carbamoyl phosphate synthase (Pf13_0044), NAD synthase (PFI1310w), asparagine synthetase (PFC0395w). Microarray analysis of *Plasmodium* available in PlasmoDB (Bahl et al., 2003) (<http://plasmodb.org/plasmo/>) shows the expression profile of these genes during the intra-erythrocytic stages of the parasite. Different aspects of *P. falciparum* GMP synthetase are presented in this thesis.

suggesting that xanthosine was an essential intermediate in guanine biosynthesis. Gehring and Magasanik reported that the enzyme converting XMP to GMP is ATP dependant and requires glutamine as an amino donor (Gehrig and Magasanik, 1955). Moyed and Magasanik (Moyed and Magasanik, 1957) first reported the isolation and purification of xanthosine 5-monophosphate aminase from *Aerobacter aerogenes*. Lagerkvist in pigeon liver and Abrams and Bentley in rabbit bone marrow extracts independently demonstrated the formation of GMP from XMP using glutamine, ATP and Mg^{2+} in the reaction (Abrams and Bentley, 1955; Lagerkvist, 1958). The studies on pigeon liver GMP synthetase using ^{18}O -labeled XMP as a substrate indicated the occurrence of adenylyl-XMP intermediate during the reaction (Lagerkvist, 1958). Fukuyama substantiated the formation of adenylyl-XMP using radiolabel substrates in the GMP synthetase reaction (Fukuyama, 1966) and was latter supported by von der Saal (von der Saal et al., 1985) and Tesmer (Tesmer et al., 1996) .

1.4.2. Structural organization of GMP synthetases

A phylogenetic analysis of ~60 non-redundant protein sequences representing GMP synthetases from different organisms showed diversity in terms of length of the sequences. While the glutaminase and the synthetase domains in eukaryotic and prokaryotic GMP synthetases reside in one polypeptide (two-domain proteins), the domains in the archaeal enzymes with few exceptions, occur as separate polypeptides (two-subunit proteins). Based on this feature, GMP synthetases can be placed in three separate groups (1) Except plants, fungi and some protozoa, eukaryotic GMP synthetases represent the longest primary sequences (600-700 residues) among these enzymes due to the presence of ~100 amino acid insertion in the dimerisation domain (2) Enzymes from prokaryotes, plants and fungi with few inclusions from protozoa are ~520-580 residue in length. (3) Archaeal enzymes with few exceptions are two-subunit enzymes with the glutaminase and the acceptor domain sequence lengths being ~ 180 and ~310 amino acids, respectively.

Figures (1.1 and 1.2) show the unrooted and rooted phylogenetic trees for GMP synthetases that expectedly classified the closely related sequences in a single group. Interestingly, fungi and protozoa though eukaryotic, have diverged from mammals, plants and insect and lie closer to the bacterial counterparts, as supported by the bootstrap values in Fig 1.2.

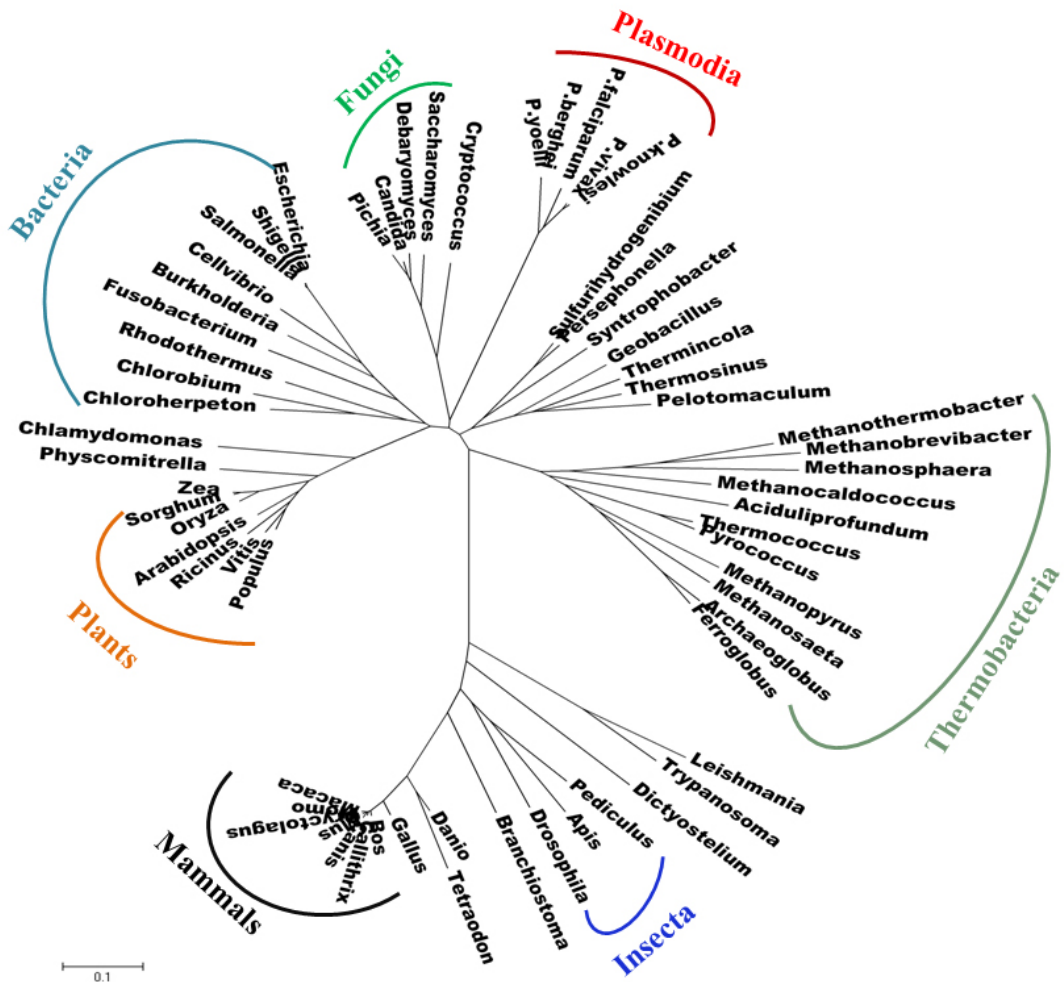


Figure 1.1. Phylogenetic tree of the GMP synthetase sequences representative of both two-domain (prokaryota and eukaryota) and two-subunit enzymes (archaea). The tree was generated by using MEGA software (Kumar et al., 2008; Tamura et al., 2007).

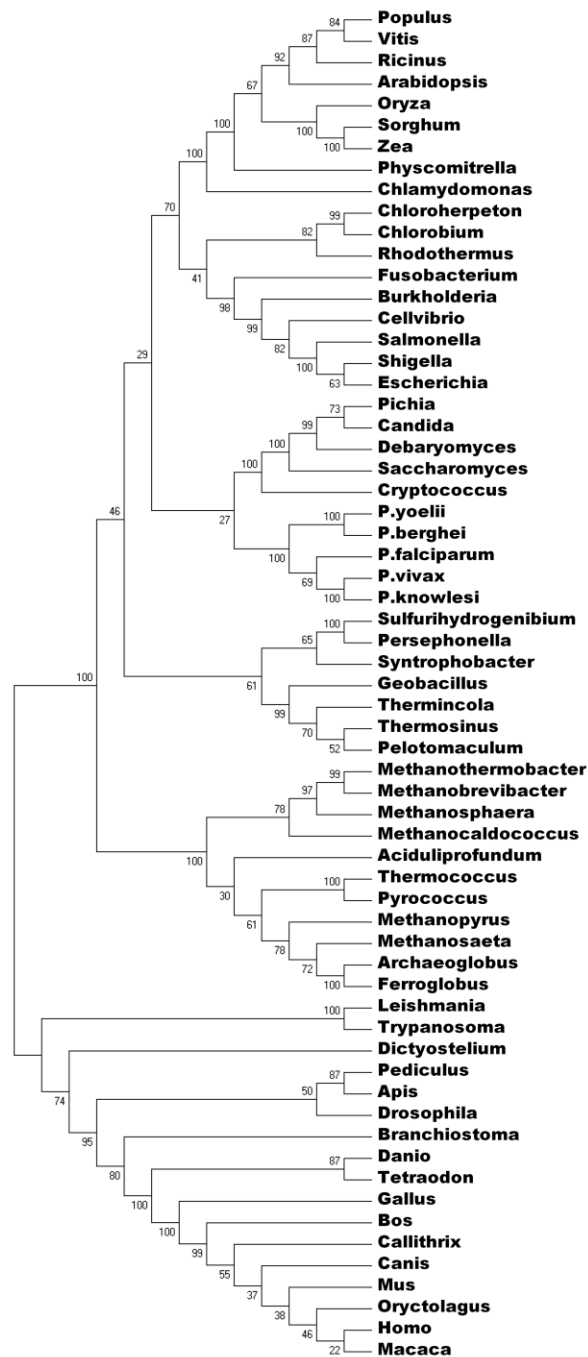


Figure 1.2. Phylogenetic tree of the GMP synthetase sequences representative of both two-domain (prokaryota and eukaryota) and two-subunit enzymes (archaea) provided

with bootstrap values. *The tree was generated by using MEGA software (Kumar et al., 2008; Tamura et al., 2007).*

Archaeal bacteria form a separate branch in the phylogenetic tree. Interestingly GMP synthetases from leishmania and trypanosoma, the two kinetoplastid protozoa, unlike their protozoan homologs, seem to be closer to that from mammalian and insect counterparts. These observations probably reflect on the different evolutionary rates with which these enzymes have evolved.

Tesmer et al reported crystal structure of *E. coli* GMP synthetase (PDB ID 1GPM) bound to AMP and PPi (Tesmer et al., 1996), nearly four decades after the establishment of its biochemical activity. At present, a PDB (<http://www.pdb.org/pdb>) query for GMP synthetase retrieves ten entries including the recently reported structure of *P. horikoshii* (PDB ID 3A4I), a two-subunit GMP synthetase. The unpublished PDB list of GMP synthetases among others holds structures of *T. thermophilus* unliganded (2YWC) and XMP bound (2YWC) and human (PDB ID 2VXO, 2VPI) enzymes. In GMP synthetases, both two-domain-type or two-subunit-type enzymes, N-terminal glutaminase domain or the glutaminase subunit catalyses the hydrolysis of glutamine to glutamate and ammonia, and the C-terminal domain or ATPase domain or ATPase subunit catalyses the ATP-XMP ligation (adenyl-XMP formation) followed by amination to form GMP.

Analysis of different crystal structures available in Protein Data Bank suggest that the core structural elements in GMP synthetases are highly recurring. The glutaminase domain generally contains α/β structures with the core mainly constructed of β -strands, with most of the conserved residues including the catalytic triad (Cys-His-Glu) residing in the core (Fig. 1.3). The catalytic triad has been proposed to be similar to that present in serine proteinases, as cysteine, a replacement for serine in the latter is surrounded by a general base (His) and a third residue glutamate, that can serve as a hydrogen bond acceptor from the imidazole ring. Glutaminase domain of GMP synthetases possess a nucleophile elbow containing the catalytic cysteine that is distinguished by disallowed backbone conformation and connects the top of a β -strand and the base of an α -helix. This feature in GMP synthetases is similar to that in α/β hydrolases where position of the nucleophile is stiffened by nucleophile elbow (Tesmer et al., 1996). Figure 1.3 presents a comparative view of GMPS glutaminase domains from different organisms,

highlighting the similarity in organization of different structural elements in the domain. The catalytic triad residues are conserved across these enzymes (Fig 1.4).

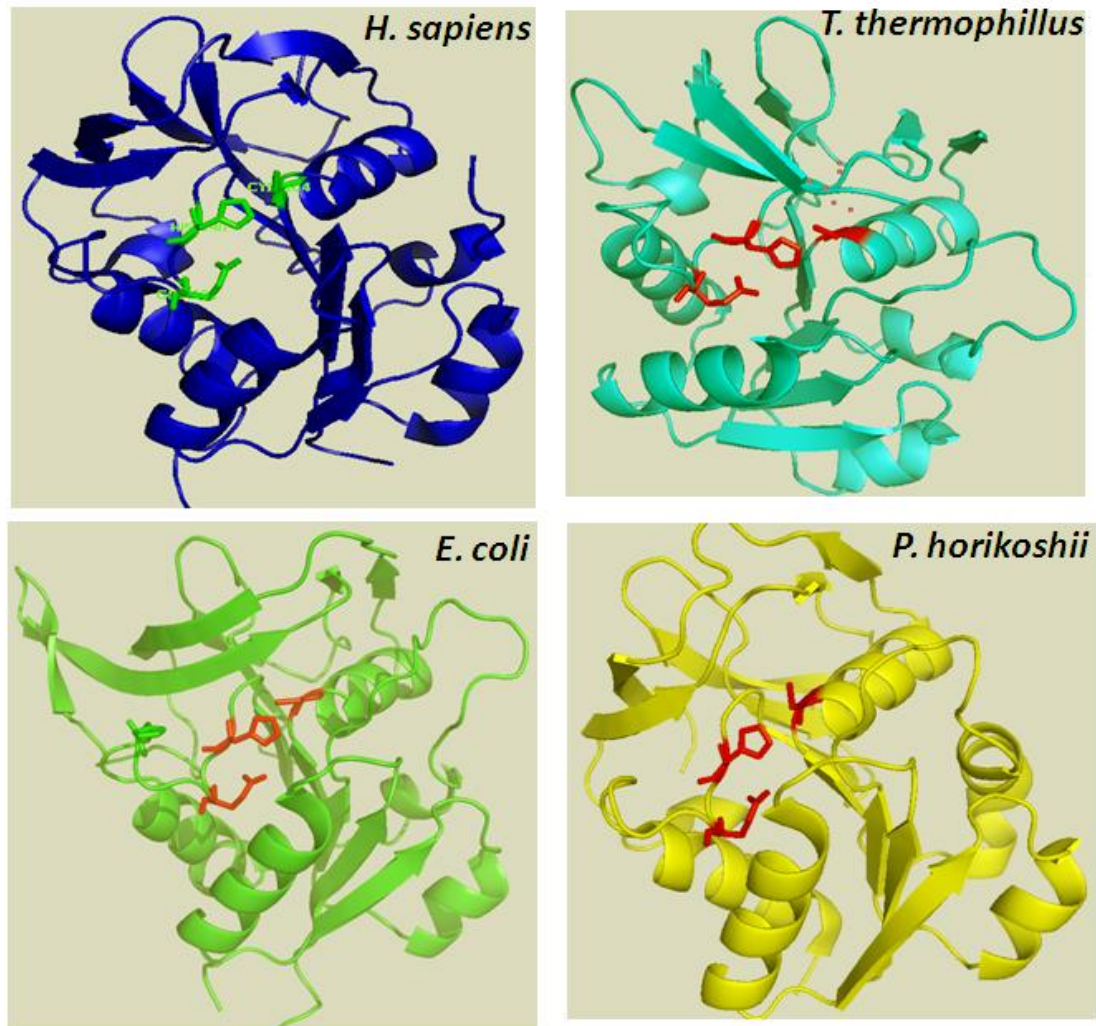


Figure 1.3. Comparison of the glutaminase domain of GMP synthetases from *H. sapiens*, *T. thermophilus*, *P. horikoshii* and *E. coli*, portraying their similarity in overall topology. The catalytic triad residues present in core of the domain are highlighted in red.

ShigellaMTENIHKH.....RILILDGFSQYTLVARRVRELGV
 EscherichiaMTENIHKH.....RILILDGFSQYTLVARRVRELGV
 SalmonellaMTENIHKH.....RILILDGFSQYTLVARRVRELGV
 BurkholderiaMHD.....KILILDGFSQYTLVARRVREANV
 SorghumMGSTAAASVLPVSAGTGQNLVILIDYGSQYTHLITRRVRQLGV
 ZeaMGSTAAASVLPVSAGSGENLVILIDYGSQYTHLITRRVRQLGV
 OryzaMGS.ASASSLPASAGFGENLVILIDYGSQYTHLITRRVRQLGV
 PopulusMDFKAVKS.....DLVLIDYGSQYTHLITRRIRSLNI
 VitisMDPENVKS.....NLVLIDYGSQYTHLITRRIRSLSV
 Methanothermobacter
 Methanobrevibacter
 Methanocaldococcus
 Thermococcus
 Pyrococcus
 PichiaMTAAEDVPIEVSKSPDITLVLDGFSQYSHLITRRRLREFNV
 DebaryomycesMVNPAVDPIEVSKVPDITLVLDGFSQYSHLITRRRLREFNV
 CandidaMSANIDVPIEVSKVPDITLVLDGFSQYSHLITRRRLREFNV
 SaccharomycesMAAGEQVSNMFDITLVLDGFSQYSHLITRRRLREFNI
 P.vivaxMEGGDYDKILVLPNFGSQYPHLIVKRLNNIKI
 P.knowlesiMEGGDYDKILVLPNFGSQYPHLIVKRLNNIKI
 P.faliciparumMEGEEYDKILVLPNFGSQYPHLIVKRLNNIKI
 P.yoeliiMEGDNYDMILVLPNFGSQYPHLIVKRLNNIKI
 P.bergheiMEGDNYDILVLPNFGSQYPHLIVKRLNNIKI
 Homo MAL.....CNG.....DSKLENAGGDLKDGHHHYEGAVVILDAGA QYGVKVIDRRVRELFPV
 Macaca MAL.....CNG.....DSKLENAGGDLKDGHHHYEGAVVILDAGA QYGVKVIDRRVREMPFV
 Mus MAL.....CNG.....DSKLENAGGDLKDGSHHYEGAVVILDAGA QYGVKVIDRRVRELFPV
 Canis MAL.....EISSIHPSAQKRLLENAGGDLKDGHHY.EGAVVILDAGA QYGVKVIDRRVRELFPV
 Bos MAL.....DSSSIHPSQKRLLENAGGDLKDGHHHNEGAVVILDAGA QYGVKVIDRRVRELFPV
 Oryctolagus MTLGIQYFSSNSYSDFSDHGLDLHGPERCAENAGGDLKDGCHHNEGAVVILDAGA QYGVKVIDRRVRELFPV

Shigella YCELWAWDVTEAQIRDPNPSGIILSGGPESTTEENSAPRAQ...YVFEAGVPVFGVYGMQTMAMQLGG
 Escherichia YCELWAWDVTEAQIRDPNPSGIILSGGPESTTEENSAPRAQ...YVFEAGVPVFGVYGMQTMAMQLGG
 Salmonella YCELWAWDVTEAQIRDPNPSGIILSGGPESTTEENSAPRALQ...YVFEAGVPVFGVYGMQTMAMQLGG
 Burkholderia YSEIHPPYDVDAFIRDPAKGVILSGGPPSSVTEEDTPRVFQ...AVPELGVVPLGICYGMQAMAQQLGG
 Sorghum LSCLCVSGTAPLASLEGLRPRAVILSGGPHSVHAPGAPAFPEGLDFAAAAGAHVLGVICYGMQLLVQSLGG
 Zea LSCLCVSGTAPLASLEGLRPRAVILSGGPHSVHAPGAPAFPEGLDFAAAAGAHVLGVICYGMQLLVQSLGG
 Oryza LSCLCVSGTAPLASLAGLRPRAVILSGGPHSVHAGSAPTFFPEGLDFAAAAGAHVLGVICYGMQLLVQSLGG
 Populus FSLCISGTSLETITSHNPKVILSGGPHSVHANSPTFFSGFVVEWAQKGGIFVLGVICYGLQLIVQRLGG
 Vitis FSLCISGTSLSKSIVDLKPRAVILSGGPHSVHSPNSPFPDGFVDYVESNGVFLGICYGLQLLVQRLGG
 Methanothermobacter
 Methanobrevibacter
 Methanocaldococcus
 Thermococcus
 Pyrococcus
 Pichia YAEMLPCTQKIADLT.WKPKGVILSGGPPSVYEDGSPHVDH...DVPKLNVPILGICYGMQEIANGK
 Debaryomyces YAEMLPCTQKISELT.WKPKGIILSGGPPSVYEDGSPHVDH...DIFKLNVPILGICYGMQELAWINGK
 Candida YAEMLPCTQKIAELS.WKPKGIILSGGPPSVYEDGSPHVDH...DIFKLNVPILGICYGMQELAWINGK
 Saccharomyces YAEMLPCTQKISELG.WTPKGVILSGGPPSVYEDGSPHVDH...AIFDLNVPILGICYGMQELAWINGK
 P.vivax FSETRDYGDVKEVEELNIKGVILSGGPHSVTEENAPHLKKEVLEFLEKKIPIFAICYGMQEIAVQMGNG
 P.knowlesi FSETRDYGIELKEVEELNIKGVILSGGPHSVTEENAPHLNKEVLEFLEKKIPIFAICYGMQEIAVQMGNG
 P.faliciparum FSETKDYGVELKDIKDMNIKGVILSGGPPSVTEAGSPHLKKEVLEFLEKKIPIFGICYGMQEIAPHMNG
 P.yoelii YSETKDYNDLKDIKNLNIKGVILSGGPHSVNAENGPHIKKEVLNYPENKIPIFGICYGMQEIAPHMNG
 P.berghei QSEIFPLETPAPFAIKEQGFRAIISGGPNSVYAEDAPWFDP...AIFTIGKPVLGICYGMQMMNKVFGG
 Homo QSEIFPLETPAPFAIKEQGFRAIISGGPNSVYAEDAPWFDP...AIFTIGKPVLGICYGMQMMNKVFGG
 Macaca QSEIFPLETPAPFAIKEQGFRAIISGGPNSVYAEDAPWFDP...AIFTIGKPVLGICYGMQMMNKVFGG
 Mus QSEIFPLETPAPFAIKEQGFRAIISGGPNSVYAEDAPWFDP...AIFTIGKPVLGICYGMQMMNKVFGG
 Canis QSEIFPLETPAPFAIKEQGFRAIISGGPNSVYAEDAPWFDP...AIFTIGKPVLGICYGMQMMNKVFGG
 Bos QSEIFPLETPAPFAIKEQGFRAIISGGPNSVYAEDAPWFDP...AIFTIGKPVLGICYGMQMMNKVFGG
 Oryctolagus QSEIFPLETPAPFAIKEQGFRAIISGGPNSVYAEDAPWFDP...AIFTIGKPVLGICYGMQMMNKVFGG

Shigella HVEASNEREPGYAQVEVVNDSALVRG.....IEDALTADGKPLLD
 Escherichia HVEASNEREPGYAQVEVVNDSALVRG.....IEDALTADGKPLLD
 Salmonella HVEASNEREPGYAQVEVLTDALVRG.....IEDSLTADGKPLLD
 Burkholderia KVDIGHLRPEFYAEVRARNHTSLLEG.....ISDPTTPEGHGMLK
 Sorghum AVVPGERQYEGKMDVQVTAASSALYG.....EAETGKRQ...T
 Zea AVVSGERQYEGKMDVEVTAASSALYG.....QAETGKRQ...T
 Oryza AVEAGEKQYEGKMEVEVTAASSALYG.....EVEGKRQ...T
 Populus QVDVGERQYEGRMEIEVEKN.LGVFG.....NKKVGDQK...V
 Vitis IVRVGERQYEGRMEIEVVRA.CGLFG.....SKEVGHKQ...T
 Methanothermobacter
 Methanobrevibacter
 Methanocaldococcus
 Thermococcus
 Pyrococcus
 Pichia GVARGDKREYGPATLNVDKSKALFA.....DVDH.....SQ
 Debaryomyces GVARGDKREYGPATLNVEDSSCSLFFK.....GVDH.....SQ
 Candida GVARGDKREYGPATLNVEDPECALFFK.....GVDH.....SQ
 Saccharomyces QVGRGDKREYGPATLNKVIDDSSNSLFFK.....GMND.....ST
 P.vivax EVKKSNSYEGCTDVNIITSKNG.....GEEKYKNYKLVLDGSGKSKCLFDGKNAEKST
 P.knowlesi EVNKSNSYEGCTDVNIITSKNG.....SEEEKYKNYKLVLDGSGKSKCLLDGKIDPEKST
 P.faliciparum EVKKSNTSEYEGCTDVNILDNDNINNIITYCRNFGDSSSAMDLYSNYKLMN.....ETCCLEPNIKS.DITT
 P.yoelii KVGKNSNSYEGSTEVTLISNDYK.....NNESYKNYKLE...KDSNCLLPDDIKNTNNMN
 P.berghei QVGRGDKREYGPATLNKVIDDSSNSLFFK.....DNELYKNYKLE...KDSNCLLPDDIKNTNNMN
 Homo TVHKSNSYEGCTDVNIITSKNG.....LQKEEV
 Macaca TVHKSNSYEGCTDVNIITSKNG.....LQKEEV
 Mus TVHKSNSYEGCTDVNIITSKNG.....LQKEEI
 Canis TVHKSNSYEGCTDVNIITSKNG.....LQKEEI
 Bos TVHKSNSYEGCTDVNIITSKNG.....LQKEEI
 Oryctolagus TVHKSNSYEGCTDVNIITSKNG.....LQKEEI

		H E
Shigella	VWMSGDKVTAIPSDPVTVAESTESCPFAIMANEKRFYGVQFHPPEVTHTRQGMHMLERFVRDQCCEALW	
Escherichia	VWMSGDKVTAIPSDPVTVAESTESCPFAIMANEKRFYGVQFHPPEVTHTRQGMHMLERFVRDQCCEALW	
Salmonella	VWMSGDKVTAIPSDPVTVAESTESCPFAIMANEKRFYGVQFHPPEVTHTRQGMHMLERFVRDQCCEALW	
Burkholderia	VWMSGDKVLEMPGPFALMASTESCPIAAMADEQRFPYGLQYHPPEVTHTRQGRAMLERFVLQICGAKADW	
Sorghum	VWMSGHDEVVTLPPQGPFEVVARVQGVAAIIEYREKRFPYGLQYHPPEVTHSAQGMETLRRPLPDCVGIKADW	
Zea	VWMSGHDEVVRLPEGPEVVARVQGVAAIENRENRFYGLQYHPPEVTHSAQGMETLRRPLPDCVGIKADW	
Oryza	VWMSGHDEVVRLPEGPEVVARVQGVAAAVENREKRFPYGLQYHPPEVTHSAQGMETLRRPLPDCVGIKADW	
Populus	VWMSGHDETVKLPYGPFEVVARVQGVAAAVENREMRFPYGLQYHPPEVTHSPEGMDLTRYPLPDCVGSVSGW	
Vitis	VWMSGHDEAAELPEGPEVVARVQGVAAAVENRERFPYGLQYHPPEVTHSPEGMDLTRYPLPDCVCRVDAGW	
MethanothermobacterMMLML	
MethanobrevibacterML	
MethanocaldococcusMF	
ThermococcusMVMP	
PyrococcusM	
Pichia	VWMSGDKLHALPTGFNIVATSDNSPYAAVANEDES IYGIQFHPPEVTHTRQGRITLKNPAVNICASTNW	
Debaryomyces	VWMSGDKLHALPTGFNIVATSDNSPYAAVANEDES IYGIQFHPPEVTHTRQGRITLKNPAVNICASTNW	
Candida	VWMSGDKLHALPTGFNIVATSDNSPYAAVANEDES IYGIQFHPPEVTHTRQGRITLKNPAVNICASTNW	
Saccharomyces	VWMSGDKLHALPTGFNIVATSDNSPYAAVANEDES IYGIQFHPPEVTHTRQGRITLKNPAVNICASTNW	
P.vivax	VWNNHTDEVTKIPDNFVLVNSDDCLICAMYNNEHN IYGVQYHPPEVTHSVDGDMQFYNPAYNICCKTKKF	
P.knowlesi	VWNNHTDEVTKIPDNFVLVNSDDCLICAMYNNEHN IYGVQYHPPEVTHSVDGDMQFYNPAYNICCKTKKF	
P.falciparum	VWNNHTDEVTKIPDNFVLVNSDDCLICAMYNNEHN IYGVQYHPPEVTHSVDGDMQFYNPAYNICCKTKKF	
P.yoelii	VWNNHTDEVTKIPDNFVLVNSDDCLICAMYNNEHN IYGVQYHPPEVTHSVDGDMQFYNPAYNICCKTKKF	
P.berghei	VWNNHTDEVTKIPDNFVLVNSDDCLICAMYNNEHN IYGVQYHPPEVTHSVDGDMQFYNPAYNICCKTKKF	
Homo	VLLTHGDSVDKVADGPKVVARSGN.IVAGIANESKLYGAQFHPPEVGLTENGKVLKKNPLYDIAGCSGTF	
Macaca	VLLTHGDSVDKVADGPKVVARSGN.IVAGIANESKLYGAQFHPPEVGLTENGKVLKKNPLYDIAGCSGTF	
Mus	VLLTHGDSVDKVADGPKVVARSGN.IVAGIANESKLYGAQFHPPEVGLTENGKVLKKNPLYDIAGCSGTF	
Canis	VLLTHGDSVDKVADGPKVVARSGN.IVAGIANESKLYGAQFHPPEVGLTENGKVLKKNPLYDIAGCSGTF	
Bos	VLLTHGDSVDKVADGPKVVARSGN.IVAGIANESKLYGAQFHPPEVGLTENGKVLKKNPLYDIAGCSGTF	
Oryctolagus	VLLTHGDSVDKVADGPKVVARSGN.IVAGIANESKLYGAQFHPPEVGLTENGKVLKKNPLYDIAGCSGTF	

		P-loop
Shigella	TPAKIIDDAVARIREQVG.DDKVILDSGGDDESVTAMLLHRAIG.KNLTCPVFDNGLIRLNLAEQVLDLM	
Escherichia	TPAKIIDDAVARIREQVG.DDKVILDSGGDDESVTAMLLHRAIG.KNLTCPVFDNGLIRLNLAEQVLDLM	
Salmonella	TPAKIIDDAVARIREQVG.DDKVILDSGGDDESVTAMLLHRAIG.KNLTCPVFDNGLIRLNLAEQVMDM	
Burkholderia	EMOHYIDEAVAKIREQVG.NEHVILDSGGDDESVAAALLHRAIG.DQLTCTVFDNGLIRLNLAEQVMAL	
Sorghum	KMQDVLDEEIKTIQSTVGPDEHVICALSGGDDESVAAATLVHKAIG.DRLHCFVFDNGLIRYKRRERMMTT	
Zea	KMQDVLDEEIKTIQSTVGPDEHVICALSGGDDESVAAATLVHKAIG.DRLHCFVFDNGLIRYKRRERMMTT	
Oryza	KMQDVLDEEIKTIQSMVGPDEHVICALSGGDDESVAAATLVHKAIG.DRLHCFVFDNGLIRYKRRERMMT	
Populus	NMENVLDEEIRVINDAVGPEEHVICALSGGDDESVAAATLVHKAIG.DRLHCFVFDNGLIRYKRRERVAET	
Vitis	NMEDVLNEEIKLIKGMVAPDDHVICALSGGDDESVAAATLVHKAIG.DRLHCFVFDNGLIRYKRRERMMET	
Methanothermobacter	NPEDPPIEEAVEEIRSTVG.NEKAIILASGGDDESVAVSLAGRAIG.DNLTAVFVNHGLIREGAEARVVKET	
Methanobrevibacter	EPKEFISDAIAKIKKEEIG.DEKTIILASGGDDESVCSVLTAQAIG.DNLTAVFVNHGLIREGAEARVCSV	
Methanocaldococcus	DPKPFIDEAVEEIKQOIS.DRKAIILASGGDDESVAAVLAHKAIG.DKLTAVPVDTGLMRKGREREVEKKT	
Thermococcus	MMKDFIREKVEEIRETVG.DSKAIILASGGDDESVAAVLAHKAIG.DRLHAVPVNTGPNRKGPEFPVVKET	
Pyrococcus	DMGRPVEEKVREIRETVG.DSKAIILASGGDDESVAAVLAHKAIG.DRLHAVPVNTGPNRKGPEFPVVKET	
Pichia	TMENFIDTEIARIQKLVGPTAEVIGAVSGGDDESVGAKINKEAIG.DRPHALVFDNGLIRKNTTSEVYKKT	
Debaryomyces	TMENFIDTEIARIQKLVGPTAEVIGAVSGGDDESVGAKINKEAIG.DRPHALVFDNGLIRKNTTSEVYKKT	
Candida	SMENFIDTEIARIQKLVGPTAEVIGAVSGGDDESVGAKINKEAIG.DRPHALVFDNGLIRKNTTSEVYKKT	
Saccharomyces	TMENFIDTEIARIQKLVGPTAEVIGAVSGGDDESVGAKINKEAIG.DRPHALVFDNGLIRKNTTSEVYKKT	
P.vivax	DPFIRYHEIELNNIKKYAK.DHYVIAAMSGGDDESVAAAFTHKIFK.ERFYGIFIDNGLIRKNGEKKVYSP	
P.knowlesi	DPFIRYHEIELNNIKKYAK.DHYVIAAMSGGDDESVAAAFTHKIFK.ERFYGIFIDNGLIRKNGEKKVYSP	
P.falciparum	DPFIRYHEIELNNIKKYAK.DHYVIAAMSGGDDESVAAAFTHKIFK.ERFPYGIFIDNGLIRKNGEKKVYTF	
P.yoelii	DPFIRYHEIELNNIKKYAK.DHYVIAAMSGGDDESVAAAFTHKIFK.ERFYGIFIDNGLIRKNGEKKVYTF	
P.berghei	DPFIRYHEIELNNIKKYAK.DHYVIAAMSGGDDESVAAAFTHKIFK.ERFYGIFIDNGLIRKNGEKKVYTF	
Homo	TVQNHRELECIIRIKERVG.TSKVLLVLSGGDDESVCTALLNRALNQDQVIAFHIDNGPNEKRSSQSVBEA	
Macaca	TVQNHRELECIIRIKERVG.TSKVLLVLSGGDDESVCTALLNRALNQDQVIAFHIDNGPNEKRSSQSVBEA	
Mus	TVQNHRELECIIRIKERVG.TSKVLLVLSGGDDESVCTALLNRALNQDQVIAFHIDNGPNEKRSSQSVBEA	
Canis	TVQNHRELECIIRIKERVG.TSKVLLVLSGGDDESVCTALLNRALNQDQVIAFHIDNGPNEKRSSQSVBEA	
Bos	TVQNHRELECIIRIKERVG.TSKVLLVLSGGDDESVCTALLNRALNQDQVIAFHIDNGPNEKRSSQSVBEA	
Oryctolagus	TVQNHRELECIIRIKERVG.TSKVLLVLSGGDDESVCTALLNRALNQDQVIAFHIDNGPNEKRSSQSVBEA	

Shigella	FGDHPG.LNIVHVPFAEDRFSLAAGENDPEPKRKITGRVFEVFDDEALK	
Escherichia	FGDHPG.LNIVHVPFAEDRFSLAAGENDPEPKRKITGRVFEVFDDEALK	
Salmonella	FGDHPG.LNIVHVPFAEDRFSLAAGENDPEPKRKITGRVFEVFDDEALK	
Burkholderia	PADHLG.VKVIHVDASERFLAAGVTDPEPKRKITGRVFEVFDDEALK	
Sorghum	FESDLH.LPVTCVDAASEFLAAGVVDPEPKRKITGRVFAVDDFAHK	
Zea	FESDLH.LPVTCVDAASEFLAAGVVDPEPKRKITGRVFAVDDFAHK	
Oryza	FESDLH.LPVTCVDAASEFLAAGVVDPEPKRKITGRVFAVDDFAHK	
Populus	FESDLH.LPVTCVDAASEFLAAGVVDPEPKRKITGRVFAVDDFAHK	
Vitis	FERDLH.LPVTCVDAATNCFSLAAGVVDPEPKRKITGRVFAVDDFAHK	
Methanothermobacter	FSERL...NPKYIDASEEFLAAGVVDPEPKRKITGRVFEVFRVAEK	
Methanobrevibacter	FEERL...NPKYIDASEEFLAAGVVDPEPKRKITGRVFEVFRVAEK	
Methanocaldococcus	PRDKLG.LNLIHVDKDRFLNALKGVTDPEPKRKITGRVFEVFEIAED	
Thermococcus	FRDEFG.LNLHYVDASERFFKALKGVTDPEPKRKITGRVFEVFEIAEK	
Pyrococcus	FRDEFG.MNLHYVDQDRFFSALKGVTDPEPKRKITGRVFEVFEIAEK	
Pichia	LTEGLG.INLTVVDASDFLGLKGVTDPEPKRKITGRVFEVFEIAEK	
Debaryomyces	LTEGLG.INLTVVDATDFLGLKGVTDPEPKRKITGRVFEVFEIAEK	
Candida	LDEGLG.INLTVVDAGDFLGLKGVTDPEPKRKITGRVFEVFEIAEK	
Saccharomyces	LKGLFPDMNLTKIDASEIFLNLKGVTDPEPKRKITGRVFEVFEIAEK	
P.vivax	LKSTFPDMNLTKIDASEIFLNLKGVTDPEPKRKITGRVFEVFEIAEK	
P.knowlesi	LKGLFPDMNLTKIDASEIFLNLKGVTDPEPKRKITGRVFEVFEIAEK	
P.falciparum	LKSTFPDMNLTKIDASEIFLNLKGVTDPEPKRKITGRVFEVFEIAEK	
P.yoelii	LKSTFPDMNLTKIDASEIFLNLKGVTDPEPKRKITGRVFEVFEIAEK	
P.berghei	LKSTFPDMNLTKIDASEIFLNLKGVTDPEPKRKITGRVFEVFEIAEK	
Homo	LKKLGL.IQVKVINAAHSEYNGTTLPISEEDRTPPKRISKTLMNMTSPPEPKRITIGDTFKIANEVIIG	
Macaca	LKKLGL.IQVKVINAAHSEYNGTTLPISEEDRTPPKRISKTLMNMTSPPEPKRITIGDTFKIANEVIIG	
Mus	LKKLGL.IQVKVINAAHSEYNGTTLPISEEDRTPPKRISKTLMNMTSPPEPKRITIGDTFKIANEVIIG	
Canis	LKKLGL.IQVKVINAAHSEYNGTTLPISEEDRTPPKRISKTLMNMTSPPEPKRITIGDTFKIANEVIIG	
Bos	LRKLG.IQVKVINAAHSEYNGTTLPISEEDRTPPKRISKTLMNMTSPPEPKRITIGDTFKIANEVIIG	
Oryctolagus	LKKLGL.IQVKVINAAHSEYNGTTLPISEEDRTPPKRISKTLMNMTSPPEPKRITIGDTFKIANEVIIG	

Shigella LEDVK...WLAQGTIYFDVIRISAA...SATGKAHVIRSHNVGGPKEMK..MGLIPLKLELFKDEVR
 Escherichia LEDVK...WLAQGTIYFDVIRISAA...SATGKAHVIRSHNVGGPKEMK..MGLIPLKLELFKDEVR
 Salmonella LEDVK...WLAQGTIYFDVIRISAA...SATGKAHVIRSHNVGGPKEMK..MGLIPLKLELFKDEVR
 Burkholderia LTDAK...WLAQGTIYFDVIRISAG...KGGKAAQTIRSHNVGGPKETLN..LKLIPLKLELFKDEVR
 Sorghum LEQKIGKRPEYLVQGTLYFDVIRISCPPPGSGRTHSHVIRSHNVGGPKDMK..LKLIPLKLELFKDEVR
 Zea LEQKIGKRPEYLVQGTLYFDVIRISCPPPGSGRTHSHVIRSHNVGGPKDMK..LKLIPLKLELFKDEVR
 Oryza LEQKIGKRPEYLVQGTLYFDVIRISCPPPGSGRTHSHVIRSHNVGGPKDMK..LKLIPLKLELFKDEVR
 Populus LEQKIGKRPEYLVQGTLYFDVIRISCPPPGSGRTHSHVIRSHNVGGPKDMK..LKLIPLKLELFKDEVR
 Vitis LEHKFGKPPVYLVQGTLYFDVIRISCPPPGSGRTHSHVIRSHNVGGPKDMK..LKLIPLKLELFKDEVR
 Methanothermobacter IGARY...LVQGTIADWIESEG...QIRSHNVVA..PHGLV..LEIVEPIRELYKDEVR
 Methanobrevibacter VDAKY...LVQGTIADWIESEG...EIRTHNVMA..PSGMV..FKVVEPVRDLYKDEVR
 Methanocaldococcus IKAEV...LVQGTIADWIEFQG...KIRSHNVVA..PHGMV..LEVVEPIRELYKDEVR
 Thermococcus INADP...LIQGTIADWIESEG...KIRSHNVGGPERLN..LKLIPLKLELFKDEVR
 Pyrococcus IGAEY...LIQGTIADWIEFQG...KIRSHNVGGPEKLN..LKLIPLKLELFKDEVR
 Pichia IKPAHQQEIEYLLQGTLYFDVIRISIS...FKGPSQTIKTHNVGGLEDMMK..LKLIPLKLELFKDEVR
 Debaryomyces IKPASGQEIEYLLQGTLYFDVIRISIS...FKGPSQTIKTHNVGGLEDMMK..LKLIPLKLELFKDEVR
 Candida IKPRDGSEIEYLLQGTLYFDVIRISIS...FKGPSQTIKTHNVGGLEDMMK..LKLIPLKLELFKDEVR
 Saccharomyces IKPRDGSEIEYLLQGTLYFDVIRISIS...FKGPSQTIKTHNVGGLEDMMK..LKLIPLKLELFKDEVR
 P.vivax INIDIEKT..YLLQGTLYFDVIRISKCS...KRLSDTIKTHNVGGPENLTK..FKLFEPPKLYLFKDDVK
 P.knowlesi INIDIEKT..YLLQGTLYFDVIRISKCS...KRLSDTIKTHNVGGPENLTK..FKLFEPPKLYLFKDDVK
 P.falciparum IDIDINKT..FLLQGTLYFDVIRISKCS...KRLSDTIKTHNVGGPENLTK..FKLFEPPKLYLFKDDVK
 P.yoelii MDIDIEKT..YLLQGTLYFDVIRISKCS...KRLSDTIKTHNVGGPENLTK..FKLFEPPKLYLFKDDVK
 P.berghei MDIDIEKT..YLLQGTLYFDVIRISKCS...KRLSDTIKTHNVGGPENLTK..FKLFEPPKLYLFKDDVK
 Homo MNLKPEE..VFLAQGTLRPDLEISAS..LVASGKAELIKTHNDTEIRKLRREGKVIPEPLKDFHKDEVR
 Macaca MNLKPEE..VFLAQGTLRPDLEISAS..LVASGKAELIKTHNDTEIRKLRREGKVIPEPLKDFHKDEVR
 Mus MNLKPEE..VFLAQGTLRPDLEISAS..LVASGKAELIKTHNDTEIRKLRREGKVIPEPLKDFHKDEVR
 Canis MNLKPEE..VFLAQGTLRPDLEISAS..LVASGKAELIKTHNDTEIRKLRREGKVIPEPLKDFHKDEVR
 Bos MNLKPEE..VFLAQGTLRPDLEISAS..LVASGKAELIKTHNDTEIRKLRREGKVIPEPLKDFHKDEVR
 Oryctolagus MNLKPEE..VFLAQGTLRPDLEISAS..LIASGKAELIKTHNDTEIRKLRREGKVIPEPLKDFHKDEVR

Shigella KIGLELGLPYDMLYHHPFPPGPPGLGVRVILG...EVKK.EYCDLLRRADAIF
 Escherichia KIGLELGLPYDMLYHHPFPPGPPGLGVRVILG...EVKK.EYCDLLRRADAIF
 Salmonella KIGLELGLPYDMLYHHPFPPGPPGLGVRVILG...EVKK.EYCDLLRRADAIF
 Burkholderia ELGVKLGGLHSMVYRHHPFPPGPPGLGVRVILG...EVKR.DPADLLRRADAIF
 Sorghum KLGSILNVVDSFLKRHPFPPGPPGLAVRVILG...DVTQGNALVLRQVDEIF
 Zea KLGSILNVVDSFLKRHPFPPGPPGLAVRVILG...DVTQGNALVLRQVDEIF
 Oryza KLGSILNVVDSFLKRHPFPPGPPGLAVRVILG...DVTQGNALVLRQVDEIF
 Populus QLGRILNVVDAFLKRHPFPPGPPGLAVRVILG...DVTQGNALVLRQVDEIF
 Vitis ELGRILNVVDAFLKRHPFPPGPPGLAVRVILG...DVTQGNALVLRQVDEIF
 Methanothermobacter EIGLELGLPREMIQRQPPFPPGPPGLAVRVILG...EITR.EKIEICRRANAIV
 Methanobrevibacter LVGTTELGLPDSIVQRQPPFPPGPPGLAVRVILG...DLTR.ENLAVCRAADAIV
 Methanocaldococcus LLAKEGLGLPDSIVYRQPPFPPGPPGLAVRVILG...EVTB.EKLNICRANAIV
 Thermococcus ELAKELGLPEKIYNRMPFPPGPPGLAVRVILG...EVTB.EKIAIVREANAIV
 Pyrococcus ELAKFLGLPEKIYNRMPFPPGPPGLAVRVILG...EVTB.EKIRIVREANAIV
 Pichia HLGELGLVPHDLVWRHPFPPGPPGLAIRVILG...EVTB.EKIRIVREANAIV
 Debaryomyces HLGELGLVPHDLVWRHPFPPGPPGLAIRVILG...EVTB.EKIRIVREANAIV
 Candida HLGELGLVPHDLVWRHPFPPGPPGLAIRVILG...EVTB.EKIRIVREANAIV
 Saccharomyces HLGELGLVPHDLVWRHPFPPGPPGLAIRVILG...EVTB.EKIRIVREANAIV
 P.vivax KLSQELNLDDEITNRHPFPPGPPGLAIRVILG...EIDK.HKLSILREVDIF
 P.knowlesi KLSQELNLDDEITNRHPFPPGPPGLAIRVILG...EIDK.HKLSILREVDIF
 P.falciparum TLSRRLNLDDEITNRHPFPPGPPGLAIRVILG...EINK.HKLNILREVDIF
 P.yoelii KLSQELNLDDEITNRHPFPPGPPGLAIRVILG...EIDK.HKLSILREVDIF
 P.berghei KLSQELNLDDEITNRHPFPPGPPGLAIRVILG...EIDK.HKLSILREVDIF
 Homo ILGRELGLPEELVSRHPFPPGPPGLAIRVILG...SASVKKPHTLLQRVKACT
 Macaca ILGRELGLPEELVSRHPFPPGPPGLAIRVILG...SASVKKPHTLLQRVKACT
 Mus ILGRELGLPEELVSRHPFPPGPPGLAIRVILG...SASVKKPHTLLQRVKACT
 Canis ILGRELGLPEELVSRHPFPPGPPGLAIRVILG...SASVKKPHTLLQRVKACT
 Bos ILGRELGLPEELVSRHPFPPGPPGLAIRVILG...SASVKKPHTLLQRVKACT
 Oryctolagus ILGRELGLPEELVSRHPFPPGPPGLAIRVILG...SASVKKPHTLLQRVKACT

Shigella IEELR...KADLYDKVSCAPTVPFLVRSVGVMDGRKKYDWWV...
 Escherichia IEELR...KADLYDKVSCAPTVPFLVRSVGVMDGRKKYDWWV...
 Salmonella IEELR...KADLYDKVSCAPTVPFLVRSVGVMDGRKKYDWWV...
 Burkholderia IETLRNTIDKETGKSWYDLTSCAPAVFLVKSQVGVMDGRKTYEYVV...
 Sorghum VQAIK...DAGLYDKIWCAPAVFLVQTVGVQGDQTHSNV...
 Zea VQAIK...DAGLYDKIWCAPAVFLVQTVGVQGDQTHSNV...
 Oryza VQAIK...DAGLYDIWCAPAVFLVQTVGVQGDQTHSNV...
 Populus IQSIK...DAGLYDSIWCAPAVFLVRSVGVQGDQTHSHVV...
 Vitis IQSIK...DAGLYDSIWCAPAVFLVRSVGVQGDQTHSHVV...
 Methanothermobacter BEEVV...ESGLHESLWYFAVLTDMVTGVKQDVEDPGYLV...
 Methanobrevibacter REEVE...KAGLDKELWYFAVLTDMVTGVKQDVEDPGYLV...
 Methanocaldococcus BEEVE...KANLDKDLWYFAVVLDCATGVKQDVEDPYNWIV...
 Thermococcus BEEVE...KAGLRP..WQAPAVLLGVKTVGVQGDTRAYKETI...
 Pyrococcus BEEVE...RAGLRP..WQAPAVLLGVKTVGVQGDTRAYKETI...
 Pichia IEAIEK...AAGLYKQISQAPAAALLVKSQVGVMDQRTYEQVI...
 Debaryomyces IEAIEK...KAGLYKDISQAPAAALLVKSQVGVMDQRTYEQVI...
 Candida IEAIEK...KAGLYRQISQAPAAALLVKSQVGVMDQRTYEQVI...
 Saccharomyces IEAIEK...KAGLYNQISQAPAAALLVKSQVGVMDQRTYEQVI...
 P.vivax INDLK...AYNLYNDISQAPAVLLVTKSVGVSGDARSYDYVC...
 P.knowlesi INDLK...AYNLYNDISQAPAVLLVTKSVGVSGDARSYDYVC...
 P.falciparum INSLK...QYGLYNQISQAPAVLLVTKSVGVSGDARSYDYVC...
 P.yoelii INSLK...EYNLYDDIGQAPAVIFPSKSVGVSGDARSYDHC...
 P.berghei INSLK...EYNLYDDIGQAPAVIFPSKSVGVSGDARSYDHC...
 Homo TEEDQE...KLMQITSLHSLNAFLLLIKTVGVQGDQRSYSYVC...
 Macaca TEEDQE...KLMQITSLHSLNAFLLLIKTVGVQGDQRSYSYVC...
 Mus TEEDQE...KLMQITSLHSLNAFLLLIKTVGVQGDQRSYSYVC...
 Canis TEEDQE...KLMQITSLHSLNAFLLLIKTVGVQGDQRSYSYVC...
 Bos TEEDQE...KLMQITSLHSLNAFLLLIKTVGVQGDQRSYSYVC...
 Oryctolagus TEEDQE...KLMQITSLHSLNAFLLLIKTVGVQGDQRSYSYVC...

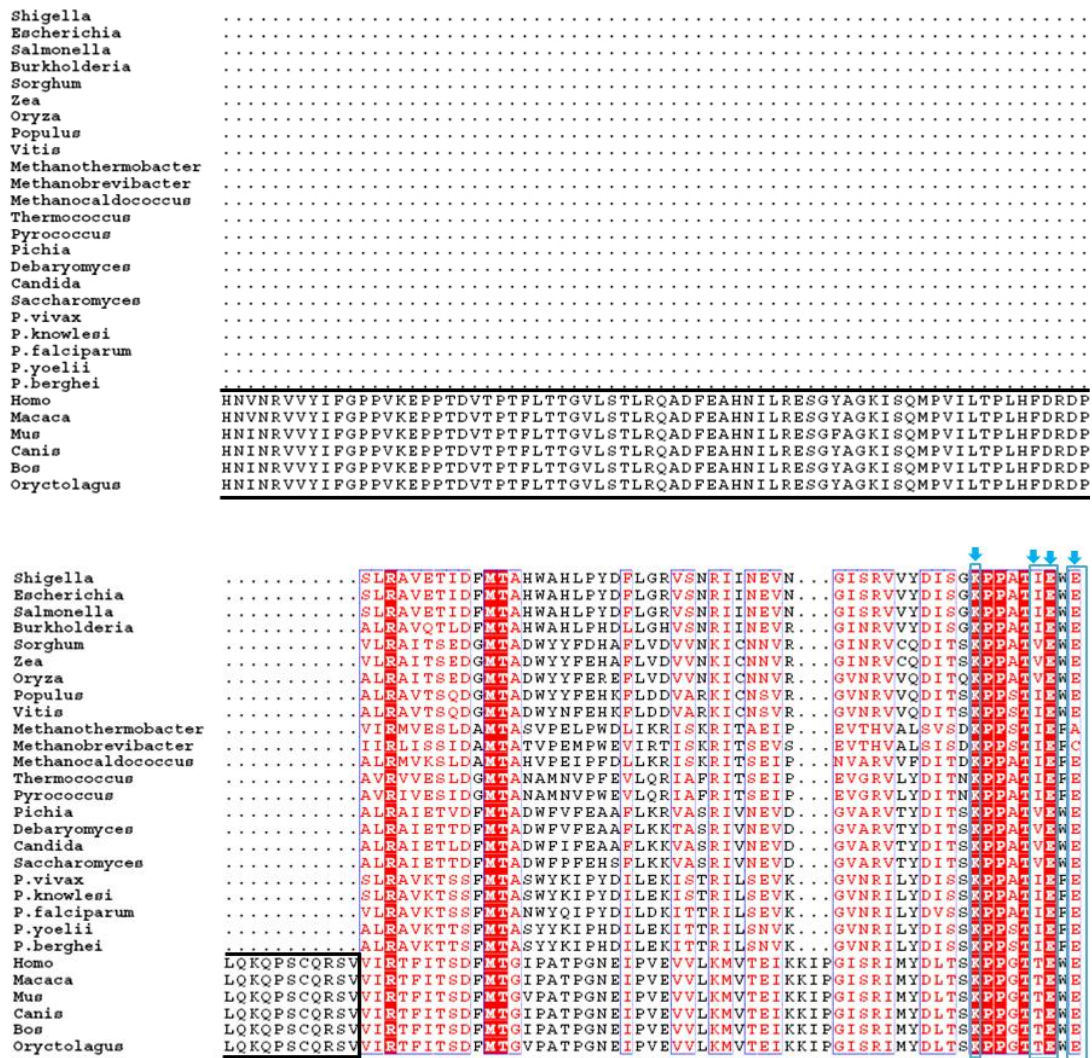


Figure 1.4. Sequence alignment of GMP synthetases, representative of prokaryotes, eukaryotes and archaea, was generated using Clustal W (Higgins D. et al., 1994) and modified by ESript 2.2 (Gouet et al., 2003). Catalytic triad residues (Cys-His-Glu) are boxed in pink. Green bar represents the residues present in the P-loop. Putative residues involved in ATP binding are solid boxed and arrow pointed in dark blue. XMP interacting residues are solid boxed and arrow pointed in light blue. The region solid boxed in black represent the dimerisation domain insertion (>100 residues) in some eukaryotes. The red shaded regions represent the residues that are identical across the GMP synthetases.

The ATPase domain in GMP synthetases is generally larger in size than the GAT domain and resembles dehydrogenases in having a typical dinucleotide binding fold characterized by sandwiching of five-strand β -sheet between α -helical layers. P-loop, a characteristic motif of ATP utilizing proteins is also conserved across the GMP synthetases (SGGVDSS/T, green marked in Fig. 1.4). Much of the information for mode of ATP binding was gained from the structural analysis of EcGMPS. Recent structures of HsGMPS and TtGMPS bound to XMP (unpublished) have highlighted the residues that interact with the bound nucleotide. Recently, a report on *P. horikoshii* GMPS (Maruoka et al., 2010) has predicted a list of residues in the ATPase domain that showed contacts with ATP (arrowed dark blue boxes in Fig.1.4) and XMP (arrowed light blue boxes in Fig.1.4). A dimerisation domain lies adjacent to the ATPase domain that contains many conserved residues and the α/β structural (Figure 1.5) motifs, forming a hydrophobic interface for inter-subunit interaction. Eukaryotic GMP synthetases, except plants, fungi and some protozoa, contain a large conserved insertion (>100 residues) in the dimerisation domain (boxed in dark, Fig. 1.4) that probably prevents them from dimerisation and also evokes the possibility of their non-enzymatic role in these organisms. Already such a role for GMP synthetases from *Drosophila* and a human cell line has been demonstrated and an account of this is provided in next section. Apart from the presence of large dimerisation domain insertion, two more conserved insertions are also seen in the above mentioned enzymes. It will be interesting to investigate whether the non-enzymatic roles of DmGMPS and HsGMPS specifically lie with the extra amino acid stretches present in the enzymes. A structural view of the ATPase domains from different organisms is given in Fig.1.5. The presence of large number of conserved residues across GMP synthetases (Fig. 1.4.) agrees well with the structural similarity observed in these enzymes.

1.4.3. Moonlighting or non-catalytic functions of GMP synthetases

Involvement of metabolic enzymes in processes independent of their enzymatic function has been known (Jeffery, 2009; Moore, 2004), with very recent addition of GMP synthetase to the list. Pegram *et al* first reported MLL-GMPS fusion in person with metastatic neuroblastoma (Pegram et al., 2000).

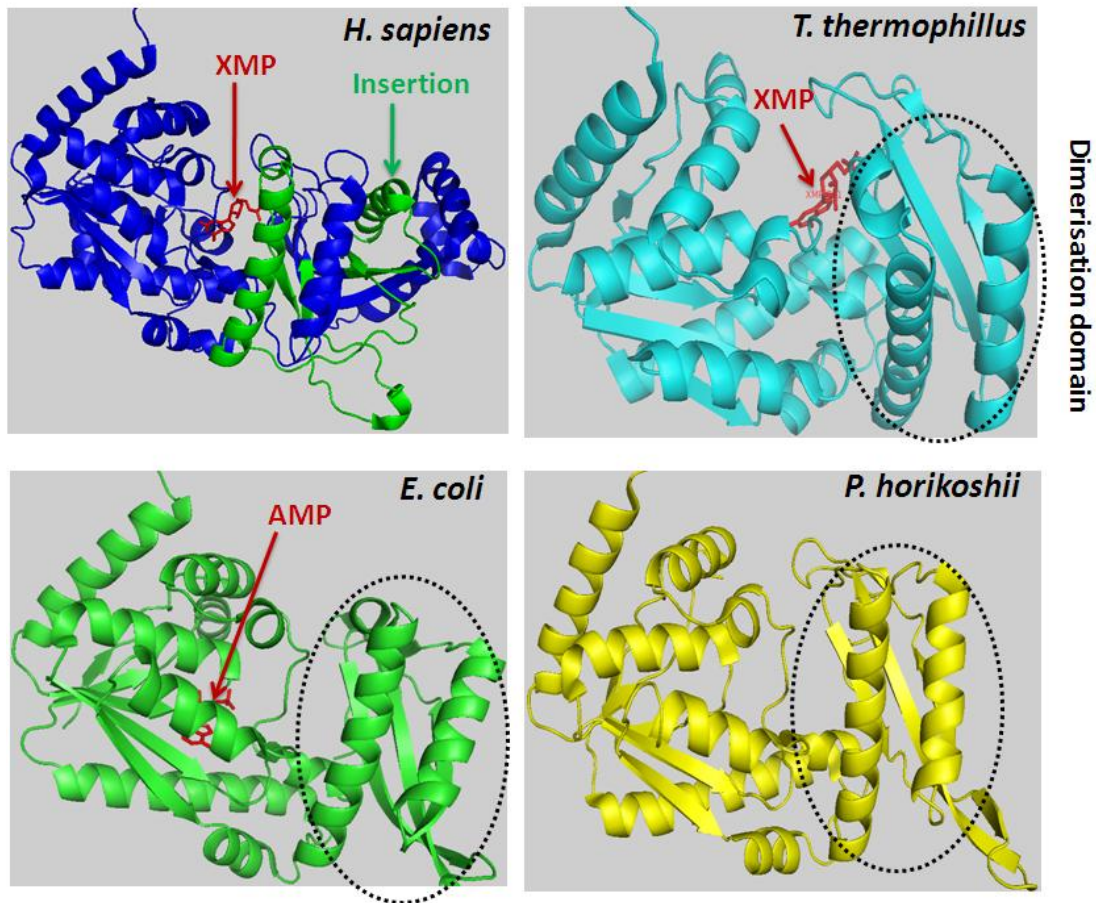


Figure 1.5. Comparison of *E. coli*, *T. thermophilus*, *P. horikoshii* and *H. sapiens* ATPase domains, highlighting overall similarity in topology. Regions highlighted in dotted circles represent the dimerisation domains.

Translocation of MLL (myeloid/lymphoid or mixed lineage leukemia), a transcription factor, has been implicated in many leulemias (Rowley, 1998). The function of GMPS as a fusion partner of MLL is yet to be determined. Two recent studies have shown that *Drosophilla* GMPS strongly interacts with the ubiquitin specific protease 7 (USP7) and deubiquitylates H2B, a function related to gene regulation. These studies highlighted that USP7-GMPS interaction and not the catalytic activity of DmGMPS is needed for this function, as the active site mutants of DmGMPS did not disrupt the activity (van der Knaap et al., 2005). These studies also highlighted the interaction of USP7-GMPS complex with ecdysone binding genes and has been proposed to act as a co-repressor of developmental gene control by ecdysone receptors (van der Knaap et al., 2010). A similar study on EBNA1, a protein of Epstein-Barr virus (EBV) essential

for the replication and persistence of its genome in the latently infected cells, has demonstrated that human GMPS-USP7 activates transcription by forming a ternary complex with the EBNA1-DNA complex via deubiquitylation of H2B (Sarkari et al., 2009). In conclusion, these studies brought off the non-enzymatic activities of GMPS that was unknown till now. It is pertinent to mention that both DmGMPS and HsGMPS contain ~100 amino acid insertion in the dimerisation domain that could be playing a role in such activities.

1.5. Purine biosynthesis and the role of GMP synthetase in *P. falciparum*

Plasmodium falciparum, a parasitic protozoan and the causative agent of cerebral malaria, causes ~1 million deaths annually (World Malaria Report 2009, http://www.who.int/malaria/world_malaria_report_2009/en/index.html). Despite availability of anti-malarial drugs, the widespread emergence of drug resistant parasites necessitates a quest for new therapies. Structure and mechanism based combinatorial approach for drug design has proved highly fruitful. All parasitic protozoa including *Plasmodium* spp. are auxotrophic for purines and use different reactions of the salvage pathway for the synthesis of purine nucleotides, (Sherman, 1998; Walsh and Sherman, 1968). That protozoan parasites including *Plasmodium* spp. are unable to synthesize purines *de novo* has been recognized long back (Booden and Hull, 1973), followed by the apicomplexan genome sequencing that failed to identify the enzymes needed for *de novo* purine biosynthesis (Gardner et al., 2002). *Plasmodium berghei* fed with [³H]-labeled adenosine and hypoxanthine showed their incorporation into the nucleic acids, while [³H]-labeled uridine and thymidine failed to be incorporated (Bungener and Nielsen, 1967; Bungener and Nielsen, 1968; Bungener and Nielsen, 1969; Van Dyke et al., 1970). *P. knowlesi* grown on monkey erythrocytes, did not incorporate [¹⁴C]-labeled thymidine, thymine, uridine and uracil into its nucleic acids, but incorporated [¹⁴C]-labeled orotate (a pyrimidine precursor) and adenine (Polet and Barr, 1968). All these studies collectively supported the presence of purine and absence of pyrimidine salvage pathways in the parasite. Moreover, incorporation of [¹⁴C]-labeled orotate into nucleic acids supported the presence of *de novo* pyrimidine biosynthetic pathway in the parasite. A schematic representation of the purine salvage pathway operating in *P. falciparum* is shown in Fig. 1.6.

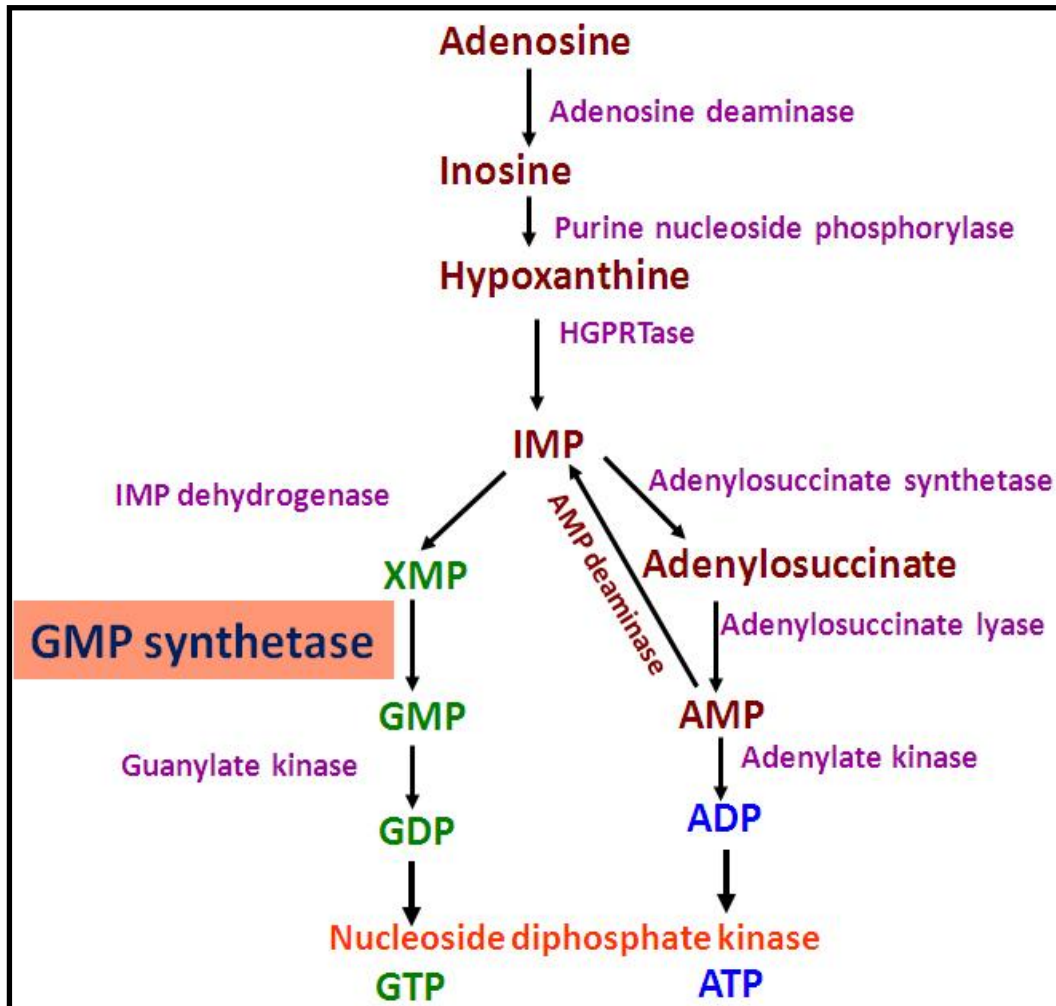


Figure 1.6. Representation of steps involved in the *P. falciparum* purine salvage pathway.

P. falciparum-encoded nucleoside transporters have been implicated in the transport of nucleosides and nucleobases from erythrocyte compartment into the parasite. PfNT1, the adenosine transporter in *P. falciparum*, has been biochemically characterized (Carter et al., 2000; Parker et al., 2000; Quashie et al., 2010) and, knockout of its gene from the parasite led to its complete dependency on high concentrations of adenosine, inosine or hypoxanthine (El Bissati, 2008; El Bissati et al., 2006). Recent studies have shown the presence of new nucleoside transporters in *P. falciparum* (Downie et al., 2010; Martin, 2005; Quashie et al., 2008).

Early studies on *P. falciparum* isolated by mechanical rupture of the host erythrocytes showed the presence of purine salvage pathway enzymes like adenosine

deaminase (ADA) purine nucleoside phosphorylase (PNP) and phosphoribosyl transferase (PRT) in the parasite (Reyes et al., 1982; Wiesmann et al., 1984). Adenosine deaminase catalyses the irreversible conversion of adenosine to inosine and ammonia and its initial characterization from *P. falciparum* was done in 1984 (Daddona et al., 1984; Wiesmann et al., 1984). PNP in the presence of inorganic pyrophosphate, carries out the reversible phosphorolysis of nucleosides into their respective nucleobases and ribose sugar. *P. falciparum* PNP (PfPNP) was first characterized in 1986 (Daddona et al., 1986) and was shown to utilize inosine, guanosine, and deoxyguanosine but not adenosine or xanthosine. Biochemical studies on PfPNP showed that the enzyme differs from human counterpart in having low K_m value for inosine, decreased preference for deoxyguanosine and reduced affinity for transition state analog inhibitors, immucillins (except 5'-deoxy-immucillin-H). Immucillin-H, showed a slow onset tight binding to PfPNP ($K_i = 0.6$ nm, $K_m / K_i = 9000$) and hence, turned out to be an effective inhibitor of parasite growth (Kicska et al., 2002a). Reversal of growth reduction by hypoxanthine and not by inosine, in the Immucillin-H treated *P. falciparum* grown in human erythrocytes, indicated the inhibition of PNP even under in vivo conditions. Inhibition of parasite growth by immucillin-H varied with the culture hematocrit leading to the conclusion that inhibition of both the erythrocyte and parasite PNPs are needed for the purine-less death of the parasite (Kicska et al., 2002b). Recent studies on PNP gene disrupted *P. falciparum* showed that the parasite has severe growth defects at physiological concentrations of hypoxanthine, highlighting importance of the enzyme for its survival (Madrid et al., 2008). Conversion of nucleobases (hypoxanthine, guanine and xanthine) to their respective nucleotides in *P. falciparum* is catalyzed by hypoxanthine guanine phosphoribosyltransferase (PfHGXPRT) (Queen et al., 1988) in a reaction where phosphoribosyl group from phosphoribosylpyrophosphate is transferred to the nucleobases and PPi is released as byproduct. The first cDNA clones of PfHGXPRT were isolated and characterized in 1987 (King and Melton, 1987) that was followed by recombinant expression of the protein in *E. coli* (Keough et al., 1998; Shahabuddin et al., 1992; Vasanthakumar et al., 1990). Detailed structural (Shi et al., 1999) and biochemical characterization (Gayathri et al., 2008; Keough et al., 1999; Li, 1999; Raman et al., 2005; Raman et al., 2004b; Sarkar et al., 2004; Subbayya and Balaram, 2002; Sujay Subbayya and Balaram, 2000) of

PfHGXPRT has led to the identification of unique features in the enzyme. Human blood contains higher levels of hypoxanthine (1.65 μM) (Scholar et al., 1973) making this purine base the key precursor for the generation of both AMP and GMP through the HGPRT reaction.

Inosine monophosphate (IMP) generated by HGXPRT activity, serves as precursor for both GMP and AMP. Conversion of IMP to AMP involves two enzymes, adenylosuccinate synthetase (ADSS) and adenylosuccinate lyase (ADSL). *In vitro* *P. falciparum* cultures treated with hadacidin, a specific inhibitor of adenylosuccinate synthetase, showed inhibition of AMP synthesis that underscored role of the enzyme in parasite metabolism (Webster, 1984). ADSS converts IMP to adenylosuccinate, in a reaction that utilizes a molecule of each GTP and aspartate. Cloning, expression, biochemical and structural characterization of *P. falciparum* ADSS (PfADSS) has provided functional insights of the enzyme (Eaazhisai et al., 2004; Gayathri et al., 2007; Jayalakshmi et al., 2002; Mehrotra et al., 2010; Raman et al., 2004a). *P. falciparum* ADSL (PfADSL) catalyses the formation of AMP from adenylosuccinate and releases fumarate as by-product. The enzyme has been cloned and characterized biochemically (Bulusu et al., 2009). The parasite enzyme has retained the property of transforming 5-aminoimidazole-4-(N-succinylcarboxamide) ribonucleotide (SAICAR) to 5-aminoimidazole-4-carboxamide ribonucleotide (AICAR) and fumarate, a reaction in the *de novo* purine biosynthesis pathway and hence, non-essential for the parasite. Formation of adenosine diphosphate (ADP) from AMP in *P. falciparum* is mediated by adenylate kinase (PfAK), whose characterization has recently been reported (Ulschmid et al., 2004).

GMP (guanosine 5'-monophosphate) is mainly formed from IMP through a two-step process involving the enzymes inosine monophosphate dehydrogenase (IMPDH) and guanosine monophosphate synthetase (GMPS). Though the formation of GMP could also occur through both human erythrocyte and parasite HGPRT, presence of low concentrations of free guanine in human blood (Scholar et al., 1973) would yield levels of GMP insufficient for the rapidly multiplying parasite. Also, both human erythrocytes and *P. falciparum* lack guanosine kinase, eliminating the possibility of generating GMP from guanosine. The potent antimalarial activities of mycophenolic acid (Queen et al., 1990) and bredinin (4-carbamoyl-1-beta-D-ribofuranosyl-imidazolium-5-olate, active as bredeinin monophosphate) (Webster,

1984), both inhibitors of IMPDH underscore the necessity of both IMPDH and GMP synthetase for the survival of intra-erythrocytic parasite. GMP synthetase converts xanthosine monophosphate (XMP) to guanosine monophosphate (GMP). In the paper describing identification of the gene for *P. falciparum* GMP synthetase, the authors have also shown that psicofuranine, a specific inhibitor of GMPS, could reduce the intra-erythrocytic growth of the parasite under in-vitro conditions (McConkey, 2000). IMPDH, that forms XMP from IMP in the purine salvage pathway of the parasite, is the only enzyme that remains to be characterized. Guanylate kinase (GK) converts GMP to GDP (guanosine diphosphate) and has been cloned, expressed and characterized (Kandeel et al., 2008). This study showed that the parasite enzyme has certain distinct biochemical and structural features when compared to its homologs from other organisms. Indeed, a recent high throughput screening for new drug targets in *P. falciparum* has listed PfGK (*P. falciparum* guanylate kinase) as one of the potential candidates (Crowther et al., 2010).

Formation of GTP and ATP from GDP and ADP respectively, is catalyzed by nucleoside diphosphate kinase (NDK). Two reports have confirmed the presence of NDK in the parasite. Biochemical analysis of the recombinant protein has shown that the nucleotides bind to the enzyme in following order; ADP ~ GDP > dGDP > dADP > dTDP > CDP > dCDP > UDP (Kandeel and Kitade, 2010; Kandeel et al., 2009).

Absence of *de novo* purine biosynthetic pathway in *P. falciparum* qualifies the salvage pathway to be a novel antimalarial drug target (Berg et al., 2010; Brady and Cameron, 2004; Bustamante et al., 2009; Choi et al., 2008; Donaldson, 2010; Downie et al., 2008; Subbayya et al., 1997; Vial, 1996). Luebke and coworkers (Luebke et al., 1991) reported that the mice treated with 2'-deoxycoformycin, an adenosine deaminase inhibitor, were able to clear the infection caused by injection of *P. yoelii* parasites. Subsequent use of L-isomers of D-coformycin by Brown, et al., in *P. falciparum* showed selective inhibition of adenosine deaminase in the picomolar range (Brown et al., 1999). Recently, 5'-methylthio coformycin and its mimics have been shown to be specific and potent inhibitors (K_i in picomolar range) of *P. falciparum* adenosine deaminase (Ho et al., 2009; Tyler et al., 2007). Crystal structure of PfPNP in the presence of Immucillin-H-SO₄ revealed (1) the protein to be homohexamer with each catalytic site occupied by a molecule of Immucillin-H and SO₄ and, (2) existence of a solvent filled cavity near 5'-hydroxyl group of Immucillin-

H, indicating the possible binding of an additional functional group (Shi et al., 2004). Biochemical studies established that 5'-methylthioinosine, a non-existent metabolite in humans, can bind to PfPNP, a feature different from the human enzyme. This laid the foundation for designing of transition state analogue, 5'-Methylthio-Immucillin-H for PfPNP, that discriminated the human and parasite enzymes by 112 fold, with K_d values of 2.7 and 303 nM, respectively. Crystal structure of 5'-Methylthio-Immucillin-H-PfPNP complex indeed located the inhibitor near the solvent filled site in the protein. A later report showed that 5'-methylthioinosine is generated by PfADA mediated recycling of polyamine biosynthetic pathway products (Ting et al., 2005) suggesting that both PfADA and PfPNP are active in combined metabolism of the two pathways. This unique characteristic rationalizes the validation of these enzymes as anti-malarial drug targets. Phosphorylated forms of immucillins (immucillin-HP and immucillin-GP) have been shown to be good inhibitors of PfHGXPRT and the structure solved with these compounds should provide a lead for designing new inhibitors for the enzyme (Shi et al., 1999). Recent study on PfHGXPRT and human HGPRT have shown differences in the binding attributes of these enzymes to different substrate and product analogs, that underscored the use of PfHGXPRT as an antimalarial drug target (Keough et al., 2009; Keough et al., 2006). Search for new drug targets in the malarial parasite is a continuous process, necessitated by the rapid evolution of drug resistance in the parasite. Towards the same goal, Crowther and coworkers using high throughput screening methods have led to the identification of new potential antimalarial targets. Interestingly, *P. falciparum* adenylosuccinate synthetase (PfADSS) has been validated as a candidate with a high druggability score of 0.8. This study also led to the identification of few compounds that not only specifically inhibit PfADSS, but also can serve as a guide for design of new inhibitors of the enzyme (Crowther et al., 2010).

The overall aim of the work undertaken in this thesis is to understand the structural and functional aspects of PfGMP synthetase, an essential enzyme for the parasite. Attributes specific to this enzyme compared to that already known in its homologs from other organisms, are mentioned later in the thesis. The specific aspects of PfGMPS highlighted by this study may allow the validation of this enzyme as a new antimalarial drug target.

CHAPTER 2

Chapter 2

Plasmodium falciparum GMP synthetase: biochemical and kinetic characterization

2. 1. Summary

Plasmodium falciparum, the causative agent of the fatal form of malaria synthesizes GMP primarily from IMP and hence, needs active GMP synthetase (GMPS) for its survival. GMPS, a G-type amidotransferase catalyzes the amination of XMP to GMP with the reaction occurring in two domains, the glutaminase domain and the ATP pyrophosphatase (ATPPase). This chapter mainly presents (1) general introduction to kinetic mechanisms operating in different enzymes, (2) the related literature on GMP synthetases and, (3) the studies undertaken for deciphering the kinetic mechanism of *Plasmodium falciparum* GMPS (PfGMPS). Results from the study on PfGMPS indicated steady-state ordered binding of ATP followed by XMP to the ATPase domain with glutamine binding in a random manner to the glutaminase domain. The irreversible, ping-pong step seen in initial velocity kinetics is attributed to the release of glutamate prior to the attack of adenylyl-XMP intermediate by ammonia. The work reported in this chapter has been published (Bhat et al., 2008).

2.2. Introduction

Enzymes are efficient catalysts for biochemical reactions, wherein they speed up the conversion of substrates to products by providing an alternative reaction pathway of lower activation energy. Unlike chemical catalysts, enzymes are very selective in nature with tight functional regulation and, catalyze physiological reactions specifically in a pool of metabolites. The enzyme catalyzed reactions progress through a high energy intermediate step called transition state that finally progresses to the formation of products (Allison and Purich, 2002; Pauling, 1946; Wolfenden, 1976). The enzyme catalyzed reactions have mainly two components; (a) the chemical part involving breaking and making of chemical bonds and, (b) the kinetics that defines rate of the reaction. Active site is the region of an enzyme where substrates bind physically and have been proposed to be complementary to the

substrates and transition states. For understanding function, the catalytic and kinetic mechanisms of an enzyme need to be understood.

2.2.1. Catalytic mechanism

At the heart of all enzyme catalyzed reactions, thermodynamic factors play an essential role. Enzymes catalyse reactions in a chemically unique surrounding (active site) which is different for different enzymes and the efficiency of turnover is mainly governed by the physiological needs of a particular cell and hence, the evolution of diverse three dimensional structures of proteins. Depending on the architecture and chemical composition of the active centers, different ways of catalysis are prevalent across enzymes. Stereo specificity, electrostatic and covalent catalysis, hydrogen tunneling and protein dynamics, all play essential roles in an enzyme catalyzed reaction. Site-specific mutations, isotope effects, use of transition state analogs and site-specific chemical labeling are the few approaches which have provided an understanding of chemical catalysis (Jencks, 1987; Kyte, 1995; Silverman, 2002).

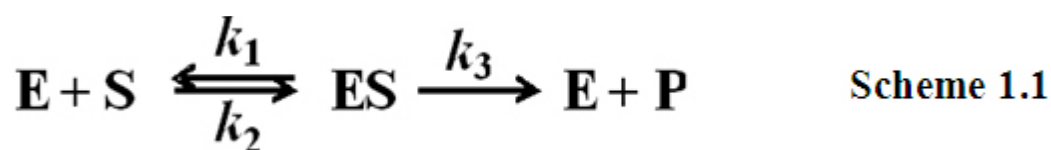
2.2.2. Kinetic mechanism

Enzyme kinetics mainly deals with the factors affecting the rate of enzyme-catalyzed reactions. The most important factors are, ligand (substrates, products, inhibitors, activators, and cofactors) and enzyme concentration, pH, temperature, ionic strength and the solvent. Kinetic mechanism of an enzyme involves the elucidation of the order of addition of substrates to or release of products from the enzyme active site.

The kinetic mechanism of a reaction is generally elucidated by a combination of pre-steady (millisecond to seconds) and steady state (seconds to minutes) kinetic methods involving the rate laws which a typical chemical reaction follows. For describing the initial rate of an enzymatic reaction under any given set of conditions, a mathematical form known as rate equation is derived (Cook and Cleland, 2007; Kaplan, 1979; Leskovac, 2003; Segel, 1993). This is achieved by following one of the assumptions described below:

(A) Rapid equilibrium assumption

In this assumption Henri Michaelis and Maude Menten (Michaelis and Menten, 1913) proposed that the binding of substrates would be rapid compared to subsequent chemical steps that convert substrate to product (Cook and Cleland, 2007; Kaplan, 1979; Leskovac, 2003; Segel, 1993). Scheme 1.1 represents the mechanism for rapid equilibrium which predicts that under saturating substrate concentration, the rate of reaction would be limited by the rate constant k_3 and the formation of intermediate(s) like ES would proceed at a faster rate. The two kinetic parameters V_{\max} (maximum rate) and K_m (the substrate affinity constant for enzyme) for rapid equilibrium assumption are represented by k_3E_t and k_2/k_1 , respectively, where, E_t represents the total enzyme concentration.



(B) Steady-state assumption

G.E. Briggs and J.B.S. Haldane (Briggs and Haldane, 1925) with modification of the above assumption proposed that binding of substrates to the enzyme need not to bring them in equilibrium, but a steady-state condition is reached in which the concentration of different enzyme forms is determined by their rates of formation and breakdown, and remains constant during the initial velocity phase of the reaction. This assumption considers substrate binding (ES formation) and dissociation of the enzyme-substrate complex (breakdown of ES) governed by the rate constants k_1 and k_2 , respectively (in scheme 1), as the rate limiting steps, while the rate of conversion of ES to products (k_3) remains the fast step. The K_m in this case is more complex than the one in rapid equilibrium assumption and is represented by the expression $(k_1 + k_3)/k_2$ (Cook and Cleland, 2007; Kaplan, 1979; Leskovac, 2003; Segel, 1993).

2.2.2.1. Initial velocity kinetics without added inhibitors

The overall rate equation of an enzyme catalyzed multisubstrate reaction is complicated due to the presence of multiple enzyme-substrate/product intermediates and is determined by the number of substrates being used in the reaction. Hence, initial velocity experiments have been devised in which the concentration of one of

the substrates is varied at a time while maintaining the other substrates at fixed concentrations with the procedure repeated for all substrates and initial rates determined. In this way, the final rate equation is simplified due to reduction in the number of intermediates whose concentration changes during the course of reaction. The graphical form of data is generally displayed by linearly transforming the Michaelis-Menten equation using the method proposed by Lineweaver and Burk (Lineweaver and Burk, 1934). In such a type of plot, reciprocal of initial velocity obtained at different concentrations of a substrate is plotted against reciprocal of substrate concentration. The different kinetic mechanisms manifested by enzymes have been classified into sequential or ping-pong mechanisms, as devised by Cleland (Cleland, 1963).

A sequential mechanism is one in which all the substrates first bind to the enzyme and then the products are released. Hence, no irreversible step occurs during the binding of substrates and, all the reaction intermediates contribute to the final rate equation. The presence of a set of intersecting lines obtained during initial velocity measurements ($1/v$ versus $1/s$) is indicative of a sequential mechanism. In a multi substrate reaction, substrate binding may be ordered or random and accordingly, the mechanism is called as ordered or random sequential. In a ping-pong or double displacement mechanism, first substrate binds to the enzyme, transfers a part of itself to the enzyme and the first product gets dissociated off before the second substrate binds. The form of enzyme bound to part of the first substrate now reacts with the second substrate and forms the final product. Hence, the presence of an irreversible step eliminates some reaction intermediates when the final rate equation is derived, that in graphical display results in a set of parallel lines (when $1/v$ is plotted against $1/s$) (Cook and Cleland, 2007; Kaplan, 1979; Leskovac, 2003; Segel, 1993). Two types of ping-pong mechanisms have been reported in different systems. (a) One-site or classical ping-pong mechanism, wherein only one site is shared by all substrates on the enzyme. Aspartate aminotransferase presents a classical example of one-site ping pong mechanism that catalyses the reversible transfer of α -amino group of L-aspartate to α -ketoglutarate to form L-glutamate and oxaloacetate. Pyridoxal 5'-phosphate, the enzyme bound covalent cofactor, accepts amino group from the aspartate forming oxaloacetate, the leaving substrate, and the pyridoxamine 5'-phosphate. The amino group from the latter is finally transferred to α -ketoglutarate (Velick and Vavra, 1962). (b) The two-site or non-classical ping-pong mechanism, wherein the

substrates bind to two physically separate sites on an enzyme. Transcarboxylase (Northrop, 1969) provides the first example of two-site ping pong mechanism in enzymes. Theorell-Chance or hit and run mechanism is a special case of ordered bi bi mechanism in which the concentration of the central ternary complex remains very low. This was first reported in alcohol dehydrogenase by Theorell and Chance (Theorell and Chance, 1951) and latter reported in many systems.

2.2.2.2. Initial velocity kinetics with added inhibitors

Initial velocity patterns under steady-state conditions are sometimes insufficient to unambiguously assign a kinetic mechanism to an enzymatic reaction. Hence, alternate approaches have been evoked to dissect the kinetic mechanism of an enzymatic reaction. One such commonly used approach is the use of inhibitors as a probe for the validation of kinetic patterns obtained under initial velocity conditions. In these studies, generally one of the substrates is varied while maintaining the inhibitor at different fixed concentrations. The other substrates (if present) are maintained at a fixed saturating concentration (Cook and Cleland, 2007; Kaplan, 1979; Kyte, 1995; Leskovac, 2003; Segel, 1993). Three types of inhibition patterns are generally observed when a reversibly binding inhibitor is used under initial velocity conditions.

(A) Competitive inhibition

A competitive inhibitor is one that competes with the varied substrate for enzyme and hence, the inhibitor and the varied substrate combine with the same form of enzyme. For the enzyme to attain the maximum velocity higher concentration of the varied substrate is required to overcome the effect of inhibitor. This type of inhibition hence, results in decreased affinity of the enzyme for substrate (high K_m) while the maximal velocity (V_{max}) remains unaffected. The plot of $1/v$ against $1/s$ for such type of inhibition is a set of lines that converge at a single point on y-axis.

(B) Uncompetitive inhibition

In this type of inhibition, the inhibitor binds only to the enzyme-substrate complex and hence, inhibition is observed even when the varied substrate is at saturating concentration, as the presence of higher substrate concentration induces the formation of more of the enzyme substrate- complex. The graphical display of this

type of inhibition is a set of parallel lines when $1/v$ is plotted against $1/s$ which suggests that both V_{\max} and K_m are altered.

(C) Non-competitive inhibition

A non-competitive inhibitor can bind both to the free enzyme and the enzyme-substrate complex. Hence, an increase in varied substrate concentration to infinity does not relieve enzyme of the inhibition completely. The graphical representation of $1/v$ against $1/s$ in such type of inhibition is a set of lines that intersect on abscissa to the left of y-axis suggesting that only the K_m is affected. A mixed type of inhibition is a form of non-competitive inhibition in which the lines in $1/v$ versus $1/s$ plot intersect either above or below the abscissa.

Based on the above inhibition patterns, kinetic mechanisms with emphasis on order of substrate binding have been elucidated. Rate equations are derived taking into consideration the presence of inhibitor bound intermediate which finally determine the line patterns during an initial velocity kinetic study. Generally, the inhibitors being used are either the products of the reaction or their analogs or varied substrate analogues.

2.2.3. Metal ion dependence of enzyme activity

There are two classes of enzyme that require bivalent metal ions for their catalytic activity; (1) metalloenzymes, which contain tightly bound metal ions that do not dissociate during their isolation, and (2) the metal-activated enzymes, that remain inactive in the absence of added metal ion. Both univalent and divalent metal ions have been shown to be involved in different kinds of enzyme reactions. Most of the enzymes that use ATP during the reaction essentially require magnesium for their activity (Cleland, 1995). In all amidotransferases that use ATP during the intermediate formation, magnesium has been shown to be indispensable for the activity. In these enzymes, though magnesium is needed for the formation of MgATP, presence of extra metal ion binding sites on the enzyme have also been elucidated. PfGMPS provides an example of this kind and the aspect is discussed in this chapter. Many kinetic methods have been devised to evaluate the role of metal ions in enzyme reactions in a detailed way (Morrison, 1979).

2.2.4. Kinetic and biochemical aspects of GMP synthetases

Though, biochemical information on many of the GMP synthetases is available, kinetic characterization has remained a topic of pursuance. The kinetic mechanism of *E. coli* GMP synthetase using initial velocity kinetic patterns and positional isotope effects was reported by von der Saal (von der Saal et al., 1985). This study was consistent with the ordered binding of MgATP followed by XMP and then NH₃. This study also confirmed the formation of adenylyl-XMP intermediate during the reaction in absence of any ammonia sources. In human GMP synthetase, Nakamura et al (Nakamura and Lou, 1995) have shown that decoyinine, an inhibitor of GMP synthetases, is an uncompetitive inhibitor of XMP and glutamine and noncompetitive with respect to ATP. This led to the conclusion that ATP may not be the first substrate to bind to human GMP synthetase, though a detailed kinetic account is still awaited. It is interesting to know that human GMP synthetase exists in two forms both following sigmoidal kinetics (with respect to XMP) with similar kinetic parameters. Utilization of both ammonium and glutamine as nitrogen source is a common feature of all GMP synthetases reported till date. This chapter presents a detailed view on kinetic mechanism of *P. falciparum* GMP synthetase.

2.2.5. GMP synthetase inhibitors

Besides the general amidotransferase modulators like acivicin and DON, few specific inhibitors have been reported for GMP synthetases. Figure 2.1 provides a list of reported GMP synthetase inhibitors. Among these, decoyinine (9-(6-Deoxy-D-β-erythro-hex-5-en-2-ulo-furanosyl)-adenine) and psicofuranine (6-amino- 9-D-psicofuranosylpurine), the two known antibacterial compounds, were first shown to inhibit the biosynthesis of guanosine-5-phosphate in *E. coli* and *Salmonella aureus* (Hanka, 1960) cell cultures and subsequently, it was reported that psicofuranine is a GMP synthetase-specific inhibitor (Slechta, 1960). Two separate biochemical studies on *E. coli* (Kuramitsu and Moyed, 1966) and human GMP synthetases (Nakamura and Lou, 1995) have established the mechanism of inhibition of psicofuranine and decoyinine. Spector and coworkers have demonstrated the inhibitory effect of a large number of nucleosides and their modified analogues on GMP synthetase activity using purified enzyme fractions from *E. coli* and Elrich ascite cells (Spector and Beacham, 1975; Spector et al., 1976). Recently, effect of psicofuranine on intra-

erythrocytic growth of *Plasmodium falciparum* has also been examined (McConkey, 2000). Bredenin monophosphate (also known as mizoribine

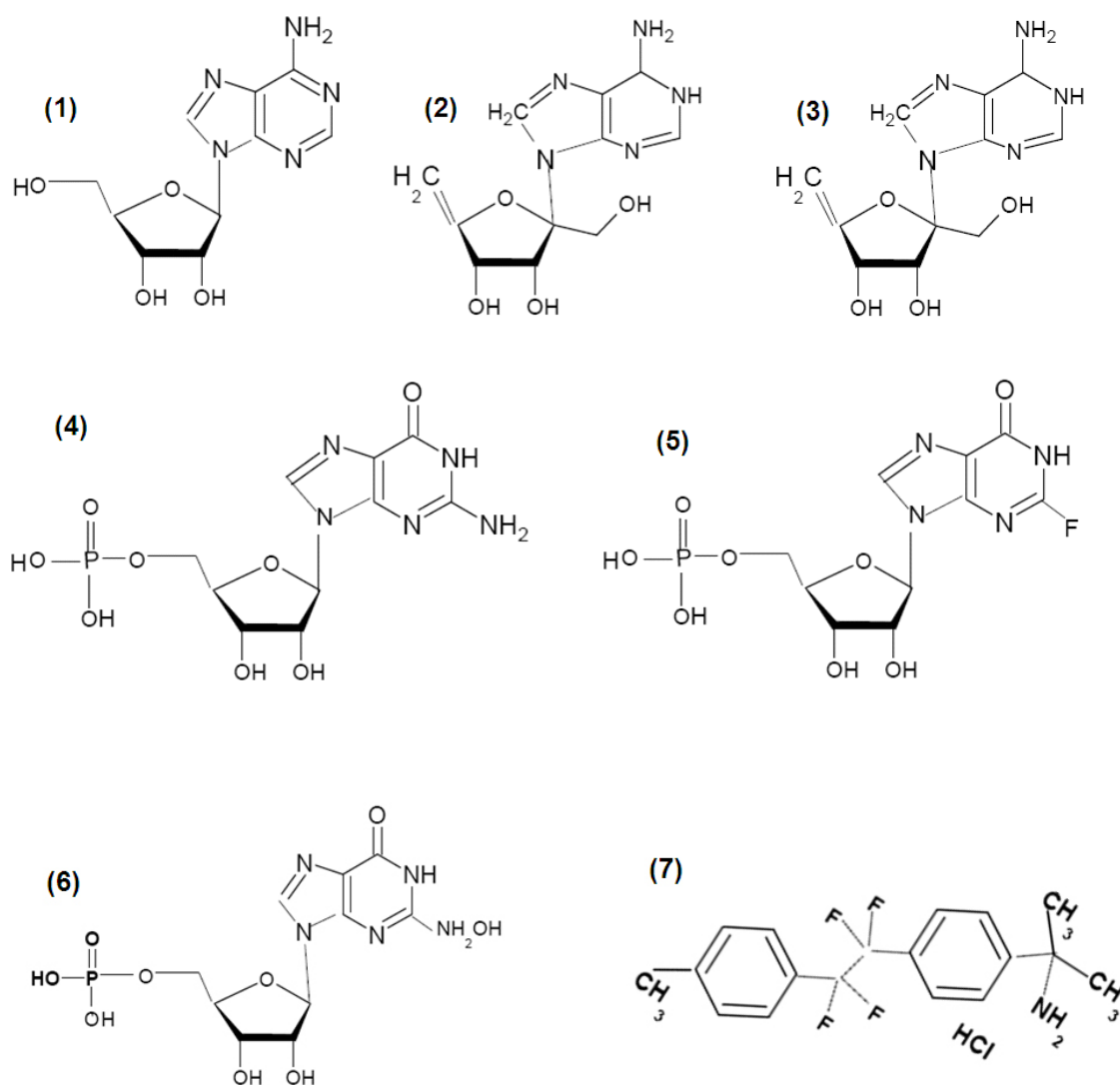


Figure 2.1. Structural mimics of adenosine and guanosine monophosphate that specifically inhibit GMP synthetase reaction. 1. Adenosine, 2. Psicofuranine, 3. Decoyinine, 4. Guanosine monophosphate, 5. 2-Fluoro-IMP, 6. N^2 -hydroxy guanosine 5'-monophosphate, 7. α, α -dimethyl-4-[1,1,2,2-tetrafluoro-2-(4-methylphenyl)ethyl] – benzenemethanamine hydrochloride

monophosphate), a phosphorylated form of an imidazole nucleoside, bredenin (mizoribine), an isolate from *Eupenicillium brefeldianum*, has been shown to inhibit GMP synthetase by competing for the XMP binding site (Kusumi et al., 1989). A more recent study on *E. coli* GMPS has evinced 2-fluorinosine 5'-monophosphate

(F-IMP, 5), and N²-hydroxyguanosine 5'-monophosphate as inhibitors of the enzyme, with the former being an electronic mimic of reaction intermediate (IC₅₀ > 2 mM) and the latter a competitive analogue of XMP (K_i = 92 nM) (Deras et al., 1999). The latest addition to the list of specific GMP synthetase inhibitors is α , α -dimethyl-4-[1,1,2,2-tetrafluoro-2-(4-methylphenyl)ethyl]-benzenemethanamine hydrochloride), a synthetic molecule that has been shown to bind to the ATPase domain of the *C. albicans* and *A. fumigatus* enzymes (Rodriguez-Suarez et al., 2007) with high affinity (K_i = 10 μ M). Though a fair understanding of mechanism of the GMPS inhibitors has been gained, a lot more is still needed to utilize these molecules as drugs to treat different diseases. A section of this chapter provides a list of inhibitors and their effect on PfGMPS.

2.3. Materials and methods

2.3.1. Materials

Restriction enzymes, *Pfx* DNA polymerase and T₄ DNA ligase were from Invitrogen, USA and Bangalore Genei Pvt. Ltd., India, and were used according to the manufacturer's instructions. *E. coli* strain AT2465 was obtained from the *E. coli* Genetic Stock Center (Yale University, New Haven, CT). Primers were custom synthesized at Microsynth, Switzerland. All chemical reagents were of high quality from Sigma Chemical Co., Missouri, USA, Alexis Biochemicals, USA or Merck India Ltd., India. Media components were from Himedia, Mumbai, India.

2.3.2. Cloning, complementation, expression and purification

Primers were designed using the annotated gene sequence of *Plasmodium falciparum* GMP synthetase (PF10_0123) available in the *P. falciparum* Genome database, PlasmoDB (www.plasmodb.org) (Bahl et al., 2003) The primers 5'GCAGGATCCATGGCAGAAGGAGAGGAATATGACAAGATTTTG 3' and 5'GTCCTCGAGCTGCAGTCATTTCGATTCAATCGTTGCTGGTG 3' that contain the restriction sites *Bam*H1 and *Pst*I (underlined) were used for amplification of the gene by PCR, with parasite genomic DNA as template. The amplified fragment was cloned into the *E. coli* expression vector pQE30 and DNA sequencing of the clone pQE30-PfGMPS with N-terminal His-tag confirmed complete identity with the PlasmoDB entry. Complementation studies were carried out using *E. coli* strain

AT2465 (λ^- , $e14^-$, *guaA21*, *relA1*, *spoT1* and *thi1*) transformed with the expression construct pQE30-PfGMPS. Single colonies were inoculated into 5 ml minimal media without guanine or guanosine, prepared according to a reported method (Hirst et al., 1994), with 100 μ g/ml ampicillin and grown overnight. The culture (100 μ l) was spread on minimal medium plates and examined for the appearance of colonies. Appropriate controls with pQE30 vectors were also grown at the same time. The *E. coli* strain AT2465 was also used for hyper-expression of PfGMPS. The hyper-expressed protein was purified using Ni-NTA beads followed by Sephacryl 200 (37.5 x 1.6 cm) size exclusion chromatography. The purified protein was stored in 20 mM Tris HCl, pH 7.4, 2 mM DTT, 10 % glycerol and 1mM EDTA at -80 °C. Protein concentration was estimated by using the method of Bradford (Bradford, 1976). The molecular weight was confirmed by MALDI-TOF (Matrix Assisted Laser Desorption Ionization-Time of Flight) mass spectrometry (Ultraflex II, Bruker, Germany). The protein sample was dialysed against water, 1 μ l of protein (3 μ g) was mixed with sinapinic acid (0.1 g sinapinic acid in 0.5 ml of 50 % acetonitrile and 0.1 % trifluoroacetic acid) in 1:1 ratio, spotted onto MALDI-TOF target plate and mass spectra recorded in the positive ion linear mode.

2.3.3. Analytical gel filtration

Analytical gel filtration was performed on Superdex-200 column (1cm x 30 cm) attached to an AKTA Basic HPLC system. The column was equilibrated with Tris HCl, pH 7.4 and calibrated with β -amylase (200 kDa), alcohol dehydrogenase (150 kDa), bovine serum albumin (66 kDa), carbonic anhydrase (29 kDa) and cytochrome c (12.4 kDa) as molecular weight markers. 30 μ M (100 μ l) of PfGMPS was injected into the column and eluted at a flow rate of 0.5 ml min⁻¹ using Tris HCl, pH 7.4 as the eluant with detection at 280 nm. To monitor the stability of the oligomer, protein samples were pre-incubated with 150 mM to 1.5 M NaCl on ice for 30 min. The elution buffer contained the appropriate concentration of NaCl.

2.3.4. Assay for PfGMPS glutaminase activity

The activity of the glutaminase domain was monitored spectrophotometrically at 340 nm as the formation of NADH, in which glutamate production was coupled to the reduction of NAD to NADH with the release of 2-oxoglutarate, using glutamate

dehydrogenase as the coupling enzyme (Wojcik et al., 2006). The assay volume of 0.1 ml containing 90 mM Tris HCl, pH 8.5, 5 mM glutamine, 0.1 mM EDTA, 0.1 mM DTT and 6 μ g of PfGMPS was incubated at 37 °C for 20 minutes with different combinations of 150 μ M XMP, 2 mM ATP, 2 mM AMP-PNP and 20 mM MgCl₂. The reaction was terminated by heating the sample in a boiling water bath for 3 minutes, chilled on ice and centrifuged for 10 minutes at 12000 rpm. Levels of glutamate in the supernatants were determined using glutamate dehydrogenase (Sigma Chemical Co., Missouri, USA). A total reaction volume of 0.3 ml containing 50 mM Tris HCl, pH 8.5, 50 mM KCl, 1 mM EDTA, 0.5 mM NAD and 2 units of glutamate dehydrogenase was incubated for 90 minutes at 37 °C and clarified by centrifugation at 12000 rpm for 5 minutes. Conversion of NAD to NADH was monitored as the absorbance at 340 nm and the amount of product formed was estimated using the extinction coefficient of 6,220 M⁻¹cm¹. All assays were performed in duplicate and the experiment was repeated twice.

2.3.5. Assay for GMP synthetase activity

PfGMPS activity was monitored spectrophotometrically using Hitachi U-2010 or U-2810 spectrophotometer. Reaction rates were monitored as decrease in absorbance at 290 nm due to conversion of XMP ($\epsilon = 4800 \text{ M}^{-1}\text{cm}^{-1}$) to GMP ($\epsilon = 3300 \text{ M}^{-1}\text{cm}^{-1}$). A $\Delta\epsilon$ value of $1500 \text{ M}^{-1}\text{cm}^{-1}$ was used to calculate the amount of product formed (Moyed and Magasanik, 1957). The standard assay consisted of 90 mM Tris HCl, pH 8.5, 150 μ M XMP, 2 mM ATP, 5 mM glutamine, 20 mM MgCl₂, 0.1 mM EDTA and 0.1 mM DTT in a total reaction volume of 0.25 ml. Reactions were initiated with 6 μ g of PfGMPS and continuously monitored at 25 °C. The assay conditions were same in all the studies unless otherwise mentioned. The effect of phosphate ions on PfGMPS activity was studied in a concentration range of 0.1 mM to 10 mM. Monovalent (Na⁺, K⁺ and Li⁺) and divalent (Ca²⁺, Mn²⁺, Co²⁺ and Zn²⁺) metal ions were examined for their effect on PfGMPS activity in the concentration range of 0 mM to 500 mM and 0 mM to 100 mM, respectively as chloride salts. To monitor the effect of different natural and modified analogs of nucleosides, nucleotides and purine bases on PfGMPS activity, the concentrations of XMP, ATP and glutamine were fixed at 45 μ M, 750 μ M and 1.5 mM, respectively. Specific activity was calculated from initial velocity and data were fitted to different equations

using GraphPad Prism, version 4.0 (GraphPad Prism 4 Software, Inc., San Diego, CA). The kinetic constants for XMP, ATP, glutamine and NH_4^+ (as $(\text{NH}_4)_2\text{SO}_4$) were determined by varying the concentration of one substrate, while keeping the other two at saturating concentrations. The substrate concentrations when fixed were, 0.15 mM XMP, 2 mM ATP, and 5 mM glutamine. The initial velocity data were fit to Michaelis-Menten equation (Eq. 2.1) and analyzed by nonlinear regression using the software GraphPad Prism 4.

$$v=V_{\max}[S]/K_m+[S] \quad (2.1)$$

2.3.6. Initial velocity kinetics

All initial velocity measurements were made under standard assay conditions at varying concentrations of substrates. For this study the method of Carl Frieden (Frieden, 1959) was used in which concentrations of two substrates were varied while maintaining the third substrate at a fixed saturating concentration. Of the two varied substrates, concentration of one was varied regularly while the second was maintained at different fixed concentrations. Each experiment was repeated 3 - 4 times to confirm reproducibility. Nonlinear analysis was done by fitting the data to rate equations, 2.2 for sequential, and 2.3 for ping-pong bireactant mechanism. For the best fit, values for standard error and 95% confidence intervals were taken as indicators. The nomenclature used in the equations is that of W.W. Cleland, (Cleland, 1963).

$$v=V_{\max}[A][B]/(K_{ia}K_B)+(K_A[B])+(K_B[A])+([A][B]) \quad (2.2)$$

$$v=V_{\max}[A][B]/K_A[B]+K_B[A]+[A][B] \quad (2.3)$$

where, v = initial velocity, V_{\max} = maximal velocity, $[A]$ and $[B]$ are concentrations of the substrates A and B, and K_A and K_B are their respective Michaelis-Menten constants. K_{ia} is the dissociation constant of the substrate A. In equation 2.2, A and B refer to substrates ATP and XMP, respectively, when glutamine was the fixed substrate. When glutamine was replaced with ammonia, A represents either substrates ATP or XMP and B is $(\text{NH}_4)\text{SO}_4$. In equation 2.3, A refers either to the substrates ATP or XMP and B to glutamine.

2.3.7. Kinetics of inhibition by products and substrate analogs

Inhibition of PfGMPS activity by products (GMP, PPI, AMP and glutamate), non-hydrolysable ATP analog AMP-PNP (β , γ -imidoadenosine, 5'-triphosphate) and the glutamine analog, glutamic acid- γ -methyl ester were examined by varying one substrate at different fixed concentrations of the inhibitor. The other two substrates were kept at fixed concentrations. All experiments were repeated at least twice. The data were fit to equations 2.4, 2.5 and 2.6 for competitive, uncompetitive and non-competitive inhibition, respectively.

$$v=V_{\max}[S]/(K_m(1+[I]/K_i)+[S]) \quad (2.4)$$

$$v=V_{\max}[S]/(K_m(1+[I]/K_i)+[S]1+[I]/K_i) \quad (2.5)$$

$$v=V_{\max}[S]/(K_m+[S](1+[I]/K_i)) \quad (2.6)$$

where, [S], K_m and K_i are the substrate concentration, Michaelis-Menten constant and inhibition constant, respectively. The other terms are same as in equations 2.2 and 2.3.

2.3.8. Dependence of PfGMPS activity on Mg^{2+} ions

The effect of varying $MgCl_2$ concentration on PfGMPS activity was monitored at fixed ATP concentration of 2 mM with XMP and glutamine at 0.15 mM and 5 mM, respectively. To estimate the number of Mg^{2+} binding sites on PfGMPS, $MgCl_2$ was fixed at 2 mM while ATP concentration was varied. Standard assay conditions were used for activity measurements. Equations 2.8 and 2.9 were solved simultaneously for the calculation of MgATP concentration (Morrison, 1979; Robertson and Villafranca, 1993).

$$[M]=[M]_t+([MATP][1+(K_1/K_2)([H]/K_H)]) \quad (2.8)$$

$$[MATP]=[ATP]_t(1+K_1/[M])+(K_1/[M])([H]/K_H)+(K_1/K_2([H]/K_H)) \quad (2.9)$$

$[M]_t$, $[ATP]_t$, $[MATP]$, $[M]$ and $[H]$ represent the total Mg^{2+} , total ATP, total $MgATP^{2-}$, free Mg^{2+} and free hydrogen ion concentrations, respectively. K_1 , K_2 and K_H represent the dissociation constants for $MgATP^{2-}$, $MgHATP^-$ and $HATP^{3-}$,

respectively and values used were according to Nakamura et al., (Nakamura and Lou, 1995).

2.4. Results

2.4.1. Functional complementation and preliminary characterization of recombinant PfGMP synthetase

The *Plasmodium* genome database PlasmoDB, carries a single annotation for GMPS that lacks introns. PfGMPS has been earlier cloned from genomic DNA and the sequence deposited in Genbank (McConkey, 2000). IPTG induced BL21DE3 cells transformed with pQE30-PfGMPS (pQE30 expression vector carrying PfGMPS gene) did not show expression of the recombinant protein on SDS-PAGE. Use of BL21DE3 cells harbouring the plasmids RIG or RIL, known to overcome codon bias (Baca and Hol, 2000) or use of M15 cells with pREP plasmid (Gottesman et al., 1981), also did not lead to expression of PfGMPS. However, pQE30-PfGMPS complemented the *gua* A (GMP synthetase) deficiency in the *E. coli* cells AT2465 (λ^- , $e14^-$, *guaA21*, *relA1*, *spoT1* and *thi1*), that were grown on minimal medium without supplementation with guanine or guanosine (Fig. 2.2A). This suggested that the clone produced functional GMPS and on SDS-PAGE the over-production of protein of the required molecular weight of 65 kDa was observed (Fig. 2.2B). Hence, the use of mutant AT2465 *E. coli* cells that lack the *gua* A gene not only confirmed the functionality of the clone, but also proved to be a good expression system for PfGMPS. Purification of recombinant PfGMPS from the induced cell lysate using Ni-NTA affinity matrix followed by size-exclusion chromatography yielded 20 mg pure protein from 1 litre of culture. The purified His-tagged protein showed a molecular mass of 65253.9 Da by MALDI-TOF mass measurement while the calculated molecular weight of the protein without the initiator methionine is 65254 Da (Fig. 2.2C).

Examination of the subunit association of PfGMPS by size-exclusion chromatography revealed a single protein peak at 12.4 ml corresponding to a molecular weight of 160 kDa (Fig. 2.3A.). The expected molecular weight of the dimer of PfGMPS is 131 kDa. On addition of NaCl over the concentration range 150 mM to 1.5 M, the peak shifted slightly towards higher retention volume of 12.7 ml,

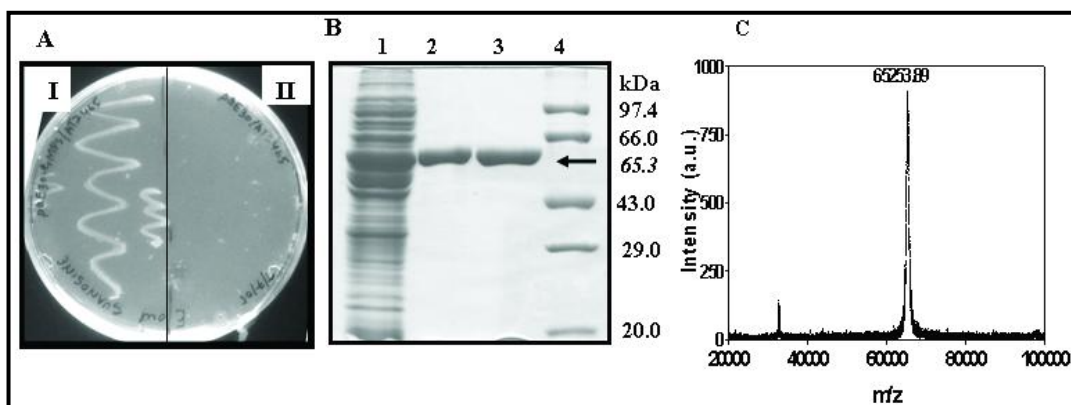


Figure 2.2. Characterization of recombinant *Plasmodium falciparum* GMP

synthetase. A. Functional complementation of *guaA* deficiency in the *E. coli* strain AT2465 (λ , *e14*, *guaA21*, *relA1*, *spoT1*, *thi1*) by PfGMPS. Cells transformed with pQE30-PfGMPS and pQE30 vector control are streaked on left (I) and right halves (II) of minimal medium agar plate, respectively. B. Purification of PfGMPS. Lane 1, crude lysate, lane 2, eluate from Ni-NTA agarose affinity chromatography, lane 3, eluate from size-exclusion chromatography and lane 4, protein molecular weight markers. C. MALDI-TOF mass spectrum of PfGMPS. The molecular mass in daltons is indicated against the peak.

corresponding to molecular weight of 144.5 kDa. However, there was no complete shift of the peak towards a monomer (14.7 ml). Hence, in the presence or absence of NaCl, the estimated molecular mass was slightly higher than that of a dimer. This possibly arises from an elongated dimeric form of PfGMPS. Tris HCl was found to be the most suitable buffer for activity measurements while the activity in 20 mM potassium phosphate, pH 7.4, was four fold lower. Addition of phosphate to the assay mixture in Tris HCl, pH 8.5 led to inhibition of enzyme activity with IC₅₀ of 2.7 mM. Magnesium was essential for catalysis and could not be replaced effectively by other divalent metal ions. Replacement of Mg²⁺ with Mn²⁺ and Ca²⁺ lead to 70 % and 85 % drop in activity, respectively. Zn²⁺ and Co²⁺ did not support activity. Monovalent metal ions Na⁺, K⁺ and Li⁺ inhibited PfGMPS activity with Na⁺ having the highest effect (Fig. 2.3B.). At 24 mM Na⁺, 25 % drop in activity was seen that increased to 90 % in 200 mM NaCl solution. K⁺ and Li⁺ also affected the activity, but to a lesser extent. This possibly indicates the presence of high affinity binding sites for Na⁺ on , which upon occupancy inhibit the catalytic activity.

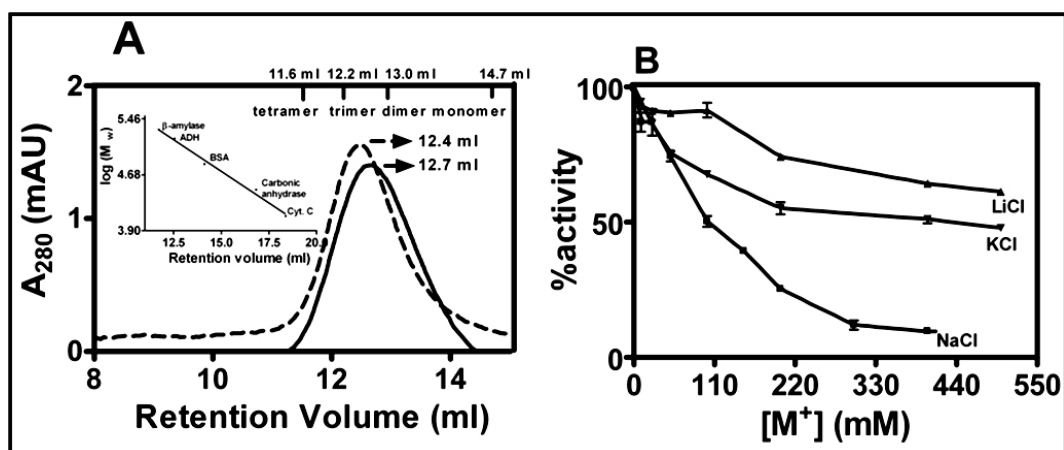


Figure 2.3. Effect of salt on PfGMPS subunit association and activity

A. Elution profile of PfGMPS upon chromatography without (...) and with (—) 1.5 M NaCl on Superdex-200 analytical gel filtration column. The elution buffer composition is as described in methods. The retention volume at the peak is indicated against each curve. Expected retention volumes for monomeric to tetrameric forms of PfGMPS are indicated on top of the plot. Inset represents column calibration plot of retention volume versus log molecular weight. ADH, alcohol dehydrogenase, BSA, bovine serum albumin, Cyt c, cytochrome c. B. Inhibition of PfGMPS activity by the monovalent metal ions Na^+ , K^+ and Li^+ , used as their chloride salts. Activity is represented as percentage of the activity in the absence of the salt.

The K_m values from saturation kinetics for XMP, ATP, glutamine and ammonium sulphate are shown in Table 2.1. The V_{max} value was found to be 450 nmoles $min^{-1}mg^{-1}$. PfGMPS has the highest affinity towards XMP and its K_m value is lower than that for human and *E. coli* GMP synthetases. The K_m value for ATP and glutamine are comparable to that for the human protein but lower than that for *E. coli* GMPS (Nakamura and Lou, 1995; Sakamoto et al., 1972). PfGMPS was also found to directly utilize ammonia for the amination of XMP, though with a significantly higher K_m . The K_m (10.8 ± 1.6) value for ammonium was 10 fold higher than that for *E. coli* GMPS (Sakamoto et al., 1972).

Table 2.1. Kinetic parameters of *P. falciparum*, *H. sapiens* and *E. coli* GMP synthetases

	XMP	ATP	Glutamine	(NH ₄) ₂ SO ₄
<i>P. falciparum</i>^a				
<i>K_m</i> (μM)	16.8 ± 2	260 ± 38	472 ± 69	10.8 ± 1.6 ^e
<i>k_{cat}</i> (sec ⁻¹)	0.43 ^b	-	-	
<i>k_{cat}/K_m</i> (μM ⁻¹ sec ⁻¹)	2.5 x 10 ⁻²	0.16 x 10 ⁻²	0.09 x 10 ⁻²	
<i>H. sapiens</i>^c				
<i>K_m</i> (μM)	35.6 ± 1.8	132 ± 7	406 ± 49	-
	45.4 ± 5.3	180 ± 12	358 ± 34	-
<i>k_{cat}</i> (sec ⁻¹)	5.4	-	-	
	5.6	-	-	
<i>E. coli</i>^d				
<i>K_m</i> (μM)	29	530	1000	1.0 ^e

^aThis study. ^bThe *k_{cat}* values with respect to the three substrates were similar. The value in this table is an average of the three *k_{cat}* values. ^cTwo values correspond to the two isoforms of human GMPS (Nakamura and Lou, 1995). ^dFrom Sakamoto et al. (Sakamoto et al., 1972). ^e*K_m* of (NH₄)₂SO₄ is in mM.

2.4.2. Kinetic mechanism of PfGMPS

PfGMPS binds three substrates ATP, XMP and glutamine, catalyzes the amination of XMP to GMP and releases the four products AMP (adenosine 5'-monophosphate), GMP, PPi and glutamate. The reaction is completed in a concerted manner in two separate domains. The steady state kinetic mechanism of PfGMPS was elucidated from patterns obtained from initial velocity and product inhibition plots that are diagnostic of a specific kinetic mechanism.

ATPPase domain. This domain binds the substrates ATP and XMP in the presence of Mg²⁺ to form the activated AMP-XMP intermediate. To determine the order of substrate binding to the ATPase domain, glutamine was held at saturating

concentration while XMP or ATP was varied at different fixed concentrations of the other. Plots of both $1/v$ versus $1/[ATP]$ and $1/v$ versus $1/[XMP]$ (Fig. 2.4 A, B) yielded intersecting line patterns with lines converging to the left of the y-axis. The point of intersection was on x-axis in the former plot and above the x-axis in the latter plot. According to the rules of Cleland (Cleland, 1963), this pattern rules out ping-pong mechanism and is indicative of either ordered or random sequential mechanism for the binding of ATP and XMP to this domain. The data did not fit to rapid-equilibrium ordered mechanism but best fitted to equation 2.2 that represents both steady state ordered and rapid equilibrium random bisubstrate models. The kinetic constants obtained from this fit (Table 2.2) were in the same range as those obtained from saturation kinetic studies and hence, validate the equation used. To differentiate between the two mechanistic possibilities (steady state ordered versus rapid equilibrium random), product inhibition studies using AMP, GMP and PPI, were carried out. AMP-PNP was also used to validate the results obtained with PPI. The results are summarized in Table 2.3 and Figure 2.5. AMP was found to be a weak inhibitor of PfGMPS activity while PPI, GMP and AMP-PNP were potent inhibitors. PPI showed competitive and non-competitive inhibition with respect to ATP and XMP, respectively (Fig. 2.5 A, B), while GMP showed competitive and uncompetitive inhibition with respect to XMP and ATP, respectively (Fig. 2.5 E, D). AMP-PNP yielded patterns similar to those obtained with PPI, being competitive and non-competitive inhibitor with respect to ATP and XMP, respectively (2.5, G, H). The slope and intercept re-plots from the primary non-competitive inhibition plots of PPI and AMP-PNP yielded K_{ii} and K_{is} values that were similar. These results indicate that ATP can bind to the free enzyme while XMP binding is conditional to the binding of ATP. Taken together, the initial velocity and product inhibition plots support steady-state ordered binding of the substrates ATP and XMP to the ATPase domain, with ATP being the first substrate to bind followed by XMP.

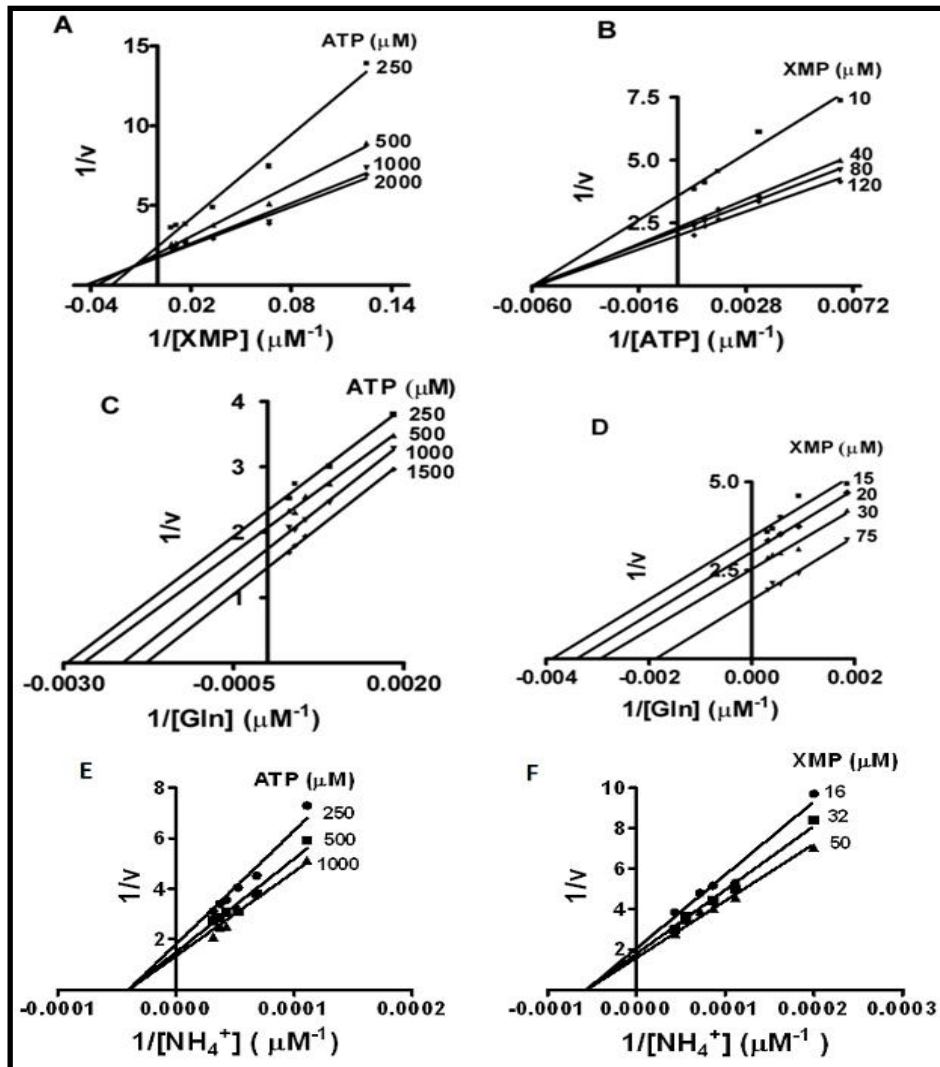


Figure 2.4. Initial velocity (v) patterns for PfGMP synthetase reaction.

Double reciprocal plots represent the initial velocity patterns with respect to XMP, ATP, glutamine and NH_4^+ . In each experiment, one substrate was varied at regular intervals keeping the other at different fixed concentrations, while the third substrate was kept at a constant saturating concentration. Assay conditions were as described in methods. In plots A, C and E, ATP is the fixed variable substrate with XMP, glutamine and $(\text{NH}_4)^+$ as the varied substrates, respectively. The concentrations of ATP are indicated against each line. In plots B, D and F, XMP is the fixed variable substrate with ATP, glutamine and ammonia as the varied substrates, respectively. The concentration of XMP is indicated against each line. The concentration of ATP, XMP and Q when maintained at saturating concentrations were, 2 mM, 0.15 mM and 5 mM, respectively. The units for $1/v$ are $\mu\text{moles}^{-1} \text{min mg}$. All the experiments were done thrice and the reproducibility was within 15%. The results of one representative experiment are presented here.

Table 2.2. Kinetic parameters and line patterns obtained from initial velocity studies on PfGMPS

Varied ^a substrates	fixed ^b substrate	apparent Michaelis constants (μM)				pattern
		MgATP	XMP	Gln	NH_4^+ ^c	
ATP vs XMP	Gln	212 ± 31	10.0 ± 1.9			I ^d
XMP vs ATP	Gln	167 ± 42	16.9 ± 3.1			I
Gln vs XMP	ATP		26.8 ± 2.4	570 ± 77		P ^e
Gln vs ATP	XMP	196 ± 31		589 ± 83		P
NH_4^+ vs XMP	ATP		7.2 ± 1.4		16.0 ± 2.3	I
NH_4^+ vs ATP	XMP	142 ± 35			16.3 ± 3.0	I

^aIn all pairs of varied substrates, the first one was varied continuously and the second at different fixed concentrations. ^bAll the fixed substrates were kept at saturating concentrations as mentioned in "materials and methods". ^c $(\text{NH}_4)_2\text{SO}_4$ was used and the apparent Michaelis constants are in mM. ^dIntersectng. ^eParallel.

Glutaminase domain. This domain hydrolyzes glutamine to glutamate and NH_3 , with the latter product channeled to the ATPase domain. The effect of varying glutamine at different fixed concentrations of ATP with XMP at saturating concentration (Fig. 2.4 C) or at different fixed concentrations of XMP with ATP saturating (Fig. 2.4 D), resulted in parallel patterns in double reciprocal plots. Similar patterns were obtained when either XMP or ATP were the variable substrates at different fixed concentrations of glutamine, with the invariant substrate at saturating concentration. Parallel plots suggest the occurrence of an irreversible step between the binding of XMP or ATP and glutamine and hence, a ping-pong mechanism. In the case of *E. coli* GMPS the parallel initial velocity pattern in $1/v$ versus $1/\text{Gln}$ plots at different fixed concentrations of ATP has been proposed to indicate that XMP binds between ATP and glutamine (von der Saal et al., 1985). This possibility is ruled out in the case of PfGMPS, as $1/v$ versus $1/\text{Gln}$ plots

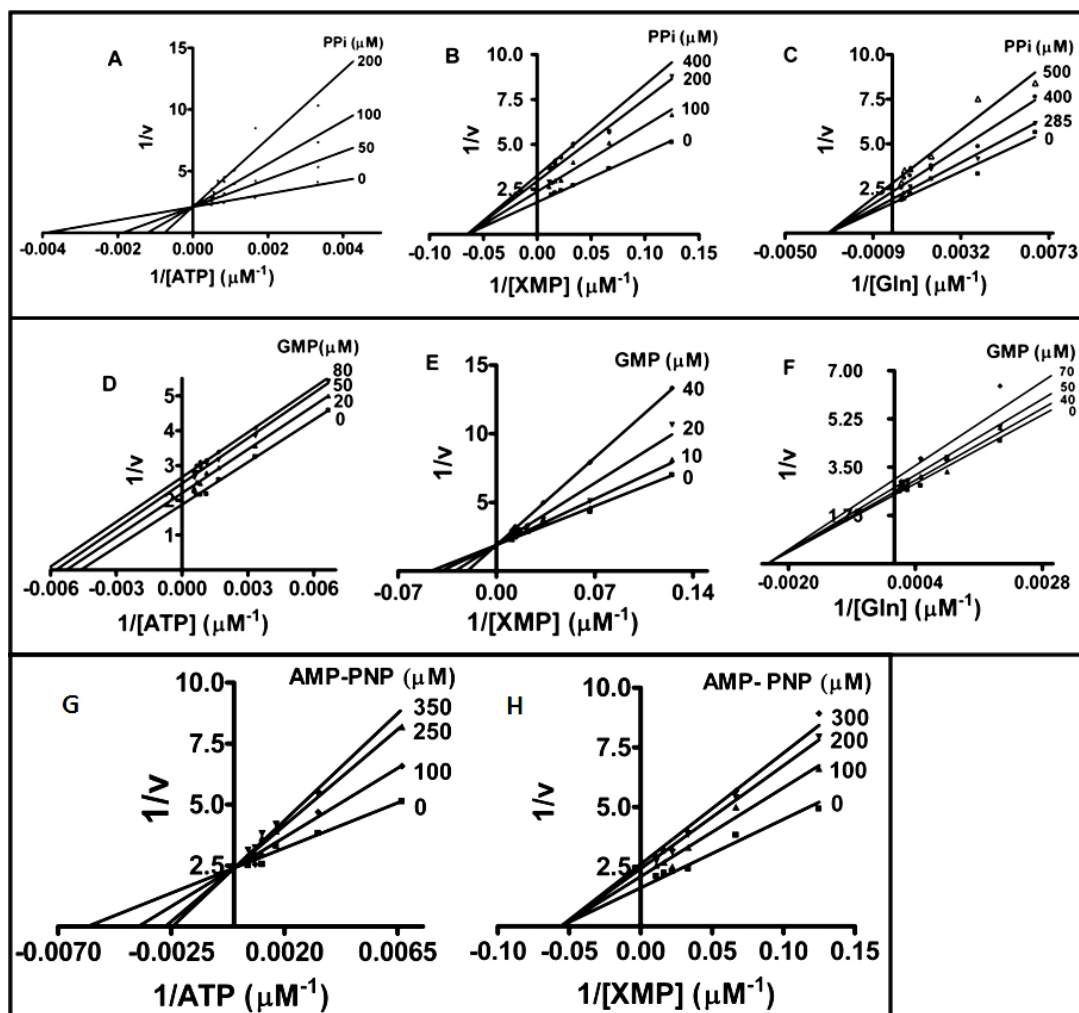


Figure 2.5. Product inhibition patterns for PfGMP synthetase reaction.

Double reciprocal plots show the effects of PPI, GMP and AMP-PNP as inhibitors with respect to the three substrates. In each plot concentration of one substrate was varied at different fixed concentrations of the inhibitor (indicated against each line) keeping the remaining two substrates at saturating concentration. Assays were done under standard conditions described in methods. When saturating, the concentration of ATP, XMP and glutamine were fixed at 2 mM, 0.15 mM and 5 mM respectively. In plots A, B and C, PPI is the inhibitor with ATP, XMP and glutamine as the variable substrates, respectively. In plots D, E and F, GMP is the inhibitor with ATP, XMP and glutamine as the variable substrate, respectively. G and H represent the plots where ATP and XMP respectively, were the variable substrates with AMP-PNP as the inhibitor. In all plots, the units for $1/v$ were $\mu\text{moles}^{-1} \text{min mg}$. Each experiment was done at least twice and reproducibility was within 10%. Shown are results from one experiment.

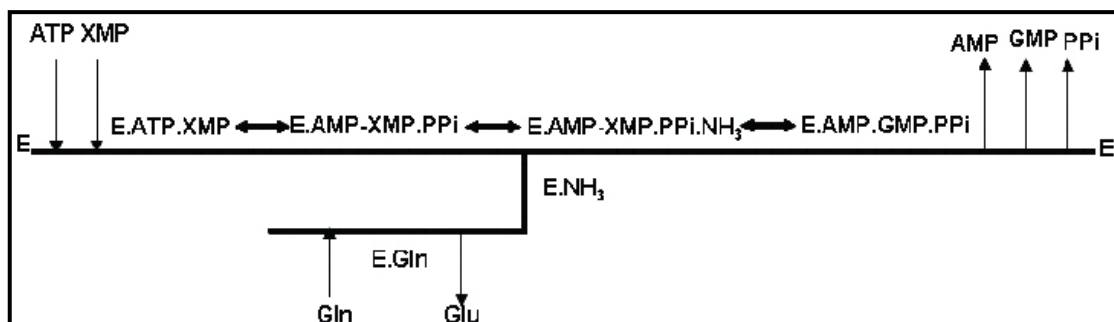
Table 2.3. Apparent inhibition constants for inhibition of PfGMP synthetase by products and substrate analogs.^a

Variable substrate	Inhibitor	K_i (μM)	Pattern
XMP	GMP	38.0 ± 6.7	Competitive
	PPi	443 ± 46	Noncompetitive
	AMP-PNP^b	611 ± 69	Noncompetitive
ATP	GMP	179 ± 16	Uncompetitive
	PPi	36.4 ± 7	Competitive
	AMP-PNP^b	210 ± 42	Competitive
Glutamine	GMP	390 ± 79	Noncompetitive
	PPi	933 ± 136	Noncompetitive

^aThe invariant substrates were held at saturating concentration, ^bAMP-PNP is an analog of ATP

at different fixed concentrations of ATP remained parallel even at subsaturating concentration of XMP. The pattern in this plot should have been intersecting if XMP bound to the enzyme in between the binding of ATP and glutamine. We also find that both PPi and GMP are non-competitive inhibitors with respect to glutamine (Fig. 2.5 C, F) suggesting that ATP and XMP bind independent of glutamine. Recently Abbott et al., (Abbott et al., 2006) have also shown that in *E. coli* GMPS, removal of GAT (glutamine amidotransferase) domain does not affect the binding of XMP and ATP to ATPase domain. Initial velocity measurements where glutamine was replaced with ammonia in the reaction also indicated that in PfGMPS, binding of XMP is not between the binding of ATP and ammonia, as $1/v$ versus $1/\text{NH}_4^+$ plots with ATP or XMP as fixed variable, were intersecting (Fig. 2.4 E, F). It is interesting to note that in the case of *E. coli* GMPS plots of $1/v$ versus $1/\text{NH}_4^+$ PfGMPS at different fixed concentrations of ATP resulted in parallel lines while $1/v$ versus $1/\text{NH}_4^+$ plots at different fixed concentrations of XMP were intersecting. The above results suggested that the parallel pattern in all the glutamine plots ($1/v$ versus $1/\text{Gln}$) could be due to

the presence of an irreversible step involving the release of products AMP, PPi or glutamate, prior to the attack of adenylyl-XMP intermediate by ammonia leading to the formation of GMP. The parallel pattern arising from the release of AMP is ruled out, as adenylyl-XMP intermediate would have to remain bound to the enzyme until attack by ammonia at the C2 of XMP. The data is also not indicative of release of PPi because a competitive inhibition pattern was seen when PPi was varied with respect to ATP and, plots of $1/v$ versus $1/\text{NH}_4^+$ at different fixed ATP or XMP concentrations were intersecting, supporting the absence of PPi release before the binding of NH_3 (Fig. 2.4 E, F). This leaves only the possibility of glutamate release prior to the reaction of ammonia with adenylyl-XMP intermediate. Glutamate and its analog, γ -glutamyl methyl ester did not inhibit PfGMPS activity (upto 5 mM), further suggesting that the enzyme cannot retain glutamate once it is formed. Coupled enzyme assays using glutamate dehydrogenase indicated glutamate release even in the absence of other substrates (Table 2.4) suggesting that glutamate release could occur prior to GMP formation, thereby giving rise to parallel pattern in double reciprocal plots. However, these studies do not indicate whether glutamate release is conditional for the movement of ammonia to the ATPase domain. The results are summarized in scheme 2.2.



Scheme 2.2. Model depicting the kinetic mechanism of PfGMP synthetase

Table 2.4. Effect of ligand binding (ATP, XMP and AMP-PNP) to ATPase domain on activity of the glutaminase domain.

Substrates	activity in the glutaminase domain ^a .
ATP, XMP, Gln., Mg ²⁺ ^b	100
ATP, Gln., Mg ²⁺	58
XMP, Gln., Mg ²⁺	57
Gln., Mg ²⁺	56
Gln.	59
AMP-PNP, XMP, Gln., Mg ²⁺	77

^aThe experiment was done twice with each assay in duplicate. The values from the two experiments agreed to within 10 %. Shown are values that are an average of the duplicates from one experiment. ^bThe amount of glutamate formed was estimated using glutamate dehydrogenase and the protocol followed was as described in methods. The amount of glutamate produced from glutamine in presence of ATP, XMP and Mg²⁺ was taken as 100 %.

2.4.3. Mg²⁺ requirement for PfGMPS activity

Shown in Fig. 2.6 A is the dependence of PfGMPS activity on Mg²⁺ ions. The data best fitted to the equation for positive cooperativity, with Hill coefficient of 4.4 and half maximal activity at 2.09 ± 0.03 mM of Mg²⁺. This suggested the presence of multiple binding sites for Mg²⁺ on PfGMPS. Maximum activity was reached at 5.5 mM of Mg²⁺, which is 2.7 fold the concentration of ATP present in the reaction, suggesting that apart from Mg²⁺ being complexed with ATP, an additional binding site necessary for activity, is present on each subunit of PfGMPS. To further confirm this observation, ATP was varied with Mg²⁺ at a fixed concentration of 2 mM and the resultant plot is shown in Figure 2.6 B. It is evident from the figure that maximum activity was not achieved at 2 mM of MgATP, but at a lower concentration of 1.2 mM.

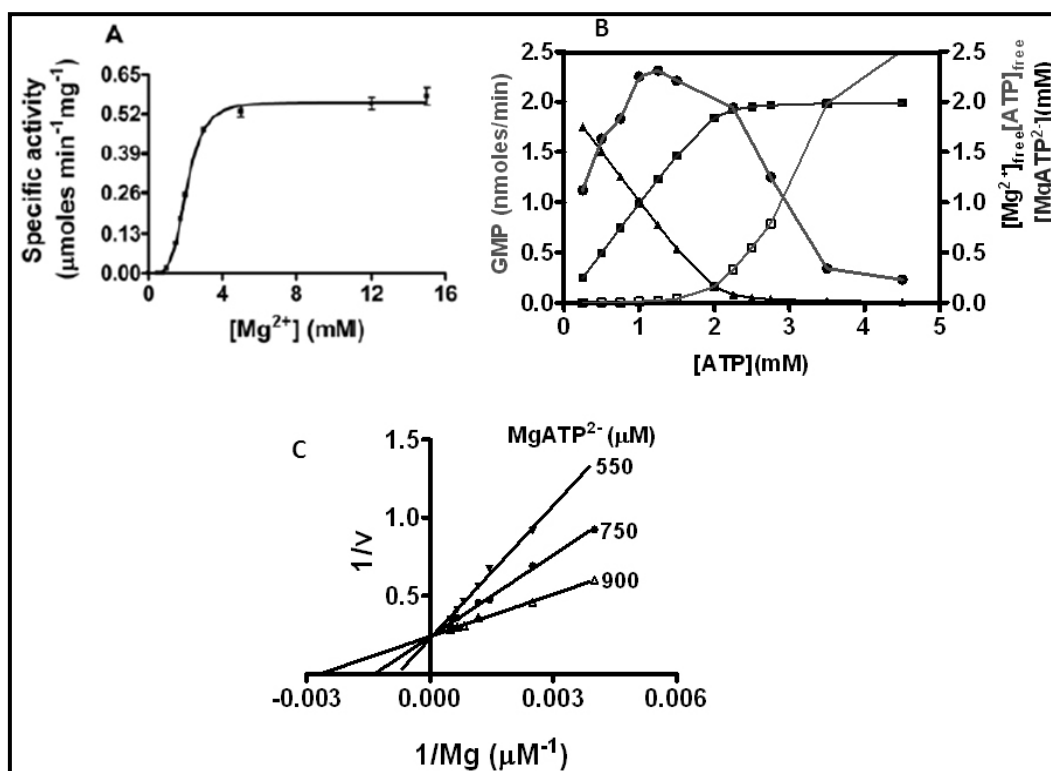


Figure 2.6. Dependence of PfGMP synthetase activity on Mg²⁺ concentration

All the assays were done using standard conditions described in methods with EDTA omitted from all reactions. A. Activity of PfGMPS with respect to Mg²⁺, at fixed concentration of ATP (2 mM). The data fitted best to positive cooperativity equation ($v = V_{max}[S]^h/[S]^h + K_{0.5}^h$, where h is the Hill coefficient and $K_{0.5}$ is the substrate concentration at which half of the sites are occupied). B. Effect of varying ATP concentration on PfGMPS activity at fixed concentration Mg²⁺ (2 mM), (●) represents the activity as the formation of GMP in nmole min⁻¹, (■) represents [MgATP²⁻], (◆) represents free [ATP] and (▲) represents free [Mg²⁺]. C. Plot of 1/v versus 1/[Mg²⁺] at different fixed concentrations of MgATP. All experiments were repeated thrice to confirm reproducibility. Shown are results from one representative experiment.

When free ATP concentration exceeded 2 mM, activity decreased as a consequence of drop in the concentration of free Mg²⁺. This suggests that either free ATP competes for MgATP binding site or that the enzyme has additional requirement for free magnesium. To confirm whether ATP is a competitive inhibitor of MgATP, Mg²⁺ concentration was varied at different fixed concentrations of MgATP, keeping XMP

at saturating concentration. The plot of $1/v$ versus $1/[Mg^{2+}]$ showed intersecting pattern (Fig. 2.6 C), which rules out the possibility of ATP being a competitive inhibitor of MgATP, as the expected plot in that case would be parallel (Nakamura and Lou, 1995). The drop in activity on increase of ATP concentration above that of Mg^{2+} is thus a consequence of the fact that PfGMPS binds free Mg^{2+} apart from MgATP (Fig. 2.6 B).

2.4.4. Inhibition by nucleosides, nucleotides and purine bases

PfGMPS is inhibited by GMP (the product of the reaction) with a low K_i value of $38.0 \pm 6.7 \mu M$, while IMP and AMP were weak inhibitors (Table 2.5). Our studies show that guanine derivatives, (8-azaguanine, 6-thioguanine, guanosine, GDP and GTP) all inhibit PfGMPS moderately. Adenosine was also found to inhibit PfGMPS while xanthosine failed to show any effect. Psicofuranine (9- β -D-psicofuranosyl-adenine), an analog of adenosine, exhibited a weak inhibitory effect while chloroadenosine and decoyinine (9- β -D-(5, 6-psicofuranoseenyl)-adenine) had no effect on PfGMPS activity. Decoyinine and psicofuranine are specific inhibitors of GMPS from other sources, indicating that *P. falciparum* enzyme has binding attributes different from other enzymes. Mizoribine monophosphate, a nucleotide analogue and α, α , -dimethyl-4-[1,1,2,2-tetrafluoro-2-(4-methylphenyl)ethyl]-benzenemethanamine hydrochloride have been to be the potent inhibitors of GMP synthetases from human and fungal sources respectively, however, the inhibitors did not exhibit any effect on the parasite enzyme.

2.5. Discussion

PfGMPS exhibits 42 % identity with *E. coli* GMPS and only 20 % with its human counterpart. Human GMPS has a large insertion in the ATPase domain common to many higher eukaryotic GMP synthetases, but absent in prokaryotic counterparts. This insertion at the C-terminus is also absent in PfGMPS, however, this enzyme has a unique insertion of 20 amino acid residues in the GAT domain which is absent even in GMP synthetases from other species of *Plasmodium*. The role of this insertion has not yet been deduced.

Table 2.5. Inhibition of PfGMPS by nucleosides, nucleotides and their derivatives^a

Inhibitor (0.5 mM)	% inhibition^b
Guanosine	50
GDP	42
8-azaguanine	40
GTP	40
Adenosine	37
6-thioguanine	27
Psicofuranine	25
AMP	22
IMP	10

^a*hypoxanthine, chloroadenosine, xanthosine, inosine and decoyinine did not inhibit PfGMPS at a concentration of 0.5 mM. ^beach value is an average of two measurements that agreed within 5 %.*

We were successful in cloning and expressing the protein to high level permitting detailed structural and functional analysis. The overexpression of the same protein attempted earlier by the consortium ‘Structural Genomics of Pathogenic Protozoa (SGPP)’ was reported to be low (Mehlin et al., 2006).

The subunit molecular weight of PfGMPS (65 kDa) is comparable to the bacterial (58 kDa) and yeast proteins (59 kDa), but smaller than the human counterpart (77 kDa), that contains a long insertion in the ATPase domain. Our studies show that PfGMPS is a dimer, with strong interface interactions and is stable even at 1.5 M NaCl concentration. The *E. coli* GMPS is a dimer (Sakamoto et al., 1972; Tesmer et al., 1994), while enzymes from higher eukaryotes including human have been shown to be monomers (Lagerkvist, 1958; Lou et al., 1995; Nakamura and Lou, 1995; Spector, 1975). The presence of large insertions near the dimerization domain in GMP synthetases of higher eukaryotes seems to preclude them from

forming dimers (Tesmer et al., 1996). This reflects the diversity in oligomeric status of this class of enzymes and hence, they probably may exhibit different modes of regulation and varied functions.

Comparison of kinetic constants of PfGMPS with that of *E. coli* and human enzyme shows that this enzyme is more related to bacterial homolog. PfGMPS does not show any cooperativity with respect to ATP, XMP and glutamine or NH_4^+ , as all the v versus $[\text{S}]$ plots exhibited Michaelis-Menten behaviour and Edie-Hofstee plots were not parabolic. Unlike the *E. coli* and *P. falciparum* enzymes, human GMPS shows cooperativity with respect to XMP. Although ammonia efficiently replaces glutamine as nitrogen source in *E. coli* GMPS, eukaryotic GMP synthetases including PfGMPS seem to prefer glutamine as the physiological substrate as evidenced by the high K_m for ammonium. Similar observations have been reported from other eukaryotic GMP synthetases (Nakamura and Lou, 1995; Page et al., 1984; Spector, 1975; Spector and Beacham, 1975). The k_{cat} of PfGMPS is 10 fold lower than that of the human enzyme. This may be a step towards the regulation of the synthesis of adenine and guanine nucleotides, as the *P. falciparum* genome has very high proportion of AT compared to GC nucleotides. A possible support for this comes from the recent studies on *P. falciparum* CTP synthetase, which has been shown to have a very low specific activity of $76 \text{ nmole min}^{-1}\text{mg}^{-1}$ (Yuan et al., 2005), suggesting lower activity with respect to CTP synthesis.

The results in this study also show that Mg^{2+} binding to PfGMPS is cooperative, a feature similar to human GMP synthetase (Nakamura and Lou, 1995). Mg^{2+} concentration in excess of ATP concentration was needed for full enzyme activity, suggesting the presence of multiple Mg^{2+} binding sites on PfGMPS. Such requirement has been shown in GMPS from *E. coli* (von der Saal et al., 1985) and human (Nakamura and Lou, 1995) and also in PEP carboxykinase, glutamine synthetase, pyruvate kinase and carbamoyl phosphate synthetase (Foster et al., 1967 ; Gupta et al., 1976; Hunt et al., 1975; Raushel et al., 1978). Though kinetic evidence for multiple Mg^{2+} binding sites is available, the specific role of the different Mg^{2+} ions has not been elucidated.

Initial velocity measurements show the occurrence of sequential and not ping-pong mechanism in the ATPase domain of PfGMPS. However, the data also indicate the presence of an irreversible step in the process of catalysis with parallel pattern in plots where glutamine was varied with respect to ATP or XMP. This pattern is akin to

the two site ping-pong mechanism (Barden and Scrutton, 1972; Fresquet et al., 2004; McClure et al., 1971; Northrop, 1969) where the coupling of two reactions leads to parallel pattern in double reciprocal plots (when a substrate from one site is varied with respect to a substrate from the other site) due to the release of a product from one site. Our results show that the parallel initial velocity plots with PfGMPS are due to the release of glutamate before the attack of adenylyl-XMP intermediate by ammonia. Product inhibition studies showed that glutamate is not an inhibitor of PfGMPS suggesting its low affinity towards the enzyme and thus the first product to get released. Nakamura et al., (Nakamura and Lou, 1995) have also shown that glutamate does not inhibit human GMP synthetase. The kinetic scheme for PfGMPS (Scheme 2.2) deduced from the results involves ordered binding of ATP and XMP, with ATP binding first followed by XMP. While glutamine binding is independent of the binding of ATP and XMP, the glutaminase assays suggest a level of co-ordination of activity between the two domains. Our kinetic scheme also shows the order of release of products, where glutamate is the first product to get released, followed by AMP which is a very weak inhibitor of PfGMPS. The scheme also suggests that the release of GMP is prior to PPi, both of which are competitive inhibitors of their respective substrates, as the value of K_m/K_i for XMP/GMP (0.56) is lower than that for ATP/PPi (4.9) suggesting the enzyme's higher affinity for PPi. This supports the suggestion by von der Saal (von der Saal et al., 1985) that PPi is the last product to be released. PPi and GMP have also been shown to be competitive inhibitors of ATP and XMP, respectively for GMPS from other sources (Nakamura and Lou, 1995; Spector and Beacham, 1975; Spector et al., 1976). Overall, this data suggests the occurrence of two-site ping-pong mechanism in which the two individual reactions are coupled to carry out the synthesis of GMP in a concerted manner.

Inhibition studies on PfGMPS using various analogs of nucleosides and nucleotides permitted differentiation of the ligand binding specificities of the human and parasite enzymes. The two adenosine antibiotics, decoyinine and psicofuranine, have been shown to specifically inhibit *E. coli* (Fukuyama and Moyed, 1964; Kuramitsu and Moyed, 1966; Slechta, 1960; Spector and Beacham, 1975; Spector et al., 1976) and human GMP synthetases (Lou et al., 1995; Nakamura and Lou, 1995). Udaka and Moyed (Udaka, 1963) have shown that psicofuranine is an irreversible inhibitor of *E. coli* GMP synthetase, however in case of human GMPS, it was shown

to be reversible. McConkey (McConkey, 2000) has shown the inhibition of growth of intraerythrocytic parasites in culture by psicofuranine, albeit at high concentration of inhibitor (IC_{50} 300 μ M). Our results show that psicofuranine is a weak inhibitor of PfGMPS compared to human enzyme (IC_{50} 46.5 μ M) supporting the McConkey's findings. Decoyinine is a weaker inhibitor of PfGMPS and did not inhibit upto 500 μ M when compared to the human enzyme (IC_{50} 17.3 μ M). Adenosine, chloroadenosine and xanthosine have been shown to inhibit GMPS from Ehrlich ascite cells (Spector et al., 1984), but no inhibition was seen in case of PfGMPS with respect to chloroadenosine and xanthosine. Overall, the studies show that guanosine and its analogs are better inhibitors of PfGMPS compared to others used in the study. The differences in inhibition between the *P. falciparum* and human enzymes highlight the utility of the parasite enzyme as a potential drug target.

In summary, this study has given a detailed insight into the kinetic mechanism operating in PfGMPS, which would help in further understanding this class of enzymes. The study also suggests that PfGMPS is more related to prokaryotic (*E. coli*) GMP synthetases than to eukaryotic (human) counterparts. This could prove to be helpful in the design of specific drugs for malaria acting through this enzyme.

CHAPTER 3

Chapter 3

Ammonia channeling in *P. falciparum* GMP synthetase: biochemical and NMR spectroscopic investigation

3.1. Summary

Ammonia channeling, a characteristic process in glutamine amidotransferases (GATs), ensures the transfer of ammonia from glutaminase domain to the acceptor domain through a structure called as ammonia tunnel. Presence of this catalytically necessary mechanism in these enzymes guarantees the obliteration of ammonia generated by glutamine hydrolysis from equilibrating with the outside medium. Biochemical, structural and theoretical evidences for the mechanism have been evoked in many of the GATs. This chapter provides detailed information on ammonia channeling that has been reported for different GATs, with a thrust on aspects of the process in *P. falciparum* GMP synthetase. A combination of biochemical assays and NMR spectroscopic measurements, site-directed mutagenesis and chemical labeling was involved to gain insight into the process in the parasite enzyme.

3.2. Introduction

3.2.1. Biochemical and structural aspects of ammonia channeling in glutamine dependent amidotransferases

Substrate channeling is a process in which a metabolite or a reactive intermediate is transferred from one active site to another without its equilibration with the bulk solvent, and may involve two or more sequential enzymes in the process (Ovádi et al., 1978). This phenomenon has many physiological implications that encompass (1) control of metabolic flux, (2) protection of reactive and/or toxic intermediates, (3) enhanced catalytic efficiency and, (4) decreased diffusion of

reaction intermediates from catalytic sites (Anderson, 1999; Keleti and Ovadi, 1988; Vertessy and Ovadi, 1987; Wakil SJ, . 1983). Tryptophan synthase (TS), a tetrameric enzyme consisting of $\alpha_2\beta_2$ subunits and catalyzing the final two steps of tryptophan biosynthetic pathway, presents one of the classical examples for intra-molecular substrate channeling. Crystal structure of TS from *S. typhimuriam* provides physical basis for the presence of 25 Å hydrophobic conduit which runs between the active sites of α and β subunits, and transports indole across the two active sites (Hyde et al., 1988; Hyde and Miles, 1990). Thymidylate synthase–dihydrofolate reductase (TS-DHFR), a bifunctional enzyme from *Leishmania major* presents a well understood example of inter-molecular electrostatic channeling. In this enzyme complex, TS catalyses the conversion of deoxy uridine monophosphate (dUMP) and 5,10-methylene tetrahydrofolate to deoxy thymidylate monophosphate (dTMP) and dihydrofolate, and then DHFR regenerates tetrahydrofolate by reduction of dihydrofolate using NADPH. The 40 Å long electrostatic highway present on surface of the enzyme is mostly lined by positively charged residues (Knighton et al., 1994; Stroud, 1994).

Ammonia channeling is a type of substrate channeling in which ammonia generated in the glutaminase domain of amidotransferases is transferred to the acceptor domain through a passage present within the protein, and involves the concerted contribution of both structural and biochemical features of the protein in driving the process. The basic hypothesis in amidotransferases for amination of the acceptor molecules envisages the nucleophilic attack of ammonia (holding a lone pair of electrons) on the electron deficient site in the acceptor molecule (Massiere and Badet-Denisot, 1998). This mechanism necessitates that ammonia must retain the lone pair of electrons to react with the acceptor molecule and hence, protection from the bulk solvent prevents its protonation. It is proposed that evolution of ammonia tunnels in amidotransferases has been a step towards the same process. Biochemical evidence for ammonia channeling in amidotransferases has been provided well before its validation by crystal structures. In *E. coli* CTP and GMP synthetases, studies involving pH dependence of glutamine and ammonia dependent activities revealed that ammonia produced from glutamine does not mix with the bulk solvent and hence, it was concluded that ammonia from glutamine is being channeled within the protein (Levitzki and Koshland, 1971; Zalkin and Truitt, 1977).

The first structural evidence for the occurrence of ammonia tunneling in amidotransferases was derived from the $\alpha\beta$ dimer of *E. coli* CPS, where a tunnel-like structure was found to exist in absence of any of its substrates (Thoden et al., 1997). This enzyme forms carbamoyl phosphate from bicarbonate, ATP and glutamine through a process involving the channeling of two intermediates, carbamate and ammonia, within the protein from one active site in the α -subunit to another in the β -domain. The distance that ammonia travels from glutamine hydrolyzing site to amination site is 45 Å and the overall length of the tunnel connecting glutaminase domain, carbamate producing site and the carbamoyl phosphate synthesis site is ~100 Å. The wall of the preformed ammonia tunnel between the active sites is mainly contributed by backbone atoms and non-polar side chains (except for the presence of Glu²¹⁷ and Cys²³¹) that protect ammonia from protonation. The average diameter of the tunnel is 3.5 Å and this is probably needed for the accommodation of the bigger carbamate molecule. In order to show that ammonia produced from glutamine hydrolysis is indeed channeled within the protein and the ammonia from bulk does not access the tunnel, ¹⁵N NMR spectroscopy was employed where ¹⁵N labeled citrulline was measured as the reaction product. This study showed that ¹⁵N NH₄Cl present in the bulk solvent is unable to access the channel in presence of glutamine (Mullins and Raushel, 1999). Further validation of the physical nature of the tunnel was elicited by mutating the potential tunnel-lining residues that either led to the blockage of the channel (Huang and Raushel, 2000a; Huang and Raushel, 2000b) or perforation of the tunnel wall (Thoden et al., 2002). In either case, the intermediate passage was affected resulting in the leakage of ammonia into the outside medium.

E. coli glutamine phosphoribosylpyrophosphate amidotransferase (GPAT) is a classic example of ammonia channeling in class II amidotransferases (Krahn et al., 1997). GPAT catalyses the transfer of ammonia from glutamine to phosphoribosylpyrophosphate that produces phosphoribosyl amine, PPi and glutamate. The crystal structure solved in presence of DON and cyclic phosphoribosyl pyrophosphate (cPRPP), representing active conformation of the protein, highlighted a 20 Å conduit lined with hydrophobic amino acids connecting the two active sites. Unlike the structure of CPS, no preformed ammonia tunnel exists in the unliganded structure of GPAT (Muchmore et al., 1998). Biochemical and mutational analysis of *E. coli* GPAT has validated the occurrence of ammonia channeling in this enzyme.

E. coli asparagine synthetase catalyses incorporation of ammonia into aspartate, either by using glutamine or external ammonium, to form asparagine. Crystal structure of this enzyme, having the catalytic cysteine in the glutaminase domain mutated to alanine, has been obtained with glutamine and adenosine monophosphate bound to the protein (Larsen et al., 1999). Analysis of the structure shows a conduit, mostly lined with a set of conserved non-polar residues, connecting the glutaminase and the acceptor domains. Recent biochemical studies on this enzyme using isotope-edited ^1H NMR spectroscopy showed that $^{15}\text{NH}_4\text{Cl}$ supplied in the external medium can access the tunnel in presence of high glutamine concentration, suggesting that ammonia channel may not be closed fully (Li et al., 2007).

Glutamate synthase, an Ntn-type amidotransferase, portrays an example of an ammonia tunnel that is patched by both polar and non-polar residues. The enzyme has a two-way mechanism for the formation of glutamate; (1) directly via glutamine hydrolysis and, (2) reductive transfer of ammonia onto 2-oxoglutarate to produce iminoglutarate and its subsequent conversion to glutamate. During this reaction Fe-S clusters are used for transfer of electrons and FMN and NADPH provide the reducing equivalents. Crystal structure from *Azospirillum brasillense* solved in presence of L-methionine sulfonate (L-MetS), a glutamine analog, FMN and 2-oxoglutarate (Binda et al., 2000) revealed a discontinuous and constricted 31Å passage between the glutaminase domain and the 2-oxoglutarate binding site. The channel in the glutaminase and the acceptor domains is lined with polar and hydrophobic residues, respectively.

Fair amount of information on mechanism and operation of ammonia channeling has come from the biochemical and structural studies carried out on yeast imidazole glycerol phosphate synthase (IGP synthase), the enzyme that converts N^1 -[(5'-phosphoribulosyl)-formimino]-5-aminoimidazole-4-carboxamide ribonucleotide (PRFAR) into 5'-(5-aminoimidazole-4-carboxamide) ribonucleotide (AICAR) using glutamine as nitrogen source. Structure of unliganded IGP synthase did not elicit any tunnel, however, the structure solved in presence of acivicin and PRFAR seems to order the two domains and a free path for ammonia was evident (Chaudhuri et al., 2001). The tunnel extending from the glutaminase domain to the cyclase domain is surrounded by charged residues. A gate-like organization of polar conserved residues, referred to as “charged gate” regulates the entry of ammonia into the cyclase domain.

Part of the tunnel within the cyclase domain is mainly surrounded by hydrophobic residues (Myers et al., 2003).

L-Glutamine:D-fructose-6-phosphate amidotransferase, (GlcN6P synthase), generates glucoseamine 6-phosphate from fructose 6-phosphate using glutamine as a ammonia source. Liganded crystal structures of the enzyme from *E. coli* containing DON and either glucose 6-phosphate or fructose 6-phosphate (Mouilleron et al., 2006) highlighted a 18 Å long tunnel between the two active sites. The unliganded structure was devoid of a similar passage (Teplyakov et al., 2001).

A recently solved crystal structure of *M. tuberculosis* NAD synthetase (LaRonde-LeBlanc et al., 2009) has provided new understanding of mechanism and architecture of ammonia tunnels. This enzyme catalyses the conversion of nicotinic acid adenine dinucleotide (NaAD⁺) to nicotineamide adenine dinucleotide (NAD) using a molecule each of ATP and glutamine. The structure was solved in presence of DON (in the GAT domain) and NaAD in the acceptor domain. The inter-molecular tunnel predicted in this protein is structurally the first of its type (intermolecular) that connects glutaminase and acceptor domains of two different subunits, G1 and G5, respectively and hence, contrasts the intramolecular amidotransferase tunnels. The length and width of the tunnel (40 and 2 Å respectively) seems to be optimum for shuttling of one molecule of ammonia at a time and patches of hydrophilic and hydrophobic residues make up wall of the tunnel.

Pyridoxal phosphate synthase (PLP synthase) catalyses the formation of pyridoxal phosphate by availing ammonia from glutamine. The liganded structure showed a 26 Å tunnel running from Cys78 in the glutaminase domain (Yaa E) to the ribulose 5-phosphate binding site in the acceptor domain (Yaa D). Most part of the tunnel that runs through the Yaa D is hydrophobic in nature (Zein et al., 2006). In *E. coli* CTP synthetase, a 25 Å channel is proposed to extend from base of the glutaminase domain to the uridine triphosphate binding site (UTP). This tunnel unlike other amidotransferase tunnels is mostly lined with polar residues and is occupied by some solvent molecules. The structure has been solved in presence of UTP and ATP with unoccupied glutaminase domain (Endrizzi et al., 2004). In formylglycinamide ribonucleotide amidotransferase, a putative 30 Å channel has been proposed to operate between glutaminase (PurS) and the acceptor domains surrounded mostly by hydrophobic residues (Anand et al., 2004). In *E. coli* GMP synthetase structure,

though the synthetase domain is liganded with AMP and PPi, no inter-domain channel is visible (Tesmer et al., 1996). Probably, complete liganding of protein changes its conformation and consequently, creates a route for ammonia transfer. In *Aquifex aeolicus* GATCAB glutamine tRNA synthetase, an amidotransferase, it has been shown that a water filled ammonia channel is open throughout the length between the glutaminase and the synthetase active sites (Wu et al., 2009).

The above survey of different amidotransferases collectively highlights that the enzymes have evolved a well defined mechanism to prevent ammonia from equilibrating with the outside medium. The channels are either fully hydrophobic or patched with hydrophilic residues, but the part contributed by the acceptor domain is generally hydrophobic and ensures the nucleophilicity of ammonia. Most of the amidotransferases whose structures have been solved in absence of ligands are devoid of any visible conduits highlighting that probably, the active conformation is a prerequisite for the creation of such structures. The overall architectural dimensions for the tunnels are different across the enzymes, suggesting their independent evolution.

3.2.2. Mechanistic basis of ammonia channeling revealed by computational approaches

Computational enzymology is a rapidly growing area, with modeling essentially being recognized as a tool for understanding the mechanistic basis of the outstanding efficiency of biological catalysts (Garcia-Viloca et al., 2004). Though computational enzymology has touched diverse aspects from understanding of enzyme catalytic mechanisms through identification of substrates for new enzymes (Hermann et al., 2007) to re-designing of enzymes (Jiang et al., 2008), its venture into mechanism of ammonia channeling in amidotransferases, has been recent. One of the earliest computational studies involving molecular dynamic simulations was conducted on IGP synthase (Amaro et al., 2005). This study demonstrated that a set of conserved residues present at the interface between two sub-domains and within the α/β barrel, are involved both in proper conduction of ammonia across the two subunits, and restriction of external water from accessing the channel. A separate study on the same enzyme (Amaro et al., 2007) using steered molecular dynamic (SMD) approach highlighted that a combined motion of different regions is essential for the allosteric regulation occurring across the two 25 Å distant catalytic sites. SMD

simulation had also been carried out in glucoseamine 6-phosphate synthase (Floquet et al., 2007) that suggested Trp74 acting as a gate for ammonia conduction and its replacement with alanine by site-directed mutagenesis led to leakage of ammonia to the outside medium. Furthermore, this study validated the role of Ala 602 and Val 605 in the transfer of ammonia across the protein. MD simulations on CPS suggested that differences in the solvation energies of ammonia and ammonium dictates the selected conduction of ammonia within the protein (Fan et al., 2008). In a separate study using a similar approach, the authors have shown that once ammonia crosses the hydrophilic part of tunnel in the glutaminase domain, further conduction of ammonia occurs in a hydrophobic environment (Fan et al., 2009). Together, these studies showed that the tunnel between glutaminase and synthetase sites is partly hydrophilic and hydrophobic in nature and underscored the role of different amino acids lining the sides of the tunnel. The overall observations from the computational studies corresponded well with the crystallographic data. A recent MD simulation done on glutamine 5'-phosphoribosylpyrophosphate amidotransferase (Wang et al., 2009) highlighted the occurrence of a set of hydrophobic residues (Phe-254, Tyr-258, Phe-259, Phe-334, Ile-335, Gly-406, and Ile-407) that restrict ammonium from accessing the tunnel. Overall, the tunnel has been described as a tube like structure which runs within the protein that is involved in the transport of ammonia between the two domains.

In summary, computational studies combined with experimental evidences have provided deeper understanding of the mechanistic basis of ammonia channeling. Exclusion of ammonium by these enzymes, using different devised mechanisms, to permit the entry of ammonia serves to satisfy their catalytic necessity.

3.2.3. Ammonia dependant activity in amidotransferases

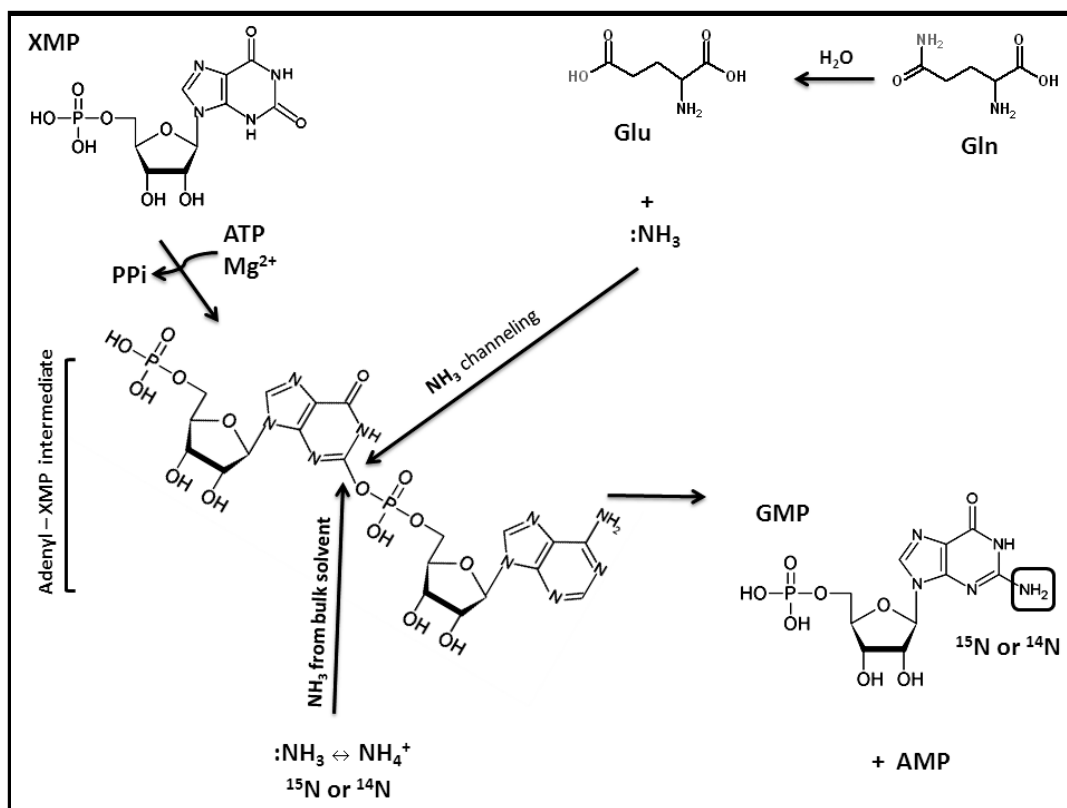
Most of the amidotransferases can by-pass glutamine hydrolysis by directly utilizing ammonia when supplied as ammonium salts. This evokes the possible evolution of these enzymes from the primitive ammonia dependent enzymes (Grieshaber, 1972; Jensen, 1976; Kane et al., 1972; Zalkin and Murphy, 1975), that led to the expansion of their substrate specificity for nitrogen incorporation through the recruitment of the glutaminase domain. *In vivo* utilization of ammonia by Gln-ATs has been demonstrated for anthranilate synthase (Paluh et al., 1985; Zalkin and

Murphy, 1975), glutamine phosphoribosyl pyrophosphate amidotransferase (Mantsala and Zalkin, 1975) and CPS (Massiere and Badet-Denisot, 1998; Rubino et al., 1986; Zalkin, 1985).

Specific utilization of either ammonia or glutamine is an interesting feature displayed by some Gln-ATs. In *E. coli* asparagine synthetase, the isoenzyme asnA is specific for ammonia alone, while asnB solely utilizes glutamine (Scofield et al., 1990). CPS across different species presents an interesting example regarding the utilization of external ammonia or glutamine that also reflects on physiology of the organism. CPS from rat and human exclusively utilizes ammonia, though a glutaminase domain with the catalytic cysteine replaced by serine, is present (Haraguchi et al., 1991; Nyunoya et al., 1985), while, *E. coli* CPS and the mammalian CPS II have been reported to be specific for glutamine only (Chaparian and Evans, 1991; Lusty, 1992; Rubino et al., 1986). In spite of the presence of all three triad residues (Cys-His-Glu) in the glutaminase domain of *Rana catesbeiana* CPS, the enzyme is unexpectedly unable to hydrolyze glutamine. Engineering of a non-triad mutation in the glutaminase domain has made the enzyme capable of hydrolyzing glutamine (Saeed-Kothe and Powers-Lee, 2002; Saeed-Kothe and Powers-Lee, 2003).

Guanosine monophosphate synthetase (GMPS), a class I glutamine dependent amidotransferase catalyzes the conversion of xanthosine 5'-monophosphate (XMP) to guanosine 5'-monophosphate (GMP) in the purine biosynthetic pathway. In this reaction a molecule of adenosine 5'-triphosphate (ATP) is consumed (Scheme 3.1). GMP synthetases, that have been characterized biochemically from eukaryotic, prokaryotic and archaeal sources, are able to utilize either ammonia or glutamine as source of nitrogen (Bhat et al., 2008; Maruoka et al., 2010; Nakamura and Lou, 1995; von der Saal et al., 1985).

Following sections of this chapter report the studies that were carried out to understand aspects of ammonia channeling in *P. falciparum* GMP synthetase.



Scheme 3.1. Conversion of XMP to GMP by GMP synthetase via the formation of adenylyl-XMP intermediate, using a molecule of ATP and glutamine or ammonia.

3.3. Materials and methods

3.3.1. Materials

Restriction enzymes, DNA polymerases and T₄ DNA ligase were either purchased from New England Biolabs, USA or Bangalore Genei Pvt. Ltd., India and were used according to the manufacturer's instructions. Primers for introducing point mutations were custom synthesized at Sigma-Aldrich, USA. Media components were obtained from Himedia, India. XMP, ATP, ¹⁵NH₄Cl, ¹⁴NH₄Cl and other biochemicals from Sigma-Aldrich, USA, were of the highest quality available. NMR (5 mm internal diameter) tubes and matrices for MALDI-TOF mass spectrometry were purchased from Sigma-Aldrich, USA. All MALDI-TOF and LC-ESI MS spectra were acquired on Ultraflex II and ESI-Q-TOF mass spectrometers (Bruker Daltonics, Germany), respectively. All the PfGMPS activity assays were done either on Hitachi U-2010 or U-2810 spectrophotometers (Tokyo, Japan). CD spectra were recorded

using J-810 Spectropolarimeter (Jasco Corporation, Tokyo, Japan). Protein expression and purification protocols for PfGMPS were same as reported (Chapter 2; Bhat et al., 2008). Protein concentration was determined by Bradford assay (Bradford, 1976) using bovine serum albumin as standard. Data fitting to different equations was done using GraphPad Prism 5.

3.3.2. Assay for PfGMPS activity

Activity was monitored under standard assay conditions, reported earlier (Chapter 2; Bhat et al., 2008). Briefly, reaction rates were monitored as decrease in absorbance at 290 nm due to conversion of XMP ($\epsilon = 4800 \text{ M}^{-1}\text{cm}^{-1}$) to GMP ($\epsilon = 3300 \text{ M}^{-1}\text{cm}^{-1}$). A $\Delta\epsilon$ value of $1500 \text{ M}^{-1}\text{cm}^{-1}$ was used to calculate the amount of product formed. The standard assay consisted of 90 mM Tris HCl, pH 8.5, 150 μM XMP, 2 mM ATP, 5 mM glutamine, 20 mM MgCl_2 , 0.1 mM EDTA and 0.1 mM DTT in a total reaction volume of 0.25 ml. Reactions were initiated with 6 μg of PfGMPS and monitored at 25 $^{\circ}\text{C}$. Kinetic constants for ammonium were determined by varying the concentration of ammonium chloride from 4 to 100 mM, while keeping the other substrates at fixed saturating concentration.

3.3.3. pH titration of glutamine and ammonium dependent activities

Assays were performed under standard assay conditions as mentioned above, except 0.15 M buffers of different pHs (range 6.5 to 10) were used with either NH_4Cl or glutamine used as ammonia source. The different buffers used were, MES (2-(N-morpholino)ethanesulfonic acid) for pH 6.5, Tris HCl for the pH range 7.0 to 8.5 and glycine for 9 to 10. In all the assays which were done at different pHs, either glutamine or ammonium chloride concentration was varied, while keeping XMP, ATP and Mg^{2+} at fixed concentrations. Data obtained at each pH were fitted to Michaelis–Menten equation for the determination of kinetic parameters k_{cat} and K_m (equation 3.1). The values for the parameter V/K obtained at different pHs were fitted to equation 3.2.

$$v = V_{\text{max}}[S]/K_m + [S] \quad (3.1)$$

$$Y = c / (1 + (H/K_1) + (K_2/H)) \quad (3.2)$$

where v represents the initial velocity, V_{max} the apparent maximal velocity, $[S]$ the concentration of varying substrate, K_m the apparent Michaelis constant, Y

represents V/K , c is pH independent value of V/K , H the hydronium ion concentration and K_1 and K_2 the dissociation constants of an acid and/ or a base.

Substrates were buffered to avoid pH change and the pH was checked before and after the reactions. All measured values are reported as average of three parallel experiments. Control experiments were performed to check the stability of PfGMPS and the ionization of ATP and XMP, the two other substrates, under extreme pH conditions (6.5 and 10) used in this study.

3.3.4. Stoichiometry of glutamate and GMP formation

To measure the stoichiometry across glutaminase and ATPase domains, end point measurements for the respective activities were performed. The reaction mixture contained 90 mM Tris HCl, pH 8.5, 150 μ M XMP, 2 mM ATP, 5 mM glutamine, 20 mM $MgCl_2$, 0.1 mM EDTA, 0.1 mM DTT and 24 μ g of PfGMPS in a total volume of 1 ml. At different time points, the reaction was quenched by boiling for 3 min and after centrifugation for 15 min, the cleared solution was divided equally into two tubes. Glutamate formation was measured using the assay conditions described earlier (Chapter 2; Bhat et al., 2008). GMP formation was measured according to the method of Sokomato (Sakamoto, 1978). In this assay perchloric acid to a final concentration of 3.2 % was mixed with the reaction mixture and absorbance was measured at 290 nm and a value of $6 \times 10^3 \text{ M}^{-1} \text{ cm}^{-1}$ was used for molar extinction coefficient of GMP. The validity of this measurement was further verified separately by estimating GMP concentration in the reaction mixture by reverse phase HPLC (on a C_{18} column) using known concentrations of GMP as standard. In a separate assay, an aliquot from the quenched reaction was used for monitoring the concentration of ammonia released if any to the medium, using α -ketoglutarate and NADPH as substrates for glutamate dehydrogenase that served as the coupling enzyme. The reaction assay contained 50 mM Tris HCl, pH 7.4, 3 mM α -ketoglutarate, 0.25 mM NADPH, 0.1 mM EDTA and 2 units of glutamate dehydrogenase in a total reaction volume of 0.3 ml, done at 25 $^{\circ}$ C for 5 min. Absorbance at 340 nm was measured after completion of the reaction and molar extinction coefficient of $6220 \text{ M}^{-1} \text{ cm}^{-1}$ was used for the estimation of ammonia.

3.3.5. Steady state competition assays in presence of both glutamine and external ammonia

The assays contained 85 µg of PfGMPS, 20 mM ATP, 10 mM XMP, 100 mM MgCl₂ and 100 mM Tris HCl, pH 8.5 in a total reaction volume of 0.6 ml. NH₄Cl and/ or glutamine were used at varied concentrations. In the assays where glutamine concentration was fixed (15 mM), NH₄Cl concentration was varied from 0 to 100 mM and similarly, when NH₄Cl was maintained at 100 mM, glutamine was varied from 0 to 15 mM. The reactions were allowed to proceed at 37 °C for 10 min, stopped by boiling for 3 min followed by incubation on ice for 5 min. Estimation of total GMP formed in the reaction was done by UV- spectrophotometry (Sakamoto, 1978).

3.3.6. Enzymatic synthesis of ¹⁵N GMP

To synthesize large quantities of ¹⁵N labeled GMP, 100 µg of PfGMPS were incubated with 10 mM XMP, 20 mM ATP, 100 mM MgCl₂ and 100 mM of ¹⁵NH₄Cl in 100 mM Tris HCl, pH 8.5, in a total reaction volume of 1ml. The reaction was incubated at 37 °C for 30 minutes and stopped by boiling for 3 min, followed by immediate chilling on ice for 5 min and centrifugation for 15 min. The supernatant was transferred to a fresh tube and stored at -20° C till further use. To purify the ¹⁵N labeled GMP, 100 µl aliquots of the supernatant were loaded on to a Q-sepharose column (Tricon column, 10 mm x 20 mm) pre-equilibrated with 10 mM potassium phosphate, pH 3.0. Elution was done with a linear gradient of 0 to 30 % of buffer B (500 mM potassium phosphate pH 3 and 0.8 M KCl) in 10 column volumes. For desalting, 500 µl aliquots of the separated ¹⁵N GMP were loaded on to Q-sepharose (Tricon column, 10 mm x 20 mm) column, using 5 mM ammonium bicarbonate pH 3.0 as both equilibration as well as elution buffer. For the removal of ammonium bicarbonate the sample was lyophilized twice, reconstituted in water and passed (100 µl aliquots) through methanol (2%) equilibrated C₁₈ reverse phase column (GE Healthcare. UK). The elution was done by using a linear gradient of 0 to 100 % methanol. The fraction containing ¹⁵N GMP was lyophilized and stored at -20 °C. All the column chromatography procedures were carried out on AKTA Basic HPLC system (GE Healthcare. UK).

3.3.7. NMR measurements

Competition assays between $^{15}\text{NH}_4\text{Cl}$ and glutamine were performed as described in section 3.3.5, except that the reactions were started with 54 μg of PfGMPS. Products of the competition assays were quantitated by ^{15}N – edited NMR spectroscopy. Standard spectra of GMP were obtained on samples that were enzymatically synthesized to contain ^{15}N at the 2-amino group. The enzymatically synthesized samples of ^{15}N – GMP were HPLC purified and characterized prior to NMR analysis (Section 3.3.6). For accurate measurement of ^{15}N GMP in the competition assays, a standard curve was generated by plotting NMR peak intensities against different known concentrations of ^{15}N GMP quantified by UV-spectrophotometry (Sakamoto, 1978). The concentrations of ^{15}N GMP used for generation of the standard curve were 0.12, 0.20, 0.40, 0.75, 1.2, 1.5 and 2.2 mM. All NMR spectra were acquired on a Bruker Avance (AV500) NMR spectrometer using a triple resonance probe equipped with a single (Z-axis) pulse field gradient accessory. NMR data were acquired on samples prepared in the assay buffer that was adjusted to contain 5% D_2O and a final pH of 4.7 prior to data acquisition. All NMR spectra were acquired at 303 K. Nitrogen – 15 labeled uracil (CIL, Andover Massachusetts, USA) dissolved in DMSO-d_6 to a final concentration of 43 mM was placed in a co-axial inner tube (2 mm internal diameter, Wilmad LabGlass, New Jersey, USA) as an internal standard. Nitrogen – 15 edited NMR spectra were acquired using the one – dimensional version of the FastHSQC experiment (Mori et al., 1995). Peak heights were measured using the NMR data processing and analysis software NMRPipe (Delaglio et al., 1995). Peak heights of ^{15}N – GMP were normalized to the uracil internal standard and then quantitated from the standard curve.

3.3.8. Chemical modification of glutaminase domain

PfGMPS (10 μM) was incubated either with 0.2 mM acivicin (L- [αS , 5S]- α -amino-3-chloro-4, 5-dihydro-5 isoxazoleacetic acid) or 0.25 mM DON (6-diazo-5-oxo-L-norlucine) at 25 $^{\circ}\text{C}$ for 30 min in 50 mM Tris HCl, pH 8.5, in two separate reactions. The ammonia and glutamine dependent activities of the modified enzyme were measured under standard assay conditions (Chapter 2; Bhat et al., 2008) using either 5 mM glutamine or 100 mM NH_4Cl as ammonia source. For analysis of the modified enzyme by MALDI-TOF mass spectrometry, excess of acivicin or DON and

the buffer components were removed by dialyzing the sample against 5 mM Tris HCl, pH 8.0. Trypsin digestion was performed at 37 °C for 30 min using trypsin to PfGMPS ratio of 1:50. The digested sample was mixed with α -cyano-4-hydroxycinnamic acid in 1:1 ratio, spotted onto a MALDI-TOF plate and spectra acquired in the positive ion reflectron mode. For obtaining the sequence of the modified peak the digested sample was passed through a nano LC column attached to an ESI-Q-TOF mass spectrometer run in positive ion mode followed by MS/MS analysis of all the eluted peptides. A linear gradient of 0-100% methanol was used for peptide elution.

3.3.9. Construction and biochemical characterization of C102A PfGMPS

Site-directed mutagenesis of cysteine 102 to alanine (C102A) was achieved by the quick change PCR method with a single mutagenic primer (Shenoy and Visweswariah, 2003). The procedure involved two steps: first an *Eco* RV restriction site was introduced using wild type pQE 30-PfGMPS clone as a template and CCAATTTTTGGTATATGATATCGTATGCAAGAG as the primer and in second step the restriction site was removed to introduce the desired mutation using CCAATTTTTGGTATAGCATATCGTATGCAAGAG as the primer. The mutant DNA generated was subcloned into pET 22b vector in which an N-terminal 6X-His sequence was introduced using GTC GCT AGC CAT CAC CAT CAC CAT CAC GGA and GCA GAG CTC TCA TTC GAA TTC AAT CGT TGC TGG as forward and reverse primers, respectively. Introduction of the desired mutation was confirmed by DNA sequencing and the clone was expressed in Rosetta pLysS strain of B121DE3 *E. coli* cells. Expression and purification conditions for the mutant protein were same as that reported for the wild type PfGMPS (Chapter 2; Bhat et al., 2008), except that the culture was grown at 37 °C for 6 hr post IPTG induction. The kinetic parameters for the C102A mutant for ammonium, XMP and ATP were determined by varying one substrate at a time, while maintaining the other two at saturating concentration and the data were fitted to equation 3.1. For analyzing the glutamine inhibition kinetic data, equations 3.3 and 3.4 were used.

$$v = V_{\max}[S]/(K_m + [S](1 + I/\alpha K_i)/(1 + I/K_i)) \quad (3.3)$$

$$y_{\text{intercept}} = (1/V_{\max}) (1 + I/\alpha K_i)/(1 + I/K_i) \quad (3.4)$$

where, definitions for V_{\max} , $[S]$ and K_m are same as in equation 3.1. $[I]$ represents inhibitor (glutamine) concentration. αK_i and K_i represent the inhibition constants of glutamine for enzyme-substrate (ES) and free enzyme (E) forms, respectively. α is the factor by which affinity of glutamine for ES is changed.

3.4. Results

3.4.1. Biochemical evidence for ammonia channeling

Channeling of ammonia under conditions of complete liganding was addressed by two biochemical assays, pH dependence of glutamine and ammonia dependent activities and, the stoichiometry of glutamate and GMP formation. Though PfGMPS can use both glutamine and external ammonia (Scheme 3.1), the kinetic parameters k_{cat} and K_m for the two substrates are different and also exhibit a pH dependent change. The optimum pH for glutamine and ammonia dependent activities was 7.4 and 9.2, respectively (Fig. 3.1a). Using the experimentally derived kinetic parameters, a theoretical k_{cat} value for a reaction, where there is leakage of ammonia, generated by glutamine hydrolysis, was computed and compared with actual k_{cat} value, to provide support for the presence or absence of channeling in PfGMPS. This was done by 1) employing the experimentally derived ammonium k_{cat} and K_m values of 56 min^{-1} and 132 mM, respectively at pH 7.4, and 2) applying initial velocity conditions where 10 % conversion of 5 mM glutamine (saturating concentration) produces a total of 0.5 mM ammonium.

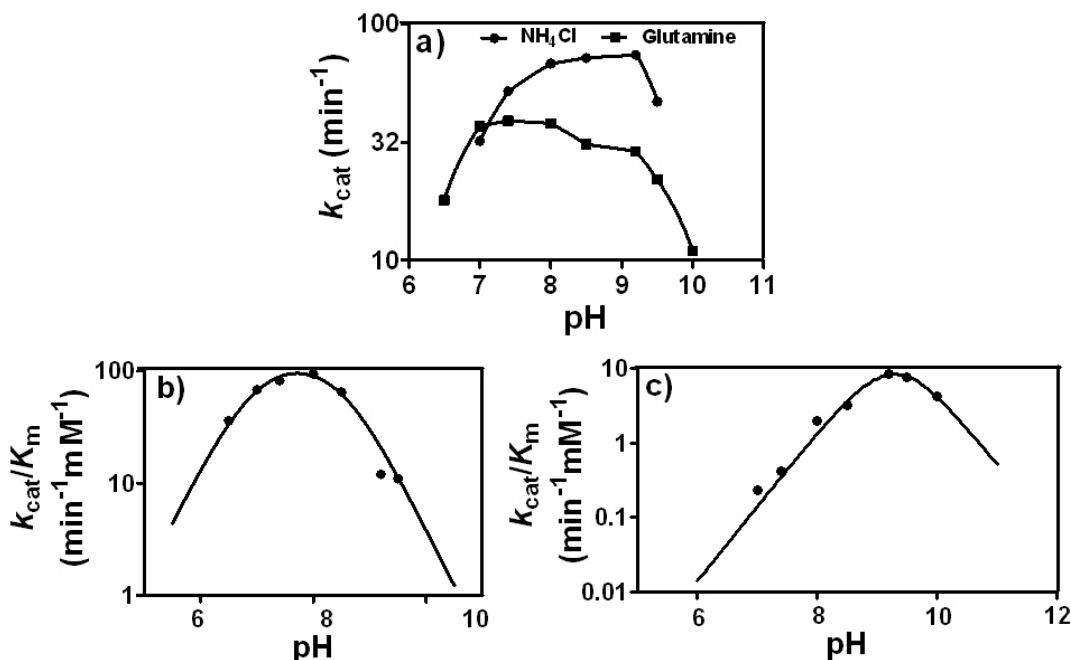


Figure 3.1. pH dependence of kinetic parameters of glutamine and ammonia dependent activities of PfGMP synthetase.

(a) Plot of k_{cat} of NH₄Cl and glutamine dependent activities versus pH, without a fit to any equation. (b) Plot of V/K versus pH where glutamine was used as ammonia source. (c) plot of V/K versus pH where ammonium chloride was used as ammonia source. Plots in (b) and (c) represent the data fitted to equation 3.2. Both glutamine and ammonium chloride dependent activities were measured in presence of saturating concentrations of the ligands, 2 mM ATP, 0.15 mM XMP and 20 mM MgCl₂. Buffer concentration at all pHs was maintained at 0.15 M. At different pHs, activity values measured over a range of glutamine and ammonium chloride concentrations were used to estimate the values of K_m and V_{max} by fitting the data to equation 3.1. Stock solutions of both glutamine and ammonium chloride were buffered to avoid any pH change upon their addition to the reaction mixture, and the pH of the assay mixture was monitored before and after the reaction.

The theoretical k_{cat} value computed for glutamine dependent reaction at pH 7.4 should have been 0.21 min⁻¹ ($56 \times 0.5/132 = 0.21$), if ammonia generated from glutamine first mixes with the bulk solvent and is then re-utilized. However, the observed k_{cat} (40 min⁻¹) is far higher than the theoretical value of 0.21 min⁻¹, ruling out the possibility that ammonia produced from glutamine equilibrates with the external medium.

When glutamine was used as ammonia source, the plot of V/K versus pH (Fig. 3.1b) highlighted the presence of two different ionization constants ($pK_{a1} = 6.9 \pm 0.08$ and $pK_{a2} = 8.5 \pm 0.08$). However, when ammonium chloride replaced glutamine, two similar pK_a values (9.4 ± 0.07 and 9.2 ± 0.05) were obtained (Fig. 3.1c), that were closer to the pK_a value of 9.2 for ammonium ionization (NH_4^+ to NH_3). This suggested that the observed pK_a values could be due to ammonium ionization and, a plot of V/K versus pH, with the K_m corrected for the actual concentration of ammonia at different pHs, yielded a horizontal line without any slope, confirming that ammonia and not ammonium is the actual substrate for PfGMPS. This is further substantiated by the drop seen in ammonium K_m as the pH was increased from 7.0 to 9.5.

Stoichiometry of the glutaminase and the acceptor domain reactions in amidotransferases has been used as an indicator for ammonia channeling. Channeling efficiency is defined as the ratio of GMP to glutamate formed in the ATPase and the glutaminase domains, respectively when glutamine is used as the source of ammonia. Data in Fig. 3.2 indicate that coupling between the two half reactions, glutamine

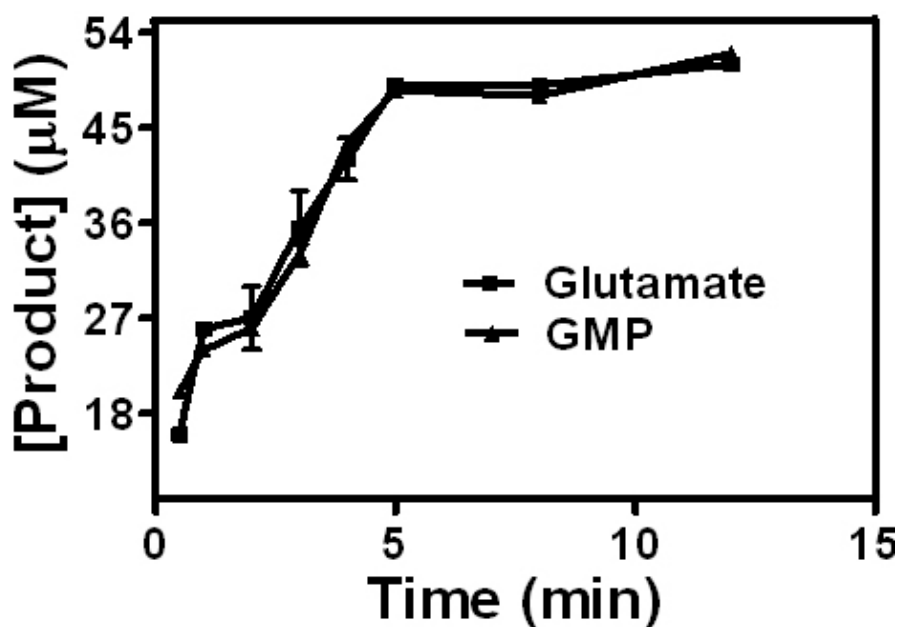


Figure 3.2. Measurement of concentration of products, glutamate and GMP in PfGMP synthetase reaction.

(■) glutamate concentration measured as formation of NAD^+ using glutamate dehydrogenase as a coupling enzyme. (▲) GMP concentration measured at 290 nm using extinction coefficient value of $6000 \text{ cm}^{-1} \text{ M}^{-1}$. The details of assay are given in “materials and methods” (section 3.3.4)

hydrolysis and GMP formation in the PfGMPS reaction was 100 % (1:1 stoichiometry). Also, the glutamate dehydrogenase coupled enzyme assays, performed for estimation of ammonia formed in the PfGMPS reaction, failed to detect any free ammonia. Overall, these results corroborated the conclusions drawn from pH dependent studies of glutamine and ammonium dependent PfGMPS activities.

3.4.2. Steady state competition assays between glutamine and ammonium

Though, ammonium and glutamine are individually used as source of ammonia by PfGMPS, albeit with different kinetic constants, the kinetics of utilization of external ammonia in presence of glutamine has not been examined. Hence, a competition assay was performed wherein both glutamine and ammonium were present together. When NH_4Cl was varied from 0 to 100 mM with glutamine maintained at 15 mM ($30 K_m$), gradual increase in GMP formation was seen. However, when NH_4Cl was fixed at 100 mM ($\sim 5 K_m$) and glutamine titrated from 0 to 15 mM, no increase in activity was observed (Table 3.1).

Table 3.1. Steady state competition assay for the formation of GMP, catalyzed by *P. falciparum* GMP synthetase in the simultaneous presence of glutamine and ammonium¹

NH_4Cl^2 (mM)	GMP (μM)	Fold increase ⁴	Gln ³ (mM)	GMP ⁴ (μM)	Fold increase ⁴
0	616 ± 20	1.00	0.0	864 ± 20	1.00
10	701 ± 32	1.13	0.5	883 ± 22	1.00
15	733 ± 32	1.20	1.0	866 ± 23	1.00
20	796 ± 31	1.30	3.0	933 ± 6	1.07
40	866 ± 8	1.40	6.0	913 ± 9	1.06
60	876 ± 45	1.42	10.0	901 ± 43	1.04
80	900 ± 28	1.46	15.0	896 ± 21	1.04
100	960 ± 30	1.56			

¹Assays were done as mentioned in “materials and methods” (section 3.3.5). All other substrates, ATP, XMP and MgCl_2 were maintained at 20, 10 and 100 mM, respectively. Reactions were started with 80 μg of PfGMPS in a total volume of 600 μl . ²Glutamine was maintained at 15 mM when NH_4Cl was titrated. ³ NH_4Cl was maintained at 100 mM when glutamine was titrated. ⁴Fold increase is with respect to the value where only glutamine or NH_4Cl was present.

These results suggested that PfGMPS is able to utilize external ammonium even in the presence of saturating concentration of glutamine.

To quantify the incorporation of external ammonia into the final product GMP, in the presence of glutamine, NH_4Cl was replaced with $^{15}\text{NH}_4\text{Cl}$ in the competition assays, and product formation was monitored by NMR spectroscopy. Shown in Fig. 3.3 is the purification and characterization of enzymatically synthesized 2-amino labeled ^{15}N GMP that served as a standard. In GMP, amino proton exchange with the bulk solvent is known to be pH dependent (Buchner et al., 1978), necessitating the optimization of a suitable pH at which the protons could be detected. Hence, ^{15}N edited ^1H NMR spectra of the synthesized ^{15}N GMP were acquired over a range of pH (1.5 to 5.5), and the presence of a sharp doublet for the 2-amino protons (6.15 ppm) between pH 4.5 to 5.5 permitted us to select pH 4.7 for all further experiments. The selected pH of 4.7 was also suitable because the ^1H peaks of $^{15}\text{NH}_4^+ / ^{15}\text{NH}_3$ present in the reaction mixture were completely broadened and hence, not detected. Earlier reports on $-\text{NH}_2$ proton exchange rates in GMP have also shown the rate to be slowest in the pH range of 4.5 to 6.5 (Buchner et al., 1978; McConnell et al., 1983). The ^{15}N edited ^1H spectrum of the purified molecule is shown in Fig. 3.3d and was similar to that recorded for the reaction mixture. Figure 3.4a and b represent stacked plot of ^{15}N -edited NMR spectra obtained at different concentrations of ^{15}N GMP and the generated standard curve, respectively.

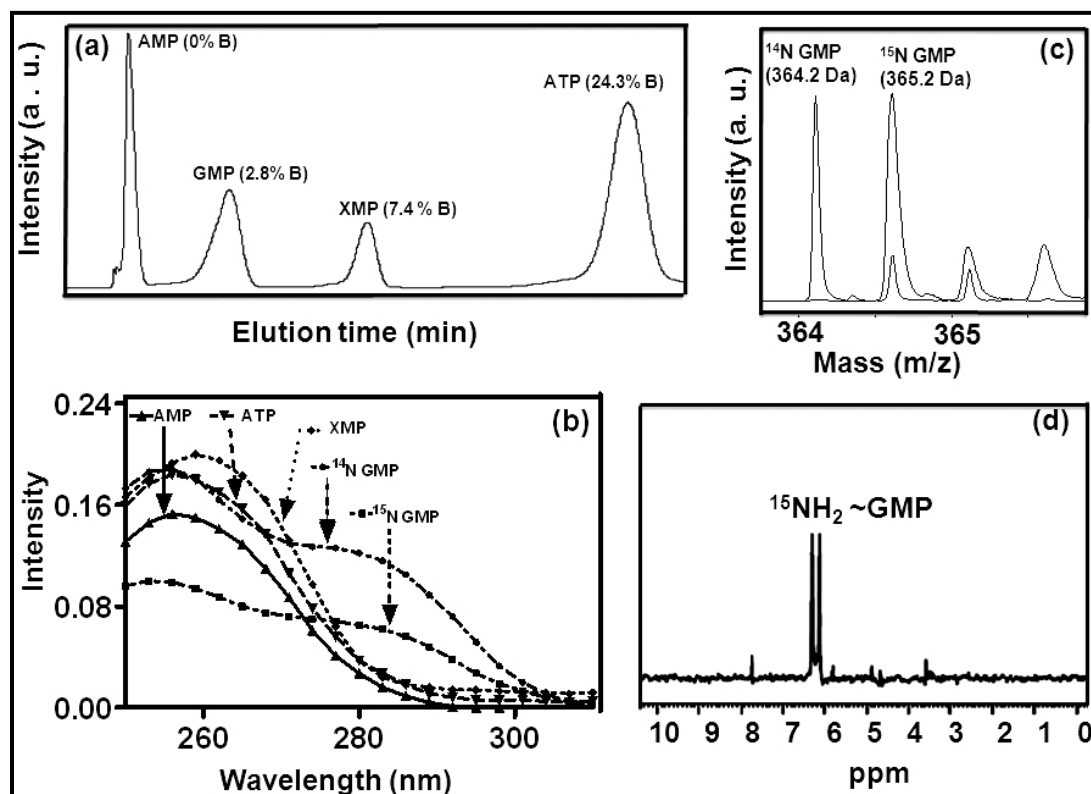


Figure 3.3. Characterization of purified ^{15}N GMP

a) Separation of the different nucleotides present in PfGMPS reaction mixture by anion exchange chromatography. AMP, GMP, XMP and ATP eluted at 0%, 2.8%, 7.4% and 24.3 % of eluent B. The conditions for chromatographic procedure are given in “materials and methods” (section 3.3.6). b) UV wavelength absorption spectrum of purified ^{15}N GMP and its comparison with commercial unlabelled GMP and other nucleotides present in the reaction mixture. All the nucleotide spectra were acquired in 3.2% perchloric acid. c) Comparison of the MALDI-TOF mass spectrum of ^{15}N GMP with that of the commercial unlabelled GMP. Spectra were acquired in positive ion reflectron mode using CHCA (α -cyano-4-hydroxycinnamic acid) as matrix. d) ^{15}N edited ^1H NMR spectrum of purified ^{15}N GMP (δ_{NH} 6.15 ppm)

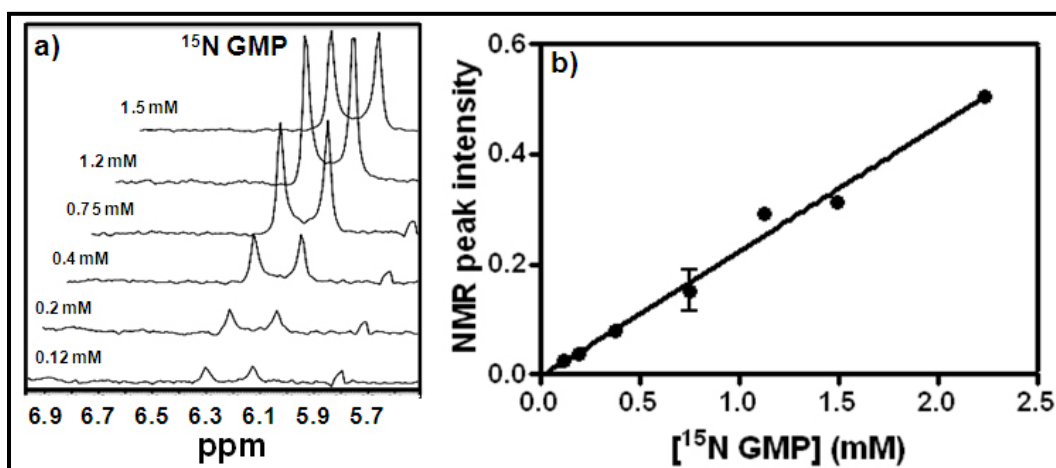


Figure 3.4. One – dimensional ^{15}N – edited proton NMR spectra representing different concentrations of ^{15}N GMP and a standard curve relating the NMR peak intensity to the ^{15}N GMP concentrations.

a) Stackplot of spectra at increasing concentrations of ^{15}N GMP. Concentration of ^{15}N GMP as determined by spectrophotometry is indicated against each spectrum. The doublet at 6.15 ppm corresponds to $^{15}\text{NH}_2$ of GMP. Conditions employed for acquisition of ^{15}N edited ^1H spectra were similar to those used for competition assays. b) Standard curve relating NMR peak intensities obtained from panel (a) to the known concentrations of ^{15}N GMP. See text for details.

With the conditions set for accurately estimating ^{15}N GMP, ^1H fHSQC NMR spectroscopy was used to quantify ^{15}N GMP in the steady state competition assays where either glutamine or $^{15}\text{NH}_4\text{Cl}$ concentration was varied, while keeping the other at a fixed saturating concentration. Figure 3.5 represents a typical spectrum obtained by fHSQC NMR spectroscopy where both glutamine and $^{15}\text{NH}_4\text{Cl}$ were together present in the reaction and shows a doublet at 6.15 ppm ($J_{\text{NH}} = 88$ Hz) that corresponds to the 2-amino group of ^{15}N GMP. As shown in Table 3.2, in assays where glutamine concentration was constant (15 mM) and ^{15}N NH_4Cl varied from 20 mM to 100 mM, presence of glutamine could not prevent the incorporation of ^{15}N label into GMP. Similarly, when $^{15}\text{NH}_4\text{Cl}$ concentration was fixed (100 mM) and glutamine varied from 3 mM to 15 mM, an initial drop in ^{15}N incorporation into GMP was seen, that subsequently plateaued.

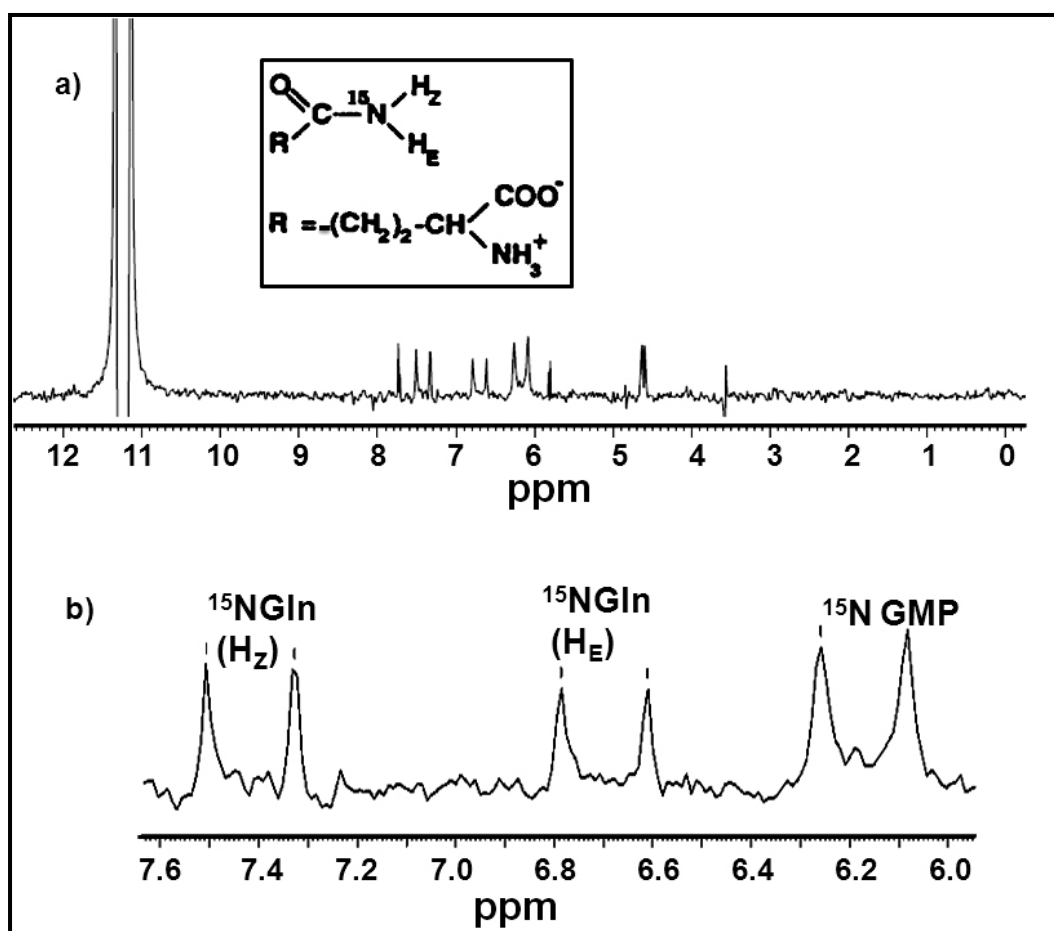


Figure 3.5. One – dimensional ^{15}N – edited proton NMR spectrum of a reaction catalyzed by PfGMP synthetase.

(a) Complete spectrum acquired after the reaction was quenched, deproteinized and pH adjusted to 4.7. The peak at $\delta = 11$. ppm corresponds to ^{15}N uracil used as an internal standard. (b) Expanded region of the spectrum in chemical shift range 6.0 – 7.6 ppm. Observable in this region are the signals arising from ^{15}N GMP (doublet, $\delta_{\text{NH}} = 6.15$ ppm), ^{15}N L-glutamine H_E (doublet, $\delta_{\text{NH}} = 6.7$ ppm) and ^{15}N L-glutamine H_Z (doublet, $\delta_{\text{NH}} = 7.4$ ppm). All the chemical shifts are reported with reference to TSP.

Table 3.2. Steady state competition assays for the measurement of ^{15}N incorporation into GMP catalyzed by *P. falciparum* GMP synthetase¹

$^{15}\text{NH}_4\text{Cl}$ (mM)	Gln (mM)	^{15}N GMP ² (mM)	^{14}N GMP (mM)	Total GMP ³ (mM)	^{14}N GMP/ ^{15}N GMP ratio
0	15	-	0.37 ± 0.04	0.37 ± 0.04	-
20	15	0.13 ± 0.01	0.34 ± 0.01	0.47 ± 0.01	2.56 ± 0.34
40	15	0.17 ± 0.01	0.36 ± 0.02	0.53 ± 0.08	2.05 ± 0.06
60	15	0.21 ± 0.01	0.36 ± 0.07	0.57 ± 0.08	1.68 ± 0.31
80	15	0.23 ± 0.03	0.37 ± 0.04	0.61 ± 0.06	1.60 ± 0.01
100	15	0.25 ± 0.02	0.41 ± 0.07	0.66 ± 0.06	1.67 ± 0.39
100	0	0.52 ± 0.07	-	0.68 ± 0.01	-
100	3	0.39 ± 0.02	0.34 ± 0.06	0.74 ± 0.04	0.88 ± 0.18
100	6	0.27 ± 0.01	0.38 ± 0.03	0.66 ± 0.04	1.41 ± 0.05
100	9	0.25 ± 0.04	0.42 ± 0.00	0.67 ± 0.04	1.67 ± 0.26
100	12	0.27 ± 0.04	0.42 ± 0.03	0.69 ± 0.01	1.56 ± 0.30
100	15	0.25 ± 0.02	0.45 ± 0.02	0.70 ± 0.00	1.78 ± 0.17

¹All assays were done under similar conditions, as mentioned in “materials and methods”. All other substrates, ATP, XMP and MgCl_2 were maintained at 20, 10 and 100 mM, respectively. ²Estimated by ^{15}N edited proton NMR spectroscopy using known quantities of enzymatically produced ^{15}N GMP as standard and all the values are corrected for the natural abundance of ^{15}N glutamine. Values are reported as mean \pm S.D of two independent experiments done with two separate preparations of PfGMPS. ³Quantified by spectrophotometry (Sakamoto, 1978). Errors reported as mean \pm S.D of two independent measurements with each having three replicates.

Apart from the presence of ^{15}N GMP peaks, two doublets at 6.70 and 7.40 ppm consistently appeared in the ^{15}N edited proton NMR spectra (Fig. 3.5a, b), except under the condition where glutamine was absent. Hence, a ^{15}N edited proton NMR spectrum of 15 mM glutamine was recorded that highlighted two low intensity doublets with same chemical shifts as seen in the spectra of assay mixtures, arising from the natural abundance of ^{15}N in L-glutamine. The NMR chemical shifts and coupling constants of the peaks correspond with those reported for the two non-equivalent amide protons of L-glutamine (Kanamori et al., 1995). These results indicated that the peaks at 6.70 and 7.40 ppm arise due the formation of ^{15}N L-glutamine in the competition assays. To check whether complete liganding of

PfATPPase domain is needed for ^{15}N L-glutamine formation, two separate competition assays were performed that contained both glutamine and $^{15}\text{NH}_4\text{Cl}$, but with either ATP, XMP or both excluded, The NMR spectra recorded of these assay mixtures indicated that ^{15}N L-glutamine was not formed, as the peak intensity did not exceed that obtained for the natural abundance of ^{15}N in 15 mM L-glutamine.

3.4.3. Effect of chemical modification and mutagenesis of cysteine 102 on glutamine and ammonium dependent activities

To examine the possible connection that the glutaminase domain may have with the entry of external ammonia, we chemically modified the glutaminase catalytic pocket with acivicin and DON, the two structural analogues of glutamine, known to specifically inhibit the glutamine dependent activity, by irreversible binding (Bhat et al., 2008; Nakamura et al., 1995; Zalkin and Truitt, 1977). To ascertain the covalent binding of acivicin to PfGMPS, a tryptic digest of acivicin treated protein was subjected to MALDI-TOF and LC-ESI-QTOF MS analysis, followed by sequence identification of the selected peptides by employing MS/MS methods (Fig. 3.6). This study allowed us to identify a peptide $\text{K}^{95}\text{-K}^{118}$ (KIPIFGICYGMQEIAVQMNGEVKK) of m/z 2695.39 Da that contained a single cysteine (C102) modified with acivicin (m/z 143 Da). Having confirmed that cysteine 102 is modified by acivicin, we monitored both glutamine and ammonium dependent activities in the acivicin and DON treated PfGMPS. As shown in Table 3.3a, the glutamine dependent activity, as expected was almost completely abolished in both acivicin and DON treated samples. However, 90 % of the activity was retained in both the samples when glutamine was replaced with ammonium in the assay. These results suggested that the modification of the glutaminase domain with acivicin and DON bound to the glutaminase domain do not impede the ammonium dependent activity.

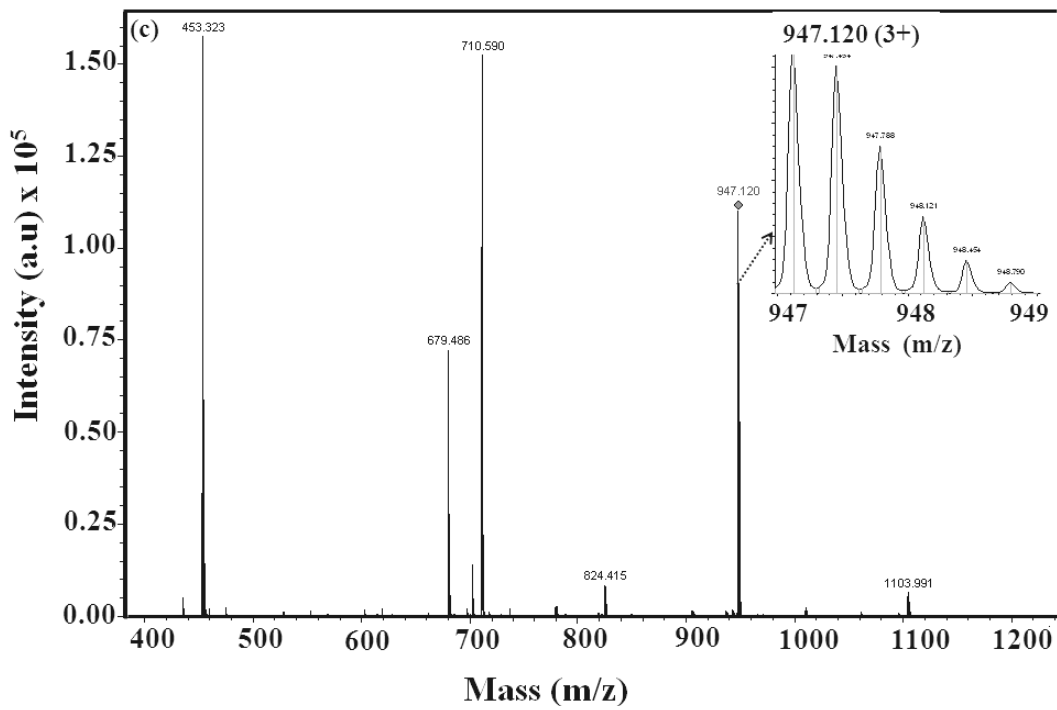
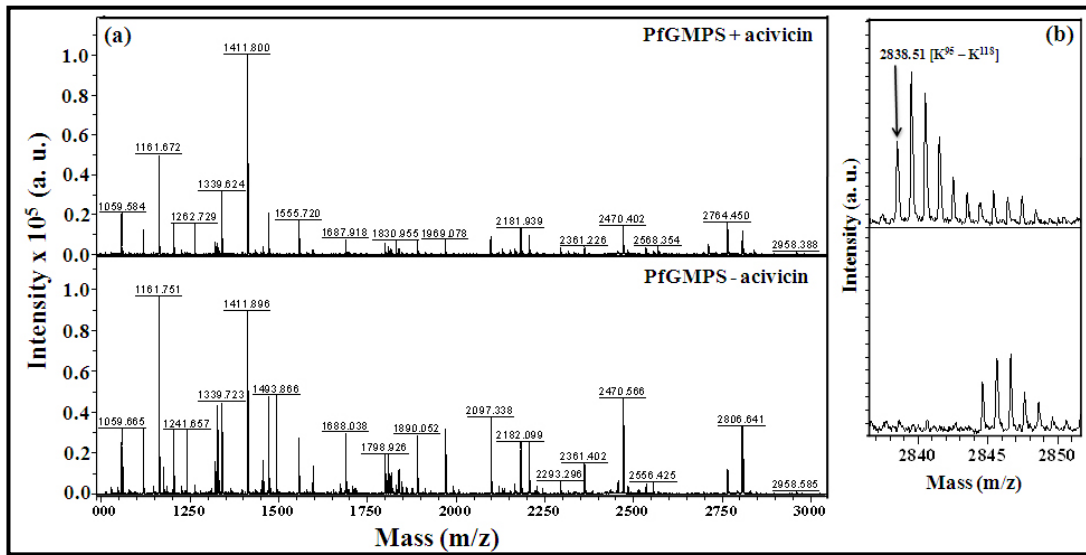


(Figure 3.6 continued)

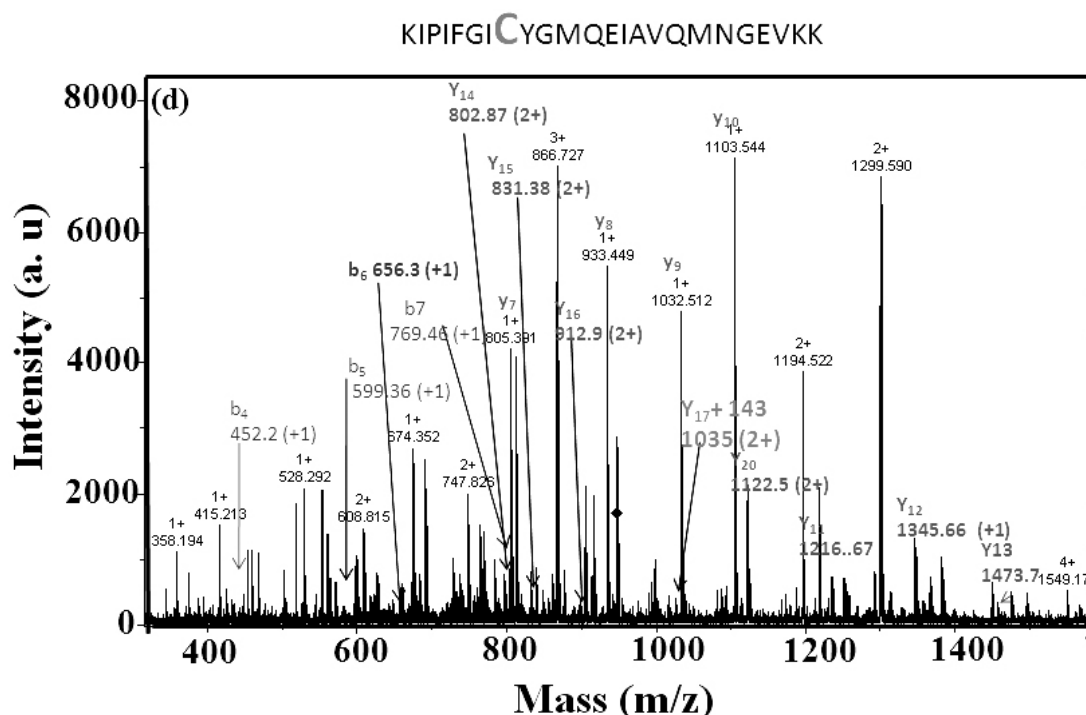


Figure 3.6. Elucidation of PfGMP synthetase covalent modification by acivicin through mass spectrometry.

(a) Complete MALDI-TOF mass spectrum of trypsin digested PfGMPS after acivicin modification and its comparison with that of unmodified PfGMPS. (b) Expansion of the MALDI-TOF mass spectrum between m/z 2837-2851 Da showing the presence of the modified tryptic fragment in acivicin treated PfGMPS and its absence in untreated PfGMPS. Spectra were taken in positive ion reflectron mode using DHB (2, 5-Dihydroxybenzoic acid) as matrix. (c) MS spectrum (between m/z 380-1240 Da) highlighting the triply charged peak of m/z 947.12 Da corresponding to acivicin modified peptide that eluted at 37.6th min. The inset shows expansion of m/z 947.12 Da highlighting quality of the spectrum (d) Spectrum showing the MS/MS of m/z 947.12 Da and assignment of the different ions to the sequence (shown on top of the spectrum). The conditions for acivicin modification and digestion of PfGMPS are mentioned in “materials and methods”.

Table 3.3a. Effect of acivicin and DON on the glutamine and ammonium dependent activities of *P. falciparum* GMP synthetase¹

Inhibitor	Activity (nmoles min ⁻¹ mg ⁻¹)	
	Ammonium dependent	Glutamine dependent
None	714 ± 10	607 ± 7
Acivicin	678 ± 15	48 ± 1
DON	631 ± 14	75 ± 7

¹*PfGMPS* was incubated either with acivicin (0.2 mM) or DON (0.25 mM) for 30 min at 25 °C. Aliquots were assayed for both glutamine and ammonium dependent activities, under standard assay conditions (detailed in “materials and methods”), with either glutamine (5 mM) or ammonium chloride (100 mM) used as source of ammonia. The values are reported as mean ± S.D, estimated from three independent measurements.

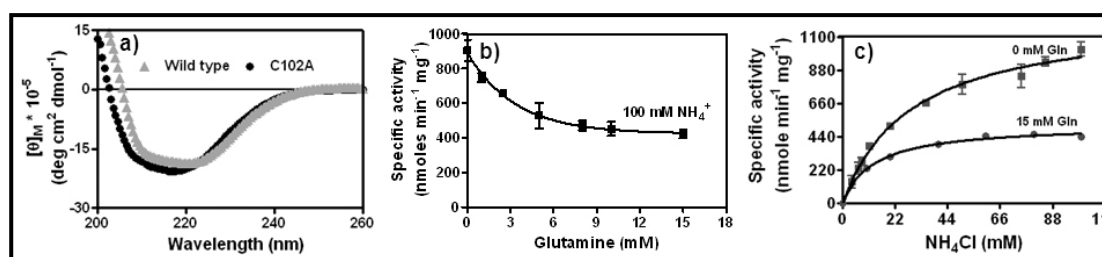
A mutant of *PfGMPS* having Cys 102 replaced with alanine was generated with the aim of having an enzyme that can bind glutamine but not catalyse its hydrolysis. The C102A mutant after purification was assayed for both glutamine and ammonium dependent activities. The kinetic constants for NH₄Cl, ATP and XMP obtained for the ammonia dependent activity of C102A mutant of *PfGMPS* (Table 3.3b) were similar to that of the wild-type enzyme. As expected, the mutant C102A was totally devoid of glutamine dependent activity, agreeing with the results from chemical modification and confirming C102 as the catalytic residue in the glutaminase domain. The CD spectra of the C102A mutant and the wild-type enzymes being similar (Figure 3.7a) ruled out the possibility of structural changes in the mutant contributing to the loss of glutamine dependent activity.

To evaluate the effect of glutamine on the ammonia dependent activity of C102A, assays were performed that contained glutamine at a fixed concentration of 15 mM and NH₄Cl concentration varied from 0 to 100 mM and vice versa, (NH₄Cl fixed at 100 mM and glutamine varied from 0 to 15 mM). Interestingly, presence of 15 mM glutamine in the reaction assays inhibited the ammonium dependent GMP formation to ~50 %, compared to the reaction where glutamine was excluded (Fig. 3.7 b and c).

Table 3.3b. Steady state kinetic parameters of PfGMPS C102A mutant¹

Substrate	K_m (mM)	k_{cat} (min ⁻¹)	k_{cat} / K_m (min ⁻¹ mM ⁻¹)
XMP	0.019 ± 0.002	65 ± 2.5	3.400×10^3
ATP	0.235 ± 0.020	64 ± 1.5	0.272×10^3
NH ₄ ⁺	27.000 ± 3.000	77 ± 2.8	0.029×10^3

¹All the steady state assays were performed under standard assay conditions (detailed in materials and methods) with NH₄Cl used as a source of ammonia. The saturating concentrations of other substrates used during single substrate titrations, were 0.2 mM ATP, 0.15 mM XMP, 100 mM NH₄Cl and 20 mM MgCl₂.

**Figure 3.7. Characterization of C102A mutant of PfGMPS.**

(a) Comparison of far-UV CD spectra of mutant C102A and the wild-type PfGMPS. Cuvettes of 0.1 cm path length were used and each spectrum was average of three scans. The protein concentration of each C102A mutant and the wild-type was 5 μ M. (b) Inhibition of ammonium dependent activity of C102A at different concentrations of glutamine, with ammonium fixed at 100 mM. (c) Inhibition of ammonium dependent activity of C102A at fixed concentrations of glutamine. All the assays were performed under standard assay conditions as detailed in “materials and methods”.

This suggested that a partial inhibition of the ammonium dependent activity in C102A mutant of PfGMPS arose from the binding of glutamine, and prompted us to carry out complete kinetics of glutamine inhibition of the ammonium dependent activity. In the kinetic assays, concentration of one of the substrates (ATP, XMP or ammonium) was varied at different fixed concentrations of glutamine while keeping the other substrates at fixed saturating concentration. The double reciprocal plots ($1/v$ versus $1/$

[S]) for the three substrates (ATP, XMP or ammonium) exhibited parallel line patterns, with the re-plots of intercept versus [glutamine] being hyperbolic (Figure 3.8). Hyperbolic re-plots obtained from the parallel linear primary plots are indicative of mixed hyperbolic or partial uncompetitive inhibition, where infinite concentration of an inhibitor (glutamine) leads to a finite inhibition and hence, the velocity of the reaction unlike the normal uncompetitive inhibition, can never be driven to zero. The parallel nature of the Lineweaver-Burk plots arises from the inhibitor (glutamine) modulating the affinity (K_m) of the substrate for the enzyme and V_{max} to an identical degree. A global fit of the initial velocity data to equation 3.3 yielded kinetic inhibition parameters for glutamine with respect to ATP, XMP and ammonium (Table 3.3c) and the values agreed well with those obtained from the fit of y-intercept values (from Lineweaver-Burk plots) versus [glutamine] to the equation 3.4, for the respective substrates.

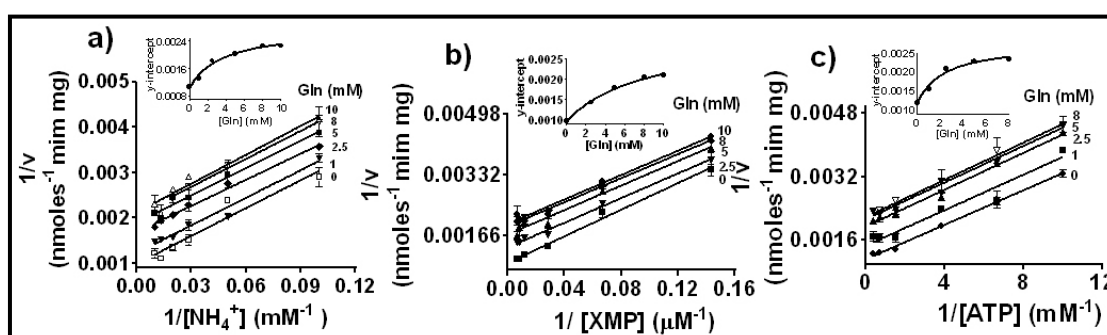


Figure 3.8. Double reciprocal plots of initial velocities ($1/v$) versus different substrate (ammonium, ATP and XMP) concentrations at various fixed concentrations of glutamine.

(a) $1/v$ versus $1/[NH_4^+]$ at 0, 1, 2.5, 5, 8 and 10 mM of glutamine. ATP and XMP were at fixed concentrations. (b) $1/v$ versus $1/[XMP]$ at 0, 2.5, 8 and 10 mM of glutamine with ATP and NH_4^+ maintained at fixed concentrations. (c) $1/v$ versus $1/[ATP]$ at 0, 1, 2.5 and 5 mM glutamine with XMP and NH_4^+ at fixed concentrations. Assay conditions were same as those used for standard assays mentioned in “materials and methods”. The fixed concentrations of substrates used were, 0.2 mM ATP, 0.15 mM XMP and 100 mM NH_4Cl .

Table 3.3c. Inhibition constants of glutamine for the ammonium dependent activity of C102A PfGMPS against different substrates

Substrate	α^1	K_i (mM)	K_m (mM)
XMP	0.30 ± 0.03	9.5 ± 2.5	0.02 ± 0.001
ATP	0.41 ± 0.03	2.7 ± 0.7	0.18 ± 0.010
NH_4^+	0.35 ± 0.03	4.2 ± 1.0	23.00 ± 2.000

All the values were obtained by global non-linear fit of the inhibition data to equation 3.3. α^1 is the factor by which affinity of glutamine for ES is changed.

3.5. Discussion

The present investigation was aimed at understanding aspects of ammonia transfer from glutaminase to ATPase domain in PfGMPS, the only two-domain GMP synthetase reported till now to possess significant leaky glutaminase activity (Chapter 2: Bhat, et al., 2008) when the ATPase domain is not completely liganded. However, during the complete catalytic cycle, the enzyme appears to have evolved a mechanism for preventing such an unwanted process, as 1:1 stoichiometry is seen in the formation of products from the glutaminase and the ATPase domains, by which leakage of ammonia from the enzyme into the outside medium is prevented (Fig. 3.2). A 1:1 stoichiometry across domains has also been reported for glutamine phosphoribosylpyrophosphate amidotransferase and IGP synthase (Bera et al., 2000; Myers et al., 2003). Whether the leaky glutaminase activity seen, when the ATPase domain is unliganded in PfGMPS, is necessary under physiological conditions remains to be investigated. A recently report on *P. horikoshii* GMP synthetase, a two-subunit two-domain GMP synthetase, has shown that the glutaminase domain possesses some glutamine hydrolysing property without involvement of the synthetase domain (Maruoka et al., 2010).

The pH-activity relationship studies with glutamine and ammonium as substrates (Fig. 3.1) agreed with the occurrence of 1:1 stoichiometry and suggested that ammonia generated by glutamine hydrolysis is channeled within PfGMPS from the glutaminase to the ATPase domain. Similar conclusions have been made from the pH kinetics done on CTP synthetase (Levitzki and Koshland, 1971) and *E. coli* GMP synthetase (Zalkin and Truitt, 1977). The two different ionization constants (6.9

± 0.08 and 8.5 ± 0.08) obtained from the plot in Fig. 3.1b could reflect the side chain ionization constants for histidine and cysteine respectively, that has been proposed to form a part of the catalytic triad involved in glutamine hydrolysis in the glutaminase domain. Similar ionization constant values of 6.0 and 8.6 have been proposed for His and Cys, the catalytic triad residues in glutamate synthase (Vanoni et al., 1994).

The ^{15}N edited ^1H fHSQC method employed in our experiments was sensitive enough to detect the different levels of ^{15}N labelled GMP produced in the competition assays permitting us to accurately quantify the molecule. As evident from Table 3.2 even in the presence of saturating concentration of glutamine (15 mM) and at a low concentration of $^{15}\text{NH}_4\text{Cl}$ (20 mM), $^{15}\text{NH}_3$ could still access the adenylyl-XMP intermediate in the ATPase domain. However, the $^{14}\text{N}/^{15}\text{N}$ ratio in total GMP will be dictated by k_{cat}/K_m for the two ammonia sources, after a correction is made for their initial concentrations (Mullins and Raushel, 1999). Such a calculation done for a condition where 20 mM $^{15}\text{NH}_4\text{Cl}$ and 15 mM glutamine were present together, suggested that the theoretical $^{14}\text{N}/^{15}\text{N}$ value of 13.5 was higher than the observed value of 2.56 ± 0.34 . This difference in the values of the theoretical and observed $^{14}\text{N}/^{15}\text{N}$ ratios persisted also in other titrations including the one where both $^{15}\text{NH}_4\text{Cl}$ and glutamine were present at saturating concentrations. The large difference seen between the theoretical and observed values of $^{14}\text{N}/^{15}\text{N}$ ratios highlighted that the ^{15}N GMP fraction in the total pool of GMP is greater than what would be expected on the basis of k_{cat}/K_m . In the competition assays where glutamine concentration was fixed at 15 mM, the value for $^{14}\text{N}/^{15}\text{N}$ ratio after an initial decrease remained constant when $^{15}\text{NH}_4\text{Cl}$ concentration was increased, and similarly, when $^{15}\text{NH}_4\text{Cl}$ was present at 100 mM, increasing concentration of glutamine led to an initial increase in $^{14}\text{N}/^{15}\text{N}$ ratio and subsequently saturated. The above ratios also indicated that absolute quantity of ^{15}N GMP in the assays never exceeded 55 % of the total GMP, suggesting that the ammonia generated from glutamine does not equilibrate with the outside medium, as in that case the ^{15}N incorporation should have been greater than 85 % (calculation based on k_{cat}/K_m ratios of the two substrates). The channeling behaviour in PfGMPS resembles that of Asn B (Li et al., 2007) where glutamine could not impede the incorporation of external ammonia into asparagine, the final product of the reaction. However, asparagine competitively inhibits the glutamine dependent Asn B reaction, with no effect on the utilisation of external ammonium, and this differential

inhibition has been proposed to be contributing to the unusual channeling behaviour seen in the enzyme. In contrast, a similar role for GMP in PfGMPS cannot be entertained, as GMP inhibits the reaction competitively with respect to XMP and manifests similar inhibitory effects (similar K_i) on both glutamine and ammonium dependent activities. In this context, it is interesting to highlight that the glutaminase domain of PfGMPS contains a unique 20 residue insertion and, whether the insertion has any role in the observed channeling behaviour remains to be investigated. In contrast to PfGMPS and Asn B, glutamine in CPS has been shown to fully impede the entry of external ammonium into the enzyme (Mullins and Raushel, 1999). Pertinently, though a biochemical evidence for ammonia channeling in *E. coli* GMP synthetase was provided earlier, no preformed channel was seen in the crystal structure (Tesmer et al., 1996).

The formation of ^{15}N glutamine from ^{14}N glutamine and $^{15}\text{NH}_4\text{Cl}$ in competition assays stems from the exchange process between ^{14}N glutamine and $^{15}\text{NH}_4\text{Cl}$ involving the thioester intermediate formed in the glutaminase domain, onto which $^{15}\text{NH}_3$ gains access leading to exchange with the side chain $-\text{NH}_2$ of L-glutamine. Similar exchange process during thioester intermediate formation has been reported earlier in asparagine synthetase (Li et al., 2007). Our inability to detect ^{15}N glutamine in assays containing both glutamine and $^{15}\text{NH}_4\text{Cl}$ but lacking either ATP or XMP or both, suggested the absence of exchange process in the glutaminase domain when the ATPase domain is unliganded. This could be due to (1) inaccessibility of glutaminase active site to external ammonia or, (2) external ammonia preventing the thioester formation and thereby, glutamine hydrolysis in the glutaminase domain when the ATPase domain is unliganded. The latter mechanism has been reported earlier in CPS (Chaparian and Evans, 1991). where high concentration of ammonium in presence of glutamine abolished the formation of thioester when ATP and bicarbonate, the two other substrates, were excluded from the assay. Detection of the PfGMPS proteolytic fragment with C102 covalently attached to acivicin using mass spectrometry supports the formation of thioester intermediate in the glutaminase domain. Similar acivicin labeled peptide has also been detected in human GMP synthetase tryptic digest (Nakamura et al., 1995). To our knowledge the studies on PfGMPS involving fHSQC experiments form the first report that provide a direct evidence for the formation of thioester intermediate in the GMP synthetase catalysis.

Partial uncompetitive nature of glutamine inhibition with respect to ATP, XMP, and NH_4^+ in C102A mutant of PfGMPS indicates that glutamine can bind to either E or ES form of the enzyme with different dissociation constants (K_i and αK_i , respectively), with the ternary complex ESI being catalytically productive, albeit with less efficiency than the ES form. The differences observed in the dissociation constant (K_i) values for glutamine for PfGMPS with respect to the different substrates (Table 3.3c) reflects on the modulation of inhibitor binding affinity for the enzyme by the substrates. These results corroborated our previously proposed kinetic mechanism (two-site ping-pong) for PfGMPS where glutamate release is the irreversible step between the binding of either ATP or XMP and glutamine. Therefore, glutamine, a mimic of glutamate when bound to the mutant C102A, switches the enzyme to a catalytically less active state. Though the irreversible binding of acivicin and DON to wild type PfGMPS could resemble the binding of glutamine to the C102A mutant of PfGMPS, inhibition of ammonium dependent activity was not seen in the chemically modified enzyme. These observations suggest that the glutamine bound C102A mutant of PfGMPS and the inhibitor (acivicin or DON) modified PfGMPS may exist in different conformational states or the inhibitor (DON and acivicin) packing in the catalytic pocket is different from that of glutamine and hence, the differences in ammonia dependent activities. It is pertinent to note that glutamine has also been shown to inhibit the ammonia dependent activity of C1A mutants of human (Sheng et al., 1993) and *E. Coli* (Boehlein et al., 1994) asparagine synthetases. However, in both the enzymes, the primary reciprocal plots, $1/v$ versus either $1/\text{ammonia}$, $1/\text{aspartate}$ or $1/\text{ATP}$ were intersecting, except for the parallel nature of $1/v$ versus $1/\text{ATP}$ plot seen for the *E. coli* enzyme. Such a pattern has been attributed to the formation of an abortive complex during the ammonia dependent catalysis in the presence of glutamine that leads to its inhibition.

In conclusion, this report provides the first detailed analysis of ammonia channeling in PfGMP synthetase that can serve as a model for comparative investigation of this phenomenon in other GMP synthetases. This study highlights the notion that the optimization of channeling efficiency during evolution in different GATs varies across this class of enzymes. Detailed catalytic and kinetic analysis of individual steps of PfGMPS reaction needs to be carried out to find answers to many unresolved questions highlighted by this study.

Furthermore, studies on other GMP synthetases would throw light on whether the specific aspects of channeling seen in PfGMPS is conserved, or a unique feature of the parasite enzyme.

CHAPTER 4

Chapter 4

Substrate-induced conformational changes in *P. falciparum* GMP synthetase: biochemical and mass spectrometric investigation

4.1. Summary

Dynamics, structural transformations and coordinated domain motions in proteins/enzymes play a pivotal role in their function/catalysis. Biochemical, biophysical and computational advancements have increased our understanding of the dynamics-related processes taking place in proteins and their link to function. Glutamine-dependent amidotransferases (Gln-ATs), modular in nature, are known to undergo substrate-induced changes in domain structure and organization. The main focus of this chapter is on the studies carried out on *P. falciparum* GMP synthetase towards understanding the conformational changes and domain cross-talk in the enzyme. A combination of biochemical assays, optical spectroscopic tools and mass spectrometry was employed to address the question. Brief account of the use of mass spectrometry for understanding the structural changes in proteins and summary of the literature available for conformational changes in Gln-ATs, is also provided in the introductory section of this chapter. Sections (4.3.3 and 4.4.1) describing the irreversible inhibition studies on PfGMPS has already been reported (Bhat et al., 2008).

4.2. Introduction

4.2.1. Conformational changes in proteins and use of high-resolution mass spectrometry.

Role of ligand-driven conformational changes in proteins is a concept widely entertained in enzyme catalysis. Protein dynamics and conformational flexibility are the broadly used terms reflecting the non-rigidity in proteins, and has been implicated to be essential in all important protein functions like, catalysis, ligand binding, protein-protein interactions, signal transduction and cell to cell communication. Over

time, large number of techniques and methodologies have been employed for assessing the dynamic nature of proteins, viz., fluorescence spectroscopy (like steady-state, pre-steady state and time-resolved fluorescence, FRET, FCS etc), circular dichroism, Raman and infrared spectroscopy, ¹⁹F NMR spectroscopy and X-ray crystallography, to name a few. With advances in mass spectrometry for probing protein structure, numerous groups have reported its use in deciphering dynamics in proteins. It is interesting to note that recent strategic advances in mass spectrometry have led to the analysis of non-covalent interactions in the native states of proteins, a step towards studying the proteins in native form (Breukera and McLafferty, 2008 ; Oh et al., 2002; Rand et al., 2009; Zhou et al., 2008). Chemical labeling, limited proteolysis and hydrogen-deuterium exchange in proteins combined to mass spectrometry are routinely used techniques for precise dissection of conformational dynamics.

4.2.1.1. Limited proteolysis in conjunction with mass spectrometry (LP-MS)

The dynamic nature of proteins was realized long back when induced-fit theory for substrate binding in enzymes was proposed by Koshland (Koshland, 1958). That protein is not a single entity, but an ensemble of different conformational states (where thermodynamic principles govern the occurrence of individual populations) has been demonstrated by the use of high resolution techniques and supports the notion that proteins are not rigid when present in solution (Barbar, 1999; Henzler-Wildman and Kern, 2007). This property provides the rationale on the basis of which limited proteolysis mass spectrometry (LP-MS) is employed in proteins to study conformational transitions. Proteases, both specific and non-specific, can act on proteins provided the sites of action are accessible. Substrate binding to protein/enzyme often shifts its conformational equilibrium and hence, the sites available for a protease in unbound form may be inaccessible in the bound form or vice versa. This differential availability of protease sites under different states leads to an altered digestion pattern. In LP-MS, proteins are generally treated with proteases of different specificity to provide complementary evidences for a given observation. The commonly used proteases known to cut at specific sites are trypsin, chymotrypsin, Lys-C, Asp-N, Arg-C and Glu-C (V8 protease) and, those without specificity such as subtilisin, proteinase K, pepsin etc (Cheng et al., 2010; Fontana et al., 2004; Hager-Braun and Tomer, 2005).

The procedure followed in LP-MS is straightforward and the data analysis is comparatively simple. In this technique, proteins with or without ligands are treated with appropriate proteases under limiting conditions (non-optimum temperature, pH and buffer, and the protease to protein/enzyme ratio) that prevent complete fragmentation of the protein. When the protein has to be studied in its holo form, the ligand(s) (substrate, product or analogues of both, a drug or another protein) is/are first allowed to equilibrate at a saturating concentration with the protein and then subjected to proteolysis. Though, SDS-PAGE analysis of the fragmented protein provides a quick view of the digestion pattern, mass spectrometry has almost taken over this step as it reliably provides the identification of different fragments in a short time span. Both MALDI-TOF and ESI MS have been employed for this analysis. Assignment of different peptides is relatively simple when a protease of known specificity is used, as in that case a theoretical peptide map can be generated and compared to the different experimental peptide masses. However, a combination of MS/MS, Edman degradation and use of region-specific antibody is occasionally involved for the unambiguous identification of a peptide. A general schematic representation of the method is given in Fig 4.1.

Two recent examples of the use of LP-MS in resolving conformational changes in proteins are briefly presented. Arrestin 2, a multifunctional adaptor protein involved in desensitization, endocytosis and alternate signaling pathways of seven-membrane spanning receptors, undergoes a conformational change on binding to the activated phosphorylated receptor. Exclusive use of LP-MS demonstrated that binding of a phosphopeptide (V₂-pp), a derivative of the C-terminal vasopressin receptor, to arrestin 2 causes the exposure of Arg³⁹⁴ in the C-terminus and shielding of Arg⁸ in the N-terminus. These studies provided a direct evidence of conformational changes in arrestin 2 associated with its change from basal inactive form to the biologically active conformation (Xiao et al., 2004). Prolyl hydroxylase, an important enzyme for oxygen sensing in humans, was subjected to treatment with different, but structurally similar, inhibitor molecules and LP-MS analysis of the treated samples indicated differential susceptibility of the protein liganded to the different molecules (Stubbs et al., 2009). These studies corresponded well with the earlier biophysical and biochemical evidences, underscoring the reliability of LP-MS technique for medicinal biochemistry.

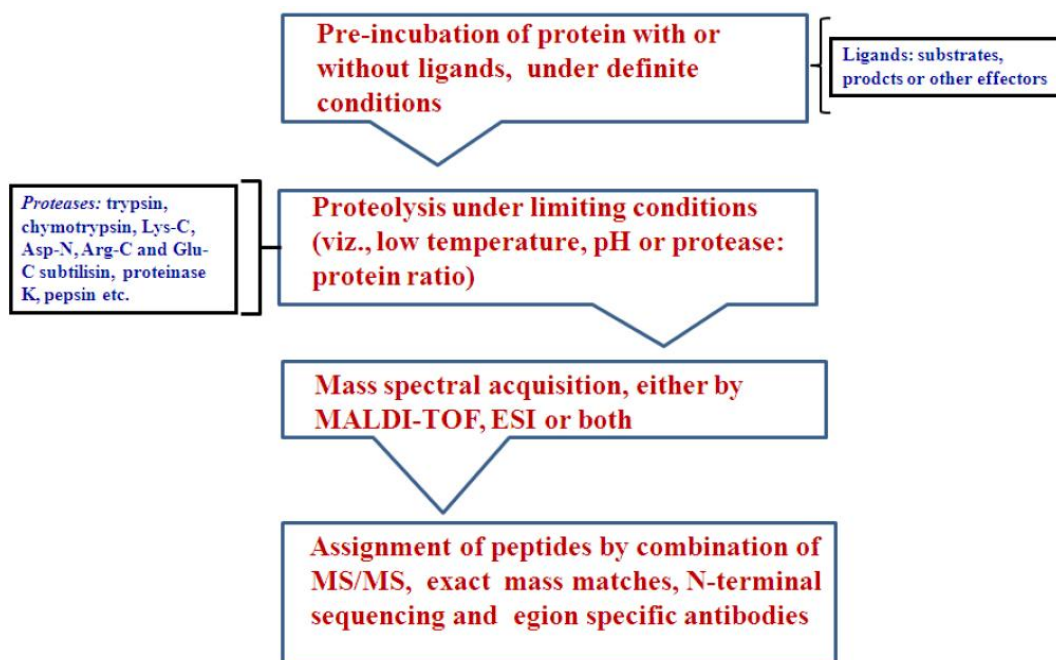


Figure 4.1. Schematic representation of the steps followed in limited proteolysis coupled to mass spectrometry.

4.2.1.2. Hydrogen-deuterium exchange coupled to mass spectrometry (H/DX MS)

In H/DX MS, proteins are labeled via hydrogen-deuterium exchange and the labeled protein is analyzed by different mass spectrometric techniques. Proteins generally contain three types of protons (Fig. 4.2), grouped on the basis of rate of exchange. (1) Protons attached covalently to carbon (marked in red) do not exchange without a catalyst. The hydrogens in polar side chains (hydrogens attached to hetero atoms; N, O, C and S, marked in green) exchange at a very fast rate (10^3 - 10^6 higher than amide protons) at neutral pH and their rates are not readily determined (Bai et al., 1993; Englander et al., 1985). Residues that contribute to the fast exchanging protons are Ser, Thr, Lys, Arg, Asp, Glu, Gln, Asn, Cys, Trp, Tyr and His. The exchange rate of these protons is highly dependent on pH (Fig. 4.3). (3) The protons attached directly to backbone amide groups (marked in blue) exchange with water at rates ranging from milliseconds to several years and are generally measured in H/D exchange studies (Garcia et al., 2004; Morgan and Engen, 2009).

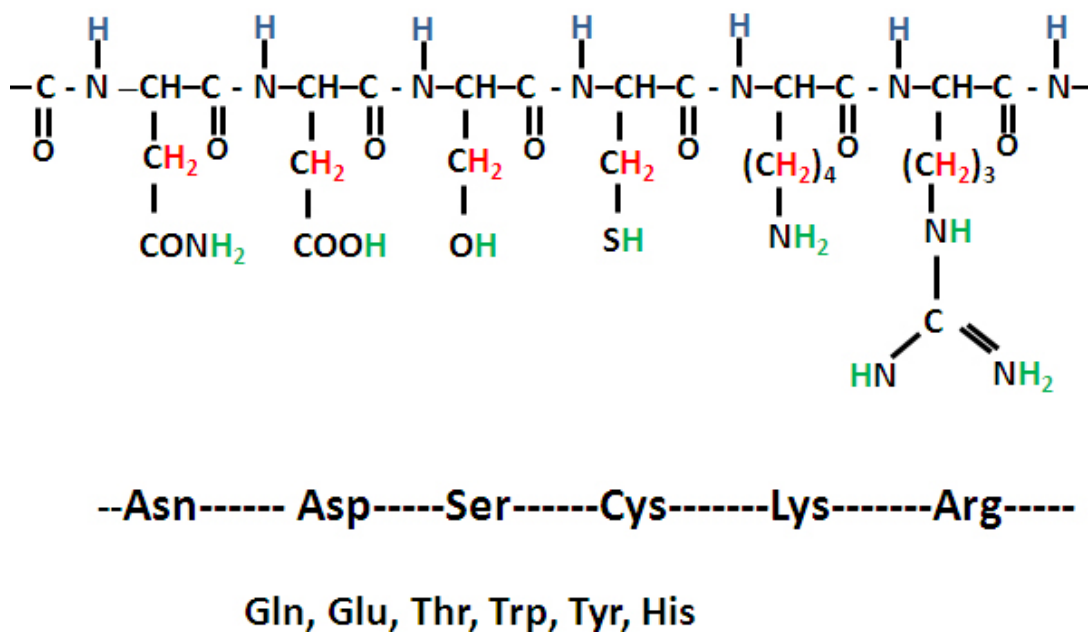


Figure 4.2. Schematic representation of a peptide showing protons with different exchange rates. Colour coded protons; *red*, *green* and *blue* refer to non-exchangeable, fast and slow exchanging protons, respectively. Hetero atom containing residues that mainly contribute the fast exchanging protons are also shown.

The rate of exchange in amide protons is influenced by local inductive effects contributed by the neighboring amino acids, degree of solvent exposure, temperature, and concentration of exchanging catalyst (H_3O^+ , OH^-). Amide protons in folded proteins that are exposed to solvent or reside in unstructured regions exchange faster than those in the core. Differences in exchange rate observed across amide protons reflects on their degree of exposure to the solvent and the networking within secondary structural elements. Protons lying in hydrophobic regions or involved in hydrogen bond formation do not exchange until perturbed by a structural change leading to their exposure to solvent and distortion of the hydrogen bonds. Hence, H/DX propensity of amide protons provides a good estimate of the conformational status, hydrogen bond nexus and solvent accessibility of a protein (Garcia et al., 2004).

Kaj U. Linderstrom-Lang in 1950's introduced the use of isotopic labeling for studying proteins and peptides

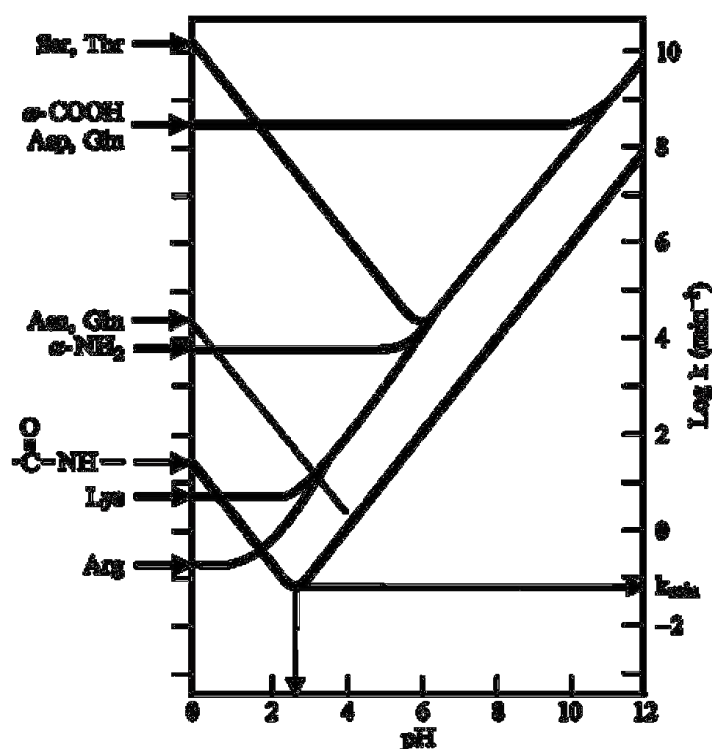


Figure 4.3. Plot of the log of exchange rate constant versus pH, indicating the dependence of proton exchange rate on solvent pH. Figure adapted from Bai et al., (Bai et al., 1993)

(Berger and Linderstrom-Lang, 1957; Hvidt and Linderstrom-Lang, 1954; Linderstrom-Lang, 1955). Early amide proton exchange in proteins was done by tritium labeling followed by separation using chromatography techniques; however, lately the methods have been replaced by hydrogen-deuterium exchange coupled to NMR spectroscopy (Wand and Englander, 1996), resonance Raman spectroscopy (Hildebrandt et al., 1993) and mass spectrometry (Englander et al., 2003), all of which can measure deuterium incorporation. Walter Englander performed experiments using amide proton exchange for folding and unfolding of proteins, where the effect of hydrogen bonding on the exchange of amide protons with solvent was monitored (Englander et al., 1997).

Amide hydrogen exchange is mainly OH^- catalyzed, down to pH 3 and below that by H_3O^+ in water based solutions. The exchange process of amide protons in water can be represented as,

$$k_{\text{ex}} \text{NH} = k_{\text{OH}} [\text{OH}]^- + k_{\text{H}} [\text{H}]^+ + k_0$$

k_{OH} , k_H , and k_0 are exchange rate constants for base, acid and direct water, respectively catalyzed exchange reactions. Using poly-DL-alanine peptide as a model, the above rate constants ($k_{OH} = 1.12 \times 10^{10}$ and $k_H = 41.7 \text{ M}^{-1}\text{min}^{-1}$ and $k_0 = 0.03 \text{ min}^{-1}$) have been derived at 20 °C. Exchange rates of side-chain and amide protons highly correlate with pH and a plot of $\log(k_{ex} \text{ NH})$ versus pH elicits a minimum at 2.5 to 3 (Fig. 4.3). It has been shown that pH change of one unit enhances the exchange rate by 10 fold, reflecting the sensitivity of pH change on the exchange rate (Bai et al., 1993; Molday et al., 1972). Hydrogen exchange rates are also temperature dependent and the rate constants follow the Arrhenius equation. Accordingly, it has been shown that every 10 K increase in temperature raises the exchange rate by three fold. At pH 7 and 25 °C temperature, the solvent exposed amide hydrogens exhibit half-life of 0.01-0.05 sec, whereas, at pH 2.7 and 0 °C, the half-life increases to 1-2 hrs. These conditions (low pH and temperature) are routinely maintained when a protein incorporated with deuterium is present in the quench buffer, during H/D/X mass spectrometry studies. Local inductive effects and steric hindrance also affect rate of the amide proton exchange. Generally, polar side chains drag electrons away from the amide bond and hence, increasing its acidity. Therefore, an increase or decrease in exchange rates will be observed in base and acid catalyzed reactions, respectively. Steric hindrance by the bulky side chains, like β and γ branched and aromatic side chains has been shown to affect the amide proton exchange rate, by shielding or protection effect. Bai et al., (Bai et al., 1993) and Moldey et al (Molday et al., 1972) and others (Englander and Kallenbach, 1983; Jeng et al., 1990) have derived protection factors for all the 20 amino acids and these are being used for making corrections in some cases. Besides the above factors, solvent composition has also been shown to affect the rate of amide exchange (Englander et al., 1985). The miscible solvents used in reverse phase HPLC generally reduce the exchange rate due to decrease in equilibrium constant of water or hydroxide ion activity (Maier and Deinzer, 2005).

Amide proton exchange in proteins generally progresses via two pathways; (1) amide protons in fully folded proteins that are solvent exposed or local breathing/transient motions makes them exposed, exchange via this pathway. These amide protons are generally not involved in hydrogen bonding. A pictorial representation of this pathway is given Fig. 4.4

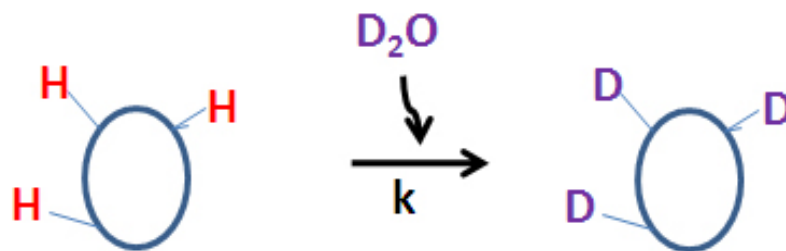


Figure 4.4. Pictorial representation of a fully folded protein showing the exchange of solvent-exposed protons with deuterium.

(2) Amide protons that are buried inside the protein and are involved in complex hydrogen bonding network follow a complex exchange pathway. This type of exchange arises due to large-scale perturbation in the hydrogen bonding network as a result of either global and sub-global transitions or local fluctuations in proteins (model shown in Fig. 4.5).

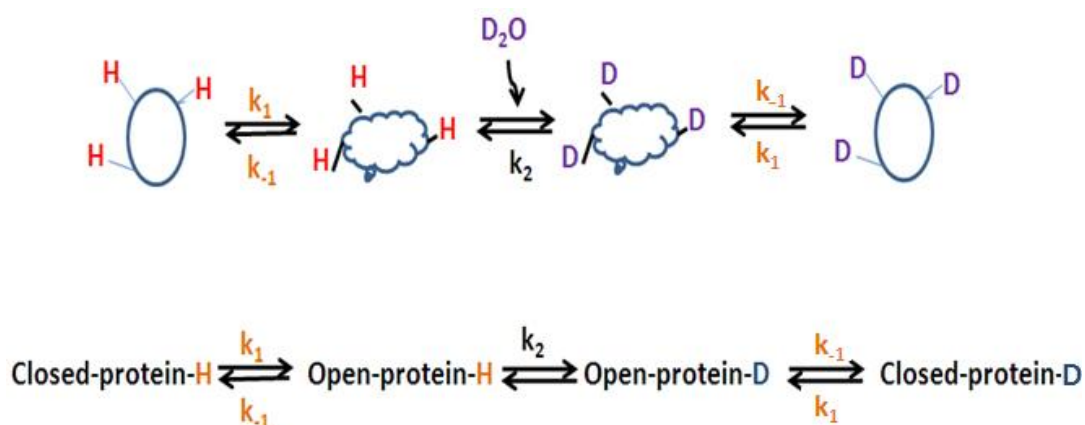


Figure 4.5. Pictorial representation of a folded protein (where protons remain involved in H-bonding network) undergoing H-D exchange.

In the above model, k_1 and k_{-1} represent the rate constants for opening and closing of a folded protein respectively, and k_2 represents the intrinsic rate constant for hydrogen –deuterium exchange in the open state of protein, that has a dependence on pH, temperature and the primary amino acid sequence. Depending on the rate of folding/ unfolding in stably folded proteins, two type of exchange mechanisms have been proposed. *EX1-type mechanism* is a first order exchange kinetic mechanism where the intrinsic rate of hydrogen-deuterium exchange is greater than rate of folding ($k_2 \gg k_{-1}$) and hence, rate of exchange (k_{ex}) is directly related to the rate of unfolding

(k_1). Protein regions that undergo slow opening and closing events generally follow the *EX1-type mechanism*. In native stably folded proteins the rate of folding is greater than the rate of intrinsic hydrogen-deuterium exchange ($k_{-1} \gg k_2$) and the observed second order rate constant is given by $k_{\text{obs}} = k_2(k_1/k_{-1})$. This exchange mechanism is common in most of the proteins undergoing hydrogen-deuterium exchange under native conditions without any denaturant (Maier and Deinzer, 2005).

Structural analysis of proteins by H-D exchange coupled to mass spectrometry provides three basic advantages over NMR spectroscopy and X-ray crystallography; (1) low protein concentration (maximum up to microgram compared to milligrams in the two former techniques), (2) studies under physiologically-relevant contexts and (3) fast and high throughput processing of data with theoretically no limitation by molecular weight. At the same time HD/X MS is limited by following factors; (1) dependence on the structure solved by other methods, like NMR and X-ray crystallography or modeled computationally, and (2) lack of residue-specific resolution (Morgan and Engen, 2009). Katta and Chait (Katta and Chait, 1991; Katta and Chait, 1993) were first to introduce mass spectrometry for monitoring the H/D exchange in proteins. In 1998, Mandell et al first time reported the use of MALDI-TOF in H/DX studies (Mandell et al., 1998).

The general procedure followed during hydrogen-deuterium exchange and analysis by mass spectrometry is pictorially represented in Fig.4.6. The steps followed are (1) deuterium incorporation or in-exchange, (2) quenching and fragmentation (3) mass spectrometry and, (4) peptide identification and assignment. The H/DX reaction for deuterium incorporation can be done either by diluting the unlabelled protein in a deuterated solvent (in-exchange) or diluting a fully deuterium-incorporated protein in a protonating solvent (off-exchange). During this step, the protein can be exchanged in presence or absence of ligands and depending on the desirability of the experiment, time dependent exchange reactions can be performed. Quenching of the reaction is achieved by simultaneous lowering of temperature (0°C) and pH (2-3) that reduces the rate of exchange to the lowest. In this step, fragmentation of the protein is done by using the proteases that function at low pH, with pepsin being the first choice in most of the studies. The fragmented protein with or without separation by HPLC is then analyzed either by ESI or MALDI-TOF mass spectrometry, with the former (ESI) being preferred mostly.

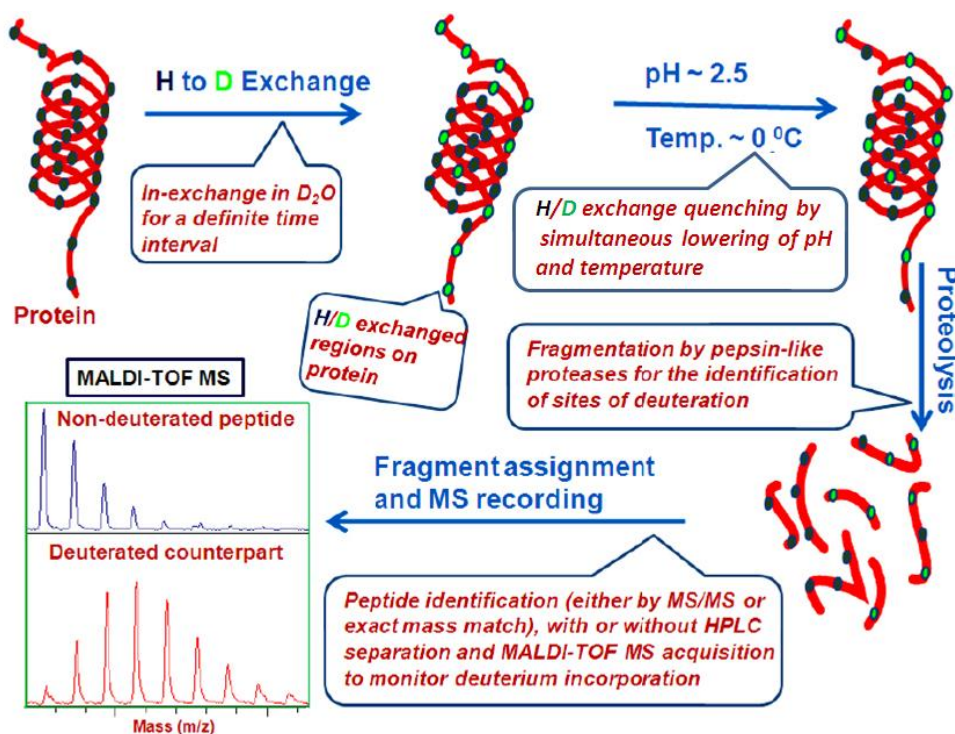


Figure 4.6. Schematic representation of the general steps followed in hydrogen-deuterium exchange coupled to mass spectrometry.

The identification of peptides is carried out by a combination of methods that include MS/MS techniques and N-terminal sequencing. The deuterated peptides if analyzed by MALDI-TOF, are directly spotted on chilled target plates after mixing with cold matrix. The spectral recording is quickly achieved to minimize the back exchange. It has been shown that residence time of the deuterated peptides on target plate affects the outcome in terms of the loss of deuterons (Mandell et al., 1998). While using ESI MS for the H/DX analysis prior to spectral acquisition, the peptides are generally fractionated by reverse phase chromatography at low pH and temperature. Though MALDI-TOF offers a straightforward analysis of the deuterium incorporated peptides, peak-overlapping after deuteration is a general drawback. Back and in-quench exchanges are the two factors that affect the final deuterium content of a peptide. Back exchange is defined as the percentage of undeuterated sites in the most deuterated peptide fragment obtained after 24hrs of continuous deuteration. Primary sequence of the peptide and the processing conditions are the two prominent factors that contribute to back exchange of a peptide. Though, exchange is slowest under low pH (pH 2.5) and temperature (0 °C), the process is never ceased and the exchange

under those conditions is generally taken as in-quench exchange. The extent of in-quench exchange is determined by the content of amino acid residues with heteroatoms (N, O, S), N and C terminal protons and the concentration of deuterium under quench conditions (Mandell et al., 2005).

Centroid masses of the deuterated peptides are used for calculating the incorporated deuterium over the undeuterated peptides. This has been eased due to the extensive use of computational approaches that are being applied to calculate the deuterium content of different peptide fragments and also takes care of the back and in-quench exchange contributions. Details of the H/DX methodology and its recent advancements have been reviewed by many authors (Engen, 2003; Engen, 2009; Engen and Smith, 2000; Engen and Smith, 2001; Floquet et al., 2009; Hochrein et al., 2006; Hoofnagle et al., 2003; Hoofnagle et al., 2004; Iacob et al., 2009; Mandell et al., 2005; Mandell et al., 1998; Morgan and Engen, 2009; Wales and Engen, 2006; Wales et al., 2008).

4.2.2. Domain cross-talk or inter-domain signaling or amidotransferase allostery

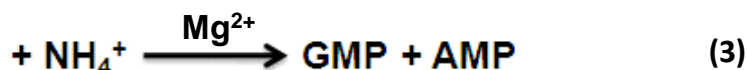
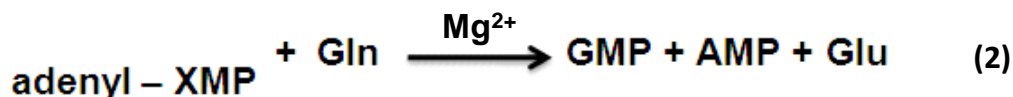
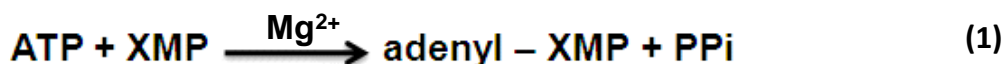
Mechanistic communication between the domains is common to all the enzymes that use substrate channeling (Anderson, 1999; Huang et al., 2001; Miles et al., 1999; Raushel et al., 1999). Most of the glutamine amidotransferases have evolved a mechanism whereby, glutamine hydrolysis in the glutaminase domain is conditional to substrate binding in the acceptor domain to prevent the process from becoming wasteful. Biochemical, structural and theoretical studies on different amidotransferases have provided an understanding of conformational changes in these enzymes and their relevance to the catalysis.

In CPS, though the two partial reactions, glutamine hydrolysis in the glutaminase domain and utilization of ATP and bicarbonate in the acceptor domain, can occur independently (Anderson and Meister, 1966), a perfect active-site synchronization operates during the full catalytic cycle. Inter-domain signaling and the effect of different allosteric ligands on the process has been shown (Miles and Raushel, 2000; Thoden et al., 2004). Use of different single tryptophan mutants of *E. coli* carbamoyl phosphate synthetase (EcCPS) generated by site-directed mutagenesis has permitted the observation of region-specific ligand-induced conformational changes in the protein and their impact on catalysis (Johnson et al., 2007). In glutamine phosphoribosylpyrophosphate amidotransferase, combination of steady

state tryptophan fluorescence and pre-steady state kinetics has shown that enzyme isomerization (conformational change) is the slowest step in catalysis (Chen et al., 1999). Biochemical, mutational and structural analysis of the yeast IGP synthase has highlighted some regulatory aspects through which the enzyme coordinates the activities of its two domains. Meyers et al (Myers et al., 2003) have shown that binding of *N*1-[(5'-phosphoribulosyl)-formimino]-5-aminoimidazole-4-carboxamide ribonucleotide (PRFAR) to the acceptor domain stimulates the glutamine hydrolysis in the glutaminase domain by 4900 fold, though the two domains lie 30Å apart. Site-directed mutagenesis in this enzyme has shown that K258 in the acceptor domain senses the binding of the acceptor substrate and a change due to its re-orientation is transmitted to the glutaminase domain. In yeast NAD synthetase, a 50 fold increase in glutaminase activity has been reported when the synthetase site was liganded with NaAD and a term “homosteric stimulation” has been coined for such a process (Wojcik et al., 2006). In formylglycinamide ribonucleotide amidotransferase, a three subunit complex, ADP has been shown to be essential for subunit assembly that catalyses the glutamine dependent amidotransferase reaction, indicating the role of the metabolite-mediated structural transitions in the process (Morar et al., 2006) . Similarly, in *P. falciparum* pyridoxal phosphate synthase, a two-subunit amidotransferase, glutamine has been reported to tighten the interaction of the glutaminase and the synthetase domains as a consequence of change in the conformational dynamics (Flicker et al., 2007). Replacement of Glu-348, a conserved residue of *E. coli* asparagine synthase B, with alanine by site-directed mutagenesis has ascribed three roles to the residue (1) mediates the formation of β -aspartyl-AMP intermediate, (2) coordination of the glutaminase and the synthetase domain activities and (3) establishment of structural integrity of intramolecular ammonia channel in the enzyme (Meyer et al., 2010)

In summary, all these studies highlight the role played by substrate-mediated conformational changes in amidotransferase function. The changes get relayed from the acceptor to the glutaminase domain by combined motion of different regions of the protein that finally leads to the coordinated hydrolysis of glutamine needed for the generation of ammonia.

GMP synthetase, catalyses the reaction in which xanthosine 5'-monophosphate is converted to guanosine 5'-monophosphate through the formation of adenylyl-XMP intermediate as highlighted in scheme 4.1.



Scheme 4.1. Reaction catalyzed by GMP synthetase

Inter-domain signaling arising due to substrate-induced conformational changes in GMP synthetases has been shown biochemically. Kuramitsu and Moyed (Kuramitsu and Moyed, 1966) reported that, cysteine reactivity to Ellman reagent (5,5'-dithiobis(2-nitrobenzoic acid) changes when the enzyme was bound to psicofuranine, an adenosine analogue, though the identity of the exposed cysteins was not shown. Similarly, Zyk et al has shown an increased stability in ATP + XMP bound form of *E. coli* GMP synthetase compared to that of unbound form. Heat denaturation and susceptibility to limited proteolysis of the enzyme were used as probes for stability (Zyk et al., 1970). In EcGMPS, inactivation rate of the glutaminase domain by DON, chloroketone and acivicin has been shown to be enhanced when the ATPase domain was completely liganded (Chittur et al., 2001; Zalkin and Truitt, 1977). Similarly, in HsGMPS (*Homo sapiens* GMPS) an increased glutamine hydrolysis activity has been reported when the enzyme was present with both MgATP and XMP. A new paradigm in PhGMPS (*P. horikoshii* GMPS) subunit assembly has been reported recently, where the presence of MgATP and XMP seems to be mandatory for the formation of GAT-ATPase complex (Maruoka et al., 2010), suggesting that a substrate-induced change is needed for the interaction. Domain coordination and conformational changes have been proposed to be a mechanism for closing the otherwise open structure of *E. coli* GMP synthetase (Tesmer et al., 1996). However, a confirmatory structural evidence for conformational dynamics and their link to catalysis in GMP synthetases is still awaited. Following sections of this chapter report the studies on substrate-induced transitions and domain cross-talk in *P. falciparum* GMP synthetase.

4.3. Materials and methods

4.3.1. Materials

Media components were obtained from Himedia, India. All the biochemicals including deuterium oxide, ATP, XMP, MgCl₂, and glutamine were obtained from Sigma-Aldrich, USA. Matrices for MALDI-TOF mass spectrometry from Bruker Daltonics, Germany or Sigma-Aldrich, USA were used. Sequence grade trypsin from Promega (Promega Corporation, USA) or Sigma-Aldrich, USA was used for PfGMPS digestion.

4.3.2. Enzyme preparation and activity assays

His-tagged PfGMPS expression and purification protocols were essentially same as described in chapter 2 (sections 2.3.2 and 2.3.5). Protein purity was judged by visualization on SDS-PAGE. Protein concentration was estimated by Bradford's method (Bradford, 1976) using bovine serum albumin as a standard.

All the activity measurements were carried out under standard assay conditions, unless otherwise mentioned. Briefly, reaction rates were monitored as decrease in absorbance at 290 nm due to conversion of XMP ($\epsilon = 4800 \text{ M}^{-1}\text{cm}^{-1}$) to GMP ($\epsilon = 3300 \text{ M}^{-1}\text{cm}^{-1}$), using a $\Delta\epsilon$ value of $1500 \text{ M}^{-1}\text{cm}^{-1}$ to calculate the amount of product formed. The standard assay consisted of 90 mM Tris HCl (pH 8.5), 150 μM XMP, 2 mM ATP, 5 mM glutamine, 20 mM MgCl₂, 0.1 mM EDTA and 0.1 mM DTT in a total reaction volume of 0.25 ml. Reactions were initiated with 6 μg of PfGMPS and monitored at 25 °C (Section 2.2.5, Chapter 2)

4.3.3. Irreversible inhibition of PfGMPS

Inhibition by two irreversible glutamine analogs, acivicin and DON was examined by preincubation of the enzyme with the inhibitors. Pre-incubation was done both in presence and absence of the substrates XMP and ATP in 50 mM Tris HCl, pH 8.5, with 20 mM MgCl₂ keeping the inhibitor concentration always in excess of the enzyme concentration. Pre-incubation in the absence of substrates was carried out both at 25 °C and 15 °C, and at 15 °C only in presence of substrates, as the inactivation was very rapid at 25 °C. In both the cases aliquots containing 2.5 μg of

the pre-incubated enzyme were taken at different time intervals and assayed under standard assay conditions. Equation 4.1 describes the mechanism of inactivation in which the first step occurs reversibly and the second step is irreversible (Kitz, 1962).

$$\ln(\varepsilon)/E^0 = k_3 t / (1 + K_I / (I)) \quad (4.1)$$

where, ε = inactivated enzyme, E_0 = total enzyme, K_I = dissociation constant for the initial reversible complex and k_3 = first order rate constant for the conversion of reversible complex to the irreversibly inhibited enzyme.

4.3.4. Circular dichroism measurements

All the CD spectra were recorded on a J-810 Spectropolarimeter (Jasco corporation, Tokyo, Japan) using a 1mm path length quartz cell. For both far-UV and near-UV CD spectral measurements, PfGMPS was pre-incubated with the ligands ATP, XMP, and MgCl₂ in different desired combinations to a final concentration of 520, 60 and 1000 μ M, respectively for 10 min at 25 °C. Far-UV CD spectra were recorded between 260 to 200 nm with a band width of 2 nm and a scan speed of 50 nm/min using 5 μ M PfGMPS in 5 mM Tris HCl, pH 7.4. Each spectrum was an average of three scans with spectral interval of 0.5 nm. PfGMPS (30 μ M) in 20 mM Tris HCl, pH 7.4 was used for the near-UV CD spectral measurements and the spectral acquisition was between 350 to 250 nm. All spectra were an average of 30 scans acquired at an interval of 0.5 nm and scan speed of 100 nm/ min. Subtraction of buffer spectra containing all ligands at the specified concentrations, from the protein spectra corrected the latter spectra for contributions from all buffer components. The resulting data was converted from millidegree to molar ellipticity using equation 4.2.

$$[\theta]_M = [\theta]_{obs} / 10cl \quad (4.2)$$

where $[\theta]_{obs}$ is the ellipticity in milli degrees after correction for buffer components, c is protein concentration (in g/ml) and l is the optical path length of the cell in cm. Molecular weight of the protein used was 65401 Da per subunit. Experiments were repeated with two different batches of purified enzyme to confirm reproducibility.

4.3.5. ANS fluorescence measurements

All the ANS (8-anilino naphthalene sulfonic acid) fluorescence recordings were performed on F-2500 FL Spectrophotometer (Hitachi, Japan) at 25 °C using 1 cm path length cell, with both the excitation and emission slit widths fixed at 5 nm. The samples were excited at 370 nm and the emission spectrum was recorded from 373 to 600 nm. ANS stock concentration was measured by spectrophotometry at 350 nm using molar extinction coefficient value of 5000 M⁻¹ cm⁻¹ (Stryer, 1965). The assays contained PfGMPS, MgCl₂, ATP and XMP to a final concentration of 5 μM, 3 mM, 1.5 mM and 150 μM, respectively in 50 mM Tris HCl, pH 7.4, with an insignificant inner-filter effect at the excitation wavelength. The ANS titration was performed from 50 to 500 μM at a fixed concentration of PfGMPS (5 μM). Protein with or without ligands was pre-incubated at 25 °C for 10 min before the addition of ANS and spectral acquisition. Spectra recorded for the samples containing all the components except PfGMPS (control spectra), were used for correcting the respective protein-ANS emission spectra for Raman-scattering and contribution from solvent.

4.3.6. Limited tryptic proteolysis of PfGMPS

PfGMPS was pre-incubated with substrate/s, digested on ice with trypsin and analyzed by SDS-PAGE, residual enzyme activity measurements and MALDI-TOF mass spectrometry. Pre-incubation conditions involved mixing of 20 μM PfGMPS with ATP, XMP and MgCl₂ (in different combinations) to a final concentration of 1.5, 0.15 and 3 mM, respectively, in 5 mM Tris HCl, pH 7.4. Wherever AMP-PNP replaced ATP, a final concentration of 1.5 mM was used. Separate assays were performed for different protein/substrate combinations and all the incubations were allowed to proceed for 10 min at 25 °C. Tryptic digestion was done on ice, with trypsin to PfGMPS ratio of either 1:100 or 1:200. For post-digestion analysis by SDS-PAGE, 10 μg PfGMPS digest was mixed with SDS loading buffer, resolved on a 15 % gel and silver stained to visualize the band pattern. For residual activity measurements after tryptic digestion, 6 μg equivalent aliquots of the digested PfGMPS were sampled at different time intervals and assayed under standard assay conditions for the conversion of XMP to GMP. Plots of log of PfGMPS residual activity versus time period of its trypsin digestion for different protein-substrate combinations were generated using GraphPad Prism 5. When MALDI-TOF mass spectrometry was applied for analysis of the PfGMPS tryptic digest, aliquots (1μg

equivalent) were collected at 3, 5, 10, 15, 20, 30, 45 and 50 min time intervals after addition of trypsin, mixed with sinnapinic acid (in 1:1 ratio) and dried after spotting onto a MALDI-TOF target plate. Six replicates of the samples pertaining to different time intervals were spotted and the spectra were recorded in positive ion linear mode on an UltraFlex II MALDI-TOF mass spectrometer (Bruker Daltonics, Germany), with each spectrum representing a sum of the data from 300 laser shots. The machine was externally calibrated using ProteinCalibStandard (provided by Bruker Daltonics, Germany) that contained a set of six proteins of m/z 5734.52 to 16952.31 Da.

4.3.7. Hydrogen-deuterium exchange (H/DX)

PfGMPS was subjected to extensive dialysis against 5 mM Tris HCl, pH 7.0 and 105 μ g aliquots of the protein were lyophilized in separate 1.5 ml Eppendorf tubes and used for H/DX studies. The protocols devised by Jeffrey J. Mandell et al (Mandell et al., 2005) were largely followed, with minor modifications. For hydrogen-deuterium exchange, 105 μ g of lyophilized PfGMPS were reconstituted in 5 μ l of buffer that contained 3 mM $MgCl_2$, 2 mM ATP or 2 mM AMP-PNP and 0.14 mM XMP in different combinations, resulting in a final protein concentration of 320 μ M in 70 mM Tris HCl, pH 7.0. Protein-ligand equilibration was allowed for 10 min at 27 $^{\circ}$ C and in-exchange was started by adding 45 μ l of 100 % D_2O , buffered with 70 mM Tris HCl, pH 7.0, making the final D_2O concentration to 90 % in the assays. The ligand ($MgCl_2$, ATP or AMP-PNP and XMP) concentrations and their various combinations in the deuteration buffer were similar to those maintained under equilibration conditions. For determining the time taken by PfGMPS to reach saturation in deuterium incorporation, in-exchange reactions at different time intervals (0.5, 1, 2, 2.5, 5, 10 and 15 min) were stopped by mixing the reaction with 300 μ l of quench buffer (0.1 % TFA, pH 2.5). Immobilized pepsin (6 %) slurry (Pierce Chemicals, Rockford, IL) was pre-activated by washing the beads twice with the quench buffer and 40 μ l of which were added to the quenched reaction containing deuterium-incorporated PfGMPS. The peptic digestion was allowed to proceed for 5 min with intermittent mixing. Pepsin beads were removed by centrifugation for 30 sec at 4 $^{\circ}$ C and the cleared solution was transferred to fresh tubes to stop the digestion. Samples were flash frozen in liquid nitrogen and stored at -80 $^{\circ}$ C till spectral acquisition. For the identification of peptides generated by pepsin digestion, PfGMPS without deuterium incorporation was processed similarly.

The extent of in-exchange after acidification (in-quench exchange) was measured by labeling the protein with D₂O after the addition of quench buffer. A total of 290 µl of quench buffer containing 40 µl pepsin beads, were added to 5 µl of protein solution on ice, followed by immediate addition of 45 µl of pre-chilled labeling buffer. Digestion and subsequent procedures were same as described above and, the experiment was independently repeated three times. Artefactual deuterium incorporation during quench conditions was 4 to 5%, as expected at the given dilution (Mandell et al., 2005; Mandell et al., 1998). For calculation of back-exchange, the protein was incubated with the labeling buffer (90 % D₂O in 70 mM Tris HCl, pH 7.0) for 24 hrs at 27 °C and further processed as described above. A peptide with non-deuterated centroid m/z of 1849.044 Da gained 7.5 ± 0.01(m/z 1856.590) deuterons after 24 hrs, that represented the highest deuterium number in any of the peptides. Calculations using this peptide suggested 58 % back exchange during the H/DX measurements. All the peptides were corrected for both in-quench and back exchange, to derive the actual amide hydrogen atoms undergoing exchange with deuterium.

4.3.8. MALDI-TOF mass spectrometric analysis of the deuterium- incorporated samples

Samples were quickly half defrosted and mixed with chilled matrix (α -cyano hydroxycinnamic acid, 5 mg/ml in 1:1:1 ratio of ethanol / acetonitrile / 0.1 % TFA, pH 2.5) and a mixture of three peptides used as internal standards. Samples (1 µl) were spotted onto a pre-chilled MALDI-TOF target plate, dried under mild vacuum and flushed with a stream of dry nitrogen to remove any residual moisture. Spectra were acquired within 5-6 min after sample defrosting including the time taken for plate docking into the instrument. All the spectra were recorded on an UltraFlex II MALDI-TOF TOF using the application flexControl 2.4 and the off-line analysis was carried out in flexAnalysis 3.0 software (Bruker Daltonics, Germany). Spectra were acquired in the positive ion reflectron mode with each final spectrum being averaged for 700 laser shots. External calibration of MALDI-TOF spectrometer was performed by PeptideCalibStandard mono (Bruker Daltonics, Germany) that contained nine peptides with m/z 757.39 to 3147.47 Da. Internal calibration was performed with three peptides having monoisotopic masses MH⁺ of 959.611Da (custom synthesized), 1552.777 Da (fibrinopeptide, Sigma-Aldrich, USA) and 1673.036 Da (neurotensin, Sigma-Aldrich, USA). Peptide identification of the peptic digest of undeuterated

protein was done by a combination of post-source decay (PSD) using MALDI-TOF, after separating the peptides through an off-line C₁₈ reverse phase column (Amersham Biosciences, UK), collision-induced dissociation (CID) using LC-ESI-Q-TOF and exact mass matches. A linear gradient of 5-100 % water/acetonitrile was used for peptide elution. PfGMPS theoretical pepsin map was generated by using Sequence Editor (Bruker Daltonics, Germany). Centroid mass of the isotopic cluster of both deuterated and undeuterated peptic fragments was calculated using MagTran software (Zhang and Marshall, 1998). Equation (4.3) was used for the estimation of deuterium incorporation into the peptides after correction for residual (5 %) and back (58 %) exchanges.

$$D(t) = [m(t)-m(0)]/(B\%)-D_s(t) \quad (4.3)$$

where, D(t) is the corrected deuterium number, m(t) is the observed mass after 10 minutes, m(0) is the undeuterated mass, B% is the % back exchange and D_s(t) is the residual side chain exchange .

4.3.9. PfGMPS modeling

PfGMPS model was generated using MODELLER 9v7 (Sali and Blundell, 1993) and *E. coli* GMPS structure complexed to AMP and PPi (PDB ID: 1GPM) as template. Alignment of primary sequences of EcGMPS and PfGMPS was performed by ClustalW (Higgins D., 1994). The model quality in terms Ramachandran parameters for the torsion angles was validated by using Whatif (Vriend, 1990) and Procheck (Laskowski and Thornton, 1993). The model was finally visualized in PyMol viewer (DeLano Scientific).

4.4. Results

4.4.1. Inter-domain cross-talk

GMPS has two domains that catalyse two different reactions with ammonia generated by the glutaminase domain being channeled to the ATPase domain to form GMP. Glutamine hydrolysis in the glutaminase domain independent of the binding of XMP and ATP to the ATPase domain would be a physiologically wasteful process and hence, coupling of GAT activity to the activity of ATPase domain would be expected. The cross-talk occurring between the two domains in PfGMPS was examined by two methods, one, by measuring the glutaminase activity

of the glutaminase domain and second, by inactivation of the domain by glutamine amidotransferase specific inhibitors. Table 2.4 (chapter 2) summarizes the effect of substrate binding to the ATPase domain on glutaminase activity. It is evident from the data that in PfGMPS, there is a high basal level of glutaminase activity that is not altered by the binding of XMP or ATP alone to the ATPase domain. But once the ATPase domain is fully liganded, glutaminase activity reaches a maximum. Replacement of ATP by AMP-PNP led to significant increase in glutaminase activity that was lower when compared to the complete reaction having both ATP and XMP. This shows that though the adenylyl-XMP intermediate is not formed, complete occupancy of the catalytic pocket in the ATPase domain is sufficient to stimulate the glutaminase activity. This also suggests that the formation of the reaction intermediate in ATPase domain signals the glutaminase domain for complete activity leading to coupling of the two reactions in the two domains. The level of leaky glutaminase activity is significantly higher than that for other glutamine amidotransferases. Under similar assay conditions, human GMP synthetase (Nakamura et al., 1995), imidazole glycerol phosphate synthase (Myers et al., 2003) and NAD synthetase (Wojcik et al., 2006) exhibited tight regulation with very low background glutaminase activity in the absence of complete liganding of the acceptor domain. However, asparagine synthetase has been shown to have significant leaky glutaminase activity (Tesson et al., 2003). It is interesting to note that while in the case of PfGMPS, liganding of ATPase domain with AMP-PNP, XMP and Mg^{2+} led to activation of the glutaminase domain, these ligands had no effect on the activity of the glutaminase domain in human GMPS (Nakamura et al., 1995). The *in vivo* significance of the partial/weak domain regulation in PfGMPS is unclear at the present stage. The presence of other modulators under *in vivo* conditions that prevent the leaky glutaminase activity cannot be ruled out.

DON and acivicin, the two antibiotics from *Streptomyces* are known irreversible inhibitors of *E. coli* (Chittur et al., 2001; Zalkin and Truitt, 1977) and human GMPS (Nakamura et al., 1995), and other amidotransferases (Miles et al., 2002). These inhibitors covalently modify the catalytic cysteine in the GAT domain, thereby inactivating the enzyme. Measurement of inactivation rates as a function of substrate binding to the ATPase domain permits evaluation of extent of cross-talk between the domains. As shown in Fig. 4.7a and b, both DON and acivicin inactivate PfGMPS.

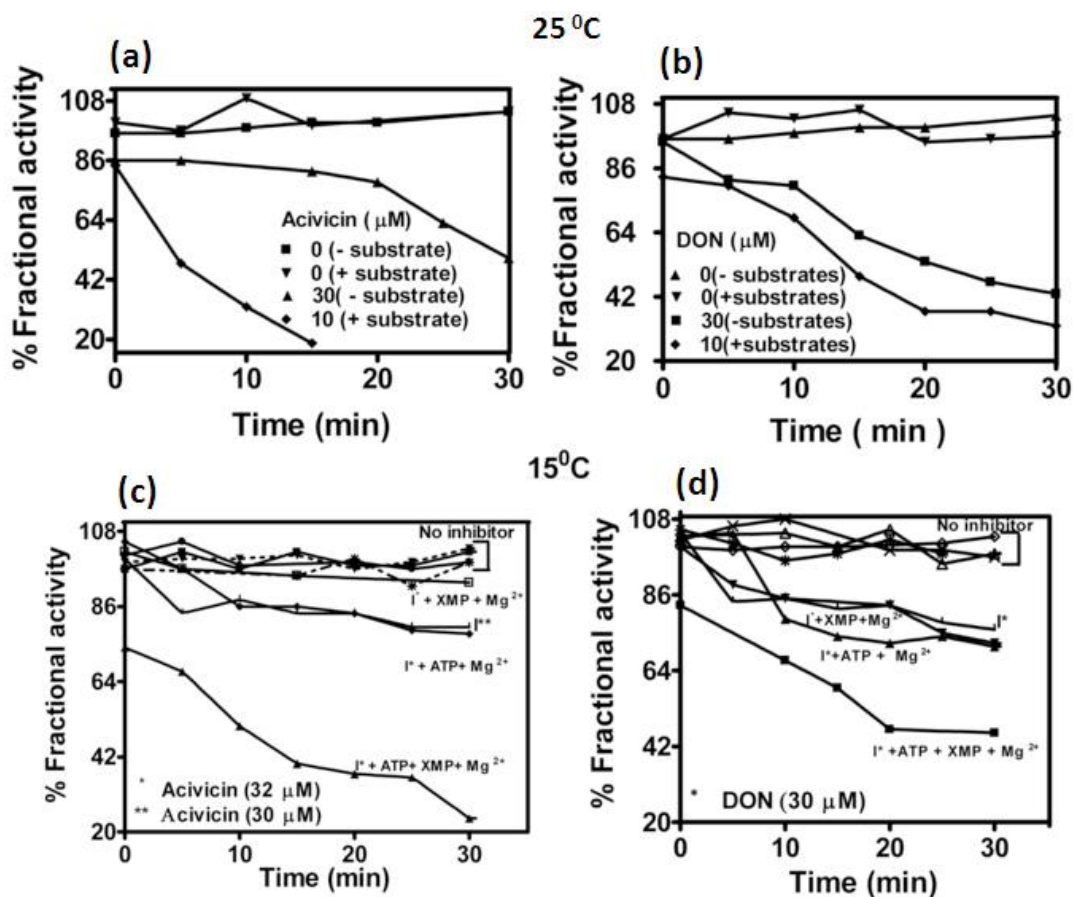


Figure 4.7. Irreversible inhibition of PfGMPS by acivicin and DON as a function of time

The inactivation is represented as % of activity remaining after incubation with the inhibitor for different time intervals. Panels a and b represent the inactivation at 25 °C by acivicin and DON, respectively. 10 and 30 μM of inhibitor (acivicin and DON) were used when PfGMPS was pre-incubated with and without substrates, respectively. Panels c and d represent the inactivation at 15 °C by acivicin and DON, respectively with different combinations of substrates. In plot c, 30 μM and 32 μM of acivicin was used in presence and absence of substrates, respectively. In plot d, 30 μM of DON was used in all the reactions. The combinations of substrates used are indicated against each line. In plots c and d, lines bracketed as “no inhibitor” represent the activity of the enzyme under different pre incubation conditions without the inhibitor. The pre incubations without inhibitor were of the enzyme alone or with different combinations of the substrates XMP and ATP.

Figure 4.7 c and d in fact show that at 15 °C, the inactivation rate by acivicin and DON both in presence and absence of substrates is reduced significantly, when compared to that at 25 °C.

The rate of inactivation is enhanced by the presence of substrates in the ATPase domain. In the absence of substrates, 30-50 % loss in activity was seen at 25 °C over 30 min, however, nearly complete inactivation was seen in 10 min when the substrates were present. It should be noted that the concentration of inhibitor in the absence of substrates was three fold higher compared to that when substrates were present. In order to evaluate the effect of substrate binding on the efficiency of inactivation, the pre-incubation temperature was lowered to 15 °C to slow down the rate of inactivation.

Plots of ln % activity versus time show a biphasic trend indicating the existence of two steps in the inactivation kinetics by acivicin (Fig. 4.8 a, c) and DON (Fig. 4.8 b, d). These plots indicate the occurrence of an initial phase with rapid loss of activity, followed by a second phase with slower inhibition rates. The secondary plot of slope (k_{app}) of the lines in Figure 4.8 versus [I] was linear indicating that saturation was not achieved at the concentrations of the inhibitors used. Hence, equation 4.1, $\ln(\varepsilon)/E^0 = k_3 t * I / I + K_I$ which describes the inactivation kinetics, was simplified to $\ln(\varepsilon)/E^0 = k_3 t * I / K_I$ to obtain an estimate of the second order rate constant (k_3/K_I) from the plots in Fig. 4.8. This value for acivicin in the absence of substrates ($0.184 \pm 0.0138 \text{ min}^{-1} \text{ mM}^{-1}$) increased by 8 fold to $1.489 \pm 0.348 \text{ min}^{-1} \text{ mM}^{-1}$ in the presence of substrates. In the case of DON, the difference is 5 fold with the values $0.188 \pm 0.009 \text{ min}^{-1} \text{ mM}^{-1}$ and $0.9498 \pm 0.081 \text{ min}^{-1} \text{ mM}^{-1}$ obtained in the presence and absence of substrates, respectively. Such biphasic behavior in the inactivation kinetics has been observed in the case of *E. coli* GMPS (Chittur et al., 2001). Unlike PfGMPS, acivicin was found to be a more potent inhibitor than DON in the case of *E. coli* GMP synthetase.

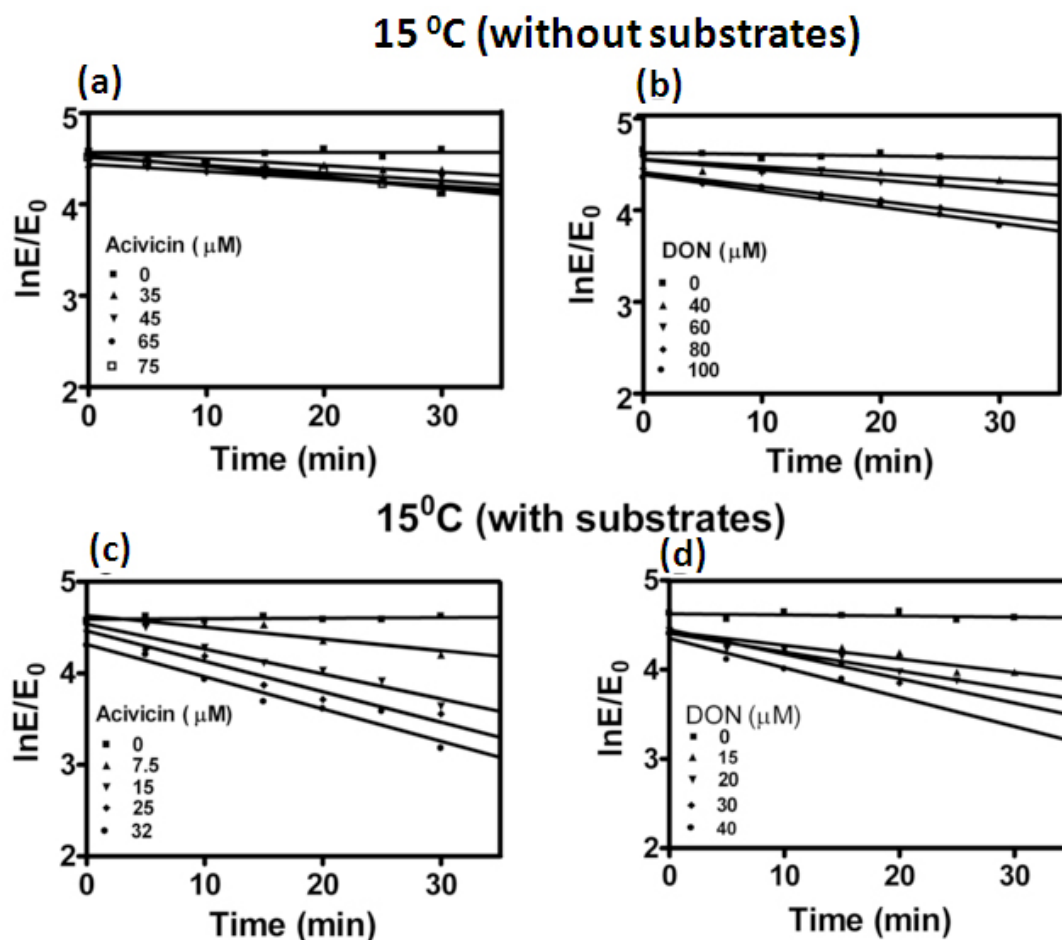


Figure 4.8. Inactivation kinetics of PfGMPS by acivicin and DON.

The inactivation is represented as \ln of residual activity as a function of time. Panels a and b represent the plots in absence of substrates with acivicin and DON, respectively at 15 °C. Plots c and d represent inactivation with acivicin and DON in presence of substrates at 15 °C. The concentration of inhibitors used in all these plots is represented as insets in each plot. The concentration of substrates used in preincubation reaction was that of standard assay.

4.4.2. Circular dichroism and ANS fluorescence spectroscopy

Far-UV CD spectra of PfGMPS incubated with different combinations of substrates did not reveal significant differences when compared to the spectrum of unliganded protein. Figure 4.9 shows the near-UV CD spectra of ligand bound and free forms of PfGMPS that report on the changes in tertiary structure of the protein.

The differences seen in the ellipticity values in the presence of ligands are mainly due to changes occurring in the environment of aromatic residues, arising

from substrate binding. The spectrum of Mg^{2+} +ATP+XMP bound form of PfGMPS was different from the spectra of protein incubated either with Mg^{2+} +ATP or Mg^{2+} alone, suggesting that the fully liganded form of enzyme has undergone a gross change in tertiary structure. Unexpectedly, the spectrum of Mg^{2+} + XMP bound PfGMPS resembled that of Mg^{2+} +ATP+XMP bound form though initial velocity kinetics supports an ordered binding scheme, with XMP binding only to the Mg^{2+} +ATP-enzyme complex (Chapter 2, section 2.4.2). PfGMPS sequence has 31 phenylalanines, 32 tyrosines and 2 tryptophans distributed across the protein that could contribute to the near-UV CD spectrum. Though the spectrum highlighted a change in the magnitude of positive Cotton effect at different wavelengths, residue specific assignment of the peaks was not possible and hence, disallowed correlation with specific regions in the protein.

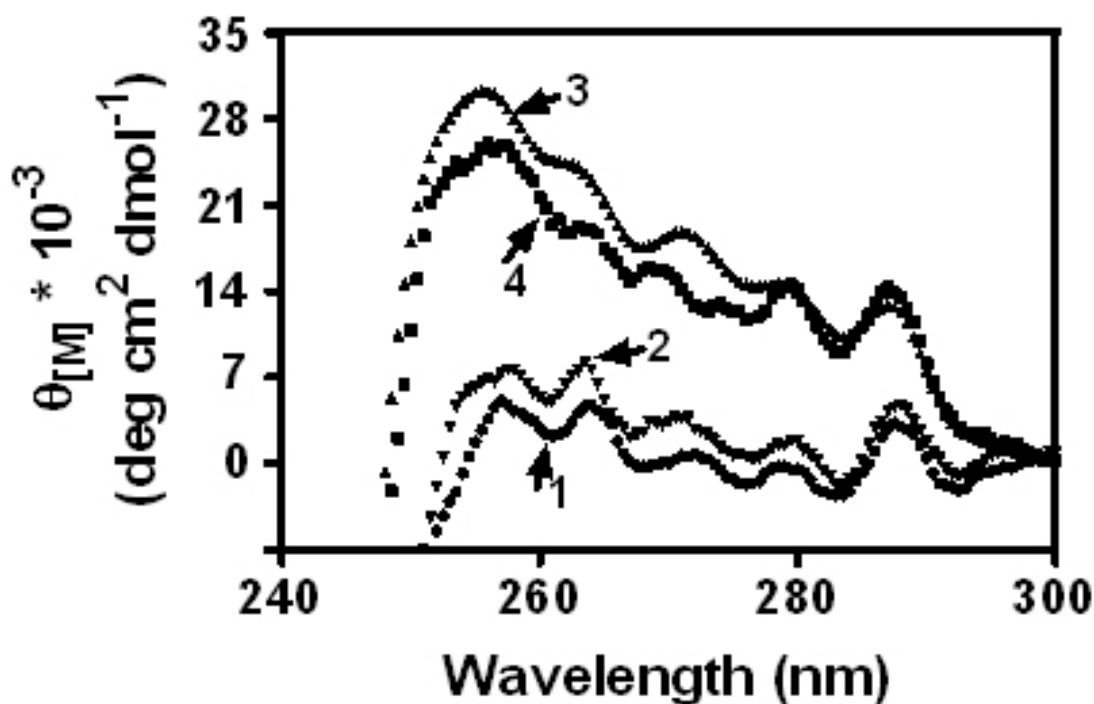


Figure 4.9. Effect of substrate binding on PfGMPS, monitored by near-UV CD spectroscopy.

Spectra were recorded after pre-incubation of the enzyme with Mg^{2+} (1), Mg^{2+} +ATP (2), Mg^{2+} +XMP (3) and Mg^{2+} +ATP+XMP (4). PfGMPS concentration in all the experiments was fixed at 30 μ M Details of spectral acquisition and processing are given in “materials and methods”.

Fluorescence spectroscopy was used as a complementary tool to validate the results obtained by CD spectroscopy. Though PfGMPS contains 2 tryptophans per molecule, intrinsic fluorescence and acrylamide quench experiments failed to report any change arising from substrate binding. Therefore, binding of ANS to PfGMPS was examined and this served as a probe for monitoring conformational change(s) in the protein emanating from ligand binding. ANS, a hydrophobic fluorescent dye, has earlier been used for such studies in proteins (Nimmegern et al., 1996; Pan and Dunn, 1996) and is known to have increased fluorescence when bound to hydrophobic surfaces (Stryer, 1965). Figure 4.10a shows ANS emission spectra of the samples containing PfGMPS with different ligand combinations. Increased fluorescence intensity and the wavelength shift (510 nm to 490 nm) in emission maximum suggested binding of ANS to hydrophobic surface on PfGMPS (Turner and Brand, 1968).

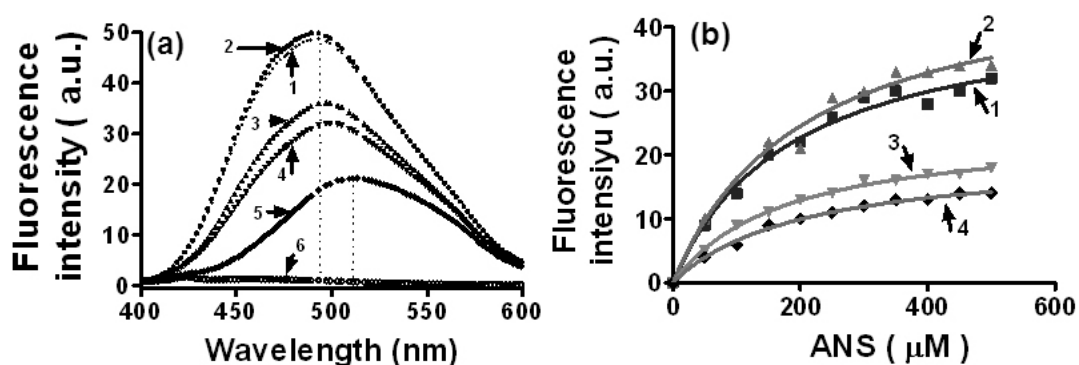


Figure 4.10. Binding of ANS to free and substrate bound forms of PfGMPS as monitored by fluorescence spectroscopy

(a) Fluorescence spectra of ANS bound to PfGMPS in the presence of different ligand combinations. 1, 2, 3 and 4 represent samples of PfGMPS containing Mg^{2+} , $Mg^{2+} + ATP$, $Mg^{2+} + XMP$, and $Mg^{2+} + ATP + XMP$, respectively. 5 and 6 are emission spectra for free ANS and free PfGMPS, respectively. All samples were excited at 370 nm. (b) ANS titration curves at fixed concentration of PfGMPS containing (1) Mg^{2+} , (2) $Mg^{2+} + ATP$, (3) $Mg^{2+} + XMP$ and (4) $Mg^{2+} + ATP + XMP$. All the fluorescence intensity values were corrected for contributions from both free ANS and protein and were fitted to the single-site binding hyperbolic equation, $[Y = I_{max} * X / (K_d + X)]$, where $Y = ANS$ emission fluorescence intensity, I_{max} = maximum ANS emission fluorescence intensity, $X = ANS$ concentration in μM and K_d = the ANS dissociation constant. See “materials and methods” for details of the assay.

Comparison of PfGMPS bound ANS fluorescence spectrum with those in the presence of different ligand combinations (Fig 4.10a) revealed emission to be lowest when the enzyme was bound to Mg^{2+} +ATP + XMP compared to that when Mg^{2+} alone or Mg^{2+} + ATP were present. To substantiate this observation, ANS was titrated at fixed concentration of PfGMPS pre-mixed with different combinations of substrates. A fit to a single binding-site equation provided a qualitative estimate of the K_d for ANS bound to the different liganded forms of PfGMPS (Fig. 4.10b).

Though significant differences were not noticed in K_d values ($198 \pm 25 \mu M$, $181 \pm 17 \mu M$, $177 \pm 12 \mu M$ and $201 \pm 17 \mu M$ for PfGMPS +, Mg^{2+} alone, Mg^{2+} +ATP, Mg^{2+} +XMP and Mg^{2+} +ATP +XMP, respectively) across the conditions, a significant change was seen in the values of maximum ANS emission intensity (45 ± 2 , 48 ± 2 , 24 ± 1 and 20 ± 1 for Mg^{2+} alone, Mg^{2+} +ATP, Mg^{2+} +XMP and Mg^{2+} +ATP+XMP, respectively). Together, these results indicate that binding of Mg^{2+} + XMP or Mg^{2+} + ATP + XMP to PfGMPS brings about a significant decrease in ANS fluorescence intensity, compared to that of the unliganded or Mg^{2+} + ATP bound forms of the protein. These results also suggested that the overall binding affinity of ANS to PfGMPS is low under all conditions employed, as judged by the high K_d values seen in these titrations. The reduced ANS fluorescence emission seen in fully liganded PfGMPS sample can be attributed to (1) competition between the fluorophore (ANS) and the substrates for the binding site, (2) a conformational change leading to change in accessible hydrophobic surface area or (3) combination of both.

4.4.3. Limited tryptic proteolysis of PfGMPS

Susceptibility of PfGMPS under different liganded conditions to trypsin proteolysis was examined by two methods viz., band pattern on SDS-PAGE and time-dependent reduction in activity. The results are summarized in Fig 4.11.

Trypsin, a serine protease, cleaves the peptide bond at the carboxyl side of lysine and arginine residues. Primary sequence analysis of PfGMPS revealed a total of 17 arginines and 51 lysines and depending on their accessibility in the tertiary structure under different liganded conditions could serve as trypsin cleavage sites. Figure 4.11a highlights the distinct SDS-PAGE profiles of PfGMPS in the presence of different substrate combinations, after trypsin digestion. Comparison of the band patterns across the lanes, showed a prominent difference in the Mg^{2+} +ATP+XMP

bound form of PfGMPS, with a reduced number of bands in the mass region of 14 to 18 kDa. Figure 4.11b shows a correlation of the effect of substrate binding on PfGMPS to the rate of its proteolysis by trypsin. Differences in the slopes of the plots of residual activity versus the time duration of proteolysis suggested differences in the rate of cleavage when the ligand combination differed.

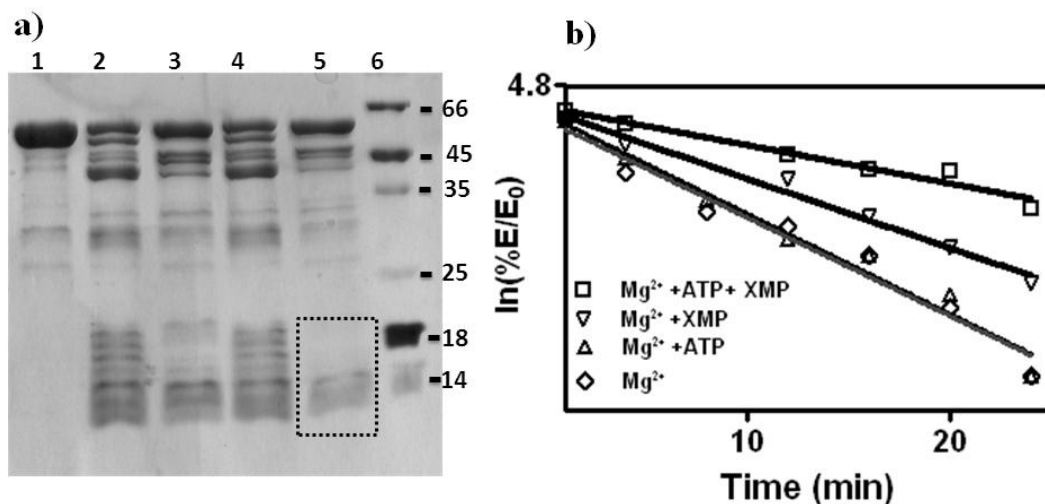


Figure 4.11. Comparison of the susceptibility of PfGMPS to limited tryptic proteolysis in the presence and absence of substrates.

(a) Tryptic digestion pattern of PfGMPS as visualized by SDS-PAGE. Intact PfGMPS (lane 1). Trypsin digest of PfGMPS after pre-incubation with Mg^{2+} , $Mg^{2+}+ATP$, $Mg^{2+}+XMP$ and $Mg^{2+}+ATP+XMP$ are in lanes 2, 3, 4 and 5, respectively. Lane 6 represents molecular weight marker with the molecular weights (in kDa) indicated to the right of the panel. The trypsin to PfGMPS ratio was maintained at 1:100. Reactions were quenched by mixing the sample with SDS-PAGE loading buffer. (b) Plot of the log of PfGMPS activity versus time period of its incubation with trypsin. E and E_0 represent PfGMPS activity with and without trypsin treatment, respectively. PfGMPS was pre-incubated with ligands in different combinations (inset). The trypsin to PfGMPS ratio was maintained at 1:200. Digested samples were collected at different time points and assayed for GMP synthetase activity under standard assay conditions. Details of the assays are described in “materials and methods”.

After 24 min of trypsin digestion, $Mg^{2+}+ATP + XMP$ bound PfGMPS could retain 42% of its activity compared to $Mg^{2+} + XMP$ (22%) and $Mg^{2+} + ATP$ or $MgCl_2$ (both 10%) bound forms. Though the results obtained from near-UV CD spectroscopy and ANS binding fluorescence measurements were complementary, region-specific changes could not be envisaged.

To establish the regions on PfGMPS that specifically undergo a ligand-induced structural change, trypsin digested samples were analyzed by MALDI-TOF mass spectrometry. Limited proteolysis has been used for probing protein structures (Fontana et al., 2004) and in combination with mass spectrometry has specifically allowed the mapping of regions undergoing ligand-induced transitions (Suh et al., 2007). MALDI-TOF mass spectra of PfGMPS in the presence of different ligand combinations after trypsin digestion were recorded between m/z 10500 to 25000 Da. The peak pattern in the spectra remained unchanged over a trypsin digestion time period of 3 to 50 min and the spectra presented in Fig. 4.12 (a, b, c and d) are representative of the 10 min time period. Comparison of the MALDI-TOF MS of $Mg^{2+}+ATP + XMP$ bound PfGMPS with that where Mg^{2+} alone was present (Fig. 4.12a and b), revealed absence of the proteolytic fragment of m/z value 15471.3 ± 1.5 Da in the former spectrum. However, the same peak was retained when the protein was bound to $Mg^{2+}+ATP$, $Mg^{2+}+XMP$ or $Mg^{2+}+AMP-PNP$, a non-hydrolysable analogue of ATP (Fig. 4.12 b and d). To ascertain that the absence of m/z 15471.3 ± 1.5 Da is not an ionization artifact arising due to the presence of $Mg^{2+}+ATP+XMP$, control experiments were performed where appropriate concentrations of the nucleotides were added after trypsin digestion, i.e. prior incubation of the protein with substrates was avoided and, the resulting mix on the MALDI-TOF plate was a real mimic of the actual concentrations of protein and ligand. Appearance of the tryptic fragment (m/z 15471.3 ± 1.5 Da) in all the spectra ruled out its artefactual presence and suggested that disappearance of the peak is a consequence of binding of $Mg^{2+}+ATP +XMP$ to PfGMPS.

To assign the tryptic fragments including the one corresponding to m/z 15471.3 ± 1.5 Da, the recombinant protein sequence was subjected to theoretical tryptic proteolysis, using Sequence Editor (Bruker Daltonics, Germany), and the experimental masses corresponding to a single possible theoretical mass within the standard deviation were listed (Table 4.1). The proteolytic fragment of m/z 15471.3 ± 1.5 Da was assigned to a theoretical fragment of m/z 15469.6 Da that corresponded to

R³⁸ - K¹⁷³ region of the glutaminase domain in PfGMPS (Fig. 4.12e). Indeed, reduction in number of bands around 15 kDa region was also evident from SDS–PAGE analysis of Mg²⁺ +ATP + XMP bound form of PfGMPS (Fig.4.11a, lane 5). These results suggested that a conformational change induced by the binding of ligands (ATP+XMP+Mg²⁺) in the ATPase domain is being transmitted to the glutaminase domain, probably leading to R³⁸ and K¹⁷³ becoming buried or reducing the overall dynamics in the protein that makes the residues inaccessible to trypsin digestion.

Table 4.1. Assignment of MALDI-TOF MS of peptides from limited trypsin digestion of PfGMPS

PfGMPS residues ^a	Theoretical mass ^b	Experimental mass ^c					
		1	2	3	4	5	6
38-173	15469.6	15471.3 ± 1.5	15471.9 ± 1.0	15470.2 ± 1.3	15471.6 ± 1.7	-	-
212-318	12713.3	12717.1 ± 0.6	12713.4 ± 4.1	12713.2 ± 1.3	12711.5 ± 2.5	12713.8 ± 0.7	12713.3 ± 1.5
247-349	11938.0	11943.5 ± 2.9	11942.1 ± 5.2	11942.8 ± 0.7	11936.3 ± 1.3	11941.1 ± 1.0	11936.4 ± 2.3
264-432	19376.1	19372.2 ± 1.4	19370.4 ± 1.6	19373.1 ± 1.1	19369.0 ± 3.7	19373.2 ± 1.5	19369.6 ± 1.5
264-468	23455.4 + (Na ⁺)	23479.4 ± 0.6	23474.8 ± 2.3	23481.6 ± 1.5	23478.5 ± 4.2	23477.6 ± 3.6	23481.4 ± 0.5
374-468	10903.9	10900.8 ± 1.7	10898.0 ± 5.6	10900.0 ± 1.6	10895.3 ± 1.5	10900.0 ± 1.5	10893.8 ± 1.7
393-568	20104.7 +(K ⁺)	20140.2 ± 1.7	20144.5 ± 1.6	20145.1 ± 0.4	20144.2 ± 1.5	20142.6 ± 1.9	20144.2 ± 1.5

Dash (-) represents absence of peak.^aPfGMPS tryptic fragments assigned by MALDI-TOF mass spectrometry. ^bTryptic peptide map was generated in silico using Sequence editor 3.0 (Bruker Daltonics, Germany). The assigned m/z values lie within the standard deviation of the experimental masses. ^cFragment masses determined experimentally. Each value is an average ± S.D of 5-6 measurements acquired under similar conditions. Protein-substrate combinations maintained during pre-incubation were Mg²⁺ alone (1), Mg²⁺+ATP (2), Mg²⁺+XMP (3), Mg²⁺+AMP-PNP (4), Mg²⁺ +ATP+XMP (5) and Mg²⁺+AMP-PNP +XMP (6). Details of the experiment are provided in “materials and methods”.

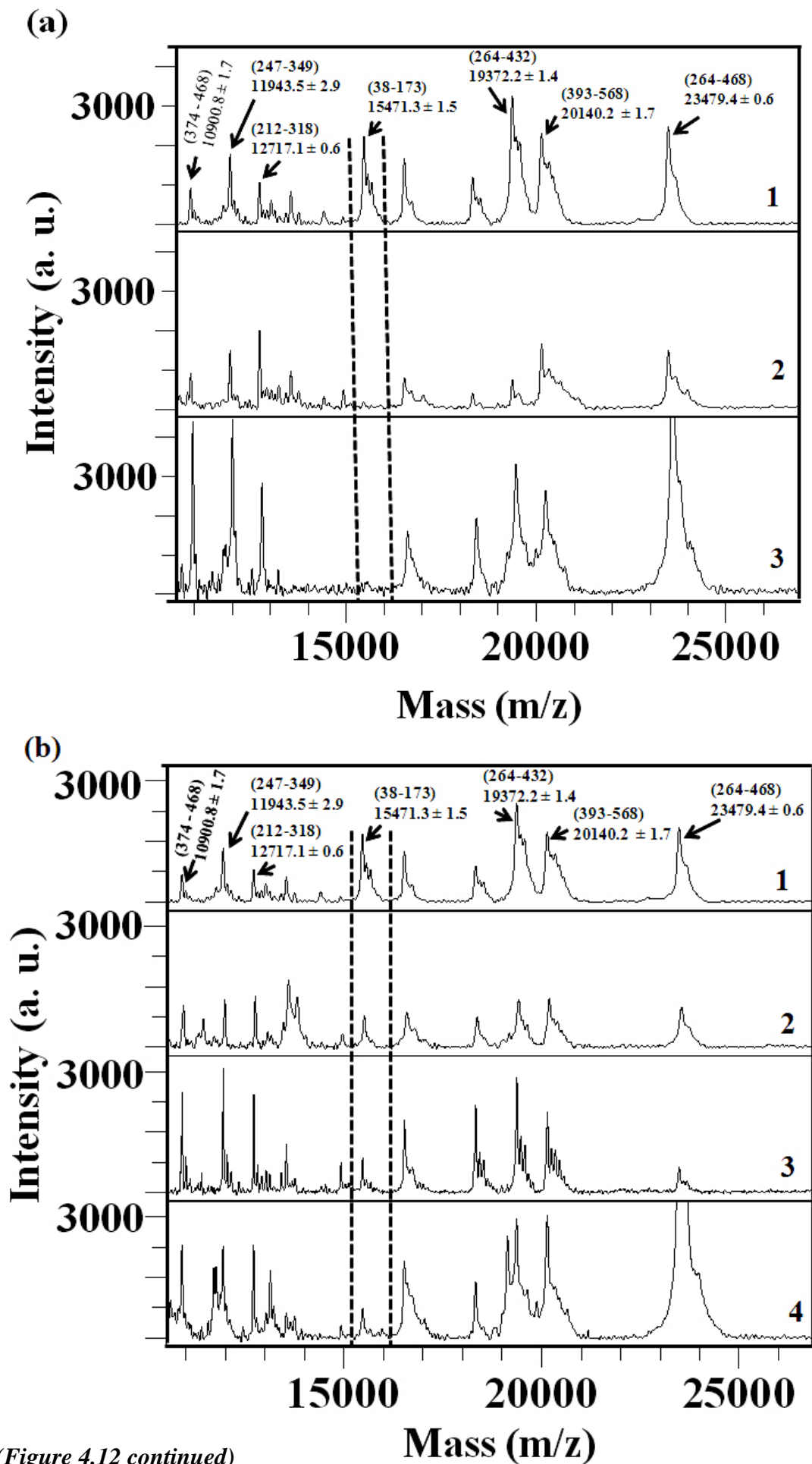


(Figure 4.12 continued)

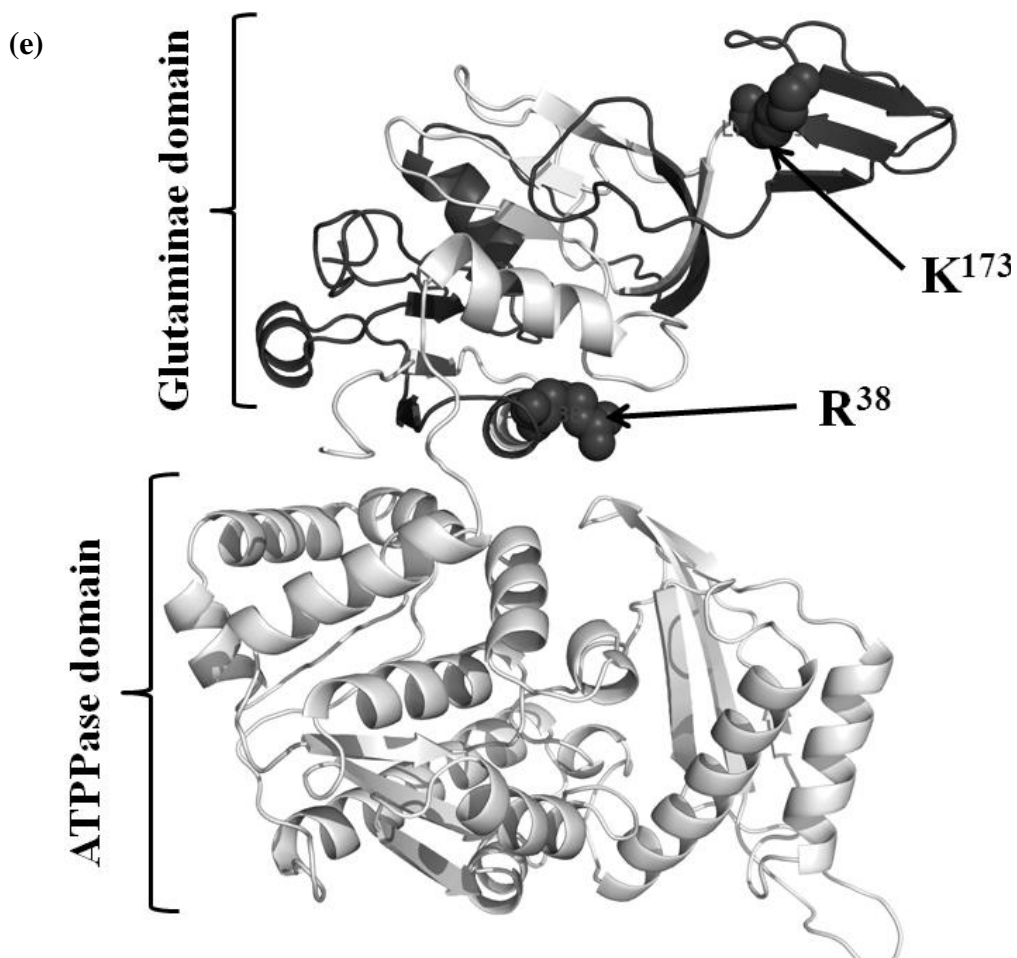
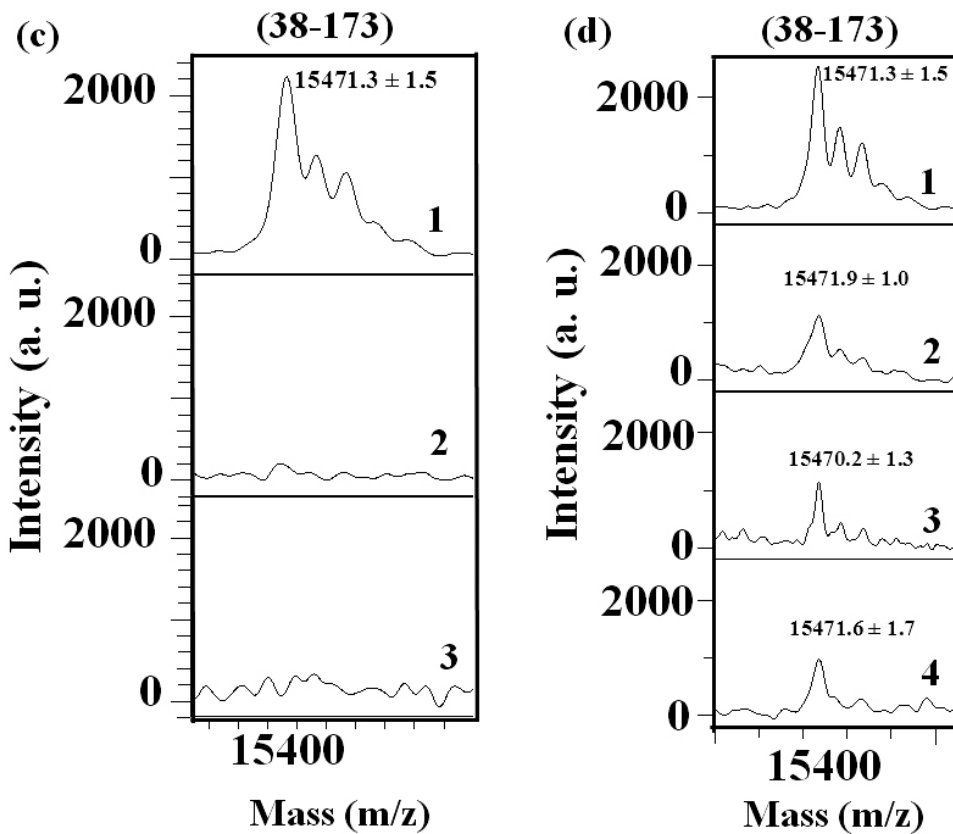


(Figure 4.12 continued)

Figure 4.12. MALDI-TOF mass spectrometric spectra of PfGMPS (between m/z 10,500 to 25,000 Da) after limited tryptic proteolysis.

(a) MALDI-TOF MS of the digested PfGMPS containing (1) Mg^{2+} (2) $Mg^{2+} + ATP + XMP$ and (3) $Mg^{2+} + AMP-PNP + XMP$. (b) MALDI-TOF MS of the proteolysed PfGMPS in presence of (1) Mg^{2+} , (2) $Mg^{2+} + ATP$, (3) $Mg^{2+} + XMP$ and (4) $Mg^{2+} + AMP-PNP$. (c) Expanded region of (a) between m/z 15000 to 16000 Da. (d) Expanded region of (b) between m/z 15000 to 16000 Da. Assignment of the tryptic fragments in panels 2 and 3 of (a) and 2, 3, 4 and 5 of (b) is given in table 4.1. The molecular mass of each peak is labeled as mean \pm S.D, calculated from 5-6 independent determinations. Spectral acquisition details are mentioned in "materials and methods". (e) Modeled structure of PfGMPS indicating the location of m/z 15471.3 ± 1.5 fragment ($R^{38}-K^{173}$) in the protein. The structure was generated and validated as described in "materials and methods" and visualized using PyMol.

4.4.4. Substrate-induced conformational changes in PfGMPS monitored by hydrogen-deuterium exchange coupled to MALDI-TOF mass spectrometry

Figure 4.13 shows a typical MALDI-TOF mass spectrum of pepsin digested PfGMPS recorded between m/z 950 to 2500 Da. **This** digestion pattern for PfGMPS under the given experimental conditions was highly reproducible across the experiments. After deuterium exchange, 17 peptic fragments remained well resolved and covered 35 % of PfGMPS primary sequence encompassing both the glutaminase and the ATPase domains (Fig. 4.14) and were used for H/DX analysis across the experiments.

Factors like protein to pepsin ratio, time period of peptic proteolysis and matrix composition affect the sequence coverage of a given protein; however, our repeated standardization efforts in this direction did not improve the coverage beyond the mentioned value. A time-dependent (30 sec to 15 min) analysis of deuterium incorporation suggested that a saturation phase was reached early at 10 min with a fast initial phase of deuteration (Fig. 4.15). To compare the relative deuteration of PfGMPS in the presence of varied combinations of ligands ($Mg^{2+}/ATP/XMP$), all the deuterium in-exchange reactions were performed for 10 min. Table 4.2a summarizes the deuterium incorporation of PfGMPS examined in the presence of five different ligand combinations. Comparison across the conditions shows varied levels of deuterium incorporation in peptides pertaining to different regions of PfGMPS and this reflects on differences in solvent accessibility of the amide protons across the

regions of the protein. To estimate the significance in the differences across the conditions, a two-way analysis of variance (ANOVA) was performed followed by paired comparison analysis of each of the conditions with the one containing Mg^{2+} alone (Table 4.2b).

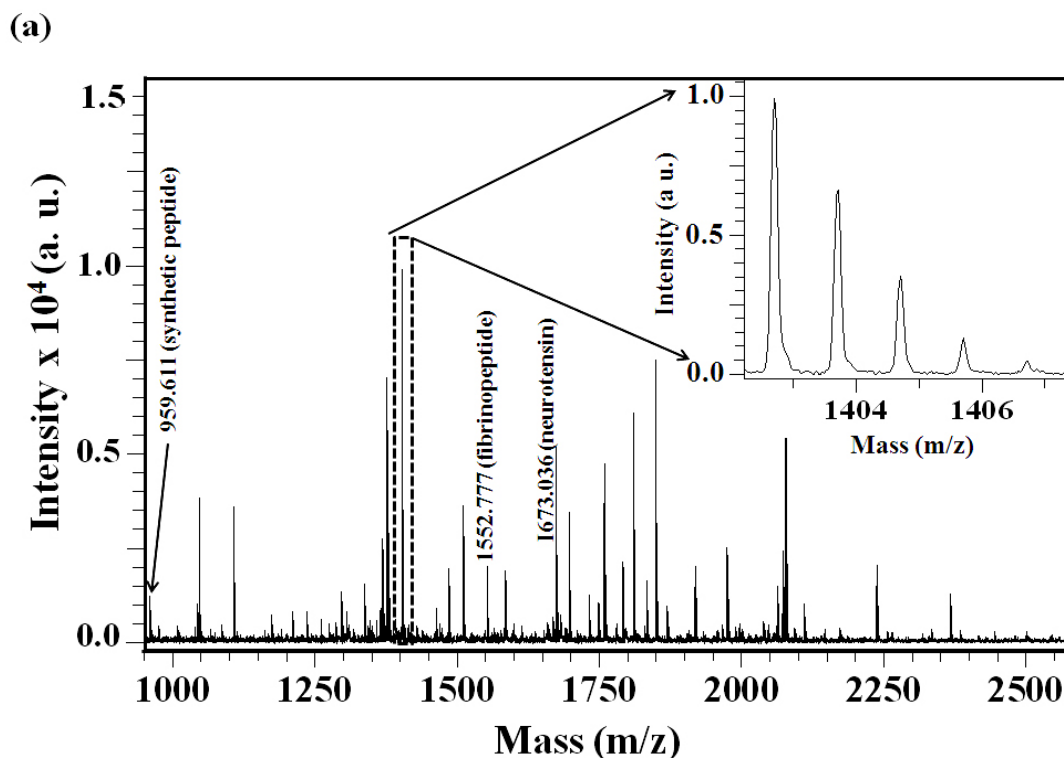


Figure 4.13. MALDI-TOF mass spectrum (between m/z 950 to 2500) of the undeuterated PfGMPS after pepsin digestion.

The marked peptides were used as internal standards for calibration. The inset shows an expanded region to highlight the quality of the spectrum. Protein digestion and conditions for spectral acquisition are given in “materials and methods”

```

MRGSHHHHHHGSMAEGEEYDKILVLNFGSQYFHLIVKRLNNIKIFSETKDYGVELKDIKDMNIKGVLS
GGPYSVTEAGSPHLKKEVFEYFLEKKIPIFGICYGMQEIAVQMNGEVKKSKTSEYGCTDVNLRNDNIN
ITYCRNFGDSSSAMDLYSNYKLMNETCCLFENIKSDITVWVMNHNDEVTKIPENFYLVSSSENCLICSIYN
KEYNIYGVQYHPEVYESLDGELMFYNFAYNICKCKKQFDPIRYHELELKNIEKYKHDHYVIAAMSGGID
STVAAAYTHKIFKERFFGIFIDNGLLRKNEAENVYTLKSTFPDMNITKIDASENFLSNLQGVTDPEQKRK
HGKLFIEEFKAVNNIDIDINKTFLLQGTLYPDIIESKCSKNLSDTIKTHHNVGGLPKNLKFKLFFEPFKYLE
KDDVKTLSRELNLPEEITNRHPFPGPLAIRVIGEINKHKLNILREVDDIFINDLKQYGLYNQISQAFVLL
SSKSVGVRGDARSYDYVCVLRVKTSSFMTANWYQIPYDILDKITRILSEVKGVNRILYDVSSKPPATIEFE
    
```

Figure 4.14. Sequence of PfGMPS showing the 17 identified peptides that were observed in a single MALDI-TOF mass spectrum.

The peptides cover 35% of the PfGMPS sequence including both the glutaminase and the ATPase domains.

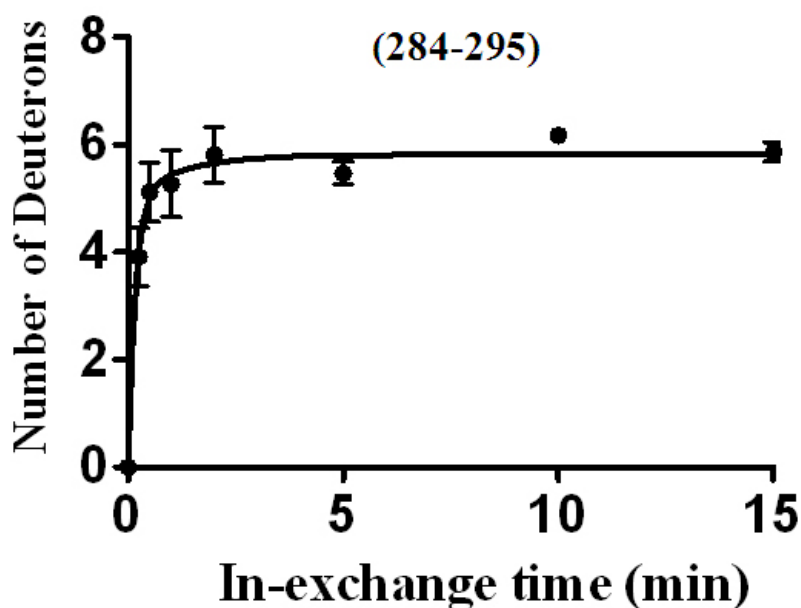


Figure 4.15. Time course of deuterium incorporation into the peptic fragment m/z 1511.9 (284-295).

The plot represents a fit of the data, using GraphPad Prism 5, to a two-phase exponential binding equation, $Y = Y_0 + A_1[1 - \exp(-k_f t)] + A_2[1 - \exp(-k_s t)]$, where Y and Y_0 represent deuterium numbers at time t and $t=0$, respectively. A_1 and A_2 represent the fast and slow phases of the exchange reaction that occur at rate constants k_f and k_s , respectively. Materials and methods (sections 4.3.7 and 4.3.8) describes the details of the experiment.

The peptic fragments that underwent significant change in deuterium incorporation compared to control belonged to both the glutaminase ([4-22] and [143-155]) and the ATPase ([300-314], [300-315] and [423-433]) domains (Fig. 4.16 and 4.17) and the change was evident only when the ATPase domain was completely liganded (bound to $Mg^{2+} + ATP + XMP$).

Table 4.2a. Summary of H/D exchange data for PfGMPS under different ligand bound conditions

PfGMPS Peptide residues ^a	Peptide mass ^b	No. of exchangeable protons ^c	No. of deuterons exchanged in 10 min ^d					
			1	2	3	4	5	6
4- 22	2238.71	18.95	12.1 ± 1.3	11.6 ± 0.1	11.0 ± 0.7	12.1 ± 0.3	9.4 ± 0.6	9.6 ± 0.7
36- 55	2367.80	20.15	9.7 ± 1.4	9.2 ± 0.7	7.8 ± 0.8	9.3 ± 1.2	9.6 ± 1.1	7.7 ± 0.3
37-51	1870.07	15.15	11.0 ± 1.0	9.6 ± 0.8	9.5 ± 0.3	10.0 ± 0.8	9.1 ± 0.6	9.6 ± 0.2
75-90	1834.44	13.17	5.6 ± 0.4	4.6 ± 0.7	5.4 ± 0.2	5.0 ± 1.0	4.1 ± 1.4	4.2 ± 0.4
128-142	1791.97	15.10	15.4 ± 1.0	15.2 ± 1.4	14.8 ± 1.7	15.4 ± 1.0	15.1 ± 0.8	14.7 ± 0.1
143-155	1403.63	12.75	9.9 ± 0.3	10.5 ± 0.3	10.1 ± 0.3	10.5 ± 0.4	8.2 ± 1.3	7.7 ± 1.4
259-272	1759.99	13.90	4.9 ± 0.4	4.2 ± 1.1	3.1 ± 0.1	5.0 ± 1.7	3.9 ± 0.4	4.1 ± 0.2
273-295	2501.45	23.00	18.1 ± 1.3	17.6 ± 1.5	15.9 ± 0.5	15.3 ± 0.6	16.6 ± 0.5	16.2 ± 0.7
284-295	1511.91	11.80	6.2 ± 0.6	6.3 ± 0.6	5.6 ± 0.5	5.7 ± 0.8	5.5 ± 0.3	5.5 ± 0.1
286-295	1370.15	9.75	4.3 ± 0.4	4.2 ± 0.6	4.0 ± 0.2	4.5 ± 0.5	4.1 ± 0.4	3.8 ± 0.2
300-314	1748.99	15.00	11.8 ± 1.5	11.0 ± 0.1	9.8 ± 0.4	10.5 ± 0.4	8.6 ± 0.3	9.0 ± 0.6
300-315	1850.06	16.05	12.9 ± 1.4	11.8 ± 0.3	11.3 ± 0.2	11.7 ± 0.3	9.3 ± 0.6	9.9 ± 0.7
314-329	1919.31	14.80	6.2 ± 1.1	5.9 ± 0.2	5.2 ± 1.1	6.2 ± 0.3	6.0 ± 0.4	5.2 ± 0.2
340-355	1811.20	15.05	7.9 ± 1.0	7.7 ± 0.3	6.9 ± 0.9	7.1 ± 0.0	6.1 ± 0.3	6.7 ± 0.2
423-433	1338.11	10.85	9.7 ± 0.7	9.4 ± 0.8	8.3 ± 0.6	10.3 ± 1.0	7.5 ± 0.7	7.9 ± 0.7
437- 452	1733.12	11.70	8.4 ± 0.4	9.0 ± 0.6	7.9 ± 0.4	8.0 ± 0.5	7.3 ± 1.0	6.6 ± 0.5
440-452	1377.79	9.60	4.0 ± 0.5	4.0 ± 0.2	3.8 ± 0.4	4.2 ± 0.6	2.9 ± 0.4	2.9 ± 0.0

^a Numbers represent peptide boundaries. ^b Centroid mass of the identified undeuterated peptic peptides. ^c Total number of the amide protons that can undergo exchange plus the fraction contributed by fast-exchanging side-chain protons at the used dilution. ^d Number of deuterons gained by the peptides after the in-exchange was allowed for 10 min under the conditions described in “materials and methods”. Numbers represent mean of at least 4 independent measurements ± S.D. All the numbers are corrected for back and in-quench exchanges. 1, 2 3, 4, 5 and 6 indicate different PfGMPS –ligand combinations subjected to deuteration as, Mg^{2+} , $Mg^{2+} + ATP$, $Mg^{2+} + XMP$, $Mg^{2+} + AMP - PNP$, $Mg^{2+} + ATP + XMP$ and $Mg^{2+} + AMP - PNP + XMP$, respectively.

Reduced deuterium exchange in the peptic fragments [300-314], [300-315] and [423-433]) reflect the short-range effects of ligand(s) binding to the ATPase domain. Though the fragment [4-22] contains the relatively flexible N-terminal 6X His-tag, the fragment [143-155] forms part of the m/z 15470.6 Da peptide that was shown to undergo a change in the limited tryptic proteolysis followed by MALDI-TOF MS experiments. These observations confirmed the long-range structural changes brought about by ligand binding in PfGMPS and again suggested that a change probably originating in the ATPase domain is relayed to the glutaminase domain.

Table 4.2b. Comparison^a of H/D exchange data for PfGMPS under different liganded conditions

PfGMPS residue	Peptide mass	Paired comparisons				
		1/2	1/3	1/4	1/5	1/6
4-22	2238.71	^b ns	ns	ns	***	**
36-55	2367.80	ns	ns	ns	ns	ns
37-51	1870.07	ns	ns	ns	ns	ns
75-90	1834.44	ns	ns	ns	ns	ns
128-142	1791.97	ns	ns	ns	ns	ns
143-155	1403.63	ns	ns	ns	*	**
259-272	1759.99	ns	ns	ns	ns	ns
273-295	2501.45	ns	ns	ns	ns	ns
284-295	1511.91	ns	ns	ns	ns	ns
286.295	1370.15	ns	ns	ns	ns	ns
300-314	1748.99	ns	ns	ns	***	***
300-315	1850.06	ns	ns	ns	***	***
314-329	1919.31	ns	ns	ns	ns	ns
340-355	1811.20	ns	ns	ns	ns	ns
423-433	1338.11	ns	ns	ns	**	**
437-452	1733.12	ns	ns	ns	ns	ns
440-452	1377.79	ns	ns	ns	ns	ns

^a Comparison was performed by two-way ANOVA using GraphPad Prism 5. ^b Results are shown as the statistical significance level. ns: not significant. * $p < 0.5$, ** $p < 0.01$ and *** $p < 0.001$. 1, 2 3, 4, 5 and 6 indicate the conditions **wherein** PfGMPS H/D exchange was carried out in presnce of Mg^{2+} , $Mg^{2+} + ATP$, $Mg^{2+} + XMP$, $Mg^{2+} + AMP - PNP$, $Mg^{2+} + ATP + XMP$ and $Mg^{2+} + AMP - PNP + XMP$, respectively.

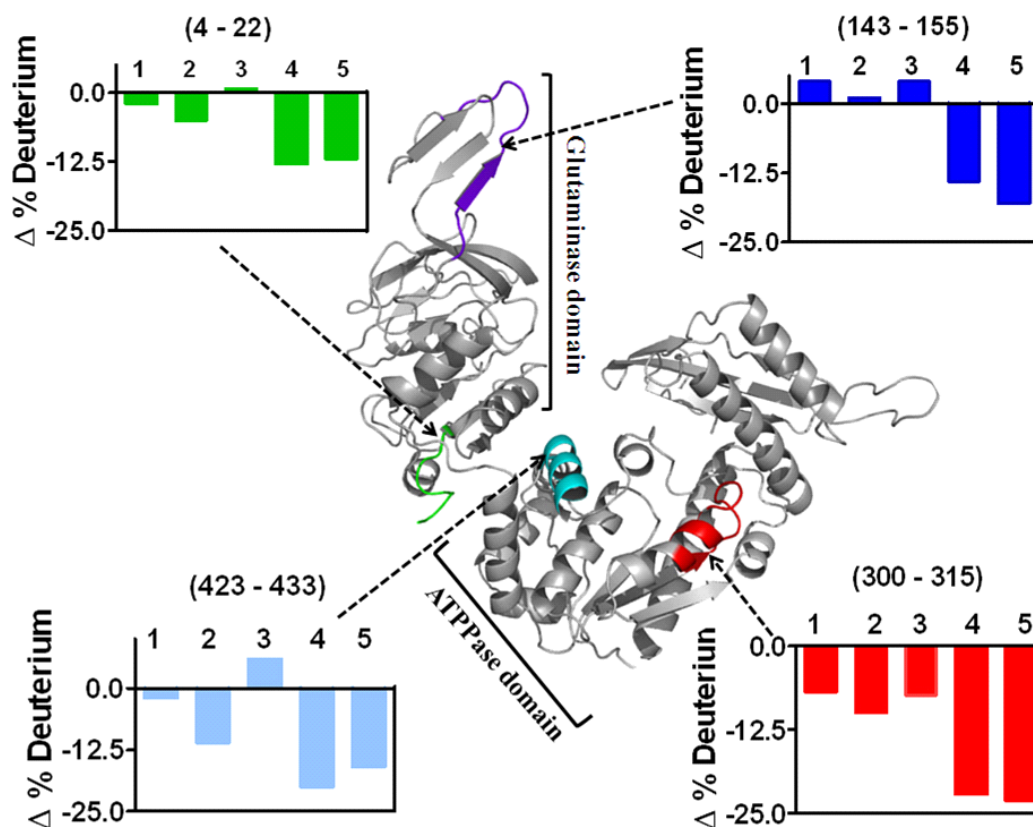


Figure 4.16. Effect of substrate binding on structure of PfGMPS as monitored by H/D exchange coupled to MALDI-TOF MS

Summary of results of H/DX mapped onto the modelled structure of PfGMPS. The bar graphs represent % difference in deuterium content in each of the relevant peptides (of liganded PfGMPS) relative to that measured for unliganded PfGMPS (Mg^{2+} bound). Numbers 1, 2, 3, 4 and 5 represent substrate combinations of PfGMPS with, Mg^{2+} +ATP, Mg^{2+} +XMP, Mg^{2+} +AMP-PNP, Mg^{2+} +ATP+XMP and Mg^{2+} +AMP-PNP+XMP, respectively. Numbers in paraenthesis represent PfGMPS residues for the respective peptides and arrows point to the location of peptide segments in the modeled PfGMPS structure, visualised in PyMol, as described in “materials and methods”. The colour coding of the peptide segments corresponds to those in the bar graphs.

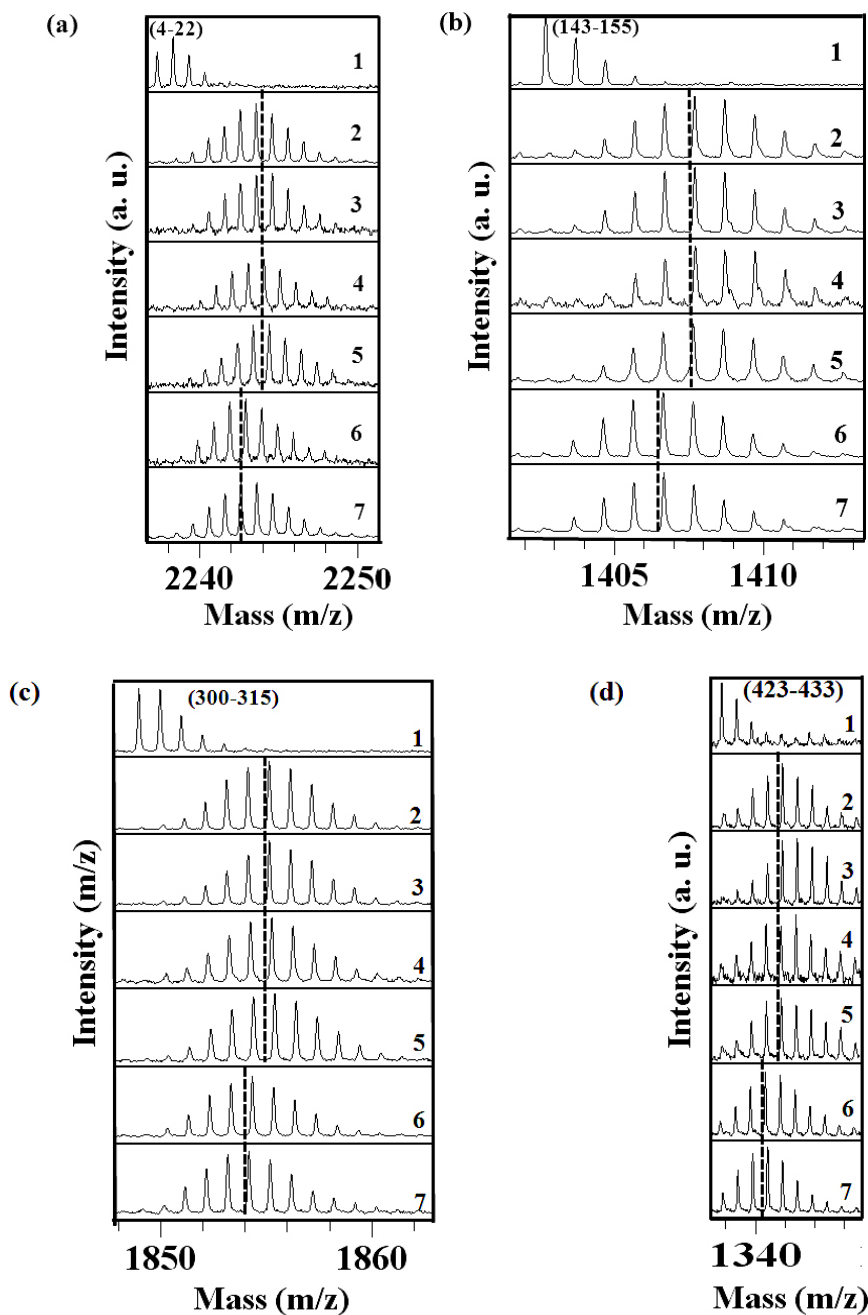


Figure 4.17. Isotopic distribution in peptides corresponding to the regions 4-22 (a), 143-155 (b), 300-315 (c) and 423-433 (d) of PfGMPS compared across different liganded states. These four peptides, under fully liganded condition, showed reduced deuterium incorporation. Numbers 1-7 in the panels correspond to Mg^{2+} , $Mg^{2+} + ATP$, $Mg^{2+} + XMP$, $Mg^{2+} + AMP-PNP$, $Mg^{2+} + ATP + XMP$ and $Mg^{2+} + AMP-PNP + XMP$, respectively the different ligand combinations that PfGMPS was pre-incubated with. Dotted line indicates centroid of the isotopic cluster of the deuterated peptides. Details of spectral acquisition and processing are given in “materials and methods”

4.5. Discussion

All amidotransferases have at least two spatially separate domains that are either fused (single subunit two-domain) or interact as two separate subunits (two-domain, two-subunit) whose coordinated activities lead to incorporation of nitrogen into their respective substrates. Two distinct functional consequences arise out of substrate-induced structural changes in GATs. The first relates to repositioning of the synthetase and the glutaminase domains that leads to the activation of the glutaminase activity. Structural evidence for the re-organization have been evoked by comparing the liganded and unliganded structures of glucoseamine-6-phosphate synthase (Floquet et al., 2009; Mouilleron et al., 2008), glutamine phosphoribosylpyrophosphate amidotransferase (Krahn et al., 1997; Muchmore et al., 1998) and imidazole glycerol phosphate synthase (Chaudhuri et al., 2003). The second pertains to the structural changes that lead to channel formation. Unlike the presence of a preformed channel in the unliganded form of CPS (Thoden et al., 1997), the channels in most of the amidotransferases are generated by structural transitions arising from complete liganding of the enzyme. (Floquet et al., 2009; Mouilleron et al., 2008; van den Heuvel et al., 2004; van den Heuvel et al., 2003).

In the absence of any experimentally deduced structure, biochemical assays, ANS fluorescence, CD spectroscopy and mass spectrometry served as probes to compare the substrate bound and unbound forms of PfGMPS in terms of the conformational transformations. Similarity in Mg^{2+} + XMP and Mg^{2+} + ATP + XMP bound forms of PfGMPS as revealed by ANS fluorescence and CD spectroscopy, suggest a similar structural alteration in the protein under the two liganded conditions. However, limited proteolysis and H/D exchange coupled to MALDI-TOF mass spectrometry suggested that the two liganded forms are structurally different, as binding of Mg^{2+} + XMP did not bring about a conformational change in the glutaminase domain. These observations corroborate our findings that Mg^{2+} +XMP neither affects the glutaminase activity nor the rate of inactivation of the glutaminase domain by acivicin and DON (Table 2.4 of chapter 2 and Fig 4. 8). Our observations also fall in-line with the studies on EcGMPS (von der Saal et al., 1985) that implicated the XMP-induced changes in protein, reported earlier (Zyk et al., 1970), to be catalytically non-productive. Also, the rate of glutaminase inactivation by covalent modifying agents in human (Nakamura et al., 1995) and *E. coli* (Zalkin and Truitt,

1977) GMP synthetases, did not alter significantly when XMP alone was bound to the ATPase domain.

Conformational changes and dynamics in proteins are routinely being monitored by H/DX in conjunction with mass spectrometry (Busenlehner and Armstrong, 2005). We have utilized this method in PfGMPS to substantiate the structural changes revealed by other probes and also to narrow down the substrate-induced changes in a region-specific manner. Though the low sequence coverage precluded the monitoring of HD/X in all the regions of PfGMPS, sufficient information was gained from the experiments to confirm that the protein undergoes a ligand-induced conformational transition that traverses across the domains. The decreased deuteration level of specific peptides in the ATPase domain (Fig. 4.16, 4.17c, d and Table 4.2a and b) could be attributed to (1) direct shielding of the amide protons by substrates from the solvent, (2) structural change that reduces the solvent exposure of the amide protons, and (3) combination of the two. Formation of adenylyl-XMP intermediate from $Mg^{2+}+ATP + XMP$ in the absence of any nitrogen donor is known in GMP synthetases (Fukuyama, 1966; Tesmer et al., 1996; von der Saal et al., 1985). In order to examine whether preclusion of the intermediate formation would still lead to conformational changes in PfGMPS, ATP in $Mg^{2+} + ATP + XMP$ was replaced by AMP-PNP. Interestingly, changes in deuterium incorporation observed in peptides [300-314], [300-315], [423-433] (ATPase domain), [4-22] and [143-155] (glutaminase domain) were similar to that when PfGMPS was bound to $Mg^{2+}+ATP+XMP$. These results suggested that the binding of $Mg^{2+}+ATP+XMP$ is sufficient to bring out a structural transition in PfGMPS. However, these results could not delineate any further contribution that the adenylyl-XMP intermediate may have in altering conformation of the protein. These results agree with the biochemical assays done on PfGMPS, where the binding of $Mg^{2+}+AMPNP +XMP$ to the protein was shown to enhance the glutaminase activity above the basal level (Table 2.4, Chapter 2). Comparison of the liganded structures of *E. coli* and *T. thermophilus* GMP synthetases with that of the unliganded *P. horikoshii* enzyme has led to the identification of 26 putative ATP and XMP binding residues (Maruoka et al., 2010) in the ATPase domain with most being conserved across GMP synthetases. Interestingly in PfGMPS, Ile³⁰⁰ and Lys⁴²⁴ belonging to the peptic fragments [300-315] and [423-433], respectively that showed reduced deuterium uptake upon complete liganding, correspond to Val⁵³ and Lys¹⁶⁶, two of the putative ATP

interacting residues in the *P. horikoshii* ATPase domain (Fig 4.18). Moreover, contact analysis of EcGMPs bound to AMP and PPi using CCP4 software (Potterton et al., 2002; Potterton et al., 2004) showed Val²⁶⁰ to be present within 4Å distance of the AMP molecule and this residue corresponds to the Ile³⁰⁰ in PfGMPS. These observations further suggest that the reduced deuteration in the two ATPase regions, arise due to the local effects of ligand binding to the protein. Further, mutational analysis of the residues should validate their role in GMP synthetase function.

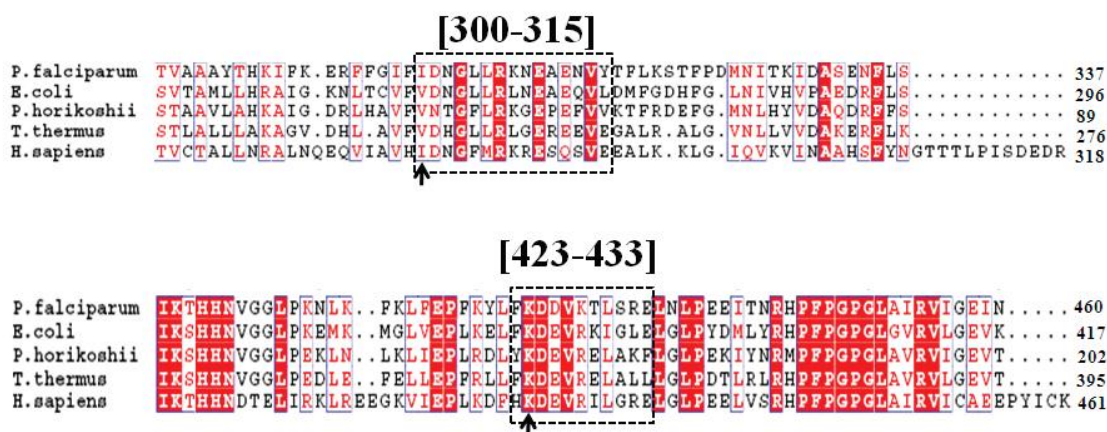


Figure 4.18. Sequence alignment of two segments of *P. falciparum*, *E. coli*, *T. thermophilus*, *H. sapiens* and *P. horikoshii* GMP synthetases, generated using ClustalW (Higgins D., 1994) and ESript 2.2. (Gouet et al., 2003). The boxed regions represent the peptic peptides of PfGMPS that showed reduced deuteration on complete liganding of the ATPase domain in *P. falciparum* GMPS and their comparison with those of other GMP synthetases. Arrows in the two panels point the putative ATP binding residues.

Reduced deuterium incorporation in the different peptic peptides of PfGMPS after complete liganding of the ATPase domain with Mg²⁺+ATP + XMP (Fig. 4.16, 4.17a, b and Table 4.2a and b) corroborated well with the change elicited by limited proteolysis MALDI-TOF experiments. Propagation of the synthetase domain originated conformational transitions to the glutaminase domain in many GATs have been implicated in catalysis. Whether the similar changes in PfGMPS, elicited as reduced deuterium incorporation in [4-22] and [143-155] peptic fragments, serves the same purpose, remains to be validated. Interestingly, the peptic fragment [143-155] locates to the unique 20 residue insertion of PfGMPS, whose function is still to be determined.

In conclusion, this study highlights that binding of ATP and XMP to the ATPase domain of PfGMPS brings about a large conformational change in the protein, probably leading to its change from open to the closed state. This change in PfGMPS, like in other amidotransferases, could be affecting both positioning of the glutaminase domain for optimum glutamine hydrolysis or ammonia channeling. Elucidating the rate constants for the individual steps including that for the conformational change, should highlight whether the conformational transformation could be the rate limiting step in PfGMPS catalysis.

REFERENCES

References

- 1) Abbott, J. L., Newell, J. M., Lightcap, C. M., Olanich, M. E., Loughlin, D. T., Weller, M. A., Lam, G., Pollack, S., and Patton, W. A. (2006). The effects of removing the GAT domain from *E. coli* GMP synthetase. *Protein J* 25, 483-491.
- 2) Abrams, R., and Bentley, M. (1955). Transformation of inosinic acid to adenylic and guanylic acids in a soluble enzyme system. *J Am Chem Soc* 77, 4179-4180.
- 3) Allison, R. D., and Purich, D. L. (2002). A survey of covalent, ionic, and radical intermediates in enzyme-catalyzed reactions. *Methods Enzymol* 354, 455-470.
- 4) Amaro, R. E., Myers, R. S., Davisson, V. J., and Luthey-Schulten, Z. A. (2005). Structural elements in IGP synthase exclude water to optimize ammonia transfer. *Biophys J* 89, 475-487.
- 5) Amaro, R. E., Sethi, A., Myers, R. S., Davisson, V. J., and Luthey-Schulten, Z. A. (2007). A network of conserved interactions regulates the allosteric signal in a glutamine amidotransferase. *Biochemistry* 46, 2156-2173.
- 6) Amuro, N., Paluh, J. L., and Zalkin, H. (1985). Replacement by site-directed mutagenesis indicates a role for histidine 170 in the glutamine amide transfer function of anthranilate synthase. *J Biol Chem* 260, 14844-14849.
- 7) Anand, R., Hoskins, A. A., Stubbe, J., and Ealick, S. E. (2004). Domain organization of *Salmonella typhimurium* formylglycinamide ribonucleotide amidotransferase revealed by X-ray crystallography. *Biochemistry* 43, 10328-10342.
- 8) Anderson, K. S. (1999). Fundamental mechanisms of substrate channeling. *Methods Enzymol* 308, 111-145.
- 9) Anderson, P. M., and Meister, A. (1966). Control of *Escherichia coli* carbamyl phosphate synthetase by purine and pyrimidine nucleotides. *Biochemistry* 5, 3164-3169.
- 10) Aoki, T., Shimogawara, R., Ochiai, K., Yamasaki, H., and Shimada, J. (1994). Molecular characterization of a carbamoyl-phosphate synthetase II (CPS II) gene from *Trypanosoma cruzi*. *Adv Exp Med Biol* 370, 513-516.
- 11) Baca, A. M., and Hol, W. G. (2000). Overcoming codon bias: a method for high-level overexpression of *Plasmodium* and other AT-rich parasite genes in *Escherichia coli*. *Int J Parasitol* 30, 113-118.
- 12) Badet, B., Vermoote, P., Haumont, P. Y., Lederer, F., and LeGoffic, F. (1987). Glucosamine synthetase from *Escherichia coli*: purification, properties, and glutamine-utilizing site location. *Biochemistry* 26, 1940-1948.
- 13) Badet-Denisot, M. A., and Badet, B. (1994). Chemical modification of glucoseamine-6-phosphate synthase by diethyl pyrocarbonate: evidence of histidine requirement for enzymatic activity. *Arch Biochem Biophys* 292, 475-478.
- 14) Bahl, A., Brunk, B., Crabtree, J., Fraunholz, M. J., Gajria, B., Grant, G. R., Ginsburg, H., Gupta, D., Kissinger, J. C., Labo, P., *et al.* (2003). PlasmoDB: the *Plasmodium*

- genome resource. A database integrating experimental and computational data. *Nucleic Acids Res* *31*, 212-215.
- 15) Bai, Y., Milne, J. S., Mayne, L., and Englander, S. W. (1993). Primary structure effects on peptide group hydrogen exchange. *Proteins* *17*, 75-86.
 - 16) Barbar, E. (1999). NMR characterization of partially folded and unfolded conformational ensembles of proteins. *Biopolymers* *51*, 191-207.
 - 17) Barden, R. E., Fung, C.H., Utter, M.F., and Scrutton, M. C. (1972). Pyruvate carboxylase from chicken liver. Steady state kinetic studies indicate a "two- site" ping-pong mechanism. . *J Biol Chem* *247*, 1323-1233.
 - 18) Bellinzoni, M., Buroni, S., Pasca, M. R., Guglierame, P., Arcesi, F., De Rossi, E., and Riccardi, G. (2005). Glutamine amidotransferase activity of NAD⁺ synthetase from *Mycobacterium tuberculosis* depends on an amino-terminal nitrilase domain. *Res Microbiol* *156*, 173-177.
 - 19) Bera, A. K., Smith, J. L., and Zalkin, H. (2000). Dual role for the glutamine phosphoribosylpyrophosphate amidotransferase ammonia channel. Interdomain signaling and intermediate channeling. *J Biol Chem* *275*, 7975-7979.
 - 20) Berg, M., Van der Veken, P., Goeminne, A., Haemers, A., and Augustyns, K. (2010). Inhibitors of the purine salvage pathway: a valuable approach for antiprotozoal chemotherapy? *Curr Med Chem* *17*, 2456-2481.
 - 21) Berger, A., and Linderstrom-Lang, K. (1957). Deuterium exchange of poly-DL-alanine in aqueous solution. *Arch Biochem Biophys* *69*, 106-118.
 - 22) Bhat, J. Y., Shastri, B. G., and Balaram, H. (2008). Kinetic and biochemical characterization of *Plasmodium falciparum* GMP synthetase. *Biochem J* *409*, 263-273.
 - 23) Binda, C., Bossi, R. T., Wakatsuki, S., Arzt, S., Coda, A., Curti, B., Vanoni, M. A., and Mattevi, A. (2000). Cross-talk and ammonia channeling between active centers in the unexpected domain arrangement of glutamate synthase. *Structure* *8*, 1299-1308.
 - 24) Boehlein SK, R. N., Schuster SM. (1994). Glutamine-dependent nitrogen transfer in *Escherichia coli* asparagine synthetase B. Searching for the catalytic triad. *J Biol Chem* *269*, 7450-7457.
 - 25) Booden, T., and Hull, R. W. (1973). Nucleic acid precursor synthesis by *Plasmodium lophurae* parasitizing chicken erythrocytes. *Exp Parasitol* *34*, 220-228.
 - 26) Bradford, M. M. (1976). A rapid and sensitive method for the quantitation of microgram quantities of protein utilizing the principle of protein-dye binding. *Anal Biochem* *72*, 248-254.

- 27) Brady, R. L., and Cameron, A. (2004). Structure-based approaches to the development of novel anti-malarials. *Curr Drug Targets* 5, 137-149.
- 28) Breukera, K., and McLafferty, F. W. (2008). Stepwise evolution of protein native structure with electrospray into the gas phase, 10^{-12} to 10^2 s *Proc Natl Acad Sci USA* 105 18145-18152.
- 29) Briggs, G. E., and Haldane, J. B. (1925). A note on the kinetics of enzyme action. *Biochem J* 19, 338-339.
- 30) Brown, D. M., Netting, A. G., Chun, B. K., Choi, Y., , Chu, C. K., and Gero, A. M. (1999). L-nucleoside analogues as potential antimalarials that selectively target *Plasmodium falciparum* adenosine deaminase. *Nucleosides Nucleotides* 18, 2521-2532.
- 31) Buchanan, C. E. (1985). Induction of penicillin-binding proteins under catabolite-repressed conditions. *J Bacteriol* 162, 1302-1303.
- 32) Buchanan, J. M. (1973). The amidotransferases. *Adv Enzymol Relat Areas Mol Biol* 39, 91-183.
- 33) Buchner P, M. W., Ruterjans H (1978). Nitrogen- 15 nuclear magnetic resonance spectroscopy of ^{15}N -labeled nucleotides. *J Magn Reson* 29, 45-63.
- 34) Bulusu, V., Srinivasan, B., Bopanna, M. P., and Balaram, H. (2009). Elucidation of the substrate specificity, kinetic and catalytic mechanism of adenylosuccinate lyase from *Plasmodium falciparum*. *Biochim Biophys Acta* 1794, 642-654.
- 35) Bungener, W., and Nielsen, G. (1967). Nucleic acid metabolism in experimental malaria. 1. Studies on the incorporation of thymidine, uridine, and adenosine in the malaria parasite (*Plasmodium berghei* and *Plasmodium vinckei*). *Z Tropenmed Parasitol* 18, 456-462.
- 36) Bungener, W., and Nielsen, G. (1968). Nucleic acid metabolism in experimental malaria. 2. Incorporation of adenosine and hypoxanthine into the nucleic acids of malaria parasites (*Plasmodium berghei* and *Plasmodium vinckei*). *Z Tropenmed Parasitol* 19, 185-197.
- 37) Bungener, W., and Nielsen, G. (1969). Nucleic acid metabolism in experimental malaria. 3. The utilization of adenine from the adenine-nucleotide pool of the erythrocytes for the synthesis of nucleic acids in malaria parasites (*Plasmodium vinckei*) in vivo. *Z Tropenmed Parasitol* 20, 67-73.
- 38) Busenlehner, L. S., and Armstrong, R. N. (2005). Insights into enzyme structure and dynamics elucidated by amide H/D exchange mass spectrometry. *Arch Biochem Biophys* 433, 34-46.
- 39) Bustamante, C., Batista, C. N., and Zalis, M. (2009). Molecular and biological aspects of antimalarial resistance in *Plasmodium falciparum* and *Plasmodium vivax*. *Curr Drug Targets* 10, 279-290.

- 40) Carter, N. S., Ben Mamoun, C., Liu, W., Silva, E. O., Landfear, S. M., Goldberg, D. E., and Ullman, B. (2000). Isolation and functional characterization of the PfNT1 nucleoside transporter gene from *Plasmodium falciparum*. *J Biol Chem* 275, 10683-10691.
- 41) Chaparian, M. G., and Evans, D. R. (1991). The catalytic mechanism of the amidotransferase domain of the Syrian hamster multifunctional protein CAD. Evidence for a CAD-glutamyl covalent intermediate in the formation of carbamyl phosphate. *J Biol Chem* 266, 3387-3395.
- 42) Chaudhuri, B. N., Lange, S. C., Myers, R. S., Davisson, V. J., and Smith, J. L. (2001). Crystal structure of imidazole glycerol phosphate synthase: a tunnel through a (beta/alpha)₈ barrel joins two active sites. *Structure (Camb)* 9, 987-997.
- 43) Chaudhuri, B. N., Lange, S. C., Myers, R. S., Davisson, V. J., and Smith, J. L. (2003). Toward understanding the mechanism of the complex cyclization reaction catalyzed by imidazole glycerolphosphate synthase: crystal structures of a ternary complex and the free enzyme. *Biochemistry* 42, 7003-7012.
- 44) Chen, S., Burgner, J. W., Krahn, J. M., Smith, J. L., and Zalkin, H. (1999). Tryptophan fluorescence monitors multiple conformational changes required for glutamine phosphoribosylpyrophosphate amidotransferase interdomain signaling and catalysis. *Biochemistry* 38, 11659-11669.
- 45) Cheng, K. W., Wong, C. C., Wang, M., He, Q. Y., and Chen, F. (2010). Identification and characterization of molecular targets of natural products by mass spectrometry. *Mass Spectrom Rev* 29, 126-155.
- 46) Chittur, S. V., Klem, T. J., Shafer, C. M., and Davisson, V. J. (2001). Mechanism for acivicin inactivation of triad glutamine amidotransferases. *Biochemistry* 40, 876-887.
- 47) Choi, S. R., Mukherjee, P., and Avery, M. A. (2008). The fight against drug-resistant malaria: novel plasmodial targets and antimalarial drugs. *Curr Med Chem* 15, 161-171.
- 48) Cleland, W. W. (1963). The kinetics of enzyme-catalyzed reactions with two or more substrates or products. II. Inhibition: nomenclature and theory. *Biochim Biophys Acta* 67, 173-187.
- 49) Cleland, W. W. (1995). Kinetic method for determination of dissociation constants of metal ion-nucleotide complexes. *Methods Enzymol* 249, 181-188.
- 50) Cook, P. F., Cleland, W.W. (2007). *Enzyme kinetics and mechanism*, Garland Science, Taylor and Francis group.
- 51) Crowther, G. J., Napuli, A. J., Gilligan, J. H., Gagaring, K., Borboa, R., Francek, C., Chen, Z., Dagostino, E. F., Stockmyer, J. B., and Wang, Y., et al. (2010). Identification of inhibitors for putative malaria drug targets among novel antimalarial compounds. *Mol Biochem Parasitol (In press)*.

- 52) Daddona, P. E., Wiesmann, W. P., Lambros, C., Kelley, W. N., and Webster, H. K. (1984). Human malaria parasite adenosine deaminase. Characterization in host enzyme-deficient erythrocyte culture. *J Biol Chem* 259, 1472-1475.
- 53) Daddona, P. E., Wiesmann, W. P., Milhouse, W., Chern, J. W., Townsend, L. B., Hershfield, M. S., and Webster, H. K. (1986). Expression of human malaria parasite purine nucleoside phosphorylase in host enzyme-deficient erythrocyte culture. Enzyme characterization and identification of novel inhibitors. *J Biol Chem* 261, 11667-11673.
- 54) Delaglio, F., Grzesiek, S., Vuister, G. W., Zhu, G., Pfeifer, J., and Bax, A. (1995). NMRPipe: a multidimensional spectral processing system based on UNIX pipes. *J Biomol NMR* 6, 277-293.
- 55) Deras, M. L., Chittur, S. V., and Davisson, V. J. (1999). N2-hydroxyguanosine 5'-monophosphate is a time-dependent inhibitor of *Escherichia coli* guanosine monophosphate synthetase. *Biochemistry* 38, 303-310.
- 56) Derrer, B., Windeisen, V., Rodriguez, G. G., Seidler, J., Gengenbacher, M., Lehmann, W. D., Rippe, K., Sinning, I., Tews, I., and Kappes, B. (2010). Defining the structural requirements for ribose 5-phosphate-binding and intersubunit cross-talk of the malarial pyridoxal 5-phosphate synthase. *FEBS Lett* 584, 4169-4174.
- 57) Donaldson, T., Kim, K. (2010). Targeting *Plasmodium falciparum* purine salvage enzymes: a look at structure-based drug development. *Infect Disord Drug Targets* 10, 191-199.
- 58) Downie, M. J., El Bissati, K., Bobenchik, A. M., Nic Lochlainn, L., Amerik, A., Zufferey, R., Kirk, K., and Ben Mamoun, C. (2010). PfNT2, a permease of the equilibrative nucleoside transporter family in the endoplasmic reticulum of *Plasmodium falciparum*. *J Biol Chem* 285, 20827-20833.
- 59) Downie, M. J., Kirk, K., and Mamoun, C. B. (2008). Purine salvage pathways in the intraerythrocytic malaria parasite *Plasmodium falciparum*. *Eukaryot Cell* 7, 1231-1237.
- 60) Eaazhisai, K., Jayalakshmi, R., Gayathri, P., Anand, R. P., Sumathy, K., Balaram, H., and Murthy, M. R. (2004). Crystal structure of fully ligated adenylosuccinate synthetase from *Plasmodium falciparum*. *J Mol Biol* 335, 1251-1264
- 61) El Bissati, K., Downie, M.J., Kim, S.K., Horowitz, M., Carter, N., Ullman, B., Ben Mamoun, C. (2008). Genetic evidence for the essential role of PfNT1 in the transport and utilization of xanthine, guanine, guanosine and adenine by *Plasmodium falciparum*. *Mol Biochem Parasitol* 161, 130-139.
- 62) El Bissati, K., Zufferey, R., Witola, W. H., Carter, N. S., Ullman, B., and Mamoun, C.B. (2006). The plasma membrane permease PfNT1 is essential for purine salvage in the human malaria parasite *Plasmodium falciparum*. *Proc Natl Acad Sci USA* 103, 9286-9291.

- 63) Endrizzi, J. A., Kim, H., Anderson, P. M., and Baldwin, E. P. (2004). Crystal structure of *Escherichia coli* cytidine triphosphate synthetase, a nucleotide-regulated glutamine amidotransferase/ATP-dependent amidoligase fusion protein and homologue of anticancer and antiparasitic drug targets. *Biochemistry* *43*, 6447-6463.
- 64) Engen, J. R. (2003). Analysis of protein complexes with hydrogen exchange and mass spectrometry. *Analyst* *128*, 623-628.
- 65) Engen, J. R. (2009). Analysis of protein conformation and dynamics by hydrogen/deuterium exchange MS. *Anal Chem* *81*, 7870-7875.
- 66) Engen, J. R., and Smith, D. L. (2000). Investigating the higher order structure of proteins. Hydrogen exchange, proteolytic fragmentation, and mass spectrometry. *Methods Mol Biol* *146*, 95-112.
- 67) Engen, J. R., and Smith, D. L. (2001). Investigating protein structure and dynamics by hydrogen exchange MS. *Anal Chem* *73*, 256A-265A.
- 68) Englander, J. J., Del Mar, C., Li, W., Englander, S. W., Kim, J. S., Stranz, D. D., Hamuro, Y., and Woods, V. L., Jr. (2003). Protein structure change studied by hydrogen-deuterium exchange, functional labeling, and mass spectrometry. *Proc Natl Acad Sci U S A* *100*, 7057-7062.
- 69) Englander, J. J., Rogero, J. R., and Englander, S. W. (1985). Protein hydrogen exchange studied by the fragment separation method. *Anal Biochem* *147*, 234-244.
- 70) Englander, S. W., and Kallenbach, N. R. (1983). Hydrogen exchange and structural dynamics of proteins and nucleic acids. *Q Rev Biophys* *16*, 521-655.
- 71) Englander, S. W., Mayne, L., Bai, Y., and Sosnick, T. R. (1997). Hydrogen exchange: the modern legacy of Linderstrom-Lang. *Protein Sci* *6*, 1101-1109.
- 72) Fan, Y., Lund, L., Shao, Q., Gao, Y. Q., and Raushel, F. M. (2009). A combined theoretical and experimental study of the ammonia tunnel in carbamoyl phosphate synthetase. *J Am Chem Soc* *131*, 10211-10219.
- 73) Fan, Y., Lund, L., Yang, L., Raushel, F. M., and Gao, Y. Q. (2008). Mechanism for the transport of ammonia within carbamoyl phosphate synthetase determined by molecular dynamics simulations. *Biochemistry* *47*, 2935-2944.
- 74) Fijolek, A., Hofer, A., and Thelander, L. (2007). Expression, purification, characterization, and in vivo targeting of trypanosome CTP synthetase for treatment of African sleeping sickness. *J Biol Chem* *282*, 11858-11865.
- 75) Flicker, K., Neuwirth, M., Strohmeier, M., Kappes, B., Tews, I., and Macheroux, P. (2007). Structural and thermodynamic insights into the assembly of the heteromeric pyridoxal phosphate synthase from *Plasmodium falciparum*. *Journal of Molecular Biology* *374*, 732-748

- 76) Floquet, N., Durand, P., Maigret, B., Badet, B., Badet-Denisot, M. A., and Perahia, D. (2009). Collective motions in glucosamine-6-phosphate synthase: influence of ligand binding and role in ammonia channelling and opening of the fructose-6-phosphate binding site. *J Mol Biol* 385, 653-664.
- 77) Floquet, N., Mouilleron, S., Daher, R., Maigret, B., Badet, B., and Badet-Denisot, M. A. (2007). Ammonia channeling in bacterial glucosamine-6-phosphate synthase (GlmS): molecular dynamics simulations and kinetic studies of protein mutants. *FEBS Lett* 581, 2981-2987.
- 78) Fontana, A., de Laureto, P. P., Spolaore, B., Frare, E., Picotti, P., and Zambonin, M. (2004). Probing protein structure by limited proteolysis. *Acta Biochim Pol* 51, 299-321.
- 79) Foster, D. O., Lardy, H. A., Ray, P. D., and Johnston, J. B. (1967). Alteration of rat liver phosphoenolpyruvate carboxykinase activity by L-tryptophan in vivo and metals in vitro. *Biochemistry* 6, 2120-2128.
- 80) Fox, B. A., and Bzik, D. J. (2002). De novo pyrimidine biosynthesis is required for virulence of *Toxoplasma gondii*. *Nature* 415, 926-929.
- 81) Fresquet, V., Thoden, J. B., Holden, H. M., and Raushel, F. M. (2004). Kinetic mechanism of asparagine synthetase from *Vibrio cholerae*. *Bioorg Chem* 32, 63-75.
- 82) Frieden, C. (1959). Glutamic dehydrogenase. III. The order of substrate addition in the enzymatic reaction. *J Biol Chem* 234, 2891-2896.
- 83) Fukuyama, T. T. (1966). Formation of an adenylyl xanthosine monophosphate intermediate by xanthosine 5'-phosphate aminase and its inhibition by psicofuranine. *J Biol Chem* 241, 4745-4749.
- 84) Fukuyama, T., and Moyed, H. S. (1964). A Separate antibiotic-binding site in xanthosine-5'-phosphate aminase: inhibitor- and substrate-binding studies. *Biochemistry* 3, 1488-1492.
- 85) Garcia, R. A., Pantazatos, D., and Villarreal, F. J. (2004). Hydrogen/deuterium exchange mass spectrometry for investigating protein-ligand interactions. *Assay Drug Dev Technol* 2, 81-91.
- 86) Garcia-Viloca M, G. J., Karplus M, Truhlar DG. (2004). How Enzymes Work: Analysis by Modern Rate Theory and Computer Simulations. *Science* 303, 186 - 195.
- 87) Gardner, M. J., Hall, N., Fung, E., White, O., Berriman, M., Hyman, R. W., Carlton, J. M., Pain, A., Nelson, K. E., Bowman, S., *et al.* (2002). Genome sequence of the human malaria parasite *Plasmodium falciparum*. *Nature* 419, 498-511.

- 88) Gayathri, P., Balaram, H., and Murthy, M. R. (2007). Structural biology of plasmodial proteins. *Curr Opin Struct Biol* 17, 744-754.
- 89) Gayathri, P., Sujay Subbayya, I. N., Ashok, C. S., Selvi, T. S., Balaram, H., and Murthy, M. R. (2008). Crystal structure of a chimera of human and *Plasmodium falciparum* hypoxanthine guanine phosphoribosyltransferases provides insights into oligomerization. *Proteins* 73, 1010-1020.
- 90) Gehrig, L. B., and Magasanik, B. (1955). Biosynthesis of nucleic acid guanine: the enzymic conversion of inosine-5'-phosphate to xanthosine-5'-phosphate. *J Am Chem Soc* 77, 4685-4686.
- 91) Gengenbacher, M., Fitzpatrick, T. B., Raschle, T., Flicker, K., Sinning, I., Muller, S., Macheroux, P., Tews, I., and Kappes, B. (2006). Vitamin B6 biosynthesis by the malaria parasite *Plasmodium falciparum*: biochemical and structural insights. *J Biol Chem* 281, 3633-3641.
- 92) Ginger, M. L. (2006). Niche metabolism in parasitic protozoa. *Philos Trans R Soc Lond B Biol Sci* 361, 101-118.
- 93) Gottesman, S., Halpern, E., and Trisler, P. (1981). Role of *sulA* and *sulB* in filamentation by *lon* mutants of *Escherichia coli* K-12. *J Bacteriol* 148, 265-273.
- 94) Gouet, P., Robert, X., and Courcelle, E. (2003). ESPript/ENDscript: Extracting and rendering sequence and 3D information from atomic structures of proteins. *Nucleic Acids Res* 31, 3320-3323.
- 95) Grieshaber, M., and Bauerle, R. (1972). Structure and evolution of a bifunctional enzyme of the tryptophan operon. *nature new biology* 236, 232-235
- 96) Gupta, R. K., Fung, C. H., and Mildvan, A. S. (1976). Chromium(III)-adenosine triphosphate as a paramagnetic probe to determine intersubstrate distances on pyruvate kinase. Detection of an active enzyme-metal-ATP-metal complex. *J Biol Chem* 251, 2421-2430.
- 97) Guy, H. I., and Evans, D. R. (1997). Trapping an activated conformation of mammalian carbamyl-phosphate synthetase. *J Biol Chem* 272, 19906-19912.
- 98) Guy, H. I., Rotgeri, A., and Evans, D. R. (1997). Activation by fusion of the glutaminase and synthetase subunits of *Escherichia coli* carbamyl-phosphate synthetase. *J Biol Chem* 272, 19913-19918.
- 99) Hager-Braun, C., and Tomer, K. B. (2005). Determination of protein-derived epitopes by mass spectrometry. *Expert Rev Proteomics* 2, 745-756.
- 100) Hanka, L. J. (1960). Mechanism of action of psicofuranine. *J Bacteriol* 80, 30-36.

- 101) Haraguchi, Y., Uchino, T., Takiguchi, M., Endo, F., Mori, M., and Matsuda, I. (1991). Cloning and sequence of a cDNA encoding human carbamyl phosphate synthetase I: molecular analysis of hyperammonemia. *Gene* 107, 335-340.
- 102) Hartmann, S. (1963). The interaction of 6-diazo-5-oxo-L-norleucine with phosphoribosyl pyrophosphate amidotransferase. *J Biol Chem* 238, 3036-3047.
- 103) Hendriks, E. F., O'Sullivan, W. J., and Stewart, T. S. (1998). Molecular cloning and characterization of the *Plasmodium falciparum* cytidine triphosphate synthetase gene. *Biochim Biophys Acta* 1399, 213-218.
- 104) Henzler-Wildman, K., and Kern, D. (2007). Dynamic personalities of proteins. *Nature* 450, 964-972.
- 105) Hermann, J. C., Marti-Arbona, R., Fedorov, A. A., Fedorov, E., Almo, S. C., Shoichet, B. K., and Rauschel, F. M. (2007). Structure-based activity prediction for an enzyme of unknown function. *Nature* 448, 775-779.
- 106) Higgins D., T. J., Gibson T., Thompson J.D., Higgins D.G., Gibson T.J. (1994). CLUSTAL W: improving the sensitivity of progressive multiple sequence alignment through sequence weighting, position-specific gap penalties and weight matrix choice. *Nucleic Acids Research* 22, 4673-4680
- 107) Hildebrandt P, Vanhecke F, Heibel G, and., M. A. (1993). Structural changes in cytochrome c upon hydrogen-deuterium exchange. *Biochemistry* 32, 14158-14164.
- 108) Hill, B., Kilsby, J., Rogerson, G. W., McIntosh, R. T., and Ginger, C. D. (1981). The enzymes of pyrimidine biosynthesis in a range of parasitic protozoa and helminths. *Mol Biochem Parasitol* 2, 123-134.
- 109) Hirotsu, K., Goto, M., Okamoto, A., and Miyahara, I. (2005). Dual substrate recognition of aminotransferases. *Chem Rec* 5, 160-172.
- 110) Hirst, M., Haliday, E., Nakamura, J., and Lou, L. (1994). Human GMP synthetase. Protein purification, cloning, and functional expression of cDNA. *J Biol Chem* 269, 23830-23837.
- 111) Ho, M. C., Cassera, M. B., Madrid, D. C., Ting, L. M., Tyler, P. C., Kim, K., Almo, S. C., and Schramm, V. L. (2009). Structural and metabolic specificity of methylthioformycin for malarial adenosine deaminases. *Biochemistry* 48, 9618-9626.
- 112) Hochrein, J. M., Lerner, E. C., Schiavone, A. P., Smithgall, T. E., and Engen, J. R. (2006). An examination of dynamics crosstalk between SH2 and SH3 domains by hydrogen/deuterium exchange and mass spectrometry. *Protein Sci* 15, 65-73.
- 113) Hoofnagle, A. N., Resing, K. A., and Ahn, N. G. (2003). Protein analysis by hydrogen exchange mass spectrometry. *Annu Rev Biophys Biomol Struct* 32, 1-25.

- 114) Hoofnagle, A. N., Resing, K. A., and Ahn, N. G. (2004). Practical methods for deuterium exchange/mass spectrometry. *Methods Mol Biol* 250, 283-298.
- 115) Huang, X., and Raushel, F. M. (2000a). An engineered blockage within the ammonia tunnel of carbamoyl phosphate synthetase prevents the use of glutamine as a substrate but not ammonia. *Biochemistry* 39, 3240-3247.
- 116) Huang, X., and Raushel, F. M. (2000b). Restricted passage of reaction intermediates through the ammonia tunnel of carbamoyl phosphate synthetase. *J Biol Chem* 275, 26233-26240.
- 117) Huang, X., Holden, H. M., and Raushel, F. M. (2001). Channeling of substrates and intermediates in enzyme-catalyzed reactions. *Annu Rev Biochem* 70, 149-180.
- 118) Hunt, J. B., Smyrniotis, P. Z., Ginsburg, A., and Stadtman, E. R. (1975). Metal ion requirement by glutamine synthetase of *Escherichia coli* in catalysis of gamma-glutamyl transfer. *Arch Biochem Biophys* 166, 102-124.
- 119) Hvidt, A., and Linderstrom-Lang, K. (1954). Exchange of hydrogen atoms in insulin with deuterium atoms in aqueous solutions. *Biochim Biophys Acta* 14, 574-575.
- 120) Hyde CC, M. E. (1990). The tryptophan synthase multienzyme complex: exploring structure-function relationships with X-ray crystallography and mutagenesis. *Biotechnology (N Y)* 8, 27-32.
- 121) Hyde, C. C., Ahmed, S. A., Padlan, E. A., Miles, E. W., and Davies, D. R. (1988). Three-dimensional structure of the tryptophan synthase alpha 2 beta 2 multienzyme complex from *Salmonella typhimurium*. *J Biol Chem* 263, 17857-17871.
- 122) Iacob, R. E., Pene-Dumitrescu, T., Zhang, J., Gray, N. S., Smithgall, T. E., and Engen, J. R. (2009). Conformational disturbance in Abl kinase upon mutation and deregulation. *Proc Natl Acad Sci U S A* 106, 1386-1391.
- 123) Isupov, M. N., Obmolova, G., Butterworth, S., Badet-Denisot, M. A., Badet, B., Polikarpov, I., Littlechild, J. A., and Teplyakov, A. (1996). Substrate binding is required for assembly of the active conformation of the catalytic site in Ntn amidotransferases: evidence from the 1.8 Å crystal structure of the glutaminase domain of glucosamine 6-phosphate synthase. *Structure* 4, 801-810.
- 124) Jayalakshmi, R., Sumathy, K., and Balaram, H. (2002). Purification and characterization of recombinant *Plasmodium falciparum* adenylosuccinate synthetase expressed in *Escherichia coli*. *Protein Expr Purif* 25, 65-72.
- 125) Jeffery, C. J. (2009). Moonlighting proteins--an update. *Mol Biosyst* 5, 345-350.
- 126) Jencks, W. P. (1987). *Catalysis in chemistry and enzymology*, Dover Publications, New York

- 127) Jeng, M. F., Englander, S. W., Elove, G. A., Wand, A. J., and Roder, H. (1990). Structural description of acid-denatured cytochrome c by hydrogen exchange and 2D NMR. *Biochemistry* 29, 10433-10437.
- 128) Jensen, R. A. (1976). Enzyme recruitment in evolution of new function. *Annu Rev Microbiol* 30, 409-425.
- 129) Jiang, L., Althoff, E. A., Clemente, F. R., Doyle, L., Rothlisberger, D., Zanghellini, A., Gallaher, J. L., Betker, J. L., Tanaka, F., Barbas, C. F., 3rd, *et al.* (2008). De novo computational design of retro-aldol enzymes. *Science* 319, 1387-1391.
- 130) Johnson, J. L., West, J. K., Nelson, A. D., and Reinhart, G. D. (2007). Resolving the fluorescence response of *Escherichia coli* carbamoyl phosphate synthetase: mapping intra- and intersubunit conformational changes. *Biochemistry* 46, 387-397.
- 131) Kanamori, K., Ross, B. D., and Tropp, J. (1995). Selective, in vivo observation of [5-¹⁵N]glutamine amide protons in rat brain by 1H-15N heteronuclear multiple-quantum-coherence transfer NMR. *J Magn Reson B* 107, 107-115.
- 132) Kandeel, M., and Kitade, Y. (2010). Substrate specificity and nucleotides binding properties of NM23H2/nucleoside diphosphate kinase homolog from *Plasmodium falciparum*. *J Bioenerg Biomembr (In press)*.
- 133) Kandeel, M., Miyamoto, T., and Kitade, Y. (2009). Bioinformatics, enzymologic properties, and comprehensive tracking of *Plasmodium falciparum* nucleoside diphosphate kinase. *Biol Pharm Bull* 32, 1321-1327.
- 134) Kandeel, M., Nakanishi, M., Ando, T., El-Shazly, K., Yosef, T., Ueno, Y., and Kitade, Y. (2008). Molecular cloning, expression, characterization and mutation of *Plasmodium falciparum* guanylate kinase. *Mol Biochem Parasitol* 159, 130-133.
- 135) Kane, J. F., Holmes, W. M., and Jensen, R. A. (1972). Metabolic interlock. The dual function of a folate pathway gene as an extra-operonic gene of tryptophan biosynthesis. *J Biol Chem* 247, 1587-1596.
- 136) Kanehisa, M., and Goto, S. (2000). KEGG: kyoto encyclopedia of genes and genomes. *Nucleic Acids Res* 28, 27-30.
- 137) Kaplan, N., Purich, D., Colowick, N. (1979). Enzyme Kinetics and Mechanism, Part A: Initial Rate and Inhibitor Methods. *Methods Enzymol* 63.
- 138) Katta, V., and Chait, B. T. (1991). Conformational changes in proteins probed by hydrogen-exchange electrospray-ionization mass spectrometry. *Rapid Commun Mass Spectrom* 5, 214-217.
- 139) Katta, V., and Chait, B. T. (1993). Hydrogen=deuterium exchange electrospray ionization mass spectrometry: A method for probing protein conformational changes in solution. *JAm Chem Soc* 115, 6317-6321.

- 140) Keleti, T., and Ovadi, J. (1988). Control of metabolism by dynamic macromolecular interactions. *Curr Top Cell Regul* 29, 1-33.
- 141) Kelly, W. L., Pan, L., and Li, C. (2009). Thiostrepton biosynthesis: prototype for a new family of bacteriocins. *J Am Chem Soc* 131, 4327-4334.
- 142) Keough, D. T., Hockova, D., Holy, A., Naesens, L. M., Skinner-Adams, T. S., Jersey, J., and Guddat, L. W. (2009). Inhibition of hypoxanthine-guanine phosphoribosyltransferase by acyclic nucleoside phosphonates: a new class of antimalarial therapeutics. *J Med Chem* 52, 4391-4399.
- 143) Keough, D. T., Ng, A. L., Emmerson, B. T., and de Jersey, J. (1998). Expression and properties of recombinant *P. falciparum* hypoxanthine-guanine phosphoribosyltransferase. *Adv Exp Med Biol* 431, 735-739.
- 144) Keough, D. T., Ng, A. L., Winzor, D. J., Emmerson, B. T., and de Jersey, J. (1999). Purification and characterization of *Plasmodium falciparum* hypoxanthine-guanine-xanthine phosphoribosyltransferase and comparison with the human enzyme. *Mol Biochem Parasitol* 98, 29-41.
- 145) Keough, D. T., Skinner-Adams, T., Jones, M. K., Ng, A. L., Brereton, I. M., Guddat, L. W., and de Jersey, J. (2006). Lead compounds for antimalarial chemotherapy: purine base analogs discriminate between human and *P. falciparum* 6-oxopurine phosphoribosyltransferases. *J Med Chem* 49, 7479-7486.
- 146) Khedouri, E., Anderson, P. M., and Meister, A. (1966). Selective inactivation of the glutamine binding site of *Escherichia coli* carbamyl phosphate synthetase by 2-amino-4-oxo-5-chloropentanoic acid. *Biochemistry* 5, 3552-3557.
- 147) Kicska, G. A., Tyler, P. C., Evans, G. B., Furneaux, R. H., Kim, K., and Schramm, V. L. (2002a). Transition state analogue inhibitors of purine nucleoside phosphorylase from *Plasmodium falciparum*. *J Biol Chem* 277, 3219-3225.
- 148) Kicska, G. A., Tyler, P. C., Evans, G. B., Furneaux, R. H., Schramm, V. L., and Kim, K. (2002b). Purine-less death in *Plasmodium falciparum* induced by immucillin-H, a transition state analogue of purine nucleoside phosphorylase. *J Biol Chem* 277, 3226-3231.
- 149) King, A., and Melton, D. W. (1987). Characterisation of cDNA clones for hypoxanthine-guanine phosphoribosyltransferase from the human malarial parasite, *Plasmodium falciparum*: comparisons to the mammalian gene and protein. *Nucleic Acids Res* 15, 10469-10481.
- 150) Kitz, R., Wilson, I. B. (1962). Esters of methanesulfonic acid as irreversible inhibitors of acetylcholinesterase. *J Biol Chem* 237, 3245-3249.
- 151) Klem, T. J., and Davisson, V. J. (1993). Imidazole glycerol phosphate synthase: the glutamine amidotransferase in histidine biosynthesis. *Biochemistry* 32, 5177-5186.

- 152) Knighton, D. R., Kan, C. C., Howland, E., Janson, C. A., Hostomska, Z., Welsh, K. M., and Matthews, D. A. (1994). Structure of and kinetic channelling in bifunctional dihydrofolate reductase-thymidylate synthase. *Nat Struct Biol* *1*, 186-194.
- 153) Koshland, D. E. (1958). Application of a Theory of Enzyme Specificity to Protein Synthesis. *Proc Natl Acad Sci U S A* *44*, 98-104.
- 154) Krahn, J. M., Kim, J. H., Burns, M. R., Parry, R. J., Zalkin, H., and Smith, J. L. (1997). Coupled formation of an amidotransferase interdomain ammonia channel and a phosphoribosyltransferase active site. *Biochemistry* *36*, 11061-11068.
- 155) Kuenzler, M., Balmelli, T., Egli, C. M., Paravicini, G., and Braus, G. H. (1993). Cloning, primary structure, and regulation of the HIS7 gene encoding a bifunctional glutamine amidotransferase: cyclase from *Saccharomyces cerevisiae*. *J Bacteriol* *175*, 5548-5558.
- 156) Kumar, S., Nei, M., Dudley, J., and Tamura, K. (2008). MEGA: a biologist-centric software for evolutionary analysis of DNA and protein sequences. *Brief Bioinform* *9*, 299-306.
- 157) Kuramitsu, H., and Moyed, H. S. (1966). A separate antibiotic binding site in xanthosine 5'-phosphate aminase. Differential alteration of catalytic properties and sensitivity to inhibition. *J Biol Chem* *241*, 1596-1601.
- 158) Kusumi, T., Tsuda, M., Katsunuma, T., and Yamamura, M. (1989). Dual inhibitory effect of bredinin. *Cell Biochem Funct* *7*, 201-204.
- 159) Kyte, J. (1995). *Mechanism in protein chemistry*, Garland Publishing, Inc. New York.
- 160) Lagerkvist, U. (1958). Biosynthesis of guanosine 5'-phosphate. II. Amination of xanthosine 5'-phosphate by purified enzyme from pigeon liver. *J Biol Chem* *233*, 143-149.
- 161) LaRonde-LeBlanc, N., Resto, M., and Gerratana, B. (2009). Regulation of active site coupling in glutamine-dependent NAD⁺ synthetase. *Nat Struct Mol Biol* *16*, 421-429.
- 162) Larsen, T. M., Boehlein, S. K., Schuster, S. M., Richards, N. G., Thoden, J. B., Holden, H. M., and Rayment, I. (1999). Three-dimensional structure of *Escherichia coli* asparagine synthetase B: a short journey from substrate to product. *Biochemistry* *38*, 16146-16157.
- 163) Laskowski, R. A., MacArthur, M. W., Moss, D.S., and Thornton, J. M. (1993). PROCHECK: a program to check the stereochemical quality of protein structures. *J Appl Cryst* *26*, 283-291.
- 164) Leskovac, L. (2003). *Comprehensive Enzyme Kinetics*. Kluwer Academic/Plenum Publisher New York.

- 165) Levitzki, A., and Koshland, D. E., Jr. (1971). Cytidine triphosphate synthetase. Covalent intermediates and mechanisms of action. *Biochemistry* *10*, 3365-3371.
- 166) Li, C. M., Tyler, P.C., Furneaux, R.H., Kicska, G., Xu, Y., Grubmeyer, C., Girvin, M.E., Schramm, V.L. (1999). Transition-state analogs as inhibitors of human and malarial hypoxanthine-guanine phosphoribosyltransferases. *Nat Struct Biol* *6*, 582-587
- 167) Li, K. K., Beeson, W. T. t., Ghiviriga, I., and Richards, N. G. (2007). A convenient gHMQC-based NMR assay for investigating ammonia channeling in glutamine-dependent amidotransferases: studies of *Escherichia coli* asparagine synthetase B. *Biochemistry* *46*, 4840-4849.
- 168) Linderstrom-Lang, K. (1955). The pH-dependence of the deuterium exchange of insulin. *Biochim Biophys Acta* *18*, 308.
- 169) Lineweaver, H., and Burk, D. (1934). The determination of enzyme dissociation constants. *Journal of the American Chemical Society* *56*, 658-666.
- 170) Lou, L., Nakamura, J., Tsing, S., Nguyen, B., Chow, J., Straub, K., Chan, H., and Barnett, J. (1995). High-level production from a baculovirus expression system and biochemical characterization of human GMP synthetase. *Protein Expr Purif* *6*, 487-495.
- 171) Luebke, R. W., Andrews, D. L., Copeland, C. B., Riddle, M. M., Rogers, R. R., and Smialowicz, R. J. (1991). Host resistance to murine malaria in mice exposed to the adenosine deaminase inhibitor, 2'-deoxycoformycin. *Int J Immunopharmacol* *13*, 987-997.
- 172) Lusty, C. J. (1992). Detection of an enzyme bound gamma-glutamyl acyl ester of carbamyl phosphate synthetase of *Escherichia coli*. *FEBS Lett* *314*, 135-138.
- 173) Madrid, D. C., Ting, L. M., Waller, K. L., Schramm, V. L., and Kim, K. (2008). *Plasmodium falciparum* purine nucleoside phosphorylase is critical for viability of malaria parasites. *J Biol Chem* *283*, 35899-35907.
- 174) Magasanik, B., and Brooke, M. S. (1954). The accumulation of xanthosine by a guanineless mutant of *Aerobacter aerogenes*. *J Biol Chem* *206*, 83-87.
- 175) Maier, C. S., and Deinzer, M. L. (2005). Protein conformations, interactions, and H/D exchange. *Methods Enzymol* *402*, 312-360.
- 176) Mandell, J. G., Baerga-Ortiz, A., Croy, C. H., Falick, A. M., and Komives, E. A. (2005). Application of amide proton exchange mass spectrometry for the study of protein-protein interactions. *Curr Protoc Protein Sci Chapter 20*, Unit 20.29.
- 177) Mandell, J. G., Falick, A. M., and Komives, E. A. (1998). Measurement of amide hydrogen exchange by MALDI-TOF mass spectrometry. *Anal Chem* *70*, 3987-3995.

- 178) Mantsala, P., and Zalkin, H. (1975). Utilization of ammonia for tryptophan synthesis. *Biochem Biophys Res Commun* 67, 8478–8484.
- 179) Mantsala, P., and Zalkin, H. (1976). Glutamate synthase. Properties of the glutamine-dependent activity. *J Biol Chem* 251, 3294-3299.
- 180) Martin, R. E., Henry, R.I., Abbey, J.L., Clements, J.D., Kirk, K. (2005). The 'permeome' of the malaria parasite: an overview of the membrane transport proteins of *Plasmodium falciparum*. *Genome Biol* 6, R26.
- 181) Maruoka S, Horita S, Lee WC, Nagata K, and M., T. (2010). Crystal structure of the ATPase subunit and its substrate-dependent association with the GATase subunit: a novel regulatory mechanism for a two-subunit-type GMP synthetase from *Pyrococcus horikoshii* OT3. *J Mol Biol* 395, 417-429.
- 182) Massiere, F., and Badet-Denisot, M. A. (1998). The mechanism of glutamine-dependent amidotransferases. *Cell Mol Life Sci* 54, 205-222.
- 183) McClure, W. R., Lardy, H. A., Wagner, M., and Cleland, W. W. (1971). Rat liver pyruvate carboxylase. II. Kinetic studies of the forward reaction. *J Biol Chem* 246, 3579-3583.
- 184) McConkey, G. A. (2000). *Plasmodium falciparum*: isolation and characterisation of a gene encoding protozoan GMP synthase. *Exp Parasitol* 94, 23-32.
- 185) McConnell, B., Rice, D. J., and Uchima, F. D. (1983). Exceptional characteristics of amino proton exchange in guanosine compounds. *Biochemistry* 22, 3033-3037.
- 186) Mehlhaff, P. M., and Schuster, S. M. (1991). Bovine pancreatic asparagine synthetase explored with substrate analogs and specific monoclonal antibodies. *Arch Biochem Biophys* 284, 143-150.
- 187) Mehlin, C., Boni, E., Buckner, F. S., Engel, L., Feist, T, Gelb, M. H., Haji, L., Kim, D., Liu, C., Mueller, N., et al.. (2006). Heterologous expression of proteins from *Plasmodium falciparum*: results from 1000 genes . *Mol Biochem Parasitol* 148, 144-160.
- 188) Mehrotra, S., Bopanna, M. P., Bulusu, V., and Balaram, H. (2010). Adenine metabolism in *Plasmodium falciparum*. *Exp Parasitol* 125, 147-151.
- 189) Mehrotra, S., Mylarappa, B.N., Iyengar, P., Balaram, H. (2010). Studies on active site mutants of *P. falciparum* adenylosuccinate synthetase: Insights into enzyme catalysis and activation. *Biochim Biophys Acta* 1804, 1996-2002.
- 190) Mei, B. G., and Zalkin, H. (1990). Amino-terminal deletions define a glutamine amide transfer domain in glutamine phosphoribosylpyrophosphate amidotransferase and other PurF-type amidotransferases. *J Bacteriol* 172, 3512-3514.

- 191) Meyer, M. E., Gutierrez, J. A., Raushel, F. M., and Richards, N. G. (2010). A conserved glutamate controls the commitment to acyl-adenylate formation in asparagine synthetase. *Biochemistry (In press)*.
- 192) Michaelis, L., and Menten, M. L. (1913). Die Kinetik der Invertinwirkung. *Biochem Z* 49, 333–369.
- 193) Miles, B. W., and Raushel, F. M. (2000). Synchronization of the three reaction centers within carbamoyl phosphate synthetase. *Biochemistry* 39, 5051-5056.
- 194) Miles, B. W., Thoden, J. B., Holden, H. M., and Raushel, F. M. (2002). Inactivation of the amidotransferase activity of carbamoyl phosphate synthetase by the antibiotic acivicin. *J Biol Chem* 277, 4368-4373.
- 195) Miles, E. W., Rhee, S., and Davies, D. R. (1999). The molecular basis of substrate channeling. *J Biol Chem* 274, 12193-12196.
- 196) Miran, S. G., Chang, S. H., and Raushel, F. M. (1991). Role of the four conserved histidine residues in the amidotransferase domain of carbamoyl phosphate synthetase. *Biochemistry* 30, 7901-7907.
- 197) Miranzo, D., Seco, E. M., Cuesta, T., and Malpartida, F. (2010). Isolation and characterization of pcsB, the gene for a polyene carboxamide synthase that tailors pimaricin into AB-400. *Appl Microbiol Biotechnol* 85, 1809-1819.
- 198) Mizobuchi, K., and Buchanan, J. M. (1968). Biosynthesis of the purines. XXX. Isolation and characterization of formylglycinamide ribonucleotide amidotransferase-glutamyl complex. *J Biol Chem* 243, 4853-4862.
- 199) Molday, R. S., Englander, S. W., and Kallen, R. G. (1972). Primary structure effects on peptide group hydrogen exchange. *Biochemistry* 11, 150-158.
- 200) Moore, B. (2004). Bifunctional and moonlighting enzymes: lighting the way to regulatory control. *Trends Plant Sci* 9, 221-228.
- 201) Morar, M., Anand, R., Hoskins, A. A., Stubbe, J., and Ealick, S. E. (2006). Complexed structures of formylglycinamide ribonucleotide amidotransferase from *Thermotoga maritima* describe a novel ATP binding protein superfamily. *Biochemistry* 45, 14880-14895.
- 202) Morgan, C. R., and Engen, J. R. (2009). Investigating solution-phase protein structure and dynamics by hydrogen exchange mass spectrometry. *Curr Protoc Protein Sci Chapter 17*, Unit 17 16 11-17.
- 203) Mori, S., Abeygunawardana, C., Jonson, M. O., and Zeil, P. C. M. V. (1995). Improved sensitivity of HSQC spectra of exchanging protons at short interscan delay using a new fast HSQC detection system that avoids water saturation. *J Magnetic Resonance B* 108, 94-98.

- 204) Morrison, J. F. (1979). Approaches to kinetic studies on metal-activated enzymes. *Methods Enzymol* 63, 257-294.
- 205) Mouilleron, S., and Golinelli-Pimpaneau, B. (2007). Conformational changes in ammonia-channeling glutamine amidotransferases. *Curr Opin Struct Biol* 17, 653-664.
- 206) Mouilleron, S., Badet-Denisot, M. A., and Golinelli-Pimpaneau, B. (2008). Ordering of C-terminal loop and glutaminase domains of glucosamine-6-phosphate synthase promotes sugar ring opening and formation of the ammonia channel. *J Mol Biol* 377, 1174-1185.
- 207) Mouilleron, S., Badet-Denisot, M. A., and Golinelli-Pimpaneau, B. (2006). Glutamine binding opens the ammonia channel and activates glucosamine-6P synthase. *J Biol Chem* 281, 4404-4412.
- 208) Moyed, H. S., and Magasanik, B. (1957). Enzymes essential for the biosynthesis of nucleic acid guanine; xanthosine 5'-phosphate aminase of *Aerobacter aerogenes*. *J Biol Chem* 226, 351-363.
- 209) Muchmore, C. R., Krahn, J. M., Kim, J. H., Zalkin, H., and Smith, J. L. (1998). Crystal structure of glutamine phosphoribosylpyrophosphate amidotransferase from *Escherichia coli*. *Protein Sci* 7, 39-51.
- 210) Mullins, L. S., and Raushel, F. M. (1999). Channeling of ammonia through the intermolecular tunnel contained within carbamoyl phosphate synthetase. *J Am Chem Soc* 121, 3803-3804.
- 211) Myers, R. S., Jensen, J. R., Deras, I. L., Smith, J. L., and Davisson, V. J. (2003). Substrate-induced changes in the ammonia channel for imidazole glycerol phosphate synthase. *Biochemistry* 42, 7013-7022.
- 212) Nakamura, A., Yao, M., Chimnarong, S., Sakai, N., and Tanaka, I. (2006). Ammonia channel couples glutaminase with transamidase reactions in GatCAB. *Science* 312, 1954-1958.
- 213) Nakamura, J., and Lou, L. (1995). Biochemical characterization of human GMP synthetase. *J Biol Chem* 270, 7347-7353.
- 214) Nakamura, J., Straub, K., Wu, J., and Lou, L. (1995). The glutamine hydrolysis function of human GMP synthetase. Identification of an essential active site cysteine. *J Biol Chem* 270, 23450-23455.
- 215) Nara, T., Gao, G., Yamasaki, H., Nakajima-Shimada, J., and Aoki, T. (1998). Carbamoyl-phosphate synthetase II in kinetoplastids. *Biochim Biophys Acta* 1387, 462-468.
- 216) Nimmegern, E., Fox, T., Fleming, M. A., and Thomson, J. A. (1996). Conformational changes and stabilization of inosine 5'-monophosphate

- dehydrogenase associated with ligand binding and inhibition by mycophenolic acid. *J Biol Chem* 271, 19421-19427.
- 217) Northrop, D. B. (1969). Transcarboxylase. VI. Kinetic analysis of the reaction mechanism. *J Biol Chem* 244, 5808-5819.
- 218) Nyunoya, H., Broglie, K. E., Widgren, E. E., and Lusty, C. J. (1985). Characterization and derivation of the gene coding for mitochondrial carbamyl phosphate synthetase I of rat. *J Biol Chem* 260, 9346-9356.
- 219) Oh, H., Breuker, K., Sze, S. K., Ge, Y., Carpenter, B. K., and McLafferty, F. W. (2002). Secondary and tertiary structures of gaseous protein ions characterized by electron capture dissociation mass spectrometry and photofragment spectroscopy. *Proc Natl Acad Sci U S A* 99, 15863-15868.
- 220) Ovádi, J., Salerno, C., Keleti, T., and Fasella, F. (1978). Physico-chemical evidence for the interaction between aldolase and glyceraldehyde-3-phosphate dehydrogenase. *Eur J Biochem* 90, 499-503.
- 221) Page, T., Bakay, B., and Nyhan, W. L. (1984). Human GMP synthetase. *Int J Biochem* 16, 117-120.
- 222) Paluh, J. L., Zalkin, H, Betsch, D, Weith, H. L. (1985). Study of anthranilate synthase function by replacement of cysteine 84 using site-directed mutagenesis. *J Biol Chem* 260, 1889-1894.
- 223) Pan, P., and Dunn, M. F. (1996). beta-Site covalent reactions trigger transitions between open and closed conformations of the tryptophan synthase henzym complex. *Biochemistry* 35, 5002-5013.
- 224) Parker, M. D., Hyde, R. J., Yao, S. Y., McRobert, L., Cass, C. E., Young, J. D., McConkey, G. A., and Baldwin, S. A. (2000). Identification of a nucleoside/nucleobase transporter from *Plasmodium falciparum*, a novel target for anti-malarial chemotherapy. *Biochem J* 349, 67-75.
- 225) Pauling, L. (1946). Molecular architecture and biological reactions. *Chem Eng News* 24, 1375.
- 226) Pegram, L. D., Megonigal, M. D., Lange, B. J., Nowell, P. C., Rowley, J. D., Rappaport, E. F., and Felix, C. A. (2000). t(3;11) translocation in treatment-related acute myeloid leukemia fuses MLL with the GMPS (GUANOSINE 5' MONOPHOSPHATE SYNTHETASE) gene. *Blood* 96, 4360-4362.
- 227) Polet, H., and Barr, C. F. (1968). DNA, RNA, and protein synthesis in erythrocytic forms of *Plasmodium knowlesi*. *Am J Trop Med Hyg* 17, 672-679.
- 228) Potterton, E., McNicholas, S., Krissinel, E., Cowtan, K., and Noble, M. (2002). The CCP4 molecular-graphics project. *Acta Crystallogr D Biol Crystallogr* 58, 1955-1957.

- 229) Potterton, L., McNicholas, S., Krissinel, E., Gruber, J., Cowtan, K., Emsley, P., Murshudov, G. N., Cohen, S., Perrakis, A., and Noble, M. (2004). Developments in the CCP4 molecular-graphics project. *Acta Crystallogr D Biol Crystallogr* *60*, 2288-2294.
- 230) Quashie, N. B., Dorin-Semblat, D., Bray, P. G., Biagini, G. A., Doerig, C., Ranford-Cartwright, L. C., and De Koning, H. P. (2008). A comprehensive model of purine uptake by the malaria parasite *Plasmodium falciparum*: identification of four purine transport activities in intraerythrocytic parasites. *Biochem J* *411*, 287-295.
- 231) Quashie, N. B., Ranford-Cartwright, L. C., and de Koning, H. P. (2010). Uptake of purines in *Plasmodium falciparum*-infected human erythrocytes is mostly mediated by the human equilibrative nucleoside transporter and the human facilitative nucleobase transporter. *Malar J* *9*, 36.
- 232) Queen, S. A., Jagt, D. L., and Reyes, P. (1990). In vitro susceptibilities of *Plasmodium falciparum* to compounds which inhibit nucleotide metabolism. *Antimicrob Agents Chemother* *34*, 1393-1398.
- 233) Queen, S. A., Vander Jagt, D., and Reyes, P. (1988). Properties and substrate specificity of a purine phosphoribosyltransferase from the human malaria parasite, *Plasmodium falciparum*. *Mol Biochem Parasitol* *30*, 123-133.
- 234) Queener, S. W., Queener, S. F., Meeks, J. R., and Gunsalus, I. C. (1973). Anthranilate synthase from *Pseudomonas putida*. Purification and properties of a two-component enzyme. *J Biol Chem* *248*, 151-161.
- 235) Raman, J., Ashok, C. S., Subbayya, S. I., Anand, R. P., Selvi, S. T., and Balaram, H. (2005). *Plasmodium falciparum* hypoxanthine guanine phosphoribosyltransferase. Stability studies on the product-activated enzyme. *FEBS J* *272*, 1900-1911.
- 236) Raman, J., Mehrotra, S., Anand, R. P., and Balaram, H. (2004a). Unique kinetic mechanism of *Plasmodium falciparum* adenylosuccinate synthetase. *Mol Biochem Parasitol* *138*, 1-8.
- 237) Raman, J., Sumathy, K., Anand, R. P., and Balaram, H. (2004b). A non-active site mutation in human hypoxanthine guanine phosphoribosyltransferase expands substrate specificity. *Arch Biochem Biophys* *427*, 116-122.
- 238) Rand, K. D., Pringle, S. D., Murphy, J. P., 3rd, Fadgen, K. E., Brown, J., and Engen, J. R. (2009). Gas-phase hydrogen/deuterium exchange in a traveling wave ion guide for the examination of protein conformations. *Anal Chem* *81*, 10019-10028.
- 239) Raushel, F. M., Anderson, P. M., and Villafranca, J. J. (1978). Kinetic mechanism of *Escherichia coli* carbamoyl-phosphate synthetase. *Biochemistry* *17*, 5587-5591.
- 240) Raushel, F. M., Thoden, J. B., and Holden, H. M. (1999). The amidotransferase family of enzymes: molecular machines for the production and delivery of ammonia. *Biochemistry* *38*, 7891-7899.

- 241) Reyes, P., Rathod, P. K., Sanchez, D. J., Mrema, J. E., Rieckmann, K. H., and Heidrich, H. G. (1982). Enzymes of purine and pyrimidine metabolism from the human malaria parasite, *Plasmodium falciparum*. *Mol Biochem Parasitol* 5, 275-290.
- 242) Robertson, J. G., and Villafranca, J. J. (1993). Characterization of metal ion activation and inhibition of CTP synthetase. *Biochemistry* 32, 3769-3777.
- 243) Rodriguez-Suarez, R., Xu, D., Veillette, K., Davison, J., Sillaots, S., Kauffman, S., Hu, W., Bowman, J., Martel, N., Trosok, S., *et al.* (2007). Mechanism-of-action determination of GMP synthase inhibitors and target validation in *Candida albicans* and *Aspergillus fumigatus*. *Chem Biol* 14, 1163-1175.
- 244) Roux, B., and Walsh, C. T. (1992). *p*-aminobenzoate synthesis in *Escherichia coli*: kinetic and mechanistic characterization of the amidotransferase PabA. *Biochemistry* 31, 6904-6910.
- 245) Rowley, J. D. (1998). The critical role of chromosome translocations in human leukemias. *Annu Rev Genet* 32, 495-519.
- 246) Rubino, S. D., Nyunoya, H., and Lusty, C. J. (1986). Catalytic domains of carbamyl phosphate synthetase. Glutamine-hydrolyzing site of *Escherichia coli* carbamyl phosphate synthetase. *J Biol Chem* 261, 11320-11327.
- 247) Saeed-Kothe, A., and Powers-Lee, S. G. (2003). Gain of glutaminase function in mutants of the ammonia-specific frog carbamoyl phosphate synthetase. *J Biol Chem* 278, 26722-26726.
- 248) Saeed-Kothe, A., and Powers-Lee, S. G. (2002). Specificity determining residues in ammonia- and glutamine-dependent carbamoyl phosphate synthetases. *J Biol Chem* 277, 7231-7238.
- 249) Sakamoto, N. (1978). GMP synthetase (*Escherichia coli*). *Methods Enzymol* 51, 213-218.
- 250) Sakamoto, N., Hatfield, G. W., and Moyed, H. S. (1972). Physical properties and subunit structure of xanthosine 5'-phosphate aminase. *J Biol Chem* 247, 5880-5887.
- 251) Sali, A., and Blundell, T. L. (1993). Comparative protein modelling by satisfaction of spatial restraints. *J Mol Biol* 234, 779-815.
- 252) Sarkar, D., Ghosh, I., and Datta, S. (2004). Biochemical characterization of *Plasmodium falciparum* hypoxanthine-guanine-xanthine phosphoribosyltransferase: role of histidine residue in substrate selectivity. *Mol Biochem Parasitol* 137, 267-276.
- 253) Sarkari, F., Sanchez-Alcaraz, T., Wang, S., Holowaty, M. N., Sheng, Y., and Frappier, L. (2009). EBNA1-mediated recruitment of a histone H2B deubiquitylating complex to the Epstein-Barr virus latent origin of DNA replication. *PLoS Pathog* 5, e1000624.

- 254) Schendel, F. J., Mueller, E., Stubbe, J., Shiau, A., and Smith, J. M. (1989). Formylglycinamide ribonucleotide synthetase from *Escherichia coli*: cloning, sequencing, overproduction, isolation, and characterization. *Biochemistry* 28, 2459-2471.
- 255) Scholar, E. M., Brown, P. R., Parks, R. E., Jr., and Calabresi, P. (1973). Nucleotide profiles of the formed elements of human blood determined by high-pressure liquid chromatography. *Blood* 41, 927-936.
- 256) Scofield, M. A., Lewis, W. S., and Schuster, S. M. (1990). Nucleotide sequence of *Escherichia coli* asnB and deduced amino acid sequence of asparagine synthetase B. *J Biol Chem* 265, 12895-12902.
- 257) Segel, I. H. (1993). *Enzyme Kinetics: Behavior and Analysis of Rapid Equilibrium and Steady-State Enzyme Systems* Wiley Classics Library.
- 258) Shahabuddin, M., Gunther, K., Lingelbach, K., Aikawa, M., Schreiber, M., Ridley, R. G., and Scaife, J. G. (1992). Localisation of hypoxanthine phosphoribosyl transferase in the malaria parasite *Plasmodium falciparum*. *Exp Parasitol* 74, 11-19.
- 259) Sheng S., Moraga-Amador, D.A., van Heeke, G., Allison, R.D., Richards, N.G., Schuster, S.M. (1993). Glutamine inhibits the ammonia-dependent activities of two Cys-1 mutants of human asparagine synthetase through the formation of an abortive complex. *J Biol Chem* 268, 16771-16780.
- 260) Shenoy, A. V., and Visweswariah, S.S. (2003). Site-directed mutagenesis using a single mutagenic oligonucleotide and DpnI digestion of template DNA. *Anal Biochem* 319, 335-336.
- 261) Sherman, I. W. (1998). *Malaria: Parasite Biology, Pathogenesis, and Protection*, ASM, Washington DC. 177-184.
- 262) Shi, W., Li, C. M., Tyler, P. C., Furneaux, R. H., Cahill, S. M., Girvin, M. E., Grubmeyer, C., Schramm, V. L., and Almo, S. C. (1999). The 2.0 Å structure of malarial purine phosphoribosyltransferase in complex with a transition-state analogue inhibitor. *Biochemistry* 38, 9872-9880.
- 263) Shi, W., Ting, L. M., Kicska, G. A., Lewandowicz, A., Tyler, P. C., Evans, G. B., Furneaux, R. H., Kim, K., Almo, S. C., and Schramm, V. L. (2004). *Plasmodium falciparum* purine nucleoside phosphorylase: crystal structures, immucillin inhibitors, and dual catalytic function. *J Biol Chem* 279, 18103-18106.
- 264) Silverman, R. B. (2002). *The organic chemistry of enzyme-catalyzed reactions* Academic Press, San Diego.
- 265) Slechta, L. (1960). Studies on the mode of action of psicofuranine. *Biochem Pharmacol* 5, 96-107.
- 266) Slock, J., Stahly, D. P., Han, C. Y., Six, E. W., and Crawford, I. P. (1990). An apparent *Bacillus subtilis* folic acid biosynthetic operon containing pab, an

- amphibolic *trpG* gene, a third gene required for synthesis of para-aminobenzoic acid, and the dihydropteroate synthase gene. *J Bacteriol* 172, 7211-7226.
- 267) Smith, J. L. (1995). Structures of glutamine amidotransferases from the purine biosynthetic pathway. *Biochem Soc Trans* 23, 894-898.
- 268) Spector, T. (1975). Studies with GMP synthetase from Ehrlich ascites cells. Purification, properties, and interactions with nucleotide analogs. *J Biol Chem* 250, 7372-7376.
- 269) Spector, T., and Beacham, L. M., 3rd (1975). Guanosine monophosphate synthetase from *Escherichia coli* B-96. Inhibition by nucleosides. *J Biol Chem* 250, 3101-3107.
- 270) Spector, T., Jones, T. E., Krenitsky, T. A., and Harvey, R. J. (1976). Guanosine monophosphate synthetase from Ehrlich ascites cells. Multiple inhibition by pyrophosphate and nucleosides. *Biochim Biophys Acta* 452, 597-607.
- 271) Spector, T., Jones, T. E., LaFon, S. W., Nelson, D. J., Berens, R. L., and Marr, J. J. (1984). Monophosphates of formycin B and allopurinol riboside. Interactions with leishmanial and mammalian succino-AMP synthetase and GMP reductase. *Biochem Pharmacol* 33, 1611-1617.
- 272) Stroud, R. M. (1994). An electrostatic highway. *Nat Struct Biol* 1, 131-134.
- 273) Stryer, L. (1965). The interaction of a naphthalene dye with apomyoglobin and apohemoglobin. A fluorescent probe of non-polar binding sites. *J Mol Biol* 13, 482-495.
- 274) Stubbs, C. J., Loenarz, C., Mecinovic, J., Yeoh, K. K., Hindley, N., Lienard, B. M., Sobott, F., Schofield, C. J., and Flashman, E. (2009). Application of a proteolysis/mass spectrometry method for investigating the effects of inhibitors on hydroxylase structure. *J Med Chem* 52, 2799-2805.
- 275) Subbayya, I. N., and Balaram, H. (2002). A point mutation at the subunit interface of hypoxanthine-guanine-xanthine phosphoribosyltransferase impairs activity: role of oligomerization in catalysis. *FEBS Lett* 521, 72-76.
- 276) Subbayya, I. N., Ray, S. S., Balaram, P., and Balaram, H. (1997). Metabolic enzymes as potential drug targets in *Plasmodium falciparum*. *Indian J Med Res* 106, 79-94.
- 277) Suh, M. J., Pourshahian, S., and Limbach, P. A. (2007). Developing limited proteolysis and mass spectrometry for the characterization of ribosome topography. *J Am Soc Mass Spectrom* 18, 1304-1317.
- 278) Sujay Subbayya, I. N., and Balaram, H. (2000). Evidence for multiple active states of *Plasmodium falciparum* hypoxanthine-guanine-xanthine phosphoribosyltransferase. *Biochem Biophys Res Commun* 279, 433-437.
- 279) Tamura, K., Dudley, J., Nei, M., and Kumar, S. (2007). MEGA4: Molecular Evolutionary Genetics Analysis (MEGA) software version 4.0. *Mol Biol Evol* 24, 1596-1599.

- 280) Teplyakov, A., Obmolova, G., Badet, B., and Badet-Denisot, M. A. (2001). Channeling of ammonia in glucosamine-6-phosphate synthase. *J Mol Biol* 313, 1093-1102.
- 281) Tesmer, J. J., Klem, T. J., Deras, M. L., Davisson, V. J., and Smith, J. L. (1996). The crystal structure of GMP synthetase reveals a novel catalytic triad and is a structural paradigm for two enzyme families. *Nat Struct Biol* 3, 74-86.
- 282) Tesmer, J. J., Stemmler, T. L., Penner-Hahn, J. E., Davisson, V. J., and Smith, J. L. (1994). Preliminary X-ray analysis of *Escherichia coli* GMP synthetase: determination of anomalous scattering factors for a cysteinyl mercury derivative. *Proteins* 18, 394-403.
- 283) Tesson, A. R., Soper, T. S., Ciustea, M., and Richards, N. G. (2003). Revisiting the steady state kinetic mechanism of glutamine-dependent asparagine synthetase from *Escherichia coli*. *Arch Biochem Biophys* 413, 23-31.
- 284) Theorell, H., and Chance, B. (1951). Studies of liver alcohol dehydrogenase. II. The kinetics of the compound of horse liver alcohol dehydrogenase and reduced diphosphopyridine nucleotide. *Acta Chem Scand* 5, 1127-1144.
- 285) Thoden, J. B., Holden, H. M., Wesenberg, G., Raushel, F. M., and Rayment, I. (1997). Structure of carbamoyl phosphate synthetase: a journey of 96 Å from substrate to product. *Biochemistry* 36, 6305-6316.
- 286) Thoden, J. B., Huang, X., Kim, J., Raushel, F. M., and Holden, H. M. (2004). Long-range allosteric transitions in carbamoyl phosphate synthetase. *Protein Sci* 13, 2398-2405.
- 287) Thoden, J. B., Huang, X., Raushel, F. M., and Holden, H. M. (2002). Carbamoyl-phosphate synthetase. Creation of an escape route for ammonia. *J Biol Chem* 277, 39722-39727.
- 288) Ting, L. M., Shi, W., Lewandowicz, A., Singh, V., Mwakingwe, A., Birck, M. R., Ringia, E. A., Bench, G., Madrid, D. C., Tyler, P. C., *et al.* (2005). Targeting a novel *Plasmodium falciparum* purine recycling pathway with specific immucillins. *J Biol Chem* 280, 9547-9554.
- 289) Trotta P. P, Platzer K. E, Haschemeyer R. H, and A., M. (1974). Glutamine-binding subunit of glutamate synthase and partial reactions catalyzed by this glutamine amidotransferase. *Proc Natl Acad Sci U S A* 71, 4607-4611.
- 290) Tso, J. Y., Bower, S. G., and Zalkin, H. (1980). Mechanism of inactivation of glutamine amidotransferases by the antitumor drug L-(alpha S, 5S)-alpha-amino-3-chloro-4,5-dihydro-5-isoxazoleacetic acid (AT-125). *J Biol Chem* 255, 6734-6738.
- 291) Turner, D. C., and Brand, L. (1968). Quantitative estimation of protein binding site polarity. Fluorescence of N-arylaminonaphthalenesulfonates. *Biochemistry* 7, 3381-3390.

- 292) Tyler, P. C., Taylor, E. A., Frohlich, R. F., and Schramm, V. L. (2007). Synthesis of 5'-methylthio coformycins: specific inhibitors for malarial adenosine deaminase. *J Am Chem Soc* *129*, 6872-6879.
- 293) Udaka, S., and Moyed, H. S. (1963). Inhibition of parental and mutant xanthosine 5'-phosphate aminases by psicofuranine *J Biol Chem* *238*, 2797-2803.
- 294) Ulschmid, J. K., Rahlfs, S., Schirmer, R. H., and Becker, K. (2004). Adenylate kinase and GTP:AMP phosphotransferase of the malarial parasite *Plasmodium falciparum*. Central players in cellular energy metabolism. *Mol Biochem Parasitol* *136*, 211-220.
- 295) van den Heuvel, R. H., Curti, B., Vanoni, M. A., and Mattevi, A. (2004). Glutamate synthase: a fascinating pathway from L-glutamine to L-glutamate. *Cell Mol Life Sci* *61*, 669-681.
- 296) van den Heuvel, R. H., Svergun, D. I., Petoukhov, M. V., Coda, A., Curti, B., Ravasio, S., Vanoni, M. A., and Mattevi, A. (2003). The active conformation of glutamate synthase and its binding to ferredoxin. *J Mol Biol* *330*, 113-128.
- 297) van der Knaap, J. A., Kozhevnikova, E., Langenberg, K., Moshkin, Y. M., and Verrijzer, C. P. (2010). Biosynthetic enzyme GMP synthetase cooperates with ubiquitin-specific protease 7 in transcriptional regulation of ecdysteroid target genes. *Mol Cell Biol* *30*, 736-744.
- 298) van der Knaap, J. A., Kumar, B. R., Moshkin, Y. M., Langenberg, K., Krijgsveld, J., Heck, A. J., Karch, F., and Verrijzer, C. P. (2005). GMP synthetase stimulates histone H2B deubiquitylation by the epigenetic silencer USP7. *Mol Cell* *17*, 695-707.
- 299) Van Dyke, K., Tremblay, G. C., Lantz, C. H., and Szustkiewicz, C. (1970). The source of purines and pyrimidines in *Plasmodium berghei*. *Am J Trop Med Hyg* *19*, 202-208.
- 300) Vanoni, M. A., Accornero, P., Carrera, G., and Curti, B. (1994). The pH-dependent behavior of catalytic activities of *Azospirillum brasilense* glutamate synthase and iodoacetamide modification of the enzyme provide evidence for a catalytic Cys-His ion pair. *Arch Biochem Biophys* *309*, 222-230.
- 301) Vasanthakumar, G., Davis, R. L., Jr., Sullivan, M. A., and Donahue, J. P. (1990). Cloning and expression in *Escherichia coli* of a hypoxanthine-guanine phosphoribosyltransferase-encoding cDNA from *Plasmodium falciparum*. *Gene* *91*, 63-69.
- 302) Velick, S. F., and Vavra, J. (1962). A kinetic and equilibrium analysis of the glutamic oxaloacetate transaminase mechanism. *J Biol Chem* *237*, 2109-2122.
- 303) Vertessy, B., and Ovadi, J. (1987). A simple approach to detect active-site-directed enzyme-enzyme interactions. The aldolase/glycerol-phosphate-dehydrogenase enzyme system. *Eur J Biochem* *164*, 655-659.

- 304) Vial, H. (1996). Recent developments and rationale towards new strategies for malarial chemotherapy. *Parasite* 3, 3-23.
- 305) Vollmer, S. J., Switzer, R. L., Hermodson, M. A., Bower, S. G., and Zalkin, H. (1983). The glutamine-utilizing site of *Bacillus subtilis* glutamine phosphoribosylpyrophosphate amidotransferase. *J Biol Chem* 258, 10582-10585.
- 306) von der Saal, W., Crysler, C. S., and Villafranca, J. J. (1985). Positional isotope exchange and kinetic experiments with *Escherichia coli* guanosine-5'-monophosphate synthetase. *Biochemistry* 24, 5343-5350.
- 307) Vriend, G. (1990). WHAT IF: A molecular modeling and drug design program. *J Mol Graph* 8, 52-56.
- 308) Wakil SJ, S. J., Joshi VC. (1983). Fatty acid synthesis and its regulation. *Annu Rev Biochem* 52, 537-579.
- 309) Wales, T. E., and Engen, J. R. (2006). Hydrogen exchange mass spectrometry for the analysis of protein dynamics. *Mass Spectrom Rev* 25, 158-170.
- 310) Wales, T. E., Fadgen, K. E., Gerhardt, G. C., and Engen, J. R. (2008). High-speed and high-resolution UPLC separation at zero degrees Celsius. *Anal Chem* 80, 6815-6820.
- 311) Walsh, C. J., and Sherman, I. W. (1968). Purine and pyrimidine synthesis by the avian malaria parasite, *Plasmodium lophurae*. *J Protozool* 15, 763-770.
- 312) Wand, A. J., and Englander, S. W. (1996). Protein complexes studied by NMR spectroscopy. *Curr Opin Biotechnol* 7, 403-408.
- 313) Wang, X. S., Roitberg, A. E., and Richards, N. G. (2009). Computational studies of ammonia channel function in glutamine 5'-phosphoribosylpyrophosphate amidotransferase. *Biochemistry* 48, 12272-12282.
- 314) Webb, E. (1992). *Enzyme Nomenclature*. Academic Press, San Diego.
- 315) Webster, H. K., Whauna, J. M., Walker, M. D., Bean, T. L., (1984). Synthesis of adenosine nucleotides from hypoxanthine by human malaria parasites (*Plasmodium falciparum*) in continuous erythrocyte culture: inhibition by hadacidin but not alanosine. *Biochem Pharmacol* 33.1555-1557
- 316) Weeks, A., Lund, L., Raushel, F. M. (2006). Tunneling of intermediates in enzyme-catalyzed reactions. *Curr Opin Chem Biol* 10, 465-472.
- 317) Wiesmann, W. P., Webster, H. K., Lambros, C., Kelley, W. N., and Daddona, P. E. (1984). Adenosine deaminase in malaria infected erythrocytes: unique parasite enzyme presents a new therapeutic target. *Prog Clin Biol Res* 165, 325-342.

- 318) Wojcik, M., Seidle, H. F., Bieganowski, P., and Brenner, C. (2006). Glutamine-dependent NAD⁺ synthetase. How a two-domain, three-substrate enzyme avoids waste. *J Biol Chem* 281, 33395-33402.
- 319) Wolfenden, R. (1976). Transition state analog inhibitors and enzyme catalysis. *Annu Rev Biophys Bioeng* 5, 271-306.
- 320) Wu J, B. W., Sheppard K, Kitabatake M, Kwon ST, Söll D, Smith JL. (2009). Insights into tRNA-dependent amidotransferase evolution and catalysis from the structure of the *Aquifex aeolicus* enzyme. *J Mol Biol* 391, 703-716.
- 321) Xiao, K., Shenoy, S. K., Nobles, K., and Lefkowitz, R. J. (2004). Activation-dependent conformational changes in {beta}-arrestin 2. *J Biol Chem* 279, 55744-55753.
- 322) Yuan, P., Hendriks, E. F., Fernandez, H. R., O'Sullivan, W. J., and Stewart, T. S. (2005). Functional expression of the gene encoding cytidine triphosphate synthetase from *Plasmodium falciparum* which contains two novel sequences that are potential antimalarial targets. *Mol Biochem Parasitol* 143, 200-208.
- 323) Zalkin, H. (1985). Glutamine amidotransferases. *Methods Enzymol* 113, 263-264.
- 324) Zalkin, H. (1993). The amidotransferases. *Adv Enzymol Relat Areas Mol Biol* 66, 203-309.
- 325) Zalkin, H., and Murphy, T. (1975). Utilization of ammonia for tryptophan synthesis. *Biochem Biophys Res Commun* 67, 1370-1377.
- 326) Zalkin, H., and Smith, J. L. (1998). Enzymes using glutamine as an amide donor. *Adv Enzymol Relat Areas Mol Biol* 72, 87-144.
- 327) Zalkin, H., and Truitt, C. D. (1977). Characterization of the glutamine site of *Escherichia coli* guanosine 5'-monophosphate synthetase. *J Biol Chem* 252, 5431-5436.
- 328) Zein F, Z. Y., Kang YN, Burns K, Begley TP, Ealick SE. (2006). Structural insights into the mechanism of the PLP synthase holoenzyme from *Thermotoga maritima*. *Biochemistry* 45, 14609-14620. 6, 582-587.
- 329) Zhang, W., Ames, B. D., Tsai, S. C., and Tang, Y. (2006). Engineered biosynthesis of a novel amidated polyketide, using the malonamyl-specific initiation module from the oxytetracycline polyketide synthase. *Appl Environ Microbiol* 72, 2573-2580.
- 330) Zhang, Z., and Marshall, A. G. (1998). A universal algorithm for fast and automated charge state deconvolution of electrospray mass-to-charge ratio spectra. *J Am Soc Mass Spectrom* 9, 225-233.

- 331) Zhou, M., Sandercock, A. M., Fraser, C. S., Ridlova, G., Stephens, E., Schenauer, M. R., Yokoi-Fong, T., Barsky, D., Leary, J. A., Hershey, J. W., *et al.* (2008). Mass spectrometry reveals modularity and a complete subunit interaction map of the eukaryotic translation factor eIF3. *Proc Natl Acad Sci U S A* *105*, 18139-18144.
- 332) Zyk, N., Citri, N., and Moyed, H. S. (1970). Alteration of the conformational response and inhibition of xanthosine 5'-phosphate aminase by adenine glycosides. *Biochemistry* *9*, 677-683